Analysis of TBM tunnelling performance in faulted and highly fractured rocks

THÈSE N^{O} 6724 (2015)

PRÉSENTÉE LE 9 OCTOBRE 2015

À LA FACULTÉ DE L'ENVIRONNEMENT NATUREL, ARCHITECTURAL ET CONSTRUIT
LABORATOIRE DE MÉCANIQUE DES ROCHES
PROGRAMME DOCTORAL EN MÉCANIQUE

ÉCOLE POLYTECHNIQUE FÉDÉRALE DE LAUSANNE

POUR L'OBTENTION DU GRADE DE DOCTEUR ÈS SCIENCES

PAR

Erika PALTRINIERI

acceptée sur proposition du jury:

Prof. I. Botsis, président du jury
Prof. J. Zhao, Dr F. Sandrone, directeurs de thèse
Prof. P. Oreste, rapporteur
Dr E. Buechi, rapporteur
Dr A. Ferrari, rapporteur

ÉCOLE POLYTECHNIQUE
FÉDÉRALE DE LAUSANNE
Suisse
2015

Acknowledgements

The thesis would not have been possible without the aid of many people who have supported me since the beginning of this experience. I would like to express my gratitude to all of them for the help I got during these "Swiss" years. Firstly, I would like to thank my supervisor, Prof. Jian Zhao, who gave me the amazing opportunity to start the PhD at EPFL and who encouraged me, always with great optimism, in the research work.

Very special thanks go to my co-supervisor, Dr. Federica Sandrone, for the immeasurable support she has given me from the professional and human point of view. She has been a perfect leader, and a friend, always ready to discuss and to provide invaluable advices.

I would like to thank also the jury members of my private defence: Prof. Ioannis Botsis, Dr Ernst Büchi, Prof. Pierpaolo Oreste and Dr. Alessio Ferrari. Their comments and recommendations have been very useful for bettering the final version of the thesis.

I also want to thank the Swiss Federal Roads Authority (ASTRA) for having financed this research. Special thanks to BG SA, the Swiss National Geological Service, Dr. Jafar Hassanpour, Prof. Eckart Schneider, for having provided part of TBM data and geological/geotechnical information.

My sincere thanks go to the team of the Rock Mechanics Laboratory (LMR), in particular to Dr. Vincent Labiouse, Laurant Gastaldo and Jean-François Mathier for the kindness and helpfulness and to Rosa Ana Turielle, Barbara Tinguely, Jessica Garcia and Michela Lotrecchiano for the sympathy and the administrative assistance. Huge thanks go to Jean-Paul Dudt, the best (and the most patient!) French teacher in the world; his help was precious for carrying out the DAT simulations. And many thanks to Dr. Pierre Christe for his valuable and appreciated "geological" contribution. I would like also to thank the staff of the Soil Mechanics Laboratory (LMS), in particular Prof. Laloui Lyesse, Gilbert Gruaz and Patrick Dubey for always being smiling and gentle with me.

I am grateful to my (new and old) colleagues at LMR and at LMS: Felipe, Donatella, Valentina, Alberto, Eleonora, Gaia, Alice, Alessandro, Francesco, Timur, Ali, Dimitrios, Giovanni S., Etienne, Andrea S., Sara, Edoardo, Samuel, Claire, Giovanni B., Chao, Danila, Roman, Lijun, Qiambing, Xing, Yang and all the other researchers. Thanks for the discussions, the complaints, the picnics and the barbecues on the lake.

Many thanks to my "Swiss" (!?!) friends: Jacopo, Gabriele, Ildi and Francesco. Thanks for all the laughs, the trips, the cakes, the concerts and the…quotations! ☺

I would like to thank also a special family: Alessio, Maria Luisa, Matteo e Luca. Thanks for the nice moments spent together, for the chats, for the movies, for the toys and for the pizza and the "rosticceria"!

Special thanks go to my old friends "scattered" around Italy and Europe: Erika, Mila, Nat, Fabio, Giuba, Piggio, Luca, Andrea (son buona..), Alessandro[2], Giorgio, Roberto, Marco, Paola, Stefania, Claudia, Daniela, Pac, Paulina, Irene, Fabrizio, Flora e tutti quelli che mi sono dimenticata! Thanks for the never-ending friendship and for all the memories.

I cannot forget Roberto, Chiara, Aurelia, Antonio e Luciana for their affection and because they always make me feel at home.

The greatest thanks go to my family. La soru, because only a sister can really understand you in particular moments. Cesare e !il pupo!, because I couldn't ask for a better brother-in-low and for a more beautiful nephew. And my parents, for the love and the continuous support, in every situation, because they always wanted the best for me and, thanks to their teachings and encouragement, I obtained this important result.

And thanks to Andrea. One word is not enough for expressing my gratitude. Thanks for believing in me and for staying always by my side. I could overcome the most difficult moments thanks to him.

Grazie!

Abstract

This thesis, financed by ASTRA, focuses on the study of the performance of Tunnel Boring Machines in highly jointed rock masses and fault zones.

The great development of TBMs in the tunnelling industry is due to their advantages with respect to conventional excavation, such as generally greater production rates in favourable ground conditions. However, the advancement could be significantly slowed down in limiting geological situations such as highly fractured and fault zones. After an introduction about the major issues resulting from tunnelling in difficult ground conditions, a brief review of the most used TBM-performance prediction models is reported. The objective is to identify the most common parameters adopted for evaluating the TBM performance.

The geotechnical characterisation of fault zones is very difficult due to their heterogeneous nature characterised by a combination of weak and strong rock components. This particular aspect is highlighted through a literature review regarding the geological and geomechanical description of fault rocks.

In order to investigate possible relationships between difficult rock mass conditions and TBM performance, data of several tunnel projects have been collected in a specific database by including information from the field, laboratory tests and literature.

Preliminary analyses have been carried out in order to identify correlations between TBM performance (namely, penetration and advance rate) and rock mass parameters (e.g. rock strength, fracturing degree, etc.). Although some trends are identified, the scattered results confirm the difficulties in predicting the machine performance in complex geological environments.

In order to obtain a more complete geotechnical description of disturbed zones, a classification system for highly fractured rock masses and fault zones has been developed. Four “fault zone” classes have been identified by considering the fracturing and the weathering degree of the rock mass. Furthermore, in order to analyse the response to mechanical excavation of the identified classes, a set of numerical simulations have been run with the aim to investigate the TBM performance at the cutter-scale.

The data recorded in the TBM-performance database have been then analysed according to the new classification system. For each "fault zone" class, a reduction rate for selected TBM-performance parameters has been defined with respect to the tunnelling performance observed in good ground conditions. The results of these analyses are of great relevance as they allow to successfully quantifying the effect of degrading rock mass conditions on the TBM performances.

The results obtained in the previous steps have been used to carry out probabilistic analyses of the tunnel construction time and costs by means of the "Decision Aids for Tunnelling" (DAT). The DAT are a methodology and a software package that can be used to evaluate the influence of the uncertainties related to both the geological/geotechnical conditions and the construction process on final tunnel construction time and costs. In this framework, the DAT have been used for assessing the effects that demanding ground conditions may have on tunnelling operations in terms of costs and delays. The advance rate reductions, previously defined for each "fault zone" class, have been input in the simulations. A reliable estimation of the effect of degrading geological conditions (from highly fractured rocks, to faulted rocks, to crushed material) on the tunnel construction process has been obtained.

The results of this research may provide useful insights regarding the reduction of the machine performance in bad grounds, with respect to an estimated good performance in "ordinary" tunnelling conditions. Moreover, the study highlights the need to better characterise, from a geomechanical point of view, the highly fractured and faulted rocks. This could be done by considering the parameters representative of the altered/degraded state of the rock mass, instead of those commonly used for estimating the TBM performance in good rocks.

Keywords

Weak rocks, fault zone classification, TBM-performance prediction, performance database, Decision Aids for Tunnelling (DAT), numerical modelling.

Résumé

Le but de cette thèse, financée par l'OFROU, est l'étude des performances des tunneliers dans les terrains très fracturés et dans les failles.

Le développement des tunneliers est principalement dû à leurs avantages par rapport aux méthodes d'excavation traditionnelles, comme de meilleures performances dans des conditions géologiques favorables. Mais dès que ces conditions se détériorent, comme c'est le cas dans des zones très fracturées et perturbées, l'avancement peut être fortement freiné. Cette thèse décrit d'abord les principaux défis occasionnés par ces conditions géologiques difficiles, puis elle présente succinctement les modèles les plus courants de prédiction des performances des tunneliers dans des conditions ordinaires, ceci afin d'identifier les principaux paramètres utilisés.

La caractérisation géotechnique des zones de faille est compliquée à cause de leur nature hétérogène due à une succession de parties faibles et de parties plus résistantes. Pour analyser cet aspect, une étude bibliographique concernant la description géologique et géomécanique des roches faillées a été menée.

Afin de pouvoir analyser la relation entre les conditions géologiques difficiles et les performances des tunneliers, des données sur plusieurs tunnels ont été récoltées dans une base de données qui comprend des informations provenant du terrain, d'essais de laboratoires et de la littérature.

Des études préliminaires ont étés conduites pour analyser les corrélations entre des paramètres de performance (en particulier la pénétration et l'avancement) et certains géo-paramètres (comme la résistance de la roche et le degré de fracturation). Même si quelques tendances ont pu être observées, la grande dispersion des résultats a confirmé qu'il était difficile de prédire les performances de tunneliers dans des géologies complexes.

Afin d'obtenir une description géotechnique complète de zones perturbées, un nouveau système de classification des masses rocheuses très fracturées et des failles a été développé. Quatre classes de «zones perturbées» ont été identifiées en se basant sur les degrés de fracturation et d'altération. De plus, pour analyser la réponse de ces classes à l'excavation mécanique, des simulations numériques ont été menées pour mieux étudier la performance du tunnelier à l'échelle des molettes.

Puis la base de données a été analysée à l'aide du nouveau système de classification. Pour chacune des classes, un facteur de réduction des performances par rapport aux valeurs obtenues dans de bonnes conditions géologiques a été défini. Les résultats de ces analyses sont très intéressants, car ils permettent de quantifier l'effet de la dégradation des conditions géologiques sur les performances des tunneliers.

Les résultats obtenus ont ensuite été utilisés pour des analyses probabilistes des temps et coûts de construction de tunnels avec le logiciel «DAT» (Decision Aids for Tunnelling). Ce logiciel permet de quantifier l'influence des incertitudes liées à la géologie et de celles liées à la méthode de construction sur les temps et coûts de construction. Dans le cas présent, il a été utilisé pour estimer l'effet de conditions géologiques particulièrement difficiles sur les coûts et les durées des opérations d'un tunnelier. Le facteur de réduction de la vitesse obtenu pour chacune des quatre classes a été utilisé comme input dans les simulations. L'analyse a conduit à une estimation fiable de l'influence de conditions géologiques dégradées (de roche fortement fracturée, en passant par des masses perturbées, jusqu'à un matériau broyé) sur l'excavation au tunnelier.

Les résultats de cette recherche permettent de mieux comprendre comment de mauvaises conditions géologiques réduisent les performances de tunneliers par rapport aux conditions «ordinaires». Ils montrent aussi le besoin d'une meilleure caractérisation géomécanique des masses rocheuses fortement fracturées et perturbées. Pour ceci, il faudrait considérer des paramètres spécifiques, en lieu et place de ceux utilisés actuellement pour estimer les performances dans de bonnes roches.

Mots-clés

Roches de mauvaise qualité, classification des zones perturbées, prévision de la performance de tunneliers, base des données des performances, Decision Aids for Tunnelling (DAT), modélisation numérique.

Table of Contents

List of symbols ..... **I**

Chapter 1 Introduction **1**

1.1 Rock TBM tunnelling 1

1.2 Major issues of tunnelling in fault zones 3

1.3 Fault zone and TBM 7

1.3.1 Pont Ventoux (Italy) 7

1.3.2 Evinos-Mornos (Greece) 8

1.3.3 Dul Hasti (Kashmir) 8

1.3.4 Pinglin (Taiwan) 9

1.3.5 Gotthard Base Tunnel (Switzerland) 10

1.3.6 Moutier Tunnel (Switzerland) 10

1.4 Objectives and structure of the thesis 11

Chapter 2 TBM-performance prediction **15**

2.1 TBM performance prediction models 15

2.1.1 The NTNU model 16

2.1.2 The CSM model 18

2.1.3 The Büchi model 19

2.1.4 The Q_{TBM} model 20

2.1.5 The RME model 21

2.1.6 Other recent studies on the TBM performance 22

2.2 Most common rock mass parameters in TBM-performance prediction 24

2.3 Final remarks 25

Chapter 3 Characterisation of fault zone and fault rocks: genetic and structural relationship, geomechanical implications 27

3.1 Fault zone definition 27

3.2 Terminology and geological classifications of fault rocks 31

3.3 Geomechanical characteristics of fault material: weak and weathered rocks 33

3.4 Final remarks 39

Chapter 4 Data collection: development of the TBM-performance database 41

4.1 Gripper TBM data 41

4.1.1 TBM specifications and performance parameters 42

4.1.2 Rock mass parameters 44

4.2 Data quality 45

4.3 Selection criteria for data collection 47

4.4 Range of variation of significant parameters 48

4.4.1 TBM performance parameters 48

4.4.2 Rock mass parameters 49

4.5 Shield TBM data 51

4.6 Final remarks 53

Chapter 5 Preliminary data analyses 55

5.1 Gripper TBM data analyses 55

5.1.1 Rock strength: correlations between UCS (and UCS_H) and TBM performance parameters 55

5.1.2 Fracturing degree: correlations between J_v and TBM performance parameters 57

5.1.3 Existing rock mass classification systems: correlations between RMR and TBM performance parameters 58

5.2 Shield TBM data analyses 60

5.3 Final remarks 62

Chapter 6 Fault zone classification 65

6.1 Significant geological/geotechnical parameters in the classification 65

6.1.1 The fracturing degree 66

6.1.2 The weathering degree 66

6.1.3 The water influence (rock mass permeability) 69

6.1.4 The depth influence (in situ stress) 69

6.2 Description of fault zone classes 69

6.2.1 Class I: highly fractured rock masses 70

6.2.2 Class II: highly fractured weathered rock masses 71

6.2.3 Class III: cohesive fault rocks (and heterogeneous rock masses) 73

6.2.4 Class IV: crushed fault rocks 74

6.3 «Fault zone» classes in the TBM-performance database 75

6.4 Numerical modelling of cracking process induced by a TBM cutter in highly fractured and faulted rocks 77

6.4.1 Brief state of the art 77

6.4.2 Two dimensional discontinuum analyses 79

6.4.3 Effect of the fracturing degree on the penetration rate 89

6.4.4 Two dimensional continuum analyses 92

6.5 Final remarks 95

Chapter 7 Fault zone classes and TBM performance reduction 97

7.1 TBM-performance database in good tunnelling conditions 97

7.2 TBM tunnelling in faulted rocks: the Q_{TBM} 100

7.3 TBM performance reduction analyses 101

7.3.1 Cutterhead rotation speed, RPM 102

7.3.2 Penetration per revolution, p 103

7.3.3 Penetration rate, PR 106

7.3.4 Daily advance rate, daily AR 108

7.4 Result discussion 111

7.5 Final remarks 112

Chapter 8 Probabilistic analysis of TBM tunnelling in highly fractured and faulted rocks with the Decision Aids for Tunnelling (DAT) 115

8.1 The Decision Aids for Tunnelling 115

8.2 Effects of highly fractured and faulted rocks on TBM tunnelling simulations with DAT 118
8.2.1 Geology related input 118
8.2.2 Construction related input 121
8.3 Simulation results 125
8.4 Application of DAT model to a real case 133
8.5 Final remarks 135
Chapter 9 Conclusions and outlook 137
ANNEX A 145
ANNEX B 155
ANNEX C 161
References 165
Curriculum Vitae 177
List of publications 181

List of symbols

Chapter 1 - Introduction

σ_{ci}	Uniaxial compressive strength of the rock
σ_{cm}	Uniaxial compressive strength of the rock mass
γ	Rock mass unit weight
H	Overburden depth
p_0	Overburden stress, $p_0 = \gamma H$
δ	Radial tunnel displacement
r_0	Tunnel radius
ε_t	Tunnel strain, $\varepsilon_t = \delta / r_0$
p_i	Internal support pressure
σ_ϑ	Tangential stress
OFM	Modified Overload Factor (Deere et al., 1969), $OFM = \sigma_\vartheta / \sigma_{ci}$
UCS_H	Uniaxial compressive strength proposed by Habimana (1999) and Habimana et al. (2002) for cataclastic rocks
RMR	Rock Mass Rating (Bieniawski, 1976)

Chapter 2 – TBM performance prediction

Q_{TBM}	Q_{TBM}-system (Barton, 2000)
RME	Rock Mass Excavability (Bieniawski et al., 2006)
RQD	Rock Quality Designation (Hudson and Priest, 1979)
UCS	Uniaxial compressive strength of the rock
σ_t	Tensile strength of the rock
RPM	Cutterhead rotation speed [rev/min]
F_n	Cutter force

DRI	Drilling Rate Index
RQD_0	Rock Quality Designation (measured in the tunnelling direction)
J_n	Joint set number parameter
J_r	Joint roughness parameter
J_a	Joint alteration parameter
J_w	Joint water reduction factor
SRF	Strength Reduction Factor
CLI	Cutter Life Index
RMR	Rock Mass Rating (Bieniawski, 1976)
BI	Boreability Index
FPI	Field Penetration Index (Klein et al., 1995)
k_{eq}	Equivalent TBM jointing factor
M_{eq}	Equivalent thrust per cutter
i_0	Net rate of TBM penetration
j_c	Joint condition factor
V_b	Block volume
c_0	Orientation of main joint set
E	Factor linked to the type of rock
σ_{ci}	(UCS) Uniaxial compressive strength of the rock
M_B	Applied thrust per disc
k_d	Correction for cutter size
k_a	Correction for cutter spacing
J_p	Jointing parameter
k_s	TBM jointing factor
Q	Q-system (Barton et al., 1974)
PR	Penetration rate [m/hr]
AR	Advance rate [m/hr]
SIGMA	Rock mass strength
F	Average cutter load
q	Quartz content
σ_ϑ	Induced biaxial stress on tunnel face
T	Time of advancement [hr]
m	Negative gradient
ARA	Average advance rate [m/day]
U	Utilization factor of the TBM

J_v	Volumetric joint count

Chapter 3 – Characterisation of fault zone and fault rocks

σ_n	Normal stress
σ_s	Tangential stress
UCS	Uniaxial compressive strength of the rock
RQD	Rock Quality Designation (Hudson and Priest, 1979)
RMR	Rock Mass Rating (Bieniawski, 1976)
Q	Q-system (Barton et al., 1974)
φ	Friction angle
c	Cohesion
GSI	Geological Strength Index (Hoek, 1994)
VBP	Block Volumetric Portion
E	Elastic modulus
MSI	Mineralogical and Structural Index
mwVh	Mean weighted Vickers hardness
TC	Texture coefficient
MC	Matrix coefficient
σ_1	Maximum principal stress at failure
σ_3	Minimum principal stress at failure
σ_{ci}	(UCS) Uniaxial compressive strength of the rock
m_b	Hoek-Brown material constant (rock mass)
a	Hoek-Brown material constant
s	Hoek-Brown material constant
t	Tectonisation degree parameter (Habimana, 1999; Habimana et al., 2002), t= $(GSI/100)^{0.55}$
C	Constant (linked to the strength contrast between block and matrix)
EBP	Equivalent Block Proportion
UCS_N	Normalised uniaxial compressive strength, $UCS_N = exp(C \times EPB)$
Δσ	Deviatoric stress, $\Delta\sigma = \sigma_1 - \sigma_3$
V_S	S-wave velocity
V_P	P-wave velocity
d	Density of the rock
r	Roundness

ABD_F	Average Block Diameter factor

Chapter 4 – Data collection: development of the TBM-performance database

RPM	Cutterhead rotation speed [rev/min]
Th	Thrust force
Tq	Torque force
RPM_{max}	Maximum installed cutterhead rotation speed [rev/min]
Th_{max}	Maximum thrust force
Tq_{max}	Maximum torque force
U	Utilization factor of the TBM
PR	Penetration rate [m/hr]
AR	Advance rate [m/hr]
FPI	Field Penetration Index (Klein et al., 1995)
p	Penetration per revolution [mm/rev]
Daily AR	Daily advance rate [m/day]
N_c	Number of cutters
∅	Tunnel diameter
UCS	Uniaxial compressive strength of the rock
BTS	Brazilian tensile strength
J_v	Volumetric joint count
RQD	Rock Quality Designation (Hudson and Priest, 1979)
UCS_{rm}	Uniaxial compressive strength of the rock mass (Hoek et al., 2002), $UCS_{rm} = (sUCS^2)^a$
σ_ϑ	Tangential stress
GSI	Geological Strength Index (Hoek, 1994)
Q	Q-system (Barton et al., 1974)
RMR	Rock Mass Rating (Bieniawski, 1976)
s_i	Average spacing of the i^{th} joint set
$N_{r(5)}$	Number of random joints along a 5 m scan line
λ	Total joint frequency
s	Hoek-Brown material constant
a	Hoek-Brown material constant
D	Disturbance factor

t	Tectonisation degree parameter (Habimana, 1999; Habimana et al., 2002), t= $(GSI/100)^{0.55}$
UCS_H	Uniaxial compressive strength proposed by Habimana (1999) and Habimana et al. (2002) for cataclastic rocks, $UCS_H = tUCS$
C.V.	Coefficient of variation

Chapter 5 – Preliminary data analyses

UCS	Uniaxial compressive strength of the rock
J_v	Volumetric joint count
RMR	Rock Mass Rating (Bieniawski, 1976)
UCS_H	Uniaxial compressive strength proposed by Habimana (1999) and Habimana et al. (2002) for cataclastic rocks
p	Penetration per revolution [mm/rev]
PR	Penetration rate [m/hr]
RPM	Cutterhead rotation speed [rev/min]
U	Utilization factor of the TBM
Daily AR	Daily advance rate [m/day]

Chapter 6 – Fault zone classification

J_v	Volumetric joint count
GSI	Geological Strength Index (Hoek, 1994)
RMR	Rock Mass Rating (Bieniawski, 1976)
UCS	Uniaxial compressive strength of the rock
UCS_{rm}	Uniaxial compressive strength of the rock mass
UCS_H	Uniaxial compressive strength proposed by Habimana (1999) and Habimana et al. (2002) for cataclastic rocks
ν	Poisson's ratio
K	Bulk modulus
G	Shear modulus
$c_{(rm)}$	Cohesion of the rock material
$\varphi_{(rm)}$	Friction angle of the rock material
$\psi_{(rm)}$	Dilation angle of the rock material
τ	Shear stress
v	Shear displacement

u	Normal displacement
k_n	Normal stiffness, $k_n = \partial\sigma_n/\partial v$
k_s	Shear stiffness, $k_s = \partial\tau/\partial u$
$c_{(j)}$	Cohesion of the joint
$\varphi_{(j)}$	Friction angle of the joint
$\Psi_{(j)}$	Dilation angle of the joint
Δz_{min}	Smallest width of the zone adjoining the joint in the normal direction
L_{xx}	Reduced cutter force
α	Joint dip angle
P_{chip}	Penetration rate expressed as chipping area over chipping stress
m_b	Hoek-Brown material constant (rock mass)
k_p	Passive earth pressure coefficient
m_i	Hoek-Brown material constant (intact rock)
s	Hoek-Brown material constant
a	Hoek-Brown material constant

Chapter 7 – Fault zone classes and TBM performance reduction

RPM	Cutterhead rotation speed [rev/min]
p	Penetration per revolution [mm/rev]
PR	Penetration rate [m/hr]
Daily AR	Daily advance rate [m/day]
J_v	Volumetric joint count
UCS	Uniaxial compressive strength of the rock
U	Utilization factor of the TBM
RPM_{max}	Maximum installed cutterhead rotation speed [rev/min]
p_{max}	The best (maximum) penetration per revolution [mm/rev]
p_{mode}	The most frequent penetration per revolution [mm/rev]
PR_{max}	The best (maximum) penetration rate [m/hr]
PR_{mode}	The most frequent penetration rate [m/hr]
Daily AR_{max}	The best (maximum) daily advance rate [m/day]
Daily AR_{mode}	The most frequent daily advance rate [m/day]
MFR	Most Frequent Reduction

Chapter 8 – Probabilistic analysis of TBM tunnelling in highly fractured and faulted rocks with the Decision Aids for Tunnelling (DAT)

GC	Ground class
GP	Ground parameter
UCS	Uniaxial compressive strength of the rock
Si	The i^{th} 'strength' ground parameter
FWj	The j^{th} 'rock mass conditions' ground parameter (fracturing degree and water inflow)
Ck	The k^{th} 'fault zone' ground parameter
L_{min}	Minimum possible segment length
L_{mode}	The most frequent segment length
L_{max}	Maximum possible segment length
PDF	Probability Density Function
AR_0	Daily advance rate in good tunnelling conditions [m/day]
EC_0	Construction cost per meter in good tunnelling conditions
t_i	Excavation time of the i^{th} construction method
RL	Round length (set equal to 2 m)
$AR_{0[best\ performance]}$	The best daily advance rate in good tunnelling conditions [m/day]
r_i	Reduction factor for the i^{th} construction method
c_i	Construction cost for the i^{th} construction method
C.V.	Coefficient of variation
Daily AR	Daily advance rate [m/day]
EC	Construction cost per meter
Daily AR_{real}	Real daily advance rate [m/day]
Daily AR_{DAT}	Simulated (by DAT) daily advance rate [m/day]

Chapter 9 – Conclusions and outlook

RMR	Rock Mass Rating (Bieniawski, 1976)
J_v	Volumetric joint count
GSI	Geological Strength Index (Hoek, 1994)
UCS_{rm}	Uniaxial compressive strength of the rock mass
UCS	Uniaxial compressive strength of the rock

UCS_H	Uniaxial compressive strength proposed by Habimana (1999) and Habimana et al. (2002) for cataclastic rocks
p	Penetration per revolution [mm/rev]
P_{chip}	Penetration rate expressed as chipping area over chipping stress
RPM	Cutterhead rotation speed [rev/min]
PR	Penetration rate [m/hr]
Daily AR	Daily advance rate [m/day]
Ck	The k^{th} 'fault zone' ground parameter in DAT simulations

Annex A

DRI	Drilling Rate Index
RPM	Cutterhead rotation speed [rev/min]
SJ	Sievers' J-value
E	Factor linked to the type of rock
σ_{ci}	Uniaxial compressive strength of the rock
k_s	TBM jointing factor
α	Angle between the tunnel axis and the plane of weakness
α_f	Dip angle of weakness planes
α_t	Direction of the tunnel axis
α_s	Strike angle of weakness planes
k_{DRI}	Correction factor
k_{si}	TBM jointing factor of the i^{th} joint set
s	Number of joint sets
k_{stot}	TBM total jointing factor, $k_{stot} = \sum_{i=1}^{s} k_{si} - 0.36 \cdot (s-1)$
k_{eq}	Equivalent TBM jointing factor, $k_{eq} = k_{stot} \cdot k_{DRI}$
M_{eq}	Equivalent thrust per cutter
i_0	Net rate of TBM penetration
k_d	Correction for cutter size
k_a	Correction for cutter spacing
PR	Penetration rate [m/hr]
F	Function of M_{eq}, $F = 0.0015 \cdot M_{eq}^{1.5}$
G	Function of M_{eq} and k_{eq}, $G = 30 \cdot k_{eq}^{-0.5} \cdot M_{eq}^{-0.8}$
U	Utilization factor of the machine
Q_{TBM}	Q_{TBM}-system (Barton, 2000)

RQD	Rock Quality Designation (Hudson and Priest, 1979)
RQD_0	Rock Quality Designation (measured in the tunnelling direction)
J_n	Joint set number parameter
J_r	Joint roughness parameter
J_a	Joint alteration parameter
J_w	Joint water reduction factor
SRF	Strength Reduction Factor
SIGMA	Rock mass strength
γ	Rock mass unit weight
Q	Q-system (Barton et al., 1974)
Q_0	Q-system (measured in the tunnelling direction)
Q_c	Function of the Q-value, $Q_c = (\sigma_{ci}/100)Q_0$
I_{50}	Point load index on 50 mm diameter core
Q_t	Function of the Q-value, $Q_t = (I_{50}/4)Q_0$
$SIGMA_{cm}$	Rock mass strength (compressive failure), $SIGMA_{cm} = 5 \cdot \gamma \cdot Q_c^{1/3}$
$SIGMA_{tm}$	Rock mass strength (tensile failure), $SIGMA_{tm} = 5 \cdot \gamma \cdot Q_t^{1/3}$
F	Average cutter load
CLI	Cutter Life Index
q	Quartz content
σ_ϑ	Induced biaxial stress on tunnel face
PR	Penetration rate [m/hr]
AR	Advance rate [m/hr]
T	Time of advancement [hr]
m	Negative gradient
m_i	Factor depending on the Q-value
D	Tunnel diameter
n	Porosity of the rock
L	Tunnel length

Annex B

RMR	Rock Mass Rating (Bieniawski, 1976)
GSI	Geological Strength Index (Hoek, 1994)
m_b	Hoek-Brown material constant (rock mass)
s	Hoek-Brown material constant

σ_1	Maximum principal stress at failure
σ_3	Minimum principal stress at failure
ε_a	Axial strain
Ω	Simulation domain

Annex C

RPM	Cutterhead rotation speed [rev/min]
PR	Penetration rate [m/hr]
Daily AR	Daily advance rate [m/day]
MFR	Most Frequent Reduction
AR	Advance rate [m/hr]
RPM_{max}	Maximum installed cutterhead rotation speed [rev/min]
PR_{max}	The best (maximum) penetration rate [m/hr]
Daily AR_{max}	The best (maximum) daily advance rate [m/day]
p	(i_0) Penetration per revolution [mm/rev]
U	Utilization factor of the machine

Chapter 1 Introduction

Switzerland is one of the countries where the underground constructions are necessary since more than 60% of the area is covered by mountains. In the past years huge TBM tunnel projects have been carried out and some are still on going. The most famous example is the Gotthard Base Tunnel (GBT), at the moment the world's longest railway tunnel.

Nowadays mechanised tunnelling is more and more considered as a valid alternative to the conventional technology (e.g. Drill-and-Blast). The great development of Tunnel Boring Machines (TBMs) in tunnelling industry is mainly due to its advantages, with respect to conventional excavation method, such as continuous operation, safer working conditions, reduced damage at ground surface and grater rate of advance. However, the TBM performances could be significantly reduced in changing ground conditions and in particular geological situations like very strong or very poor rock masses, where lower advance rates are generally recorded, mainly due to the lack of versatility of the machine. In particular, one of the main issues, especially for what concerns gripper TBMs, is the crossing of weakness (e.g. fault) zones. Although the presence of important fault zones is generally identified along the tunnel alignment already in the project phase, in some cases it may still represent an unexpected incident due to either a lack of warning during excavation or an underestimation of the problem seriousness (Barla and Pelizza, 2000). Tunnelling in such difficult ground conditions might cause project costs increase (mainly due to additional ground improvements and consequent substantial delays) and plays a central role for the safe completion of the works. Although, as reported by Palmström and Berthelsen (1988), this kind of problems generally occur along only 1-15% of a tunnel, a better understanding of the geological development and occurrence of weakness zones is important in the planning and construction phases of a tunnel.

1.1 Rock TBM tunnelling

Rock tunnelling machines can be grouped into three main categories:

- Open (Gripper) TBM: for rock characterised by medium to high strength. During the boring operation two laterally mounted gripper plates anchor the rear part of the machine to the tunnel walls, while the rotating cutterhead (equipped with disc cutters) is

pressed against the tunnel face. Due to the rolling movement of the cutters, single pieces (chips) of rock are cut out from the face and removed.

- Shield TBM: for rock characterised by low to high strength or when the tunnel walls cannot support/contrast the action of the grippers. The body of the TBM is enclosed in a shield and precast concrete segments are assembled by an erector to form closed rings (the final support) directly behind the TBM. The TBM advancement is guaranteed by the concrete ring erected behind the shield. Hydraulic thrust cylinders allow the machine to push against the ring, thus the installation of segments and excavation cannot be done simultaneously.
- Double Shield TBM: for good to fractured/weak rocks. The TBM consists of two main components: a front shield with cutterhead, main bearing and drive, and a gripper shield with gripping unit, auxiliary thrust cylinders and tail steel jacket (the overlap of front shield and gripper shield forms the extendible telescopic shield). The TBM simultaneously excavates and erects the tunnel lining (continuous cycle of excavation). The machine unifies the functional principles of gripper and single shield TBMs being equipped by two possible "thrust systems" (adopted on the basis of the ground conditions): the jacks that push against the segment ring to create the thrust for the TBM as well as the grippers (located on the second shield) that push against the excavated tunnel. In this sense the double shield machine can be considered as one of the most flexible types of machine.

Table 1.1 shows the main advantages and disadvantages characterising the different TBM types.

Table 1.1 Schematic comparison among various types of TBMs, after Barla and Pelizza (2000)

Open TBM	**Single Shield TBM**	**Double Shield TBM**
Advantages		
Easy to operate Applicable only in hard rocks Flexibility of supports Construction cost Limited investment	Application range more widespread than for open TBMs Safety Precast lining installation High performances	Larger application range Safety Support and lining flexibility High performances Drive in difficult ground condition
Disadvantages		
Gripping in soft or unstable rock Support installation in unstable rock	Two work phases Not applicable in weak ground Need of precast lining Higher initial investment Complex to operate Squeezing ground risk of TBM jamming	High investment Complex to operate Higher maintenance costs (need of cleaning the telescopic joint) Squeezing ground risk of TBM jamming

Although the technological improvements of recent years allow reaching acceptable/good performances also in difficult grounds, the selection of the most appropriate TBM type still remain a very uncertain task. This is principally due to the significant fix costs (i.e. initial

investments required for this technique), and to the potential serious consequences (e.g. TBM loss due to jamming) that can occur if weakness zones are encountered (e.g. highly deformable and squeezing grounds, water bearing rocks, etc.).

1.2 Major issues of tunnelling in fault zones

Weakness ground conditions, besides referring to weak (sandstone, siltstone, shale, mudstone, marl and chalk, tuff, agglomerate) and weathered (hydrothermal and chemical) rocks of all types, could be caused by jointing and shear zones or faults present in the rock mass (Klein, 2001). As reported by several authors (Schubert and Riedmüller, 1997; Schubert and Riedmüller, 2000; Habimana et al., 2002; Loew et al., 2010; Ramoni and Anagnostou, 2010), the most common geotechnical problems resulting from tunnelling in faulted/highly fractured zones are:

- instability of the excavation face;
- excessive overbreak of the tunnel contour;
- excessive deformation when squeezing ground is encountered;
- frequent changes (i.e. both magnitudes and direction) of stresses and displacements;
- large water inflows.

The possible instability phenomena (such as collapses, ravelling, slabbing, softening and slaking, swelling, squeezing and flowing ground) are generally due to the low strength and to the high deformability of the involved weak and weathered rocks, furthermore, they can be influenced by groundwater conditions and by discontinuities (bedding planes, joints, foliation and faults) in the rock mass (Klein, 2001).

The tunnel collapse is a sudden cave-in inwards which could interest the face, the side-walls and the lining (e.g. when it occurs after excavation). Moreover, a gradual overbreak at tunnel roof and/or walls can be associated to ravelling ground that implies a time-dependent loss of strength of the weathered rocks (Sturk et al., 2011). Significant ravelling could develop because of the combined effect of stress slabbing in a thinly-bedded rock formation and loosening along steeply dipping joints orientated nearly parallel to the tunnel (Klein, 2001). The ravelling behaviour considerably reduces the rock mass stand up time, mainly depending on the degree of weathering (Sturk et al., 2011).

One of the worst geological hazards of tunnelling in weak rocks is represented by flowing ground in which unconsolidated and saturated material can enter the tunnel flowing for great distances and for a significant time. It is generally associated to fault zones and crushed zones, where a great amount of available water at high pressure must be present and the rock must be characterised by no or low cohesion (Sturk et al., 2011).

Softening and slaking are typical of rocks with high clay content that are prone to moisture changes. Softening represents a significant loss of strength and slaking results in disintegration of the rock (Klein, 2001). For tunnels, slaking means problems in stand-up time, overbreak, need of construction and support procedures to minimise deterioration, and it contributes to

time-dependent instability of large blocks progressing along surfaces of fractures behind rock slabs (Hartman, 1992).

One of the most common problems observed in weak rocks is the squeezing behaviour of the rock mass, caused by overstress conditions around the tunnel. Squeezing can occur both in weak rock formations (such as schists, claystones, shales, etc.) and in highly jointed rock masses and it is characterised by yielding under the redistribution state of stress during and after excavation (Palmström, 1995) that results in the reduction of the tunnel cross-section. The magnitude of the ground movements (tunnel convergence) depends on the type of rock, rock mass strength and deformation properties, and in situ stress conditions (Klein, 2001). Squeezing is enhanced by unfavourable orientation (parallel to the tunnel axis) of discontinuities (bedding planes, schistosity), and it is found to occur frequently in contact and tectonised zones and faults (Loew et al., 2010). As reported by Barla (2002) several empirical (e.g. Singh et al., 1992; Goel et al., 1995) and semi-empirical (e.g. Jethwa et al., 1984; Aydan et al., 1993; Hoek and Marinos, 2000) approaches are available in literature to predict squeezing. All these methods use as starting point the ratio of uniaxial compressive strength σ_{ci}/σ_{cm} of intact rock/rock mass to overburden stress $p_0=\gamma H$, where γ is the rock mass unit weight and H is the overburden depth (Loew et al., 2010). According to Loew et al. (2010), the most used approach is the one proposed by Hoek (2001). By means of axisymmetric finite element analyses, he provided an approximate relationship to calculate the tunnel strain ε_t (defined as ratio of radial tunnel displacement to tunnel radius) as a function of the ratio σ_{cm}/p_0 and the internal pressure p_i:

$$\varepsilon_t(\%) = 0.15\left(1-\frac{p_i}{p_0}\right)\frac{\sigma_{cm}}{p_0}^{-\frac{\left(\frac{3p_i}{p_0}+1\right)}{\left(\frac{3.8p_i}{p_0}+0.54\right)}} \qquad 1.1$$

The curve defined by Equation 1.1 (without support pressure p_i) may give a first estimate of tunnel squeezing problems associated with different tunnel strain levels (Figure 1.1).

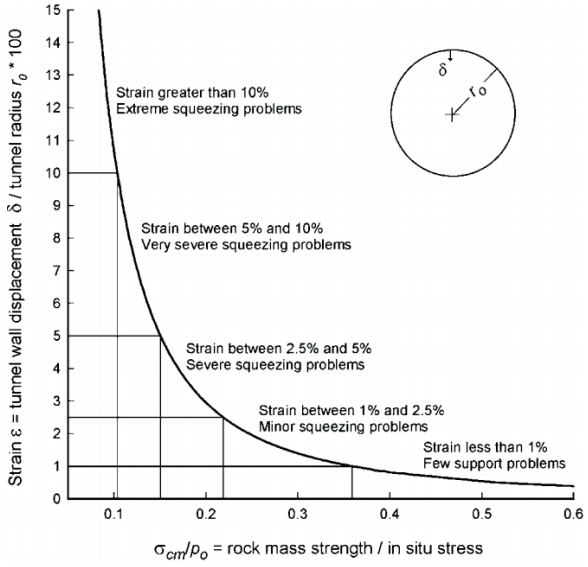

Figure 1.1 Squeezing associated with different levels of strain (Hoek, 2001).

It is important to observe that, squeezing ground is one of the most common hazards connected to a fault zone in deep Alpine tunnelling, together with high water inflows and structurally controlled failures (Figure 1.2).

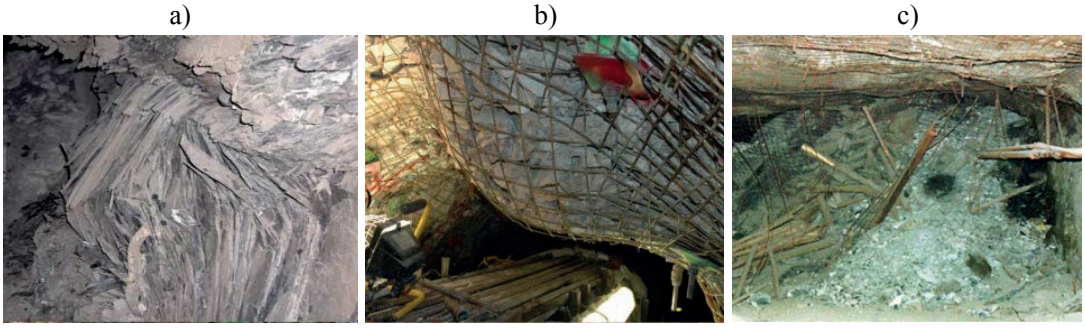

Figure 1.2 Examples of structurally controlled instabilities in fault zones: a) highly anisotropic failure at the tunnel sidewalls due to the presence of well-developed foliation or sub-parallel fractures with small spacing; b) progressive block destabilisation at the tunnel walls/crown; c) complete collapse resulting from total loss of confinement; after (Loew et al., 2010).

All described instability phenomena might affect the performance of the TBMs. As a matter of facts, one of the main drawbacks of TBM tunnelling in faulted/highly fractured zones is a significant reduction of the advancement rate due to large/very large construction delays which are generally associated to the following problems:

- heavier supports should be installed in very fractured/bulking rocks;
- ground treatments are often required, causing major delays (i.e. need to stop the excavation process) and cost increase;
- additional drainage systems and waterproofing becomes necessary to deal with significant water inflows;
- the need to free the machine cutterhead (or shield) if it jams, especially in case of very high tunnel displacements (this also tremendously affects the tunnel crew safety).

Furthermore, it is also important to observe that encountering faulted/heavily jointed tunnel faces may strongly affect the interaction between rock mass and TBM cutters, since the excavation may not proceed anymore via the usual chipping process.

Figure 1.3 illustrates schematically the tunnelling and stability problems that could be encountered when a TBM crosses fault rocks (Habimana et al., 2002).

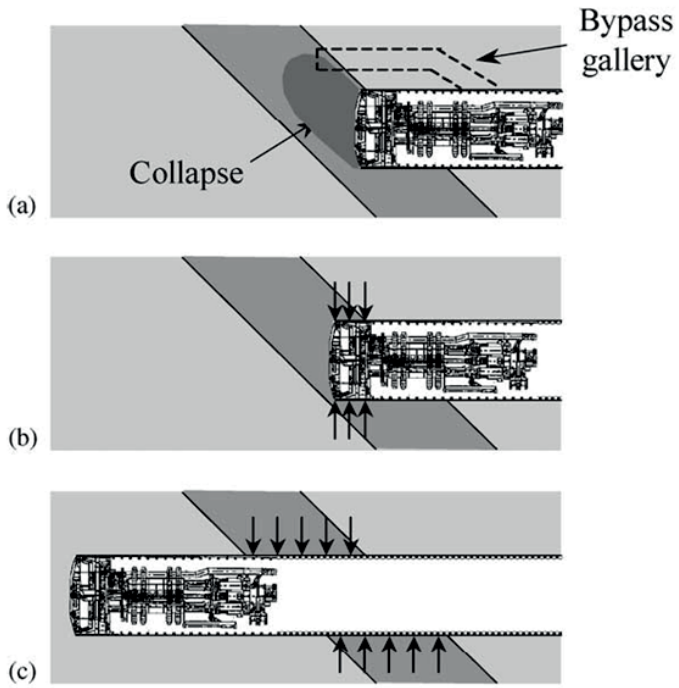

Figure 1.3 Progress difficulties of a TBM in tectonically crushed rock zone: a) excavation face instability; b) decompression and blocking of the TBM; c) creep phenomenon (Habimana et al., 2002).

In order to avoid/reduce the consequences of the problems listed here before, a constant observation of rock mass behaviour during tunnel construction becomes necessary, as well as a constant update of the ground model by taking into consideration all the information collected during excavation. Besides an adequate ground investigation activity (i.e. before and during excavation), the prediction of the TBM performance in difficult ground conditions becomes extremely important, since it will allow a more appropriate selection of the excavation method as well as a better planning of the tunnel construction.

For evaluating the immediate response of weak rocks to tunnelling, Klein (2001) developed the flow chart reported in Figure 1.4. As it is possible to see, he defined the mass behaviour as "a function of the stresses imposed on the rock surrounding the tunnel and the strength of the rock". In order to assess the potential for overstressed conditions, the modified overload factor (OFM), expressed by Equation 1.2 (Deere et al. 1969), has been used:

$$OFM = \frac{\sigma_\vartheta}{\sigma_{ci}} \qquad 1.2$$

where σ_ϑ is the tangential stress and the σ_{ci} is the uniaxial compressive strength of the rock. By this equation it is possible to deduce that overstressed rock conditions develop around the tunnel when OFM is greater than one; otherwise stable conditions are expected. According to Klein (2001), mainly depending on the stress-strain characteristics of the rocks, the behaviour under overstressed conditions changes: for example, rocks characterised by brittle failure (e.g. typically coarse-grained rocks such as sandstone and conglomerate) will break; while ductile

rocks (e.g. typically fine-grained rocks such as shale, marl and weathered/altered rocks) will yield causing convergences of the tunnel walls.

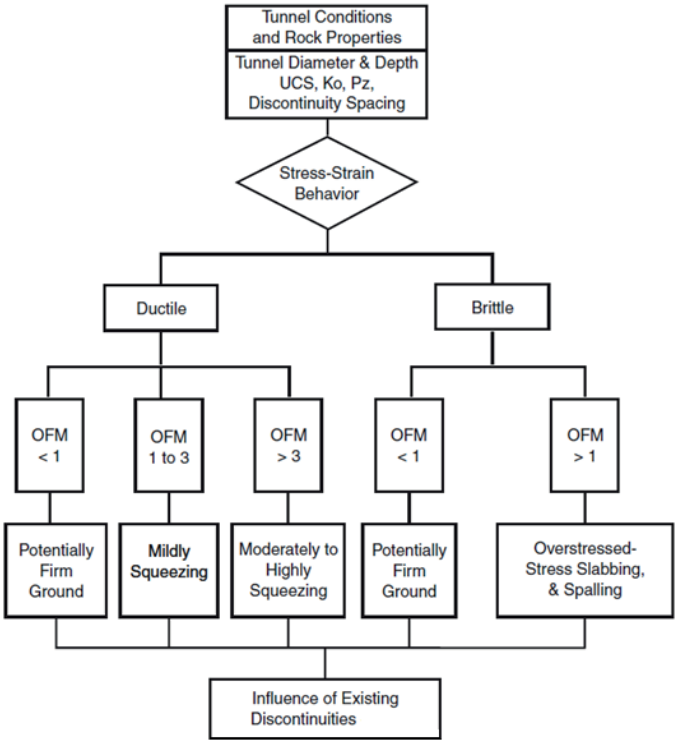

Figure 1.4 Immediate response of weak rocks to tunnelling (Klein, 2001).

1.3 Fault zone and TBM

Several cases of TBM tunnelling in fault zones have been recorded in these last decades in different parts of the world. Some of them, collected by Barton (2006) on the basis of his "fault zone experiences" in Italy, Greece, Kashmir and Taiwan, are reported in the following sections as well as two famous cases in Switzerland. The aim is to better understand the possible consequences on TBM tunnelling of such bad conditions.

1.3.1 Pont Ventoux (Italy)

The Italian Pont Ventoux HEP headrace tunnel, excavated by a gripper TBM, was characterised by several fault zones that had disastrous results on the machine progress (Figure 1.5). The biggest problem was the combination of adverse water pressures, erosion of faulted material and major void formation due to generally sub-parallel fault orientation. The cutterhead was stuck for 6 months, because of the need to probe ahead of the tunnel face, mapping the extent of fracture zones (by means of tomographic images) and then deciding the stabilisation measures to be adopted (Barla and Pelizza, 2000). This resulted in an advancement of only 20 m in 7 months. Moreover, the TBM grippers represented a further complication due to the pressure exerted on the continuous steel liner (flange-to-flange), which was installed in the most adverse

rock conditions. This loading caused the crushing of the steel sets with consequent tunnel walls instability.

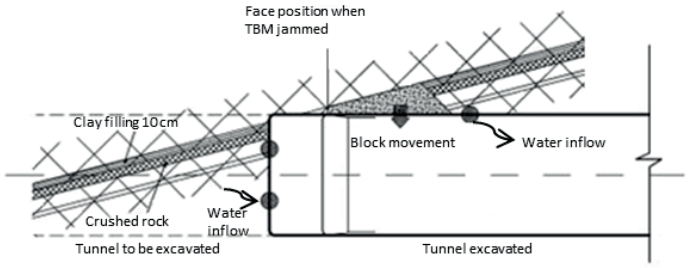

Figure 1.5 The TBM jamming as a consequence of overstressing and a 25 cm block movement of the right sidewall in the Pont Ventoux tunnel, Italy, after Barla and Pelizza (2000).

1.3.2 Evinos-Mornos (Greece)

Another TBM project characterised by adverse geological conditions is the Evinos-Mornos tunnel (Greece), one of the longest hydraulic tunnels in the world. A big collapse occurred in front of the TBM cutterhead (Figure 1.6) when the double shield TBM entered a very disturbed zone characterised by a disintegrated rock mass structure. The result was the creation of a large cavity, i.e. more than 10 m height, above the machine area. Hand-mining operations were required to restart the TBM excavation which caused about a 50 days standstill (Grandori et al., 1995).

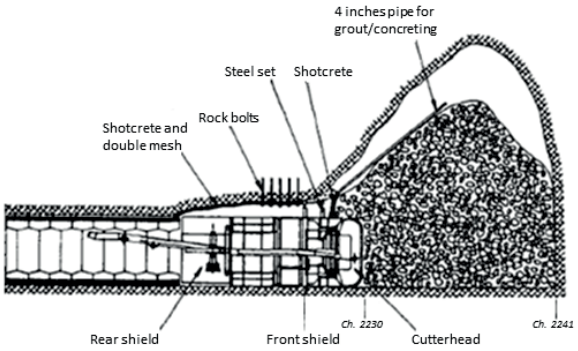

Figure 1.6 The big collapse in front of the cutterhead that creates a cavern of more than 10 m high in the Evinos-Mornos tunnel, Greece, after Grandori et al. (1995).

1.3.3 Dul Hasti (Kashmir)

The excavation of Dul Hasti Hydroelectric Project (Kashmir, India) was partly performed by an open TBM and it was characterised by serious difficulties. Due to several geological accidents, such as extreme pebble/sand blow-out and stand-up time problems, accompanied by water discharge up to more than 1000 lit/sec (Figure 1.7), the machine stick many times. As a consequence, the average advance rate reduced to 22 meters per month (Vibert et al., 2005). Although additional supports, grouting of the cavities in the machine area, drilling of drainage holes and a final modification of tunnel alignment were performed, the heavily damaged TBM

was abandoned after a further blockage, and the excavation was resumed with the Drill-and-Blast method.

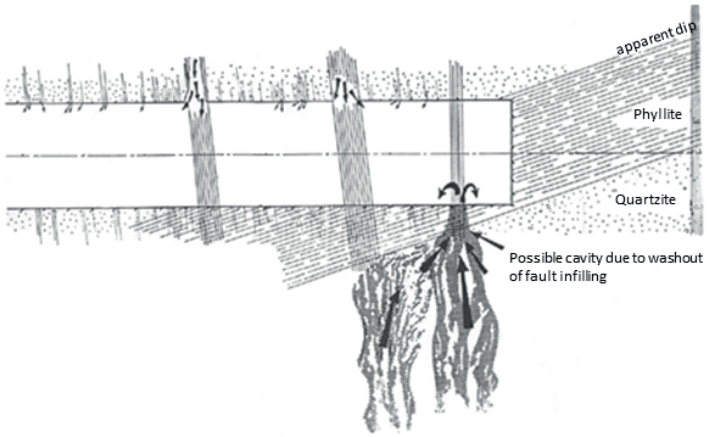

Figure 1.7 Cavity formation in the right part of the invert as a consequence of a very important water inflow carrying silt, sand and debris, in the Dul Hasti tunnel, India, after Vibert et al. (2005).

1.3.4 Pinglin (Taiwan)

The Pinglin Highway tunnel in Taiwan is an example of particularly complex geological conditions such as sudden inrush of great quantities of groundwater through zones of faulted and fractured rocks. As illustrated in Figure 1.8, several face collapses, causing TBM jamming, were observed during its excavation (Barla and Pelizza, 2000). In particular, the delays were so important that also in this case it was decided to abandon the TBM and continue the excavation using the Drill-and-Blast method. The 15 km long tunnel could be completed after about 12 years.

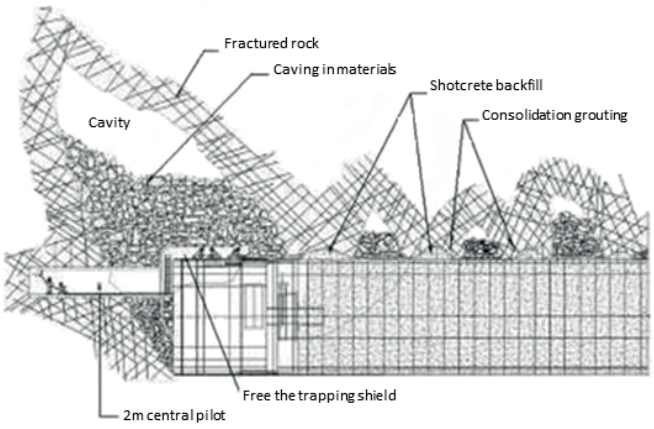

Figure 1.8 Example of instability problem at the tunnel face of the Pinglin Highway tunnel, Taiwan, after Barla and Pelizza (2000).

1.3.5 Gotthard Base Tunnel (Switzerland)

The Gotthard Base Tunnel (GBT) is a Swiss railway tunnel expected to open in 2016. It is part of the AlpTransit project, also known as the New Railway Link through the Alps (NRLA). Despite most of problematic zones along the tunnel alignment could be identified in advance, some relevant unexpected events occurred during the tunnel excavation. In the south part of the GBT, after about 200 meters, the TBM bumped into a sub-horizontal fault zone characterised by kakirite, cataclasite and highly fractured rocks. It was a few meters thick zone and it affected the west tube for about 100 meters and the east tube for 400 meters, especially at the crown. The detachment of loose material, above and just behind the cutterhead, caused the formation of cavities till 6 m high, which were filled with shotcrete and, in some cases, with in-situ casted concrete. The support was immediately installed, adopting steel sets, welded wire mesh and shotcrete. Because of the difficult ground conditions, the TBM advancement could not exceed 2.5 meters per day. Toward the end of the same excavation section, two nearly parallel sub-vertical fault zones were encountered (Figure 1.9). Moreover, some cataclastic rocks and kakirite layers, about 3-5 m thick, with highly fractured rocks in between were encountered. When TBM crossed these zones, the great pressure exercised on the cutterhead shield led to the machine jamming, with a downtime of ten days. The convergence of the tunnel caused also important deformations and damages to the supports, and reprofiling works became necessary. Without considering the stoppage of the TBM, the advancement was between 7 and 15 meters per day.

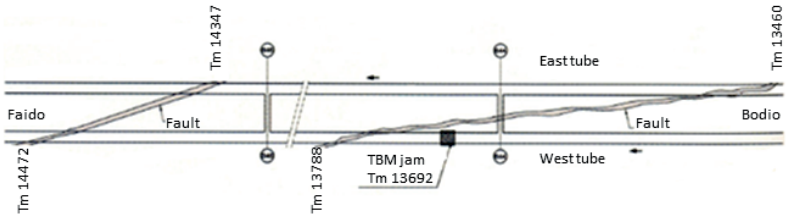

Figure 1.9 Location and orientation of the two sub-vertical fault zones encountered during excavation of the GBT, Switzerland, after Ferrari (2006).

1.3.6 Moutier Tunnel (Switzerland)

The Moutier Tunnel is situated on the Motorway A16 (Transjurane) in the Canton of Bern (Switzerland). During the excavation of this tunnel several disturbed zones, generally constituted of strongly tectonised and partially weathered molasses layers, in some cases water bearing, were crossed (Koenig et al., 2006). In particular, one of these zones was encountered after less than 200 m of TBM excavation causing a cave-in at face and subsidence at surface. The shielded TBM was blocked for several months after that the immediate measures adopted for consolidating the ground proved to be useless for the restarting of the machine. The excavation of the top heading of the tunnel was then conducted with conventional method from the opposite site until reaching the TBM that was finally used only for excavating the tunnel bench and invert (Figure 1.10) up to the northern portal, where the machine could be finally dismantled (Koenig et al., 2006).

Figure 1.10 Moutier tunnel, Switzerland, the TBM cutterhead was exposed after a stop of more than two years (http://www.a16.ch).

1.4 Objectives and structure of the thesis

In the present chapter the major issues resulting from tunnelling in difficult ground conditions and the description of the main geotechnical problems encountered in famous case-histories have been introduced.

TBM performance prediction in adverse environments, has often roused researchers' interest, especially because of its great importance in the engineering practice (e.g. see what has been described in the previous section) from an economic point of view and for a purely scientific aspect regarding the interaction between machine and rock mass. However, in the past, a great amount of research has principally focused on the prediction of TBM performance in very hard rocks, where the main issues are the rock boreability and the abnormal cutters and buckets wear. This thesis analyses the reduction of the machine performance that can take place in highly fractured rocks and fault zones, with respect to an estimated good performance in favourable tunnelling conditions. The research was part of a project financed by ASTRA (Bundesamt für Strassen), the Swiss Federal Roads Authority, where the aim was mainly to provide some recommendations for TBM design and performance prediction in difficult ground conditions.

In particular, the main objectives of the thesis can be summarised as follows:

- Establishment of a TBM-performance database in both bad and good ground conditions, compiling data from several tunnel projects; evaluation of the effects of highly fractured and faulted rocks on the TBM penetration and advancement by means of statistical analyses.
- Choice of main parameters influencing TBM tunnelling in disturbed zones and development of a geomechanical classification system for highly fractured rocks and fault zones; numerical simulations characterising their different behaviour under the action of the cutting tool.
- Definition, for each "fault zone" class, of a reduction rate with respect to the best and the most frequent performances for selected TBM-performance/operational parameters.

- Probabilistic simulations of tunnel excavation (by the DAT) for evaluating the effects of degrading rock mass conditions on the final tunnel construction time and cost.

According to the objectives listed above and apart from this introduction, the thesis is structured in seven chapters. Chapter 2 and Chapter 3 compile two literatures reviews necessary to develop the main topics of the thesis, in particular:

– In Chapter 2 the most common TBM-performance prediction models is presented. These models are not representative of bad tunnelling conditions where it is generally suggested to use them with caution. The most common parameters used for evaluating the TBM performance in "ordinary" advancing conditions are finally pointed out.

– In Chapter 3 a brief description of the fault zone genesis and structure is introduced as well as a non-exhaustive review of the existing geological and geomechanical classifications systems for fault rocks.

In Chapter 4 a TBM-performance database is developed with data of several tunnel projects. The main goal is to investigate possible relationships between difficult rock mass conditions and TBM performance. The database is subdivided into two sections: the first one contains the tunnel characteristics, TBM specifications and TBM performance parameters; while the second one considers the geological-geotechnical parameters of the intact rock and rock mass. The compiled data are obtained directly from the field, laboratory tests and literature. Although the data quality varies from one project to another and nevertheless difficulties in gaining complete TBM and detailed geological information, enough data are collected in order to have an idea of the distribution of important parameters related to the boring process and the TBM advancement.

In Chapter 5 preliminary analyses are carried out with the aim to identify correlations between TBM-performance parameters and rock mass parameters generally used in common TBM performance prediction models, such as rock strength and fracturing degree. In order to take into account the tectonisation and the weathering degree of the rock materials, a new rock mass strength parameter (called UCS_H) is considered. Finally, with the aim to introduce a more global approach for characterising rock mass behaviour, possible correlations between rock mass classification systems (RMR) and machine performances are also investigated.

In Chapter 6 a new classification system of highly fractured rocks and fault zones is developed and described. In order to identify the specific classes, several geological/geotechnical parameters are taken into account (in particular the fracturing degree of the rock mass and the weathering degree of the rock and of the joint surfaces). The choice of specific parameters is done mainly referring to the literature review presented in Chapter 2. In order to improve the geomechanical characterisation of the classes, numerical discontinuum and continuum models are developed trying to establish the main failure mechanisms and the chipping process, for each fault zone class, induced by a TBM cutter.

In Chapter 7, after the evaluation of the best (and the most frequent) TBM performance recorded during excavation in good tunnelling conditions, the comparison with the behaviour of the machine in faulted and highly fractured rock masses is carried out. For each "fault zone"

class a reduction rate with respect to the best and the most frequent performance is defined for the most important TBM-performance parameters.

In Chapter 8 the "Decision Aids for Tunnelling" (DAT) is used to carry out probabilistic analyses of tunnel construction time and costs. For assessing the effects that demanding ground conditions, such as fault zones, may have on tunnelling operations, the tunnel construction is simulated by introducing several geological profiles characterised by changing ground rock mass conditions as described by the "fault zone" classification system developed in Chapter 6. The advance rate reductions defined for each class in Chapter 7 are also used as input for the simulations. A real case is then simulated in order to validate the results previously obtained.

In the last part the final conclusions achieved in this work are summarised and potential developments and improvements are introduced.

Chapter 2 TBM-performance prediction

Because of generally higher advancement rates and better safety conditions with respect to conventional methods, TBMs are widely used nowadays for the excavation of long tunnels in a variety of ground conditions. For construction planning and for the selection of the most suitable excavation technology, the estimation of the TBM performance, in terms of rate of penetration, utilization factor, daily advancement, etc., has become a primary topic in rock mechanics and tunnelling engineering.

During the last decades a number of models have been developed for the prior-to-construction prediction of the TBM performance. In this chapter a brief review of some of these models is presented.

2.1 TBM performance prediction models

TBM performance prediction models may be divided in two main categories: the empirical models, which represent the largest group, and the theoretical or semi-theoretical models.

The empirical models are mainly based on back-analyses of machine performances of past tunnelling experiences. They are obtained through regression analyses by considering both rock mass parameters (e.g. rock strength, rock fracturing, joint orientation, etc.) and TBM parameters (e.g. rate of penetration, cutter force, advance rate, etc). These methods are quite interesting since they combine and consider ground and excavation “as a whole system”. This actually means that all the effects of ground conditions, rock properties, machine parameters and operational and logistic constraints are directly or indirectly taken into account (Rostami et al., 1996). Among these empirical models, the one developed at the Norwegian Institute of Technology (NTNU) (Bruland, 1998; Bruland et al., 1995; Bruland and Nilsen, 1995; Palmström, 1995) is certainly the most widely used.

The theoretical and semi-theoretical (or mechanical) models can combine theoretical bases and some empirical relations. With respect to the machine design parameters, they are more flexible than empirical methods. They generally analyse the forces acting on the cutters or the specific energy required to excavate a unit volume of rock and relate them to the intact rock and rock mass properties, as well as to the machine specifications. Within this category, the most famous

is the model developed by the Colorado School of Mines (CSM) (Nilsen and Ozdemir, 1993; Rostami, 1997; Rostami and Ozdemir, 1993; Rostami et al., 1996) which estimates the advance rate from relationships that combine thrust, torque and penetration, with the aim to improve the TBM cutterhead design.

In addition to these models it is important to mention the expanded rock mass classification systems, such as the Q_{TBM} (Barton, 2000) and the Rock Mass Excavability (RME) Indicator (Bieniawski et al., 2006; Bieniawski et al., 2007a; Bieniawski et al., 2007b; Bieniawski et al., 2008). They have been specifically developed for predictive purposes as well as for selecting the most suitable TBM to be used during the planning phase of a tunnel project. Moreover, several authors (e.g. Büchi, 1984; Gong and Zhao, 2009; Hassanpour et al., 2011; Sapigni et al., 2002) tried to estimate the boreability of the rock mass by introducing empirical equations mainly based on relationships among intact rock and rock mass parameters like strength, brittleness, RQD, joint spacing and orientation.

As suggested by Gong and Zhao (2009), another possible classification of TBM performance prediction models can be done according to the number of geological and geotechnical parameters required as input (i.e. single factor models and multiple factor models).

Table 2.1 summarises some of the most referred performance prediction models as well as their main input parameters in terms of both rock mass and machine factors. Furthermore, the following sections present a brief description of the most well-known and widespread models, trying to focus on the limits encountered in their application in disturbed rocks (e.g. highly fractured and fault zones).

2.1.1 The NTNU model

The NTNU prediction model (Bruland, 1998; Bruland et al., 1995; Bruland and Nilsen, 1995; Palmstrom, 1995) is an empirical model primarily based on correlations between geological/geomechanical parameters and actual TBM performance (see also Annex A). For developing this method, time and cost curves for the various tunnelling operations have been established by collecting and analysing a large amount of information on machine parameters and rock mass properties, coming from several tunnels in Europe. The model has been constantly upgraded and improved with data from new projects whenever available. The 1998 version is based on data from about 230 km of bored tunnels (Bruland, 1998).

The NTNU model is based on two main groups of data: the main rock mass parameters, and the main TBM factors (Table 2.1). As represented in Figure 2.1, the methodology used in this model can be described as follows:

- The rock mass parameters are combined into one factor that represents rock boreability, called “the equivalent fracturing factor” or “the equivalent TBM jointing factor”, k_{eq}.
- The machine parameters are combined into one machine (or cutterhead) factor called “the equivalent thrust per cutter”, M_{eq}.

These two parameters are then used to estimate the net rate of TBM penetration i_0.

Table 2.1 Summary of existing and most common TBM performance prediction models and expanded classification systems and main input parameters

Reference	Prediction value	Rock mass factors	Machine factors
Tarkoy, 1974	Penetration rate [ft/hr]	Total hardness	*
Graham, 1976	Penetration rate [m/hr]	Uniaxial compressive strength (UCS)	Cutter force
Wanner and Aeberli, 1979	Penetration (intact rock) [mm/rev] Specific penetration rate (jointed rock) [mm/MN]	UCS, tensile strength (σ_t), joint characteristics	Cutter spacing, tip width, and radius, cutter force, TBM diameter, RPM
Robbins, 1980	Penetration rate [in/rev]	UCS	*
Büchi, 1984	Penetration rate [m/hr] Advance rate [m/hr]	UCS, tensile strength, correction factors (depending on rock type, anisotropy/schistosity, fracture spacing, mica volume %)	Cutter spacing, cutter tip width, cutter radius, cutter force, TBM diameter, RPM
Hughes, 1986	Penetration rate [m/hr]	UCS	Cutter force, cutter diameter
CSM (Rostami and Ozdemir, 1993)	Penetration rate [m/hr] Advance rate [m/hr] Some TBM parameters	UCS, σ_t	Cutter spacing, tip width and radius, cutter force, TBM diameter, RPM
Gehring, 1995	Penetration rate [mm/rev]	UCS and correction factors for joints, specific fracture energy, etc.	Cutter force F_n
Thuro and Spaun, 1996; Thuro and Plinninger, 1999	Specific penetration [mm/kN]	UCS, Young`s modulus, σ_t, destruction work	Destruction work
NTNU (Bruland, 1998)	Penetration rate [m/hr] Advance rate [m/hr]	UCS, drilling rate index (DRI), no. of joint sets, joint frequency and joint orientation, porosity	Cutter force, RPM, cutter spacing, cutter size and shape, installed power
Q_{TBM} (Barton, 2000)	Penetration rate [m/hr] Advance rate [m/hr]	RQD_0, J_n, J_r, J_a, J_w, SRF, rock mass strength, cutter life index (CLI), quartz content, induced biaxial stress at the face, porosity	Cutter force, TBM diameter
Sapigni et al. 2002	Penetration rate [m/hr] Specific penetration [mm/rev/kN] Utilization factor	RMR	*
RME (Bieniawski et al., 2006)	Penetration rate [m/hr] Advance rate [m/hr] Specific energy [KJ/m^3]	UCS, abrasiveness, rock mass jointing at the face, stand-up time, water flows.	Total cutterhead thrust, RPM and torque
Gong and Zhao, 2009	Boreability Index (BI) [kN/mm/rev]	UCS, volumetric joint count, brittleness index, angle between discontinuities and tunnel axis.	Cutter force
Hassanpour et al., 2011	Field Penetration Index (FPI) [kN/mm/rev]	UCS and RQD	Cutter force, RPM

*Based only on geomechanical parameters

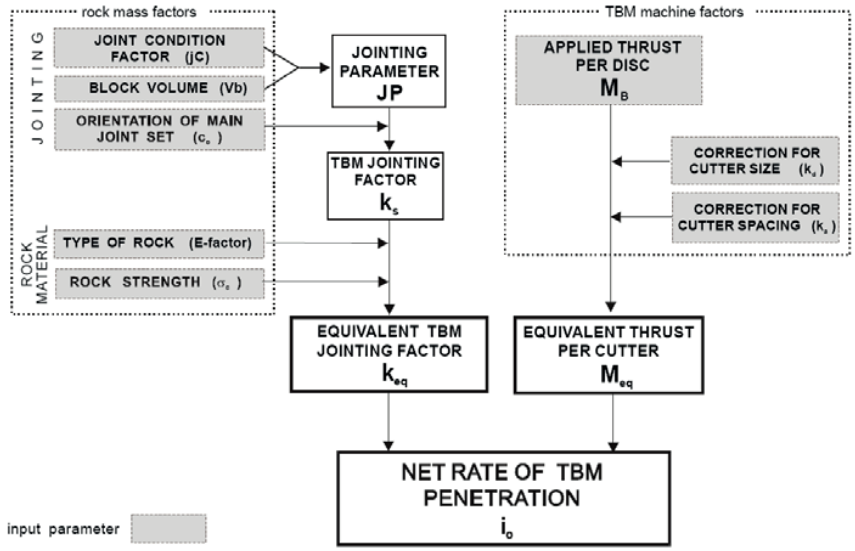

Figure 2.1 Layout of the NTNU methodology (Palmström, 1995).

One of the main advantages of the NTNU model is the generally comprehensive empirical database which allows taking into account the influence of the joints. In order to do that, NTNU has derived a set of relationships between the TBM penetration rate and the "fracturing factor", depending on discontinuity spacing and orientation with respect to the tunnel axis. Moreover, being an empirical model, it actually combines the effects of the ground and the excavation system in their entire complexity (Rostami et al., 1996). The main disadvantage of the model, as every empirical model, is that it should be applied very carefully to cases which differ significantly from those included in the original data-set.

2.1.2 The CSM model

The CSM model (Rostami, 1997; Rostami and Ozdemir, 1993) is a theoretical model which incorporates some empirical relations as well. In order to evaluate the overall thrust, torque and power requirement on the entire cutterhead, it considers the individual cutter forces (i.e. both normal and rolling forces, see also Table 2.1).

The basic assumptions of the model can be summarised as follows:

- The crushed zone beneath a disc cutter is circular (Figure 2.2).
- The size of the particles increases from the centre towards the rock media surrounding the crushed zone.
- The extension of the crushed zone is a function of cutter tip geometry and rock properties.
- The pressure distribution in the crushed zone is uniform.
- Tensile fracture initiation and propagation is assumed to be the predominant failure mode.

For an optimum cutter spacing, cracks are ideally propagated towards the neighbouring cuts through a straight line, which represents the shortest distance for crack propagation and is equal to half the cutter spacing (Figure 2.2).

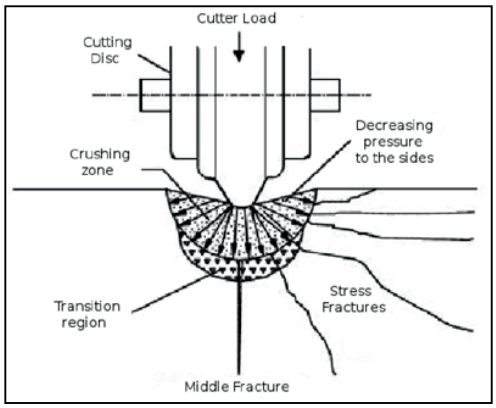

Figure 2.2 Crushed zone under a disc cutter (Rostami et al., 1996).

For calculating the real penetration rate, the model introduces an iterative procedure starting from a very low value of penetration rate. The machine thrust, torque and power are then computed according to a set of equations and compared to the machine specifications. If the computed values are below the machine specifications, the penetration rate needs to be increased and the procedure repeated. This iterative estimation ends when one of the machine requirements is met (i.e. exceeded).

It is important to observe that one of the main limitations of this model is that it predicts the penetration rate without any consideration given to the influence of existing joints/fissures in the rock mass. However, in order to take into account the joint effects, the model uses the correlation factors developed by the Norwegian Technical University (NTNU) as well as the so-called fracturing factor (see previous section). Further development in this framework has been carried out by Ramezanzadeh et al. (2005 and 2008).

2.1.3 The Büchi model

A critical review of the CSM model has been provided by Büchi (1984) who, in addition to a review of geological factors mostly affecting TBM performance and wear, provides an investigation of the effects of anisotropy (schistosity) and fracture spacing on the penetration rate (Table 2.1).

The proposed model correlates the cutter force, obtained in a full-scale linear cutting machine as in the Colorado School of Mines (CSM), with rock anisotropy and rock mass fracturing. The background data of this model come from about 38 km of tunnels excavated with TBMs. The study investigates the effect of the rock schistosity on the TBM penetration rate and concludes that a favourably oriented foliation (i.e. perpendicular to the tunnel axis) may significantly increase the TBM penetration rate.

2.1.4 The Q_{TBM} model

Barton (2000) extended the original Q-system for rock mass classification to a new Q_{TBM} system which allows predicting TBM penetration and advance rates (see also Annex A). The system accounts for average cutter force, abrasive nature of the rock, stress field at the tunnel depth and joints orientation and conditions (Table 2.1). The Q_{TBM} mainly depends on basic geological and geotechnical parameters which can be simply estimated by an experienced engineering geologist (Sapigni et al., 2002).

The main hypothesis of the method is based on the consideration that, both extremely good (Q up to 1000) and extremely bad conditions (Q down to 0.001) are unfavourable for the TBM advancement. In particular, in the first case a lower penetration rate can be observed due to increasing maintenance times for cutters replacements; in the second case the hindrance is represented by longer stops of the machine for allowing heavier support installation as well as rock consolidating treatments. Starting from these considerations, Barton identified general trends for the penetration rate (PR), for continuous boring process, and for the actual advance rate (AR), evaluated as functions of the rock mass quality (Figure 2.3).

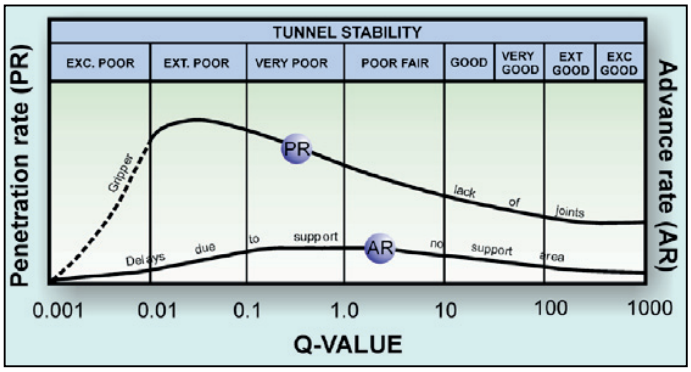

Figure 2.3 Conceptual relation between Q index, penetration rate (PR) and advance rate (AR) (Barton, 2000).

The Q_{TBM} is calculated by Equation 2.1, starting from the equation and the parameters used for estimating the original Q value:

$$Q_{TBM} = \frac{RQD_0}{J_n} \cdot \frac{J_r}{J_a} \cdot \frac{J_w}{SRF} \cdot \frac{SIGMA}{F^{10}/20^9} \cdot \frac{20}{CLI} \cdot \frac{q}{20} \cdot \frac{\sigma_\vartheta}{5} \qquad 2.1$$

where: RQD_0 is the Rock Quality Designation (RQD, %) interpreted in the tunnelling direction, J_n, J_r, J_a and J_w are the parameters used for describing the joints conditions, SRF is the Strength Reduction Factor, SIGMA refers to the rock mass strength, F is the average cutter load (tnf) through the same zone normalised by 20 tnf, CLI is the cutter life index, q is the quartz content (%) and σ_ϑ is the induced biaxial stress on tunnel face in the same zone normalised to a depth of 100 m.

The relationships between Q_{TBM} and TBM penetration rate (PR) and advance rate (AR) are reported below:

$$PR \approx 5Q_{TBM}^{-0.2} \quad 2.2$$

$$AR \approx 5Q_{TBM}^{-0.2} \cdot T^{m} \quad 2.3$$

where T is the time (in hours) and m is a negative gradient that expresses the decelerating average advance rate which is observed as the unit of time (hours, days, weeks, months) increases.

Although the Q_{TBM} can be applied to a wide range of rock mass conditions, the great number of parameters involved in the calculation strongly limits its utilisation in the practice.

2.1.5 The RME model

The RME indicator (Bieniawski et al., 2006; Bieniawski et al., 2007a; Bieniawski et al., 2007b; Bieniawski et al., 2008) estimates the performance of double-shield and open-type TBMs on the basis of statistical analyses of data from more than 500 tunnel case records. Similarly to the original RMR rock mass classification index, the RME is calculated using five input parameters specifically related with the ground TBM interaction: e.g. abrasion, joints spacing and orientation with respect to the tunnel alignment, stand-up time, uniaxial compressive strength of intact rock and water inflow at the tunnel (Table 2.1). With the same philosophy of the traditional RMR method, each parameter is associated to a specific rating according its value. The sum of them gives the value of the RME index.

This index is correlated with the average rate of advance ARA, computed as the ratio between the length of a given tunnel section and the total time needed to excavate that section. This correlation is based on a regression analysis performed on a dataset composed by data coming from three tunnels excavated by double shield machines (Figure 2.4).

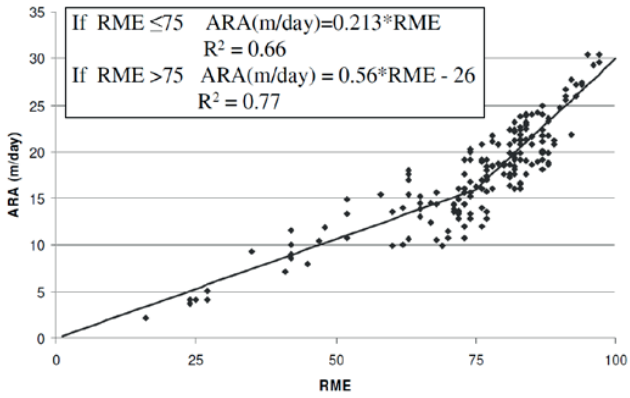

Figure 2.4 Correlation between ARA and RME (Bieniawski et al., 2006).

By using a dataset of 49 tunnel sections of the San Pedro tunnel (Spain), the performance of double shield and gripper TBMs could be compared, considering separately rock characterised by UCS < 45 MPa and UCS > 45 MPa (Figure 2.5 and Figure 2.6). This study allowed concluding that for less resistant rocks (i.e. UCS < 45 MPa), double shield TBMs always provide better results than open TBMs, while for more resistant rocks (i.e. UCS > 45 MPa), characterised also by higher values of RME (i.e. > 75), the use of gripper TBMs gives better

performances. For intermediate rock conditions (i.e. 65 < RME < 75), double shield and open TBMs provide quite similar results. Finally, for decreasing values of rock conditions (i.e. 50 < RME < 65), double shields generally had better advancements than open machines (Bieniawski et al., 2007a; 2007b).

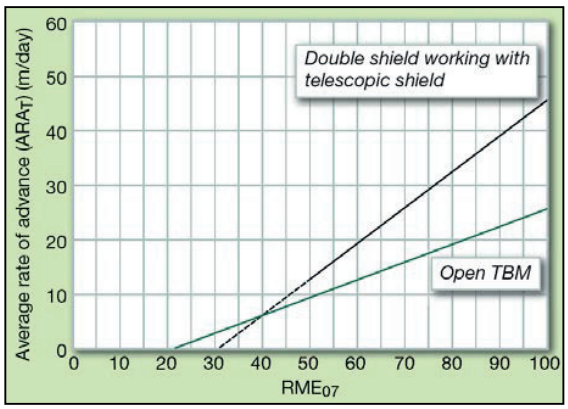

Figure 2.5 Comparison of the performance of double shield and open TBMs for UCS < 45 MPa (Bieniawski et al., 2007b).

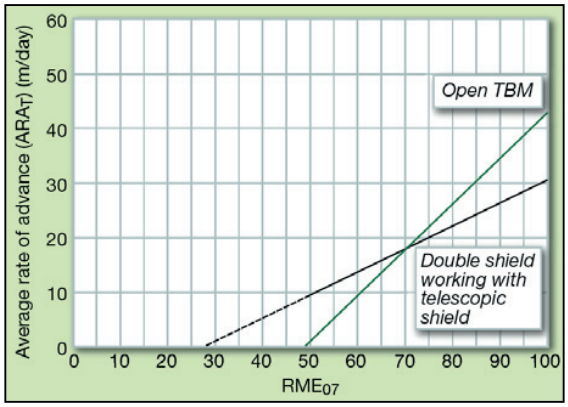

Figure 2.6 Comparison of the performance of double shield and open TBMs for UCS > 45 MPa (Bieniawski et al., 2007b).

2.1.6 Other recent studies on the TBM performance

More recent studies have been done by Hassanpour et al. (2011), Gong and Zhao (2009) and Sapigni et al. (2002), see also Table 2.1.

Hassanpour et al. (2011) proposed to evaluate the rock mass boreability starting from the rock strength and the rock mass fracturing degree. This empirical model is based on the analysis of data obtained from four tunnelling projects, covering total length of 55 km excavated in different geological conditions. Strong connections have been found between rock mass parameters such as uniaxial compressive strength, RQD and joint spacing, with the so-called Field Penetration Index (FPI) (Klein et al., 1995). Although the model is applicable in a quite wide range of geological conditions (like layered and jointed sedimentary rocks or blocky

rocks), it has to be adopted with extreme caution in highly fractured rock masses, fault zones and water sensitive rocks, since the results provided by the proposed correlation could be misleading.

Gong and Zhao (2009) focused their attention on the combination between a rock mass conceptual model, for evaluating rock mass boreability, and an established database developed during the construction of the DTSS project (Deep Tunnel Sewer-age System) in Singapore. By analysing the rock fragmentation mechanism, the theoretical model identifies the influence of rock mass properties on TBM penetration rate, showing that the rock uniaxial compressive strength and the volumetric joint count seem to have the most relevant effect. However, the model presents some limitations and attention must be paid for predicting the TBM performance in other critical tunnelling conditions.

Sapigni et al. (2002) analysed possible relationships between the machine performance (i.e. penetration rate of the machine) and the geological/geotechnical characteristics of the rock mass, expressed in terms of value of Rock Mass Rating (RMR) (Figure 2.7).

a) b)

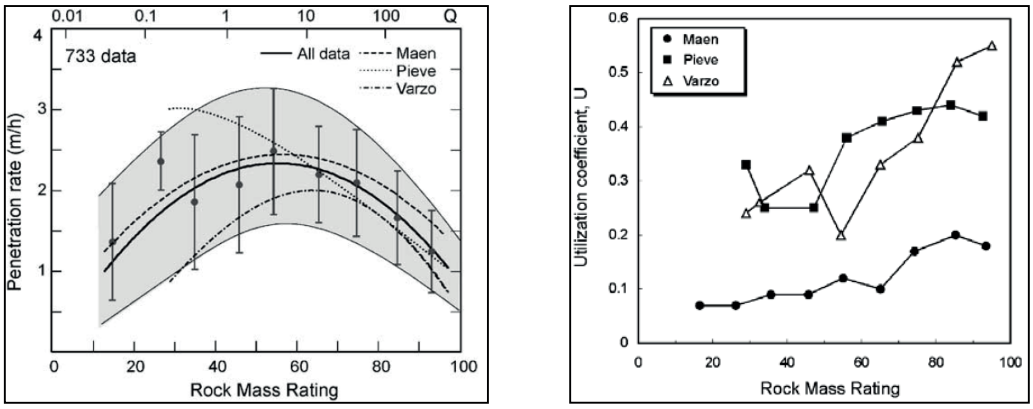

Figure 2.7 a) Correlation between the rate of penetration of the TBM and Rock Mass Rating; b) Correlation between TBM utilization factor derived from daily average data and RMR (Sapigni et al., 2002).

The empirical correlation, shown in Figure 2.7a, seems to follow a bell-shaped curve, with the maximum TBM performance reached for rock masses of medium quality (i.e. RMR = 40 ÷ 60). The penetration rate of the TBM decreases more or less in the same way for very poor or very hard rock masses. This result, especially for what concerns adverse ground conditions, is described as a possible consequence of mucking problems, as well as face instabilities that limit the potentially high penetration rate as a consequence of thrust reduction (Sapigni et al., 2002). The authors also provide a relationship between the TBM utilisation factor, defined as the fraction of total construction time in which the TBM has been used for boring, and RMR. Figure 2.7b shows that even in favourable conditions (i.e. RMR > 70-80) U is less than 0.5 and that those values strongly decrease (i.e. up to 0.05-0.1) for poor rock mass conditions (i.e. RMR ~ 20-30).

Finally, in the literature, it is also possible to find other examples of rating system formulations used for estimating the utilisation factor of the TBM (Bilgin et al., 1999a; Bilgin et al., 1999b; Bilgin et al., 1993), where an important role is played by the operator experience (especially in the thrust force control). However, it is important to underline that, as reported by Einstein (1996), the exact prediction of the TBM performance can be practically impossible. As a matter of fact, the definition of the utilisation factor is based on a combination of parameters which are not only related to the rock mass conditions and/or to the machine factors. A very important role is indeed played by non-quantifiable factors such as the skills of the tunnel crew, the variable performance of the equipment as well as accidents/breakages occurring at various intervals during construction.

2.2 Most common rock mass parameters in TBM-performance prediction

The most common TBM performance prediction models presented in this chapter have been compared with the aim to identify the most used geological-geotechnical parameters and in which frequency they are adopted as rock mass input. Figure 2.8 shows the results of this analysis.

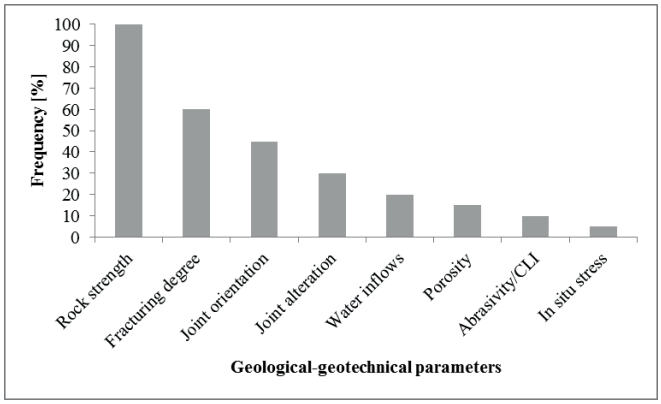

Figure 2.8 Geological-geotechnical parameters generally evaluated for TBM-performance prediction. The frequency refers to a sample of 20 existing prediction models.

As it is possible to observe, the most common parameters involved in the TBM performance prediction, are the strength of the rock (i.e. present in 100% of the models considered as sample for this analysis) and the degree of fracturing (i.e. present in 60% of the models). The term "rock strength" here refers to closely related parameters such as uniaxial compressive strength, brittleness as well as rock hardness. Also, "fracturing degree" refers to several factors (joint spacing, RQD and the volumetric joint count J_v) representative of the same information. The other rock mass characteristics highlighted by this analysis are related to the joint orientation and alteration, the potential water inflows, the porosity of the rock, the abrasion/quartz content as well as the cutter life index and the in situ stress. Apart from the joints quality parameters (orientation and alteration), which are used in about 30-40% of the models, the other parameters are employed in less than 20% of the cases.

Thus, based on these results and considerations, uniaxial compressive strength (UCS) and volumetric joint count (J_v) have been considered in this framework (i.e. see Chapter 5) as the two main representative parameters for evaluating the TBM performance.

2.3 Final remarks

By compiling some of the most relevant TBM performance prediction models it has been possible to identify the most relevant rock/rock mass and TBM parameters commonly included in the TBM performance prediction/estimation models.

Among the geological/geotechnical factors, on one side, the existing models mainly focus on parameters related to the rock mass fracturing (expressed via RQD, volumetric joint count, joint spacing and orientation, etc.) as well as on rock strength (expressed via uniaxial compressive strength (UCS), drilling rate index (DRI), tensile strength, etc.).

However, the majority of the reviewed models have been developed for "ordinary" tunnelling situations and their application to difficult ground conditions may lead to misleading results. As a matter of facts, the existing models seem to be strongly limited for applications to highly fractured and faulted zones. This can be due both to a lack of information (the majority of the existing models are based on empirical studies) and to a more difficult characterisation of such weak rocks.

Chapter 3 Characterisation of fault zone and fault rocks: genetic and structural relationship, geomechanical implications

As already discussed, a fault zone is one of the greatest challenges to face during underground construction works. For this reason a proper understanding of its genesis and a thorough assessment of its internal structure are prerequisites for the development of a reliable geological model that helps better predict the geomechanical behaviour of the fault rocks. In this way, a number of geotechnical problems during the construction process could be efficiently anticipated.

Fault rocks are extremely complex and heterogeneous by nature, due to a combined contribution of weak and strong rock components that can vary significantly inside a same fault zone. For this reason, the geotechnical characterisation of the fault rocks, that will often be referred to as either "soil-like" or "rock-like" materials, presents difficult tasks in rock engineering and rock mechanics. The mechanical behaviour of fault rocks is also very sensitive on the water content and fault zones are generally sites of sustained water circulation and/or accumulation, meaning additional risks for engineers that have to be properly taken into account.

In this chapter a review about the genetic and structural relationship of fault zones is reported, in reference to a number of existing geological and geomechanical classifications developed for fault rocks.

3.1 Fault zone definition

In rock engineering, a "fault zone" commonly refers to a localized weakness in the Earth's crust, formed mostly under brittle conditions, and susceptible to accommodate various amount of shear (Figure 3.1).

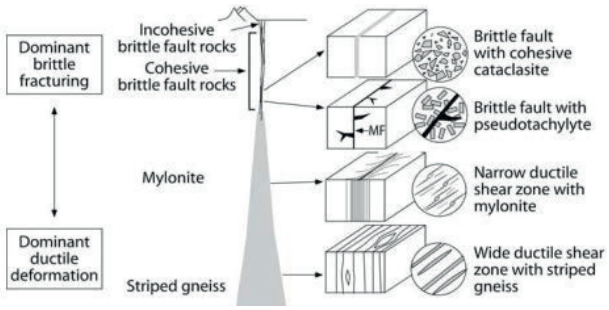

Figure 3.1 Conceptual model showing the distribution of shear zones with depth (Passchier and Trouw, 1996).

Shear zones are usually much longer than thicker and the resulted fault rocks will depict typical structural elements that are directly related to the amount of strain that has been accommodated. There is a spatial gradient in the amount of strain that is generally highest within the centre of the shear zone, decreasing outward into its adjacent rocks (Loew et al., 2010), meaning also a gradient in the resulting structural relationships.

The response of the rock to the shear rate to which it has been subjected, depends on pressure and temperature conditions and determines how the rock accommodates the deformation. The mechanism of shearing can occur at brittle, ductile or intermediate conditions, identifying, according to several authors, four main types of shear zones (Sibson, 1977; Ramsay and Huber, 1987; Davis and Reynolds, 1996; Loew et al., 2010):

- brittle shear zones ("fault zones" in this research), that contain products of brittle deformation mechanisms (cataclasis), considering the potential subsequent weathering or cementation by migrating fluid (Riedmüller et al., 2001) promoted by the high permeability of the fractured material;
- ductile shear zones, where the deformation processes are mainly achieved by crystal plasticity, involving a minor amount of fracturing;
- semi-brittle shear zones, that involve mechanisms such as cataclastic flow and pressure solution;
- brittle-ductile shear zones, that show evidence of both brittle and ductile deformation.

The ductile (and semi-brittle) shear zones do not generate instability problems in underground construction (Loew et al., 2010), whereas the most problematic type for rock engineering purposes are brittle and plastic shear zones and their related type of fault rocks, referred to as cataclasite (Christe, 2009).

Cataclastic rocks result from both a mechanical and chemical weathering related to tectonic activity. This particular degradation process (cataclasis) is friction and time dependent and involves high deformation by brittle fracturing, grinding, crushing and rotation of rock components. On one hand, mechanical processes inherent to cataclasis will be responsible for a high degree of fracturing at different scales by stress and strain localisation. The Mohr-Coulomb diagram in Figure 3.2 details the general process of cataclastic fracturing. On the other hand,

chemical processes will further impact on rock quality by progressive weathering of the primary rock mineralogy leading to the development of secondary mineral phases (phyllosilicates, clay minerals). The rate at which weathering occurs will moreover be controlled by the fluid-rock interaction.

Such rocks will therefore show a vast panel of mechanical properties ranging from hard rock to soil-like material behaviour. In reference to the respective ratio of gouge matrix to rock blocks, fault rocks will be more or less cohesive. The degree of this "cohesion" can be further influenced by the sizes, shapes and strengths of the blocks (see Medley (1994), who defined as "bimrocks" the block-in-matrix rocks characteristic of fault rocks). This is the reason why fault rocks inherited from brittle processes are often characterised by generally low mechanical strength with a high deformability involving non-linear constitutive laws, a strong strength dependence on water saturation and temperature, and a great susceptibility to weathering.

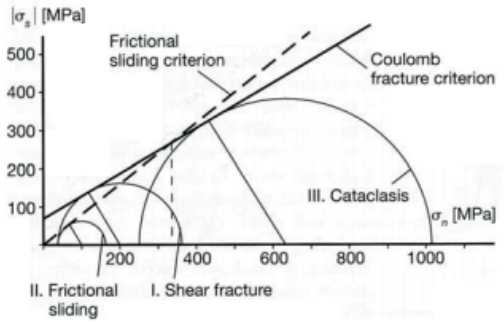

Figure 3.2 Representation on a normal vs. tangential stress diagram of Coulomb fracture criterion and frictional sliding criterion for sliding on a pre-existing fracture. Cataclasis occurs in a regime where continuous fracturing becomes the energetically most favourable deformation mode, while movements along pre-existing discontinuities, governed by a frictional sliding criterion, are made impossible. Mohr circle I: critical stress conditions for shear fracture. Mohr circle II: frictional sliding on a fracture plane at the same confining pressure. Mohr circle III: critical stress conditions for cataclasis process (Christe, 2009).

Structurally speaking, a common model used to describe brittle fault zones involves three different structural elements:

1. the fault core;
2. the damage zone;
3. the protolith (e.g. host/country/parent rock).

A conceptual model of the fault zone architecture is illustrated in Figure 3.3. Each of these elements is shortly summarized hereafter and a view of a small fault zone is reported in Figure 3.4.

The **fault core** (characterised by the occurrence of fault rocks) is a "structural, lithologic and morphologic part of a fault zone where most of the deformation is accommodated" (Caine et al., 1996). It consists of low permeability fault rocks, characterised by a high amount of fine-grained rock matrix in comparison to clasts (Christe, 2009). According to Brosch et al. (2006), the most important parameters within the fault core are the cohesiveness (cementation)

regarding the behaviour with access of water, the grain size distribution and matrix material, the proportion of rock fragments in the matrix, the clay mineral content/composition (and the vulnerability to water) and the (residual) shear strength of the matrix.

The **damage zone** bounds the fault core and is characterised by subsidiary structures such as small faults, veins, fractures and fold, causing heterogeneity and anisotropy in fault zone permeability that is controlled by the hydraulic properties of the fracture network (Bruhn et al., 1994; Caine et al., 1996). The damage zone will be greatly responsible for the permeability of the fault zone as shown in Figure 3.5. The fluid flow within and near the fault zone is controlled by the distribution of each component (Caine et al., 1996).

Finally, the **protolith** surrounds the fault core and damages zone. The protolith can be virtually any type of petrology of sedimentary, magmatic or metamorphic origin and it is referred to as the country, parent or host rock. Its mechanical properties and fluid flow properties are generally well known and reflect the unfaulted host rock (Caine et al., 1996).

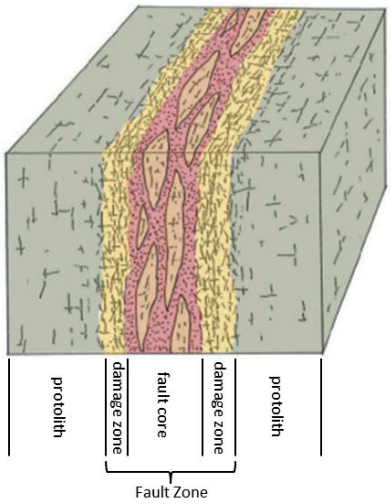

Figure 3.3 Conceptual model of internal fault zone architecture in the host rock (protolith), after Fasching and Vanek (2011).

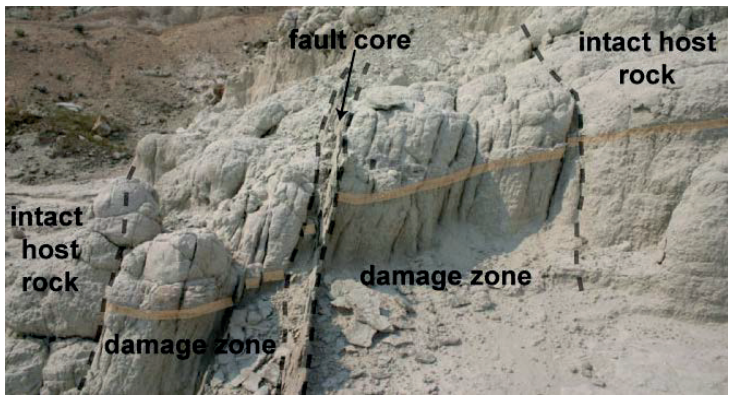

Figure 3.4 View of a small fault in the Brule Formation strata of Slim Buttes, South Dakota, with the fault core and damage zones labelled, after Maher (2014).

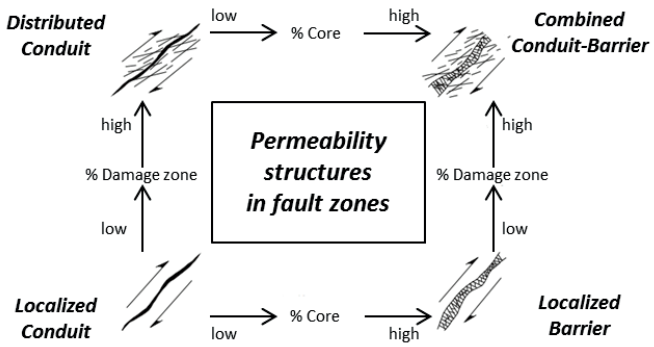

Figure 3.5 Conceptual scheme for fault-related fluid flow. Permeability loss due to grain-size reduction and/or mineral precipitation (filling open pore spaces) is responsible for fault cores acting eventually as barriers to fluid flow (Caine et al., 1996).

Brosch et al. (2006) report that fault zones might not fully develop, resulting in an apparent lack of a fault core. In rock engineering, fault zones with these "damage zone only" or "intensified fracturing" characteristics have however to be considered in the same way as fully developed fault zones since they also cause distinct deterioration to the rock mass and permeability increase.

3.2 Terminology and geological classifications of fault rocks

Several geological classifications of fault rocks have been proposed in the literature (e.g. Higgins, 1971; Sibson, 1977; White, 1982; Wise et al., 1984; Zhang et al., 1986; Riedmüller et al., 2001). They are generally based on parameters such as fabric, texture and clasts size or they take into account the cohesive/non-cohesive character of materials.

In a conventional geological engineering terminology, fault rocks can be classified as follows (Table 3.1):

- fault breccia, it consists of large fragments of rock in a fine-grained matrix that could include mineral veins formed in voids between the clasts. It may have a non-cohesion (with visible fragments > 30%) or a cohesion character. In the cohesive (and cemented) fault breccia the proportion of matrix is less than 10% and, based on the fragments dimension, it is possible to define crush breccia (> 0,5 cm), fine crush breccia (> 0,1 cm and < 0,5 cm), crush microbreccia (< 0,1 cm);
- fault gouge, a non-cohesive clay-rich and fine-to-ultrafine-grained material (with visible fragments < 30%) that may possess a schistosity. Geologists and engineers sometimes refer to it as "kakirite" (Figure 3.6) to define a type of material that will readily collapse once extracted or excavated;
- cataclasite, normally cohesive and non-foliated, consisting of angular clasts in finer-grained matrix (Figure 3.7). It may be subdivided according to the relative proportion of finer-grained matrix into protocataclasite (10-50%), mesocataclasite (50-90%) and ultracataclasite (90-100%);

- pseudotachylite, a cohesive and ultrafine-grained rock, is a vitreous-looking material and dark in colour. It is generally found along a fault surface or as thin planar veins injected into the fractures in the host rock. Pseudotachylite normally forms during earthquake events (ultra-fast movement along the slip plane during instantaneous relief of strain).
- mylonite, a fine-grained cohesive rock looking somehow similar to a gneiss with at least microscopic foliation (Wise et al., 1984), formed by ductile processes occurring at depth, below the brittle shear zones (ductile shear zones involving already greenschist metamorphic facies condition, see Figure 3.1).

Table 3.1 Textural classification of fault rocks, after Sibson (1977). The terminology adopted in this table (especially "fault breccia" and "fault gouge") is frequently assumed in engineering geology for describing the most problematic and arduous zones encountered in tunnelling

<table>
<tr><td></td><td colspan="3">RANDOM-FABRIC</td><td colspan="4">FOLIATED</td></tr>
<tr><td rowspan="2">INCOHESIVE</td><td colspan="3">FAULT BRECCIA
(visible fragments > 30% of rock mass)</td><td colspan="4">?</td></tr>
<tr><td colspan="3">FAULT GOUGE
(visible fragments < 30% of rock mass)</td><td colspan="4">?</td></tr>
<tr><td rowspan="5">COHESIVE</td><td>Glass/devitrified glass</td><td colspan="2">PSEUDOTACHYLYTE</td><td colspan="4">?</td></tr>
<tr><td rowspan="4">NATURE OF MATRIX
Tectonic reduction in grain size dominates grain growth by recrystallization and neomineralization</td><td colspan="3">CRUSH BRECCIA (fragments >0.5 cm)
FINE CRUSH BRECCIA (0.1 cm< frag.s <0.5 cm)
FINE MICROBRECCIA (fragments <0.1 cm)</td><td>0 - 10 %</td><td rowspan="4">PROPORTION OF MATRIX</td></tr>
<tr><td>PROTOCATACLASITE</td><td rowspan="3">CATACLASITE SERIES</td><td colspan="2">PROTOMYLONITE</td><td rowspan="3">MYLONITE SERIES</td><td>10 – 50 %</td></tr>
<tr><td>CATACLASITE</td><td rowspan="2">PHYLLONITE VARIETIES</td><td>MYLONITE</td><td>50 – 90 %</td></tr>
<tr><td>ULTRACATACLASITE</td><td>ULTRAMYLONITE</td><td>90 – 100 %</td></tr>
<tr><td>Grain growth pronounced</td><td colspan="2">?</td><td colspan="4">BLASTOMYLONITE</td></tr>
</table>

Figure 3.6 Drill core photo, example of non-cohesive fault rock (kakirite), after Fasching and Vanek, (2011).

Figure 3.7 Drill core photo, example of cohesive fault rock depicting blocks of various dimensions (cataclasite), after Fasching and Vanek (2011).

For specific civil engineering applications, where it is important to derive precise geomechanical information from geological/structural observations, a characterisation of the fault zones based on additional parameters such as the degree of cementation/consolidation, the water susceptibility and the permeability, the mass homogeneity and its isotropy/anisotropy, the rock strength and the properties of the discontinuities is however recommended (Fasching and Vanek 2011).

The following section will focus on the geomechanical aspects of fault rocks. Some of the most important contributions in this field will be summarized in order to highlight the main conclusions and outcomes. This will represent the starting point for the development of a fault zone classification to be related to the tunnelling performance.

3.3 Geomechanical characteristics of fault material: weak and weathered rocks

For geomechanical studies, the characterisation of particularly weak fault rocks (highly crushed and weathered rocks) proves to be very difficult because of the extreme complex structure and heterogeneous nature of the material which is the result of combined contributions of weak and

strong rock components (Figure 3.8). Moreover, the flow pattern of water through the rock mass must be assessed properly.

Geomechanical and hydrological properties of fault rocks can therefore be defined by rheology of host rocks, petrography and age of fault activity (Sausgruber and Bradner, 2003):

- brittlely deformed incompetent host rocks, such as phyllite, marl and shale, form zones (also known as cohesive kakirites or fault gouge) with soil-like features, characterised by a low compressive strength, low values of Young's modulus and a high squeezing potential. From the hydrological point of view they are characterised by a low permeability which hinders the flow of cementing solutions, as already mentioned before. For this reason the older fault rocks do not show a very high grade of cementation and the properties do not change significantly compared to younger fault zones;
- brittlely deformed competent host rocks, such as granite, massive carbonate and quartzite, form nearly non-cohesive zones (cohesionless kakirites), extremely permeable, with a high potential of water circulation. The older fault rocks (cataclasite) show a higher rate of cementation due to high permeability, and geomechanically, they have a quality similar to that of intact rocks (high compressive strength and high values of Young's modulus).

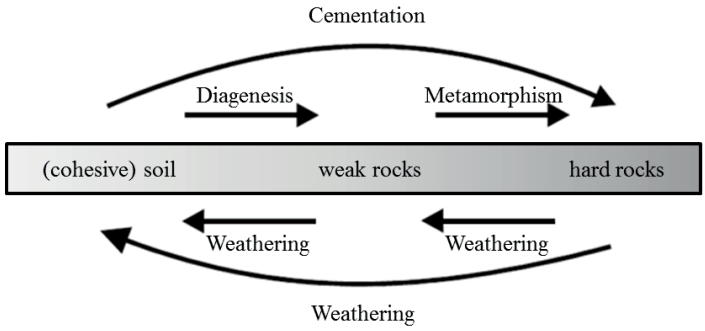

Figure 3.8 Position of weak rocks between cohesive soil and hard rocks, after Nickmann et al. (2006).

In order to better describe weak and weathered rocks, several classifications have been developed (e.g. Little, 1969; Lee and De Freitas, 1989; Thuro and Scholz, 2003; Santi, 1995; Santi, 2006). Most of these systems were created for granitic materials and some of them have then been improved in order to be applicable to a wider range of rocks.

For the purposes of this research, in order to describe fault rocks as weak rocks, a summary of geological and geotechnical properties has been reported in Table 3.2. It is mainly based on a technical literature review compiled by Santi (2006) and integrated by information collected by other authors (Hoek et al., 1998; Marinos and Hoek, 2001; Thuro and Scholz, 2003; Marinos et al., 2007).

Table 3.2 Summary of engineering properties of weak rocks, after Santi (2006)

Property	Value or range for weak rocks	Reference
Compressive strength UCS [MPa]	1-40	Afrouz, 1992; Santi, 2006; Thuro and Scholz, 2003
Rock quality designation RQD [%]	< 25-75	Santi and Doyle, 1997; Santi, 2006
Ratio between weathered matrix and unweathered blocks	> 75 % matrix	Geological Society Engineering Group Working Party, 1995
Natural moisture content	> 1 % for igneous and metamorphic rocks; > 5-15 % for clayey rocks	Santi and Doyle, 1997
Dearman weathering classification	≥ category IV (50%-100% of the rock is decomposed and/or disintegrated to a soil; the original mass structure and material fabric can be destroyed)	Santi, 1995; Dearman, 1976
Friction angle φ [◦] (Weathered granites)	Highly/completely weathered: 10-30	Thuro and Scholz, 2003
	Residual soil: 30-40	
Cohesion c [kPa] (Weathered granites)	Highly/completely weathered: 50-10	Thuro and Scholz, 2003
	Residual soil: 15-35	
RMR (Bieniawski, 1976)	< 35-60	Santi, 1995
Norwegian Geotechnical Institute "Q" rating	< 2	Santi, 1995
Extended GSI	< 30	Hoek et al., 1998; Marinos and Hoek, 2001; Marinos et al., 2007

It must be stressed that characterising fault rock properties (e.g. uniaxial compressive strength) can be a tough task mainly due to the difficult preparation of regularly shaped and smooth specimens. To solve this issue and in order to provide proper predictive models for geomechanical properties of weak rocks, many authors proposed adequate methodologies that have been successfully applied to a variety of geologically complex geo-materials such as melanges, sheared serpentinites, coarse pyroclastic and fault rocks (e.g. Chester and Logan, 1986; Medley, 1994, 2001 and 2002; Lindquist and Goodman, 1994; Medley and Goodman, 1994; Bürgi, 1999; Ehrbar and Pfenniger, 1999; Goodman and Ahlgren, 2000; Habimana et al. 2002; Laws et al., 2003; Sonmez et al., 2004 and 2006; Kahraman and Alber, 2006 and 2008; Kahraman et al., 2008; Christe, 2009; Coli et al., 2011). The main aspects and conclusions of the works of some of the authors cited above are summarized in Table 3.3.

Table 3.3 Geomechanical characterisation of fault rocks: non-exhaustive review of results provided by authors studied in this research

References	Tested type of fault rocks	Main research/Methodology	Main results and/or comments
Chester and Logan, 1986	*Brittle Punchbowl fault zone*: sandstone samples containing single and/or multiple subsidiary faults (representative of the damaged zone) or consisting of **fault gouge** material	Field investigations of fault zone structure and laboratory tests for the determination of e.g. strength and deformability parameters, relative ductility, etc. of fault rocks	Gradual reduction in strength and elastic modulus and increase in ductile rock behaviour with increasing fracture density and clay content Permeability contrast between damaged zone (high) to fault gouge (low)
Madley 1994, 2001 and 2002; Madley and Goodman, 1994; Madley and Lindquist, 1995	Heterogeneous rocks characterised by a mixture of strong blocks within a bonded weaker matrix of finer (block-in-matrix rocks)	Characterisation of melanges (complex mixture) and similar block-in-matrix rocks and estimation of block volumetric proportion (*VBP*=total volume of the blocks/total volume of the mass)	Introduction of the term "**bimrock**" for melanges and mixture (e.g. breccias, weathered rocks with corestone, tectonically fragmented rocks) characterised by: • Significant strength contrast between block and matrix ($\tan\varphi_{block}/\tan\varphi_{matrix} \geq 2$) • $25\% \leq VBP \leq 75\%$ • Block size varies between 5% and 75% of the characteristic engineering dimension (e.g. tunnel diameter, specimen) If blocks size < 5% of characteristic dimension, blocks are assumed as matrix with negligible effect on rock strength
Lindquist and Goodman, 1994; Lindquist, 1994	Physical model of melange made up of stronger blocks in a weaker matrix (melange **bimrock**)	Study of the potential effect on strength and deformability properties of *VBP* and block orientation (by uniaxial compressive tests)	*VBP* increases → cohesion (c) decreases elastic modulus (E) increases $25\% < VBP < 75\%$ → φ increases with *VBP* $VBP > 75\%$ → Uniform φ $VBP < 25\%$ → The rock strength "reflects" the matrix strength
Burgi, 1999; Burgi et al., 2001; Christe, 2009	Cataclastic fault rocks: quartzite, quartzo-phyllite, carbonatic breccia (**kakirites**), carbonatic cataclasite	Definition of possible correlations between structural, mineralogical and geomechanical properties of fault rocks (by macro- and microscopic scale analyses) and study of hydrogeological aspects of fault zone	Quantitative characterisation based on a clast-matrix model → geomechanical behaviour as function of rock fabric and mineralogical composition Geomechanical properties (MSI) = f [$mwVh$(TC+MC)] – *MSI*=Mineralogical and Structural Index – *mwVh*=mean weighted Vickers hardness → quantifies mineralogy – *TC*=texture coefficient (arrangement of clasts) → quantifies rock fabric – *MC*=matrix coefficient (matrix/discontinuity conditions) → quantifies rock fabric

Table 3.3 continued

References	Tested fault rock	Main research/Methodology	Main results and/or comments
Habimana, 1999; Habimana et al., 2002	Cataclastic fault rocks: quartzitic sandstone and phyllitic schists characterised by different degree of folding, faulting and fracturing	Geomechanical characterisation of fault rocks (by uniaxial and triaxial compressive tests; shear tests; traction tests; creep tests) and definition of a corresponding failure criterion	The proposed failure criterion is an extension of Hoek and Brown failure criterion: $\sigma_1 = \sigma_3 + t\sigma_{ci}\left(m_b \frac{\sigma_3}{t\sigma_{ci}} + s\right)^a$ – σ_1 and σ_3=maximum and minimum principal stress at failure – σ_c=*UCS* of intact rocks – m_b, a and s=modified H-B parameters related to rock mass characteristics – $t = (GSI/100)^{0.55}$, refers to the tectonisation degree; it varies from 0 (soil-like material) to 1 (intact rock)
Laws et al., 2003	*Aar Massif* granite- and gneiss-hosted shear zones (strongly foliated zone, fractured zone and heavily fractured/cohesionless zone): **mylonite/ultramylonite** and **microbreccia** composed of mylonite fragments in a fine-grained matrix	Investigation of the geomechanical properties of shear zones and their dependence on structural characteristics (by triaxial compressive tests)	The increasing degree of tectonic damage corresponds to: • Increase in stress-strain non-linearity • Decrease in elastic stiffness • Decrease in peak strength • Increase in residual strength • Transition from brittle failure (along a single, discrete shear plane) to ductile failure (encompassing a definite yield zone) As fracture density increases (i.e. lower influence of discrete, persistent discontinuities on rock mass strength) the sample becomes more and more representative of the in-situ behaviour.
Sanmez et al. 2004 and 2006	*Ankara Agglomerate*: volcaniclastic mixture of pink and andesite blocks cemented by weak tuff matrix (volcanic **bimrock**)	Development of an empirical model to determine the rock strength (by uniaxial compressive tests)	$UCS_N = \exp(C \times EBP)$ – UCS_N=normalized *UCS* (overall strength of the fault rock) – *C*=constant depending on the strength contrast between block and matrix – *EBP*=equivalent block proportion depending on *VBP* and on the strength of individual blocks The relation is valid only for *VBP* < *80%* and when the strength between block and matrix is approximately equal to that of matrix alone Strength anisotropy (due to blocks shape and orientation) is not considered

Table 3.3 continued

References	Tested fault rock	Main research/Methodology	Main results and/or comments
Kahrman and Alber, 2006	*Ahauser fault breccia*: cemented tectonic breccia characterized by slate components partly weathered and/or altered by Fe-rich fluids, where weaker blocks are surrounded by stronger matrix (**non-conventional bimrock**)	Development of a predictive model to determine strength and deformability properties from *VBP* (by uniaxial compressive tests)	$UCS = -22.43 \ln VBP + 115.44$ *20% < VBP < 70%* → *UCS* decreases with *VBP* a dependence between *VBP* and *E* has been observed *VBP < 20%* → The rock strength "reflects" the matrix strength *VBP > 70%* → *UCS* tends to be uniform The scale effect influences the strength (the effect is not clear for *E*)
Kahrman and Alber, 2008	*Ahauser fault breccia*: cemented tectonic breccia characterized by slate components partly weathered and/or altered by Fe-rich fluids, where weaker blocks are surrounded by stronger matrix (**non-conventional bimrock**)	Study of the effect on triaxial strength ($\Delta\sigma = \sigma_1$-σ_3) of block proportion (*VBP*) and texture coefficient (*TC*) (by triaxial compressive tests)	$\Delta\sigma = 184.5e^{-0.0233VBP}$ $\Delta\sigma = 16.3TC^{-0.7}$ $\Delta\sigma$ decreases with increasing *VBP* For low *VBP* the rock strength "reflects" the matrix strength (high $\Delta\sigma$) $\Delta\sigma$ and *UCS* almost converge with high *VBP* (at ≈20MPa) The scale effect influences the strength
Kahrman et al., 2008	*Misis fault breccia*: dolomitic limestone strong blocks embedded in a weaker fine-grained matrix of red-coloured claystone containing Fe-rich clay (**bimrock**). Block and matrix are strongly cemented together.	Study of potential effect on strength and deformability parameters (*UCS, E*, $\Delta\sigma$) of geomechanical properties such as density (*d*), *P*- (V_P) and *S*-wave (V_S) velocities, *VBP*, average block diameter, average block diameter factor (ABD_F), aspect ratio, roundness (*r*) (by uniaxial and triaxial compressive tests; density tests; ultrasonic tests)	Simple regression analyses (if *25% < VBP < 75%)*: $UCS = 32.53V_S - 44.97$ No other significant correlations are found with simple regression analyses (probably due to the wide strength range of blocks and matrix) Multiple regression analyses: $UCS = -205.07 - 0.46VBP + 66.30d + 30.43V_S + 20.23r + 0.73ABD_F$ $E = -103.88 - 0.16VBP + 39.65d + 4.20V_P + 4.33V_S$ The model for the prediction of *E* is not very significant $\Delta\sigma = 73.17 + 19.77V_P - 161.92r$ Lack of correlations between $\Delta\sigma$ and some properties (probably due to the wide strength range of blocks and matrix)

3.4 Final remarks

A detailed characterisation of fault zones is very important in rock mechanics and engineering geology applications. In this chapter different methods for describing, characterising and classifying fault rocks have been compiled, considering both geological and geotechnical points of view. A simpler system for classifying this type of rocks is still necessary since an ambiguous use of terms and definitions have been often found. In addition, due to the practical difficulties in taking and preparing samples from weak rocks and due to the great variability of the test results observed in literature, the characterisation of fault rocks from a geomechanical perspective cannot be easily representative of the effective behaviour encountered during real-time excavation.

Based on the above comments, one of the goals of this study is to provide a simpler methodology for classifying fault rocks by considering their interaction with mechanized tunnelling and their effects on the TBM performance.

Chapter 4 Data collection: development of the TBM-performance database

In order to investigate the correlations existing between TBM performance parameters and geological/geotechnical characteristics of a highly fractured and faulted rock mass, a TBM-performance database has been developed by compiling data coming from several tunnel projects. The attention has been focused on longitudinal tunnel sections in which highly fractured rock masses and fault zones hindered the TBM operations. The sections, selected according to specific criteria, are characterised by homogeneous geological/geotechnical conditions and mostly constant machine performance over a length from about 8-10 meters to several tens of meters. Data coming from tunnels excavated with gripper and shield TBM machines have been considered, as well as different type of projects (e.g. high speed railway, headrace and tailrace tunnels).

The most significant TBM-performance parameters and rock mass characteristics have been then selected and, for each type of machine, their range of variation within the database has been investigated.

4.1 Gripper TBM data

An open-type machine is generally used in hard rock and good geological conditions or where considerable deformations are expected. In less favourable ground conditions, such as highly fractured rocks and fault zones, the required additional supports, the potential need of ground consolidation and significant problems for the crew security can strongly affect the performance of a gripper TBM. The main specifications of the gripper TBMs employed in the studied projects are reported in Table 4.1.

After the specification of the general tunnel geometry (i.e. overburden, azimuth and diameter) for each project, the data compiled have been structured into two main sections:

1) TBM specifications and TBM performance parameters.
2) Geological-geotechnical parameters of the rock mass.

Table 4.1 Main specifications of the gripper TBMs used for the tunnel projects analysed in this research

TBM specification	Value
Diameter [m]	6 ÷ 10
Maximum thrust force [kN]	15000 ÷ 18150
Maximum revolutions per minute (RPM) [rev/min]	5.1 ÷ 8.2
Maximum torque [kNm]	2300 ÷ 9860
Number of cutters	42 ÷ 68
Cutter diameter [mm]	419 ÷ 432

For what concerns geological-geotechnical parameters, it is important to emphasise that they have been partly gathered directly from tunnel projects and partly estimated using existing formulations, commonly used in rock mechanics. Moreover, it is important to observe that, since the data come from real projects, their quality varies from one project to another in terms of degree of details as well as in type (e.g. quantitative vs. qualitative information).

4.1.1 TBM specifications and performance parameters

For each compiled section, the information related to boring operations, such as the bored length, the effective boring time and the total time needed to complete the excavation of a given tunnel section, has been collected in the database (Table 4.2).

Table 4.2 Boring information, TBM specifications and TBM performance recorded for each section

	Boring information	**TBM specifications**	**TBM operational parameters**
Tunnel section (first chainage-last chainage)	Bored length [m] Total time [hr] Boring time [hr]	RPM_{max} [rev/min] Th_{max} [kN] Tq_{max} [kNm]	RPM [rev/min] Th [kN] Tq [kNm]

The TBM specifications have also been included, as well as some TBM operational parameters such as the cutterhead rotation speed (RPM, rev/min), the thrust force (Th, kN) and the torque (Tq, kNm) recorded by the on-board acquisition system. These latter are called operational parameters as they are varied by the TBM operator according to the encountered ground conditions. Based on these data sets it has been possible to estimate other important factors usually taken into account while describing TBM performance:

- the ratio between boring time and total shift time, i.e. the utilisation factor (U) of the TBM (Equation. 4.1, Table 4.3) which expresses the amount of time in which the machine has been effectively used for boring;

- the penetration rate (PR), in m/hr, defined as the distance excavated divided by the operating time during a continuous excavation phase (i.e. without considering time required for installing supports, TBM maintenance, etc.) (Equations 4.2a and 4.2b, Table 4.3);
- the advance rate (AR), in m/hr, i.e. the TBM advance speed computed by considering the TBM delays due to rock supporting, maintenance, etc., calculated via the utilisation factor U and the penetration rate PR (Barton, 2000). Commonly, the daily advance rate is reported (Equation 4.3, Table 4.3);
- the field penetration index FPI (Klein et al., 1995; Barton, 2000; Hassanpour et al., 2011) calculated as the ratio between average cutter load and attained penetration per revolution p measured in mm/rev (Equation 4.4, Table 4.3);
- the power consumed by machine (Equation 4.5, Table 4.3);
- the net production rate (Equation 4.6, Table 4.3);
- the specific energy needed to excavate a unit volume of rock (Equation 4.7, Table 4.3).

Table 4.3 TBM parameter equations in the TBM-performance database

TBM parameter	**Equation No.**	
$U = \frac{Boring\ time\ [hr]}{Total\ time\ [hr]}$	4.1	
$PR\ \left[\frac{m}{hr}\right] = \frac{Bored\ length\ [m]}{Boring\ time\ [hr]}$	4.2	a
$p\ \left[\frac{mm}{rev}\right] = \frac{PR \times 1000}{RPM \times 60}$		b
$Daily\ AR\ \left[\frac{m}{day}\right] = (PR \times U) \times 24$	4.3	
$FPI\ \left[\frac{kN \cdot rev}{cutter \cdot mm}\right] = \frac{T_h}{N_c \times p}$, $N_c = number\ of\ cutters$	4.4	
$Power\ [kW] = \frac{2\pi \times T_q \times RPM}{60}$	4.5	
$Net\ Production\ Rate\ \left[\frac{m^3}{hr}\right] = \frac{RPM \times p \times 60 \times \pi \times \emptyset^2}{1000 \times 4}$, $\emptyset\ [m] = tunnel\ diameter$	4.6	
$Specific\ Energy\ \left[\frac{MJ}{m^3}\right] = \frac{3.6 \times Power}{Net\ Production\ Rate}$	4.7	

4.1.2 Rock mass parameters

For what concerns the rock mass characteristics, attention has been focused on the following parameters:

- Uniaxial Compressive Strength, UCS [MPa];
- Brazilian Tensile Strength, BTS [MPa];
- joint orientation;
- joint spacing;
- joint surface weathering conditions;
- volumetric joints count, J_v [joint/m^3];
- Rock Quality Designation, RQD ;
- rock mass global strength, UCS_{rm} [MPa];
- measured water inflow;
- tangential stress, σ_ϑ [MPa];
- Geological Strength Index, GSI;
- Q Index;
- Rock Mass Rating, RMR.

The intact rock properties for each lithotype included in the TBM-performance database, such as the Uniaxial Compressive Strength (UCS) and the Brazilian Tensile Strength (BTS), have been evaluated from laboratory tests on rock samples collected during excavation as well from detailed geological/geotechnical reports. When the information was available, the rock and joint conditions as well as the foliation attitude (e.g. orientation, spacing and surface conditions) have been gathered directly from face mappings, face/side-walls pictures and from tunnel profiles obtained during construction. The volumetric joint count J_v, defined as the average number of joints in a cubic meter of rock, has been also calculated by considering the average spacing of the identified joint sets (Equation 4.8, Table 4.4), and on this basis also an approximated Rock Quality Designation value, RQD (Hudson and Priest, 1979) has been computed (Equation 4.9, Table 4.4). The recorded information about water inflows, as described in the geological reports of the projects or from the tunnel surveys, has also been included in the database. In addition, the Rock Mass Rating (RMR), the Q index and the Geological Strength Index (GSI) are computed (or evaluated) on the basis of all above collected data. The rock mass uniaxial compressive strength (UCS_{rm}) (Hoek et al., 2002) is computed by using Equation 4.10a (Table 4.4). The uniaxial compressive strength of intact rock (UCS) is reduced by the Hoek and Brown parameters, s and a, which depend on the GSI index (Equations 4.10b and 4.10c, Table 4.4). The factor D depends on the degree of disturbance due to blast damage and stress relaxation: it varies from 0, for undisturbed in situ rock masses, to 1, for very disturbed rock masses, in the present case, due to the fact that only TBM excavation has been considered, this parameter has been set equal to 0. For better taking into account the behaviour of cataclastic and weak rocks, the strength parameters calculated as proposed by Habimana (1999) and by Habimana et al.

(2002) have been also included in the database. As reported in Chapter 3 (see Table 3.3), the uniaxial compressive strength of the weathered material can be reduced according to t (Equation 4.11a, Table 4.4), a coefficient describing the tectonisation degree, which depends on GSI and varies between 1, in case of intact rock, and 0, in case of a soil-like material (Equation 4.11b, Table 4.4).

Table 4.4 Equations used for evaluating some of the rock mass parameters included in the TBM-performance database

Rock mass parameter	**Equation No.**	
$J_v\ [joints/m^3] = \sum\left(\frac{1}{s_i}\right) + \left[\frac{N_{r(5)}}{5}\right]$ $s_i\ [m] = average\ spacing\ of\ the\ i^{th}\ joint\ set$ $N_{r(5)} = number\ of\ random\ joints\ along\ a\ 5\ m\ scan\ line$	4.8	
$RQD\ [\%] = 100e^{-0.1\lambda}(1 + 0.1\lambda)$ $\lambda = total\ joint\ frequency$	4.9	
$UCS_{rm}\ [MPa] = (sUCS^2)^a$	4.10	a
$s\ [-] = \frac{\exp(GSI - 100)}{9 - 3D}$ with $D = 0\ (TBM\ tunnelling)$		b
$a\ [-] = \frac{1}{2} + \frac{1}{6}\left(e^{-GSI/15} - e^{-20/3}\right)$		c
$UCS_H\ [MPa] = tUCS$	4.11	a
$t\ [-] = \left(\frac{GSI}{100}\right)^{0.55}$		b

4.2 Data quality

According to the different nature of the sources, a preliminary analysis has been done to show the distribution of compiled data as well as their quality. In Table 4.5 and Table 4.6 the distributions of the different sources of compiled data are reported both for TBM performance and geological-geotechnical parameters. As it can be clearly seen in Table 4.5, though the calculation of the basic machine parameters has been generally performed on the basis of the measures carried out by the TBM on-board acquisition system during construction, it was not possible to gain complete TBM data for all tunnel projects. This is due to the fact that the contractors are often unable to share easily data especially when on-going claims have not been solved yet. However, although important TBM performance parameters could not been compiled for all projects (for example penetration per revolution, thrust force and torque are

unavailable for up to 70% of the collected data), it has been possible to obtain the daily advance rate (meters per day) per each section included in the analysis, mainly by referring to available time-way diagrams, and by using information gathered from the literature (e.g. delays and stoppages of the machine).

Table 4.5 The different sources of the compiled TBM-performance data

TBM-performance parameter	**TBM on-board acquisition system**	**Time-way diagram/Literature**	**No data**
Penetration Rate	62 %	-	38 %
Advance Rate (delays)	62 %	38 %	-
RPM	62 %	-	38 %
Thrust force	62 %	-	38 %
Torque	31 %	-	69 %

With regard to the rock mass characterisation (Table 4.6), it is important to underline that, mainly due to the fact that they belong to the tunnel owner and not to the contractor, geological-geotechnical descriptions of tunnel projects are easier to obtain than TBM performance data. As it is possible to see, several sources have been considered: geological-geotechnical reports, laboratory tests, stereographic projections, tunnel profile survey, face and side-wall pictures and literature. Except for the information describing joints orientation (38% of data were not available), all parameters have been collected, though with variable detail and reliability degrees. As already specified in Chapter 3, in extremely challenging environments, it might be very difficult, or impossible, to perform standard laboratory tests. Thus, literature values represented in such cases the reference for charactering the rocks.

Table 4.6 The different sources of geological-geotechnical parameters

Geological-geotechnical parameter	**Geological-geotechnical reports**	**Laboratory tests**	**Literature**	**Face and side-walls photos**	**Tunnel profile surveys**	**Stereographic projections**	**No data**
Rock strength	-	62 %	38 %	-	-	-	-
Joint orientation	31 %	-	-	-	-	31 %	38 %
Joint spacing	-	-	-	-	100 %	-	-
Joint surface/rock weathered conditions	31 %	-	-	31 %	38 %	-	-
Water flows	62 %	-	38 %	-	-	-	-

4.3 Selection criteria for data collection

In order to select the tunnel sections to be included in the TBM-performance database, attention has been focused firstly on stretches identified as difficult/very difficult ground conditions (such as highly fractured or faulted rocks) over a length of at least 8-10 m. The parameters and representative values already specified in Chapter 3 for characterising difficult rocks have been here used as a reference.

In particular, the selected zones are generally characterised by RMR values lower than 40, characterising poor (IV class) to very poor (V class) rock quality according to the classification provided by Bieniawski (1976). These sections are also generally characterised by large to very large water inflows (> 60 l/min) that contribute to the low values of RMR.

For what concerns the joint spacing (s_i), five classes have been considered (Table 4.7) and only the sections belonging to classes C, D and E have been included in the database. When only a qualitative description of the rock mass conditions was available (i.e. from "slightly fractured" to "disintegrated" in Table 4.7), the tunnel sections characterised by "Highly Fractured" (corresponding to classes C and D) and "Disintegrated" (corresponding to class E) rocks have been included in database. On the basis of the joint spacing, the volumetric joint count (J_v) has been computed. Though J_v is always rather high in the database, some sections are characterised by lower values of J_v. This is due to the fact that other factors (such as the weathering degree or water inflows) were considered for including those sections in the database. As a matter of facts, rock masses characterised by a significant weathering degree of the rock and/or of the joint surfaces are not necessarily described by high values of J_v.

Due to the available data quality (i.e. the characteristics of the joints such as roughness, opening and alteration/filling are not always clear or well-defined), the identification of the information describing quantitatively the weathering degree of the joint surfaces was not an easy task. This is the case, for example, of extremely fractured rock masses where it is no more possible to identify joint sets. Thus the rock conditions become the most relevant information. As a matter of facts, weathering and weakness of the material can be considered as results of faulting and folding processes. Table 4.8 summarises the criteria used for describing the rock conditions. Based on the nature and on the detail degree of the available data, at least one of the three criteria has been used to identifying and specifying the class.

Table 4.7 Quantitative and qualitative description of fracturing degree

Fracturing degree class *(according to the quantitative description)*	**Quantitative description** *Joint spacing, s_i [m]*	**Qualitative description**
A	$s_i > 5$	Slightly fractured
B	$1 < s_i < 5$	Fractured
C	$0.1 < s_i < 1$	Highly fractured
D	$s_i \leq 0.1$	
E	$s_i \leq 0.01$	Disintegrated

Table 4.8 Conditions and behaviour of the rock

Class	Rock behaviour	Rock weathering	Rock strength (UCS, MPa)
1	Good	Unweathered	Very strong (> 100)
2	Fair	Slightly weathered	Strong (60-100)
3	Mediocre	Weathered	Medium strong (40-60)
4	Very poor	Highly weathered	Weak (< 40)

Finally, to complete the description of the section, also the available information about the (temporary) supports has been taken into account: in particular, only sections characterised by heavy to very heavy supporting measures have been considered.

4.4 Range of variation of significant parameters

Among the compiled data significant parameters concerning the TBM performance (p, daily AR) and geological-geotechnical characteristics (J_v, GSI and UCS_H) have been selected in order to study their range of variation in the database.

4.4.1 TBM performance parameters

The choice of the TBM parameters based on the fact that the penetration per revolution (p) and the daily advance rate (daily AR) allows evaluating the performance of the machine with or without possible delays due to temporary supports installation, consolidation measures, TBM maintenance etc.

The penetration per revolution (p) is characterised by a range of variation comprised between 1 mm/rev to more than 11 mm/rev, with a mean of 5.76 mm/rev and a mode range of 5 to 7 mm/rev (Figure 4.1). These rather high recorded values are due to the significant fracturing degree of the rock mass that improves TBM performance in terms of penetration. This is because the crushing and chipping processes are favoured by the discontinuities which enhance fracture propagation and interaction beneath the disc cutters. It is important to underline that the higher values of p (> 9 mm/rev), recorded during construction, can be assumed negligible for the purposes of these analyses.

The potential delays occurring during excavation are taken into account through the utilisation factor (U) of the machine. Therefore, they affect the daily advance rate (see Equation 4.3, Table 4.3). As already mentioned, U includes downtimes due to increasing rock support requirements, additional drainage systems, gripper bearing failure etc. As a matter of fact, the obtained daily advance rates show an important lowering compared to the penetration rates (Figure 4.2). The range of variation includes values lower than 5 m/day (down to performance lower than 1 m/day) as far as values greater than 30 m/day, with a mean of 7.31 m/day and a mode range of 5 to 15 m/day. More than 90% of the tunnel sections show a daily advance rate lower than 15 m/day and about half of them do not reach 5 m/day. The higher values (especially greater than

20 m/day) correspond to percentages so low to be negligible. The large data scatter, expressed by a high coefficient of variation (C.V. = 0.76), underlines the high uncertainty related to the estimation of the TBM utilisation factor which involves both geological/geotechnical and construction-related parameters. Despite machine delays mainly depend on the TBM-rock mass interaction, they can indeed be affected also by unpredictable events (often due to the human factor) which is almost impossible to quantify.

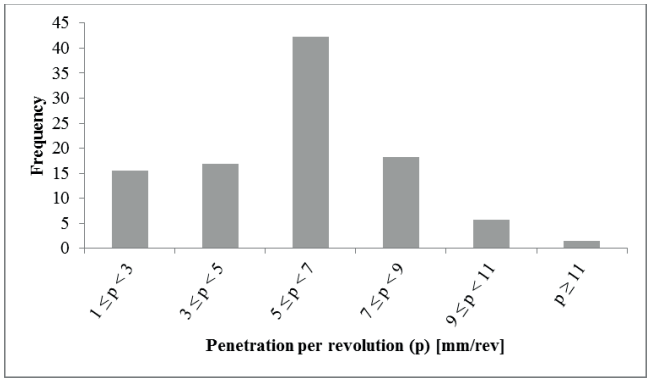

Mean p [mm/rev]	5.76
Standard deviation [mm/rev]	2.16
C.V.	0.37

Figure 4.1 Histogram plot for the penetration per revolution (p) of the TBM with indication of mean, standard deviation and coefficient of variation (C.V. = standard deviation/mean).

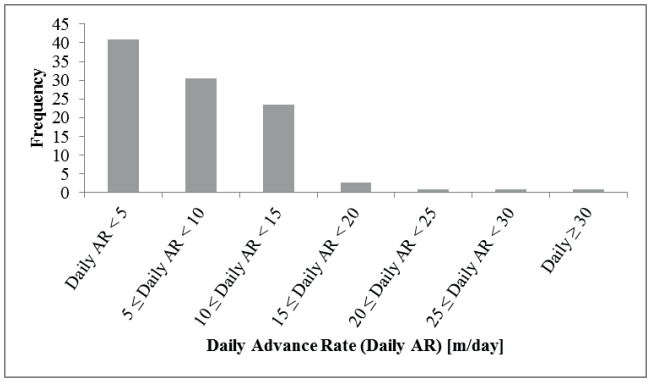

Mean Daily AR [m/day]	7.31
Standard deviation [m/day]	5.56
C.V.	0.76

Figure 4.2 Histogram plot for the daily Advance Rate (AR) of the TBM with indication of mean, standard deviation and coefficient of variation (C.V. = standard deviation/mean).

4.4.2 Rock mass parameters

For what concerns the geological-geotechnical characteristics, the degree of fracturing (expressed by J_v) has been considered as one of the most representative parameter, as well the

weathering conditions of the rock matrix and of the joint surfaces (considered in the definition of GSI and UCS_H).

The range of J_v is comprised between values lower than 15 joints/m^3 and values greater than 30 joints/m^3 (Figure 4.3). However, the mode (J_v > 30 joints/m^3) and the mean (about 28 joints/m^3) underline the generally high (and extremely high) fracturing degree which characterises the rock masses of the chosen tunnel sections. The highly jointed structure contributes, together with the conditions of the joint surfaces, to obtain rather low values of the Geological Strength Index, GSI (Figure 4.4).

The GSI values vary between 5 and 50 in the database (Figure 4.4), with a mode value in the range 30-40 and a mean value of about 30. As previously shown (see Chapter 3), according to the modified version of GSI (Marinos and Hoek, 2001; Marinos et al., 2007), values lower than 40 describe strongly disturbed and folded rock masses, characterised by important degree of tectonisation and faulting as far as disintegrated material.

The rock strength estimated according to Habimana (1999) and Habimana et al. (2002) covers a range between 10 MPa and 120 MPa (Figure 4.5), with a mean and a mode value of 58.2 MPa and 36.7 MPa respectively. More than 50% of tunnel sections are characterised by rock with a reduced strength lower than 60 MPa (33% with UCS_H lower than 40 MPa and about 22% with UCS_H between 40 MPa and 60 MPa). These values correspond to weak and medium strong rocks (see Table 4.8) while about 36% and only 8% refer to rocks defined respectively as strong and very strong. Since the database compiles data of several projects, the different rock types (e.g. schist, limestone, gneiss, greenstone, granite etc.) justify the large range of UCS_H which obviously is a function of the uniaxial compressive strength of these (intact) rocks. For what concerns the values obtained for the strength of the altered rocks it is important to observe that they strongly depend on the high fracturing and/or weathering degrees expressed by low values of GSI.

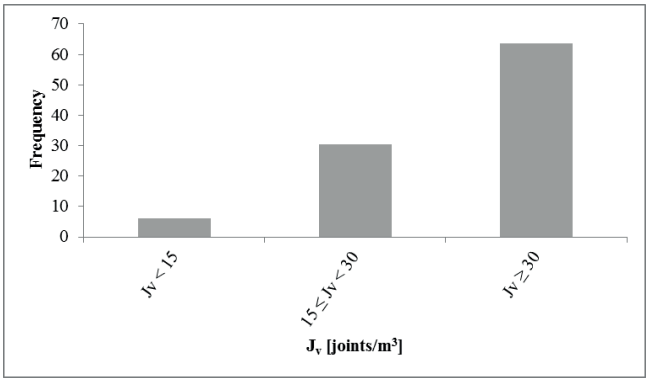

Mean J_v [joints/m^3]	27.77
Standard deviation [joints/m^3]	9.33
C.V.	0.34

Figure 4.3 Histogram plot for the volumetric joint count (J_v) with indication of mean, standard deviation and coefficient of variation (C.V.= standard deviation/mean).

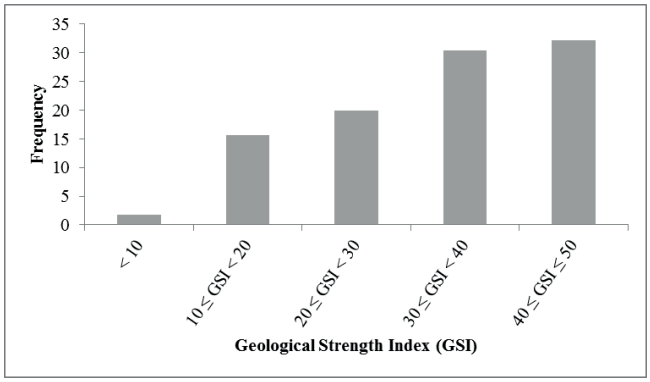

Mean GSI [-]	29.00
Standard deviation [-]	11.24
C.V.	0.39

Figure 4.4 Histogram plot for the Geological Strength Index (GSI) with indication of mean, standard deviation and coefficient of variation (C.V.= standard deviation/mean).

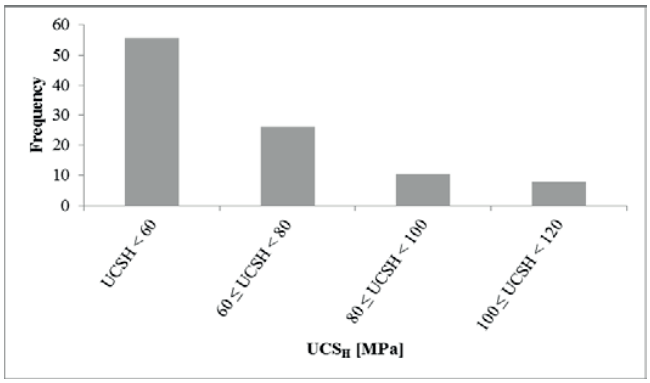

Mean UCS_H [MPa]	58.25
Standard deviation [MPa]	23.29
C.V.	0.40

Figure 4.5 Histogram plot for the Uniaxial Compressive Strength of the rock (UCS_H) calculated by Habimana (1999) and Habimana et al. (2002) with indication of mean, standard deviation and coefficient of variation (C.V.= standard deviation/mean).

4.5 Shield TBM data

Although main problems can be expected with gripper TBM crossing disturbed zones, it has been decided to include in the database also values coming from projects where shield TBMs were used. The main specifications of the considered shield TBMs are shown in Table 4.9.

The available shield TBM data are similar to those already described for gripper machines. These include operational parameters such as applied thrust force, torque and cutterhead rotational speed, and performance parameters such as daily advancement (daily AR) and rate of penetration (both p and PR). Unfortunately, for those projects, less information could be found

for what concerns geological-geotechnical data. In particular, only general information could be gathered (e.g. rock strength and RMR, but no fracturing degree). However, in order to compare the performance with the one of the open TBMs, Figure 4.6 and Figure 4.7 show respectively the ranges of variation of p and of daily AR for shield-TBMs.

Table 4.9 Main specifications of the shield TBMs used for the tunnel projects analysed in this study

Diameter [m]	10
Maximum thrust force [kN]	130000
Maximum revolutions per minute (RPM) [rev/min]	5
Maximum torque [kNm]	25000
Number of cutters	69
Cutter diameter [mm]	432

As for the gripper TBMs, significant rates of penetration (p), i.e. reaching values higher than 15 mm/rev, could be recorded. The mean penetration is equal to 14.90 mm/rev and the mode range is comprised between 13 and 15 mm/rev (Figure 4.6). Also in this case, the high p-values are probably due to important degree of fracturing, supposed quite high on the basis of low RMR values recorded (20 < RMR < 50) for the majority of the tunnel sections. Better penetration values, with respect to the ones observed for the open machines, can be associated both to lower strengths of the rocks (UCS ≤ 60 MPa) as well as to higher thrust force of the cutterhead.

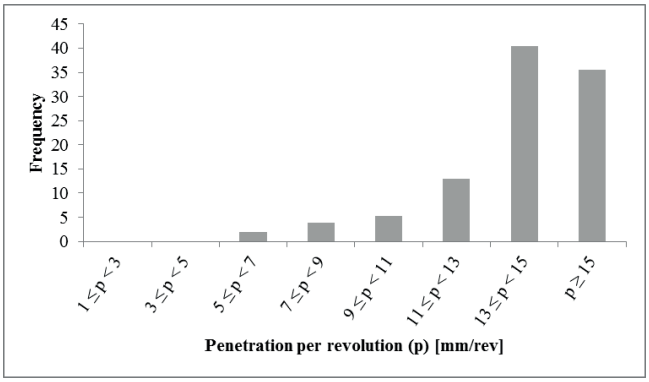

Mean p [mm/rev]	14.90
Standard deviation [mm/rev]	5.20
C.V.	0.35

Figure 4.6 Histogram plot for the penetration per revolution (p) of the shield TBM with indication of mean, standard deviation and coefficient of variation (C.V. = standard deviation/mean).

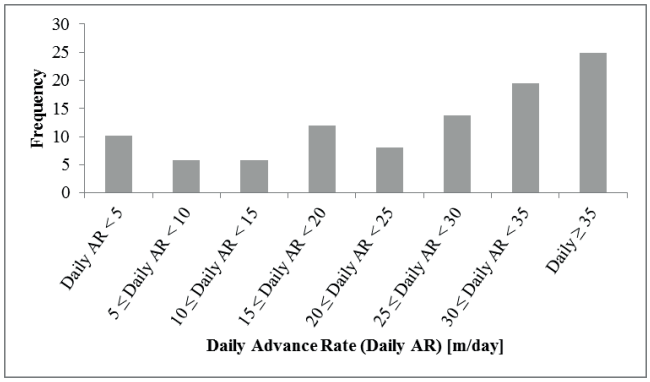

Mean Daily AR [m/day]	25.40
Standard deviation [m/day]	12.58
C.V.	0.49

Figure 4.7 Histogram plot for the daily Advance Rate (AR) of the shield TBM with indication of mean, standard deviation and coefficient of variation (C.V. = standard deviation/mean).

Finally, it is interesting to observe that for the shield TBMs, high advance rates have been recorded (though with large data scattering). As a matter of facts, values greater than 35 m/day have been reached for the majority of the tunnel sections. This result is the exact opposite of what has been observed for the gripper machines, where the majority of the sections are characterised by daily AR lower than 5 m/day. This important difference may result from higher rate of penetration and from an overall better performance (i.e. U) of the shield TBMs recorded in highly fractured rocks (this is also related to the fact that the rock supporting time, i.e. ring assembling, does not change significantly to one section to another).

4.6 Final remarks

A TBM-performance database has been developed with the aim to compile data from several tunnel projects where both gripper and shield machines have been employed. A detailed procedure has been adopted in order to identify tunnel sections characterised by highly fractured and faulted rock masses. In order to select the sections to be included in the database, the attention has been focused on significant parameters such as strength and fracturing degree of the rock mass, weathering conditions of rock and joint surfaces as well as recorded water inflows and type of supports.

The variation range of significant geological/geotechnical parameters and TBM performances has been studied. The data quality varies from a project to another and some information has been obtained by other sources (e.g. literature). Due to a different degree of the information detail, it was not possible to investigate the same rock mass characteristics for gripper and shield machines. On the other hand, with regard to the TBM performance parameters, the first analyses of the variation ranges show an important difference between the two types of machine for what concerns the daily AR. In particular, higher values have been observed for the shield TBMs which are not affected by significant delays in terms of rock supporting time.

Chapter 5 Preliminary data analyses

Starting from the information compiled in the database, preliminary investigations have been performed in this chapter in order to analyse the correlations between the TBM performance and the rock mass characteristics. The parameters commonly adopted in the existing performance prediction models, such as the rock strength and the fracturing degree of the rock mass, have been considered in the analyses.

The gripper TBM and the shield TBM data have been studied separately due to the changing characteristics of the machines which, as already observed in the previous chapter, differently affect the excavation process and significant performance (e.g. the advance rate).

5.1 Gripper TBM data analyses

According to the review performed in Chapter 2 (see paragraph 2.2), the most relevant parameters commonly used in the existing TBM-performance prediction models are the strength and the fracturing degree of the rock. In the following sections several analyses have been performed in order to find if some correlation can be highlighted also in case of bad tunnelling conditions, by considering the performances recorded while tunnelling with open (gripper) TBMs.

Based on the available information concerning the strength and the fracturing degree of the rock mass, the potential relationships with the uniaxial compressive strength of the rock (UCS), the volumetric joint count (J_v) as well as the Rock Mass Rating (RMR) have been investigated.

5.1.1 Rock strength: correlations between UCS (and UCS_H) and TBM performance parameters

As shown in Figure 5.1a, although the UCS data compiled in the database are mainly characteristic of strong to very strong rocks (UCS = 60-180 MPa), it has already been observed that these values are not representative of the disturbed conditions considered in this framework (i.e. highly fractured and faulted rocks). For this reason, instead of UCS values of the intact rock it has been decided to adopt the uniaxial compressive strength reduced by Habimana (1999) and Habimana et al. (2002), for evaluating possible correlations with the TBM performance. Despite

a significant lowering (Figure 5.1b) of the strength values (that become more representative of the real conditions), a large data scattering can be observed and the correlation with both p and PR is almost meaningless (Figure 5.2 and Figure 5.3).

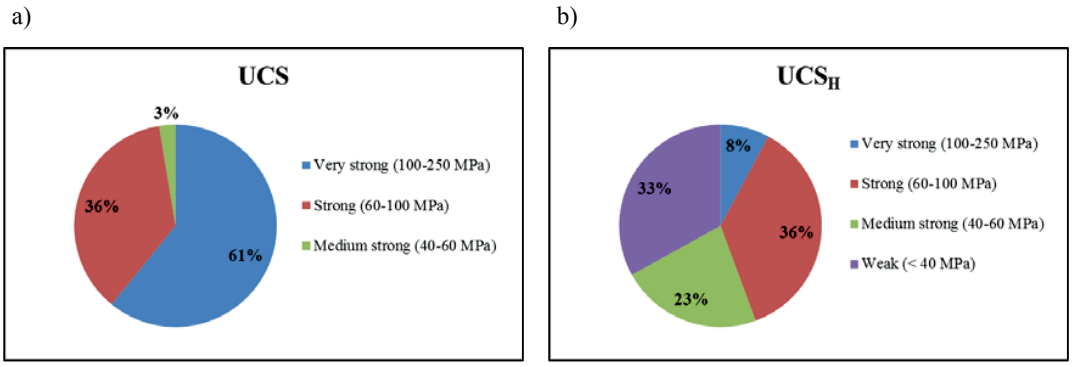

Figure 5.1 Classes of strength of the rocks included in the database: a) Uniaxial Compressive Strength (UCS); b) reduced Uniaxial Compressive Strength (UCS_H).

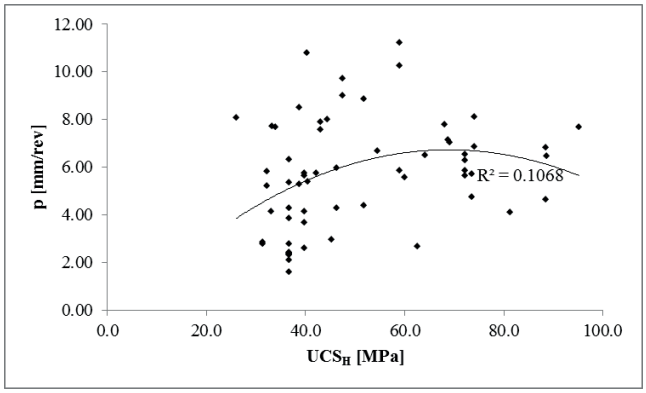

Figure 5.2 Correlation between penetration per revolution (p) and the reduced Uniaxial Compressive Strength (UCS_H).

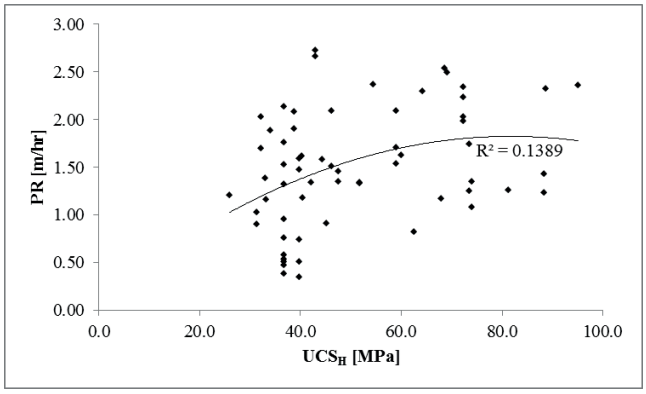

Figure 5.3 Correlation between Penetration Rate (PR) and the reduced Uniaxial Compressive Strength (UCS_H).

5.1.2 Fracturing degree: correlations between J_v and TBM performance parameters

Regarding the fracturing degree of the rock mass, the first analysis investigated the relationship between the penetration per revolution (p) and J_v. In this case the best fitting of the data is provided by a polynomial curve (Figure 5.4).

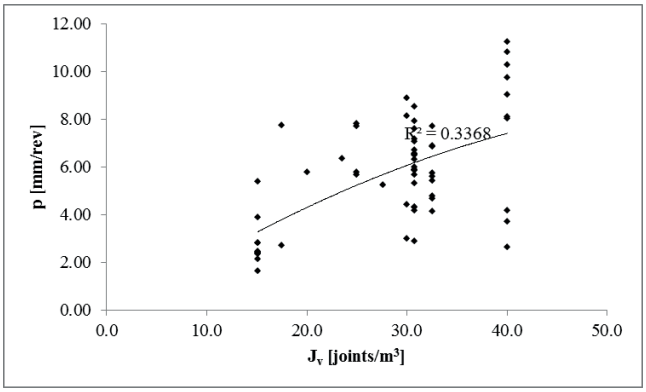

Figure 5.4 Correlation between penetration per revolution (p) and Volumetric Joint Count (J_v).

Although the accuracy of the relationship is not very high (R^2=0.34), due to the large scattering of data, a general increase of p may be observed for increasing J_v. This can be explained by the fact that the discontinuities are planes of weakness in the rock mass, and they assist the crushing and chipping of the rock during excavation, beneath and adjacent to the cutters, as already observed by Dollinger and Raymer (2002) and by Gong et al. (2006). For this reason, it is important to remark that, although a high number of joint sets generally does not represent a hindrance to the boring process, it might, however, generate other difficulties mainly linked with face/wall stability problems and increasing TBM downtimes. Furthermore, it should be noticed that, once a certain threshold of rock mass fracturing is exceeded, its effect on the TBM performance seems to start decreasing. In Figure 5.4 this behaviour is actually represented by the downward concaveness of the fitting curve.

Figure 5.5 shows the correlation between PR and J_v. Compared to p, PR undergoes a more evident decrease for values greater than 30 joints/m^3. As a matter of facts, while p refers to the penetration for one cutterhead revolution, PR is affected by the rotational speed (RPM) which in its turn is clearly affected and reduced in case of high fracturing degrees of the rock mass. As already observed by Delisio and Zhao (2014), this reduction is probably due to the fact that, in highly fractured rocks, other operational issues, such as the efficiency of the muck removal system to evacuate the excavated material from the face, may affect the applicable RPM and, therefore, achievable rate of penetration.

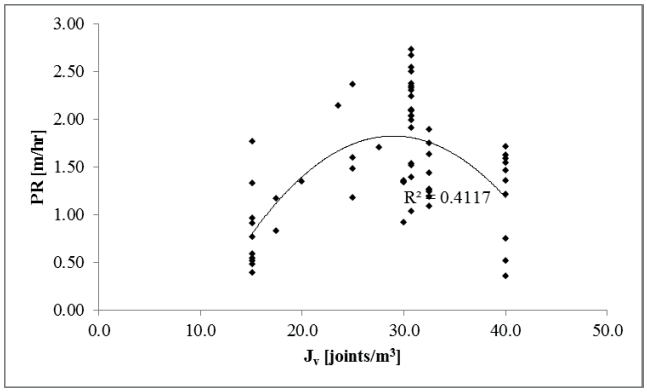

Figure 5.5 Correlation between Penetration Rate (PR) and Volumetric Joint Count (J_v).

The computation of the potential construction delays and the prediction of the TBM utilisation factor and advance rate can be considered within the most important issues when back-analysing the performance of the machine in difficult ground conditions. In these analyses, despite of good penetration rates (i.e. PR between 0.38 and 2.73 m/hr), the TBM utilisation factor (U) is quite often very low, reaching extreme values of about 3%. As a consequence of this, the advance rates (estimated according to Equation 4.3) could be also extremely low (i.e. about 1.0 m/day), since it includes downtimes for TBM maintenance, potential machine breakdown and tunnel failures.

5.1.3 Existing rock mass classification systems: correlations between RMR and TBM performance parameters

Due to the difficulties observed in the previous section in finding satisfying relationships among the TBM performance and individual geological-geotechnical parameters, the Rock Mass Rating, providing a general geomechanical description of the rock mass, has been then selected as reference index. Thus, further analyses have been performed for investigating existing correlations between RMR and both PR and daily AR (Figure 5.6 and Figure 5.7).

Together with the raw information (Figure 5.6a and Figure 5.7a), data have been grouped in 5 RMR classes and plotted as bar charts: the central point of the bars represents the average value of PR (Figure 5.6b) and daily AR (Figure 5.7b) for each class, while the bar length indicates the standard deviation. As it can be observed in Figure 5.6 and Figure 5.7, respectively for PR and daily AR, although a quite large data scattering exists, a certain trend can be identified: if RMR increases both average PR and daily AR also increase.

These results seem to confirm the trend reported in Sapigni et al. (2002). However, since only sections characterised by RMR lower than 40 have been included in the database, only the increase of PR with increasing rock mass quality could be investigated (which corresponds to the left part of the bell shape curve represented in Figure 2.7a). Moreover, as already observed by Sapigni et al., (2002), the scatter around the mean value is rather high and it is probably related to the difficulty in maintaining a constant thrust during excavation.

The correlation between daily AR and RMR follows the same trend. The reason of that is twofold: in one hand, PR increases for increasing RMR and, at the same time, also an increase of the TBM utilisation factor (U) can be assumed due to better conditions for excavation. In an attempt to find a possible relationship between U and RMR, despite of a high data scatter, nearly constant levels of utilization factor has been detected for the worst ground conditions while an increasing U has been observed for higher values of RMR (Paltrinieri and Sandrone, 2014). The uncertainties are mainly due to the fact that the Rock Mass Rating depends on several factors (i.e. fracturing degree, water inflow, rock strength, joints conditions) and each of them might influence the utilisation factor with a different weight that should be considered according to the specific encountered conditions.

In addition, it is necessary to remind that the conventional RMR system has been originally developed to provide support guidelines for underground construction excavated by the Drill-and-Blast method. In this sense, it might not be the most appropriate parameter to be taken into account for this kind of analyses.

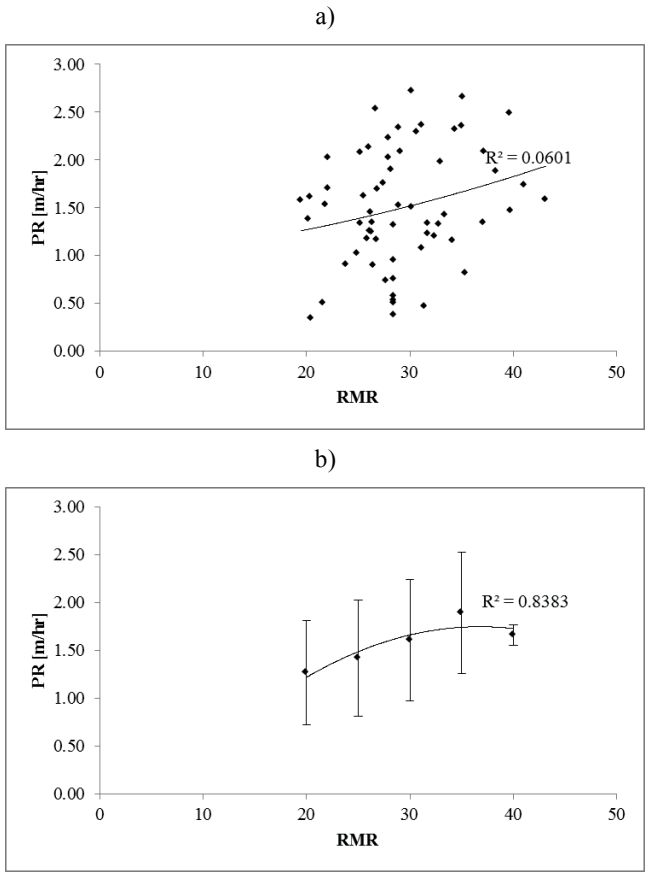

Figure 5.6 a) Correlation between Penetration Rate (PR) and Rock Mass Rating (RMR) (raw data); b) correlation between average PR and average RMR in each class.

a)

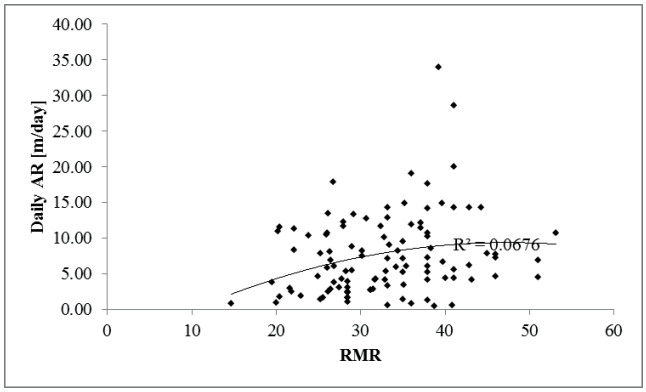

b)

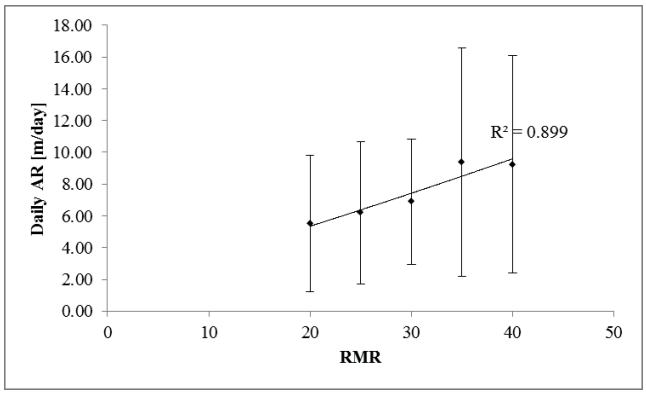

Figure 5.7 a) Correlation between Advance Rate (AR) and Rock Mass Rating (RMR) (raw data); b) correlation between average AR and average RMR in each class.

5.2 Shield TBM data analyses

As reported in the previous chapter, the available geological and geotechnical information collected in the database for shield TBM projects is not as much detailed as what has been obtained for the tunnels excavated with the gripper TBMs. Thus the analyses considering J_v and UCS_H could have not been performed and only the relationships between the TBM performance parameters and RMR have been investigated (Figure 5.8 and Figure 5.9).

a)

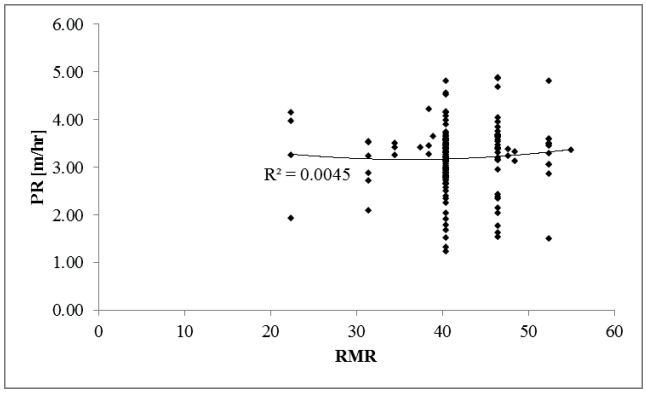

b)

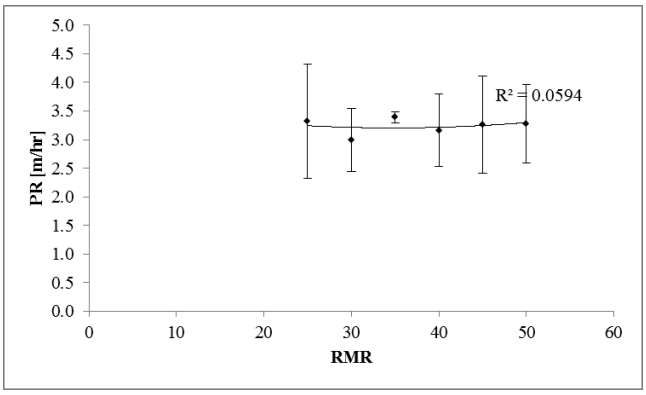

Figure 5.8 Correlation between Penetration Rate (PR) and Rock Mass Rating (RMR) (raw data); b) correlation between average PR and average RMR in each class.

The results clearly show that it is not possible to define any kind of correlation between RMR and the TBM-performance parameters such as PR and daily AR. The accuracy is almost negligible (i.e. $R^2 \approx 0$), both considering the row data (Figure 5.8a and Figure 5.9a) or RMR classes (Figure 5.8b and Figure 5.9b).

However, it is interesting to observe that the mean values of PR and daily AR seem to follow a constant trend for the different RMR ranges. This can be due to the fact that, with a shield TBM, it could be harder to identify variations of the rock mass conditions (unless very problematic ones) because they may not cause significant reductions in the utilisation factor of the machine (e.g. rock supporting time, unlike for what happens with a gripper TBM, remains unchanged). However, since the data scattering is quite important and the accuracy is quite low (i.e. $R^2 \sim 0.22$), it is rather difficult to confirm these hypotheses.

a)

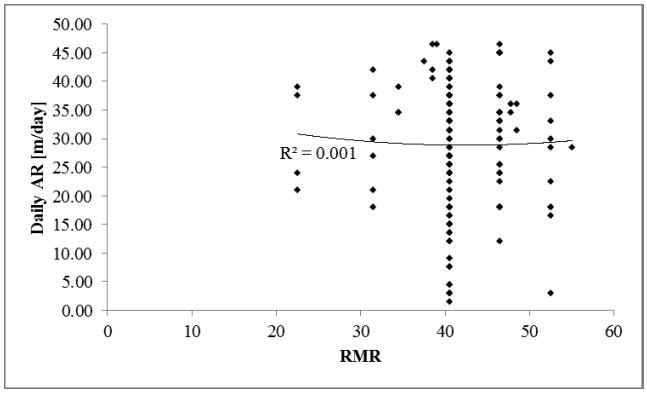

b)

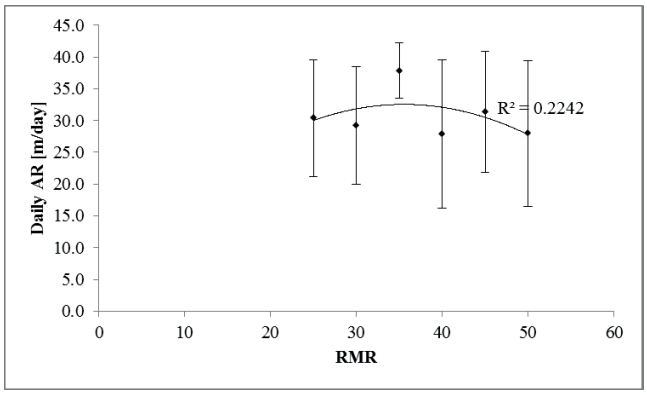

Figure 5.9 a) Correlation between Advance Rate (AR) and Rock Mass Rating (RMR) (raw data); b) correlation between average AR and average RMR in each class.

5.3 Final remarks

The preliminary results reported in this section highlight the great difficulty of describing the TBM-performance in highly fractured and fault zones through parameters commonly used in the existing predictions models (see Chapter 2). Both gripper TBM data and shield TBM data have been investigated. Although any consistent correlations could be found for what concerns the shield TBMs, some significant observations have been made in the case of gripper TBMs.

In particular, it has been underlined that the properties of the intact rock (e.g. UCS) are no more relevant parameters for characterising weak and weathered materials. However, also if a first attempt of taking into consideration the alteration degree of the rock mass has been done by introducing the reduced strength UCS_H, any relevant correlations with the TBM performance parameters could be found.

Finally, it has been observed that, the introduction of a "more global" characterisation of the rock mass may be necessary to find better correlations with performance parameters and rock quality. With this purpose, referring to the existing rock mass classification systems seemed to be a valid starting point. However, although the analyses performed by considering the Rock

Mass Rating (RMR), showed results in agreement with previous works reported in literature, the RMR system proved to be still not the most appropriate way for describing how difficult ground conditions affect the TBM performance (and thus finding good correlations for a prediction model). Furthermore, it is important to point out that some factors, which are basic for RMR definition (e.g. the rock strength), are extremely significant for predicting performances in hard rock tunnel boring, but they may play a very marginal role in the definition/estimation of the machine performance in highly fractured and faulted zones.

As a consequence of these previous analyses it can be observed that, in order to better characterise the TBM behaviour in difficult ground conditions, it is necessary to describe the weak rocks and the fault zones that can be encountered mainly focusing on the geological/geotechnical parameters which more affect the TBM performance and the possible delays.

Chapter 6 Fault zone classification

Due to the very complex structure and nature of the fault zones and their difficult geomechanical characterisation, detailed criteria have been chosen for developing a specific classification method mainly focusing on their mechanical behaviour during tunnel excavation. Thus in this framework, the term "fault zone" basically refers to the difficult ground conditions encountered in TBM tunnelling, characterised by extremely jointed rock masses or faulted/sheared rocks. The most common and approved terminology and the existing geotechnical characterisation systems for fault rocks, already presented in Chapter 3, have been here adopted to describe and characterise each group of the proposed classification system.

Numerical modelling has been used for simulating the interaction between a TBM cutter and the different categories of fault zone. In order to better describe the different behaviour characterising the identified "fault zone" classes both discontinuum and continuum models have been performed. The aim is to obtain a better description of the TBM performance at the tool-scale, by studying the cracking and chipping processes induced by the cutter.

6.1 Significant geological/geotechnical parameters in the classification

Though in literature fault rocks (generally termed 'cataclastic rocks") result from a mechanical and chemical weathering related to tectonic activities (Christe, 2009), in this framework, the term "fault zone" refers with a more general approach to difficult ground conditions encountered in TBM tunnelling, thus starting from extremely jointed rock masses up to completely faulted/sheared rocks. From a geomechanical point of view, this kind of rocks can be also described as weak and weathered rocks.

The review reported in Chapter 3 about the formation and structure of a fault zone and about the characterisation of fault rocks, provides the bases for the proposed classification. In particular, Table 3.2 (Chapter 3) summarises geological and geomechanical parameters (as well as their relative ranges of values) generally used for describing weathered and weak rocks that will be taken into account in this study.

According to what has been presented in the review proposed in Chapter 3, in order to identify the "fault zone" classes, the following aspects have been firstly taken into consideration:

- The fracturing degree of the rock mass;
- The weathering degree of the rock mass;
- The possible influence of the water;
- The effect of the depth (in-situ stress)

In this framework, the fracturing degree of the rock mass and the weathering degree of the rock and of the joint surfaces will represent the basic parameters for defining the "fault zone" classes, while the potential water inflows and depth of faulted/fractured zones will be considered only as additional factors which contribute to the reduction of the TBM performance independently of the class. The following sections describe more in detail the influence of each of these aspects.

6.1.1 The fracturing degree

According to how the fault zones are described by various authors (see Chapter 3) the blockiness of the rock mass represents a valid base of departure to identify the different classes. Thus, the volumetric joint count (J_v) has been selected as the most appropriate parameter to represent the degree of fracturing. J_v is generally given as a range and it is an average measurement of the number of joints that intersect a volume of the rock mass. The ISRM (1978) describes the block size according to J_v as follows:

- very large blocks: $J_v < 1$ joints/m^3;
- large blocks: $1 < J_v < 3$ joints/m^3;
- medium-sized blocks: $3 < J_v < 10$ joints/m^3;
- small blocks: $10 < J_v < 30$ joints/m^3;
- very small blocks: $J_v > 30$ joints/m^3.

For the proposed fault zone classification, only blocks with small to very small sizes have been considered, adopting J_v equal to 10 joints/m^3 as lower limit, below which the rock mass cannot be described anymore as highly fractured. Regarding the upper limit, the exact definition of the threshold beyond which the rock is completely crushed is not immediate. For this reason a reference value of 35 joints/m^3 has been considered as the highest J_v for a rock mass where individual joint sets can be still identified.

6.1.2 The weathering degree

Another important factor involved in the definition of the "fault zone" classes is the weathering degree of the rock and of the discontinuity surfaces. In order to take into account this aspect, the existing classification systems for weak and weathered rocks have been considered to describe the different weathering degree suffered by the rock mass and its influence on some engineering properties.

For a qualitative characterisation of the rock mass it has been decided to refer to the Geological Strength Index (GSI).

The GSI is a system of rock mass-characterisation (Hoek, 1983; Hoek and Brown, 1988) used to determine the rock mass strength and the rock mass deformation modulus. This system provides an estimation of the rock mass properties based on qualitative descriptions of the blockiness of the mass and of the conditions of the joint surfaces. It has been modified over the years (Hoek et al., 1998; Marinos and Hoek, 2001; Marinos et al., 2007) in order to accommodate different geological situations, such as sheared rock masses characterised by a very poor quality and heterogeneous and tectonically disturbed lithological formations. The general chart for estimation of the Geological Strength Index (GSI) for jointed rock masses is shown in Figure 6.1.

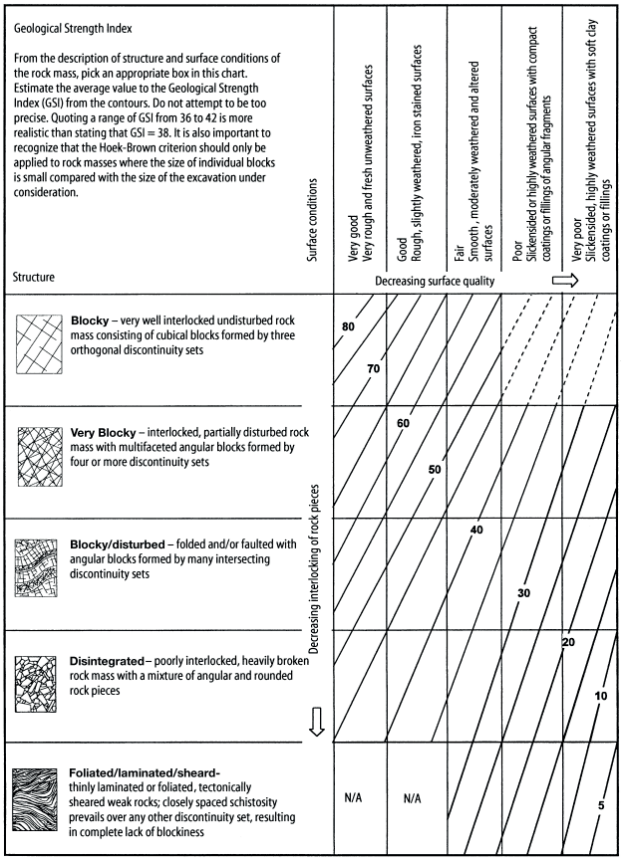

Figure 6.1 The Geological Strength Index for jointed rock masses (Hoek et al., 1998).

The "foliated/laminated/sheared" class shown in the bottom row of the chart consists of rock masses of non-blocky structure with a low strength and a high deformability, where a well-defined persistent and closely spaced lamination (or foliation) is dominant with respect to any other discontinuity set and shows slickensided surfaces characterised by an important weathering degree. Unlike the disintegrated category, where the rock-to-rock contacts govern strength and deformability, the mechanism of deformation in foliated/laminated/sheared class is

controlled by the displacements along the foliation planes and by the shear strength of the fines along the surfaces (Hoek et al., 1998).

The description of foliated/sheared category in the GSI system is very close to the structural and geological characteristics taken into account to define the classes of the classification developed in this work for highly fractured and faulted rocks. In particular, the pre-sheared nature of the rock mass is a condition easily encountered in fault zones. Based on these considerations, extremely low values of GSI (down to 5) have been considered in the characterisation of the identified classes.

In order to take into account the complex nature of a fault zone, often constituted of a combination of material with different characteristics of strength and deformability (rock and soil-like materials), the more recent Geological Strength Index, developed for heterogeneous rock masses (Marinos and Hoek, 2001; Marinos et al., 2007) is particularly interesting because it has been introduced to describe rock masses, such as flysch, composed of frequently tectonically disturbed alternations of strong and weak rocks (Marinos and Hoek, 2000). This new version of GSI (Figure 6.2) refers to the composition and structure of the mass, in terms of tectonic disturbance and alternation of the weaker layers, rather than to the blockiness and interlocking of rock pieces, while the surface conditions of the discontinuities predominantly refer to the bedding planes. A detailed description of the weak and weathered rock masses used in this context is mainly based on this chart where also the tectonic disturbance is taken into consideration.

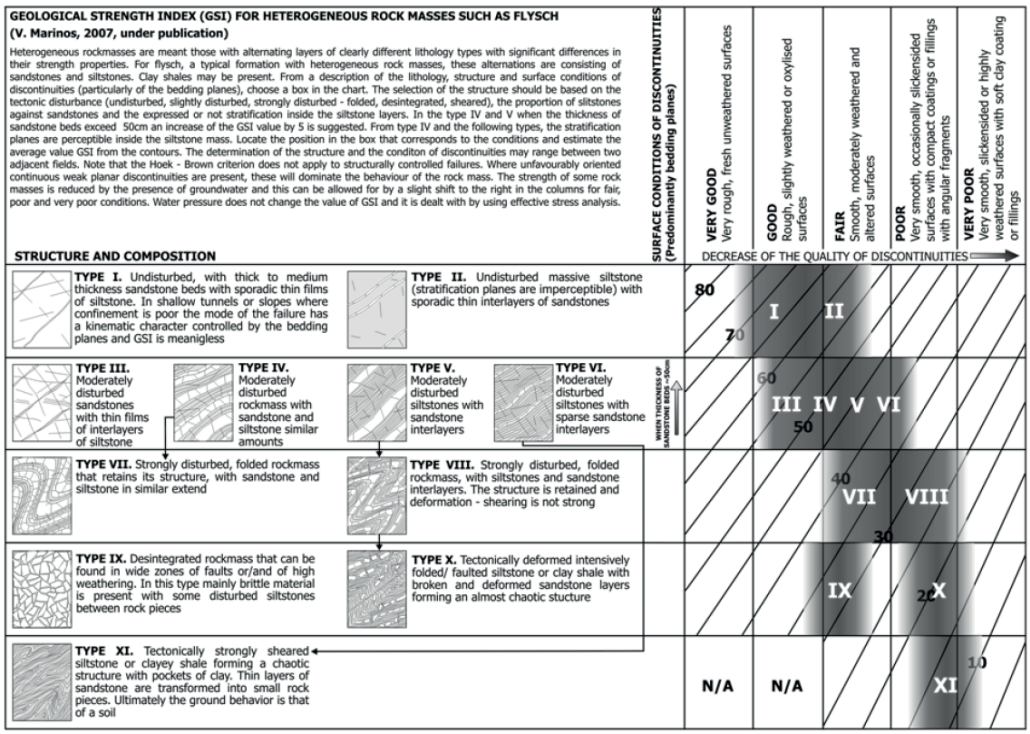

Figure 6.2 The Geological Strength Index for heterogeneous rock masses such as flysch (Marinos et al., 2007).

6.1.3 The water influence (rock mass permeability)

The potential water inflows might strongly influence the rock mass behaviour. While crossing a fault zone, they may vary from low to extremely high mainly depending on the rock mass permeability and porosity. Thus, as previously described (see Chapter 3), a fault zone may behave as a conduct or as a barrier and in some cases as a combined system depending on the fracture network and on the amount of generally less permeable fine-grained matrix (Caine et al., 1996). Moreover, the weathering degree of the rock (and of the joint surfaces) can be a reference parameter in order to describe the potential fluid flow in a disturbed zone since the products of rock alteration (generally fine-grained material) might significantly affect (i.e. reduce) the permeability.

In this framework, the aim is to study the TBM performance in each proposed fault zone category. Therefore, the potential degree of permeability will be qualitatively defined for all classes, in order to identify possible correlated risk scenarios during the tunnelling operations. Since it may significantly affect the excavation also in good ground conditions, the potential water inflow (which may vary from low to high in each class) is not assumed as basic factor in the geomechanical characterisation of the "fault zone" classes, but only as additional aspect. This consideration bases also on the fact that a high flow contributes to the reduction of the TBM performance independently of the class where it occurs.

6.1.4 The depth influence (in situ stress)

The depth has not only an indirect influence on the in-situ stress, but also on the uncertainties characterising hydrological and geotechnical conditions, playing an important role in the definition of potential risks and stability issues in tunnelling. Problematic events are more frequent in weakness zones such as heavily tectonised and fractured rocks characterised by poor mechanical and anisotropic conditions. As reported by Kaiser et al. (2000), the combined effect of rock mass conditions and tunnel depth influences the rock mass behaviour: in rocks of poor quality (RMR < 50), the deeper the tunnel the higher is the risk of encountering difficult environments such as squeezing and/or swelling rock masses. Furthermore, it is also significant to observe that groundwater related problems might have significant impact on excavation hindering with increasing depth (e.g. higher water pressure).

The depth has surely had an important influence in the formation of each "fault zone" type, but this aspect is not taken into consideration for the purpose of the classification which is considering the effects on tunnelling. Thus, in this framework, similarly to the potential water inflows, the depth represents only a secondary factor. This is due to the fact that, dealing with rock masses of poor quality (RMR < 50) in each class, the effect of depth may be the same in terms of stability problems during the tunnelling operations (i.e. it may affect the TBM performance independently of the "fault zone" class).

6.2 Description of fault zone classes

The new classification methodology introduced in this research for describing the effect of disturbed zones on the TBM performance, takes into consideration the fracturing degree and the

weathering degree of the rock mass as most representative factors. The potential water inflows and depth will be considered only as complementary parameters since they can affect tunnelling operations (and thus the TBM performance) also outside from a fault zone. Thus, based on these considerations and on the review performed in Chapter 3, four classes have been introduced: they will be the basis for the TBM performance analyses which will be presented in the next Chapters. In the following sections the classes will be described and characterised from a geomechanical point of view, by identifying for each of them the most significant parameters as well as representative intervals of values.

6.2.1 Class I: highly fractured rock masses

The first class consists of rock masses characterised by a high fracturing degree without visible sign of weathering of the rock material. Though the original fresh rock and the discontinuity surfaces might be affected by a slightly discolouration, the geomechanical properties of the intact rock are not subjected to any alteration. The "mechanical degradation" (i.e. fracturing and potential opening of the joints) is therefore the only involved process, while the "chemical weathering" (i.e. alteration and decomposition of the rock) does not affect the rock mass.

In the first class the fracturing degree can be extremely high, but not enough to describe the rock mass as "crushed and totally fragmented". Thus, since a blocky-structure is still evident, the volumetric joint count (J_v) can be evaluated based on the available information about the number of joint sets and the spacing of discontinuities. According to ISRM recommendations, small (10 joints/m^3 < J_v < 30 joints/m^3) to very small (J_v > 30 joints/m^3) blocks have been considered for charactering this class, in particular:

$$10 < J_v \left[\frac{joints}{m^3}\right] < 35$$

As mentioned before, only if J_v is greater than 35 joints/m^3, the rock mass can be considered as totally crushed, which is not the case of this class.

In Class I the tectonisation degree is not taken into account, therefore, there is no reference to "fault" rocks with respect to the definitions and terminology reported in the literature. For what concerns a more qualitative description of the jointed rocks, this class corresponds to the "very blocky" and "blocky/disturbed" groups reported in Figure 6.1 (where no faulting and folding processes are considered). According to this, GSI varies between 15 and 60, depending on the conditions of the discontinuity surfaces. Moreover, being the weathering degree of the rock negligible, the quality of the joint surfaces is supposed corresponding to fair conditions, i.e. moderate alteration. Thus, based on all these considerations, the variation range for the GSI narrows to the following limits:

$$30 < GSI < 60$$

If the fracturing degree and the slightly weathered conditions of the joint surfaces (and rock) are sufficiently described by J_v and GSI, the uniaxial compressive strength of the rock mass UCS_{rm} (Hoek and Brown, 1997) can be a representative parameter of the class since it takes into account the blockiness of the mass and the weathering degree of the discontinuity surfaces. UCS_{rm} is expressed by the following formulation (Equation 4.10a, Chapter 4):

$$UCS_{rm} = (sUCS^2)^a$$

where UCS is the uniaxial compressive strength of the intact rock, s and a are parameters depending on the geological strength index of the rock mass.

For what concerns the water inflows, due to the well-developed fracture network, this kind of "fault zone" behaves as a "distributed conduit" by referring to the terminology introduced by Caine et al. (1996).

In tunnelling, the main geological hazards linked to this class are related to squeezing phenomena, possible instability of the excavation face, frequent blocks falls and large water inflows due to greater permeability of the rock mass (i.e. extremely high fracturing degree). Thus Class I corresponds to the ground conditions more frequently encountered during excavation, where stability problems often occur and lead to increasing requirements of supporting measures. In Table 6.1 the main characteristics of Class I are summarised.

Table 6.1 Class I: highly fractured rock masses

Fracturing degree	
Small to very small blocks	$10 < J_v$ [joints/m^3] < 35
Weathering degree	
No visible sign of weathering of rock material and/or joint surfaces	$30 < GSI < 60$
Geomechanical characterisation	
Uniaxial compressive strength of the rock mass	$UCS_{rm}=(sUCS^2)^a$
Water inflow	
Distributed conduit	
(Most frequent) tunnelling problems	
Squeezing; instability of the excavation face; block fall; large water inflows	

6.2.2 Class II: highly fractured weathered rock masses

The second class consists of highly fractured rocks with more significant weathering conditions of the rock and of the discontinuity surfaces. The weathering degree may largely influence the geomechanical behaviour of the rock mass and affect its response to excavation. The rocks have undergone certain alteration (in particular along joints, significant discolouration can be observed without signs of material decomposition) and for this reason they can be treated as "weathered rocks".

Regarding the fracturing degree, accordingly to what has been already observed for Class I, a blocky structure characterises the rock mass and it is still possible to evaluate the volumetric joint count on the basis of the joint sets number and frequency. Thus, J_v varies within values

representative of small and very small blocks, and the upper and lower limits are the same of the ones considered in the first class:

$$10 < J_v \left[\frac{joints}{m^3}\right] < 35$$

For what concerns the GSI classification system (Figure 6.1), the worst conditions of the discontinuity surfaces are now taken into account. Thus, the reference to the "poor" category (i.e. highly weathered surfaces) brings down significantly the GSI value that varies now within the following limits:

$$20 < GSI < 40$$

The tectonisation degree, resulting from important faulting processes, is still not taken into account since the chemical weathering introduced here is mainly a consequence of the water action which causes chemical alteration of the joint surfaces. Based on the same considerations made for Class I, UCS_{rm} can be again used as representative parameter since it describes the rock mass strength mainly by taking into account the degree of fracturing and the joints conditions.

For what concerns the water inflows, due to the high fracturing degree, also the rock masses described by Class II mainly behave as a "distributed conduit" (Caine et al., 1996). However, the generally high permeability may be affected by the potential clay filling of the weathered joints that could represent a hindrance to the water flow.

The most common tunnelling risks related to this class are more or less the same encountered in the first class. However, the weathered conditions of the discontinuity surfaces could strongly affect the rock mass strength and stand-up time (e.g. ravelling) leading to stability problems such as rock falls, slides and collapses (e.g. lower shear strength due to clay fillings). In Table 6.2 the main characteristics of Class II are summarised.

Table 6.2 Class II: highly fractured weathered rock masses

Fracturing degree	
Small to very small blocks	$10 < J_v$ [joints/m^3] < 35
Weathering degree	
Significant weathering of joint surfaces	$20 < GSI < 40$
Geomechanical characterisation	
Uniaxial compressive strength of the rock mass	$UCS_{rm}=(sUCS^2)^a$
Water inflow	
Distributed conduit (but the potential clay filling could hinder the water flow)	
(Most frequent) tunnelling problems	
Squeezing; ravelling; block fall/slides/collapses (e.g. lower shear strength due to clay filling)	

6.2.3 Class III: cohesive fault rocks (and heterogeneous rock masses)

This class mainly refers to faulted and tectonised rocks. It represents all the zones where the rock behaviour depends on the intensity of the tectonic faulting, thus where cataclasis occurred. The cohesive cataclastic rocks of Class III are characterised by original rock fragments (clasts) in a fine-grained matrix (Bürgi, 1999). The major parameters describing their mechanical behaviour must therefore consider the significant alteration due to the tectonic faulting which gradually transforms the rock from the original intact state to a completely crushed soil-like material (Habimana, 1999; Habimana et al., 2002). Nevertheless, for Class III only the early stages of this process have been taken into account. The chaotic structure typical of the rock masses of this class (i.e. block-in-matrix) results in a complete lack of blockiness which cannot be anymore characterised by a fracturing degree (i.e. J_v).

Since the weathering (tectonisation) degree remains the main factor for describing the rocks of this class, the new versions of the GSI system, developed for better representing sheared weak rocks and heterogeneous rock masses, have been considered. In particular, Class III is partly represented by the "foliated/laminated/sheared" type of the GSI chart for jointed rock mass (Figure 6.1). As already mentioned, this last GSI category has been introduced for describing rock masses with reduced strength and greater deformability, resulting from significant weathering of the intact rock and intense shearing along the lamination or foliation planes (Hoek et al., 1998).

At the same time, Class III can be described by referring to some categories defined in the GSI chart developed for heterogeneous rock masses (Figure 6.2). In particular, rock masses showing a certain deformation after tectonic disturbance (e.g. Type VII, Type VIII, Type IX and Type XI of Figure 6.2) are considered. Regarding the quality of lamination/foliation surfaces, only fair to very poor conditions are supposed, due to the pre-sheared nature of the discontinuities (Hoek et al., 1998). According to these observations, the variation range of GSI in Class III becomes:

$$5 < GSI < 40$$

Since the fracturing degree of the rock (expressed by J_v) is not estimated in this class, the uniaxial compressive strength of the rock mass (UCS_{rm}) cannot be anymore considered for the geomechanical characterisation of Class III. In this framework, the uniaxial compressive strength proposed for cataclastic rocks (UCS_H) by Habimana (1999) and Habimana et al. (2002) is taken into account since it depends on the tectonisation degree quantified by GSI, as expressed by Equation 4.11a (Chapter 4):

$$UCS_H[MPa] = \left(\frac{GSI}{100}\right)^{0.55} \cdot UCS$$

For what concerns the water inflows, it has to be observed that, the permeability of the rock masses described by this class is quite variable. As reported in Chapter 3, if a significant damage zone bounds the fault rocks, a "combined conduit-barrier" behaviour can be assumed.

Regarding the main problems encountered in TBM tunnelling, instabilities in front of the cutterhead, squeezing of the cataclastic material, potential flowing ground, and consequent increase of the pressure on the support represent the most common hazards for the rock masses

described by Class III, where additional heavier support systems and ground treatments are often required. In Table 6.3 the main characteristics of Class III are summarised.

Table 6.3 Class III: cohesive fault rocks (and heterogeneous rock masses)

Fracturing degree	
Faulted and tectonised rocks → blocks-in-matrix structure → no blockiness	
Weathering degree	
Significant weathering (tectonisation) → "new version" of GSI	$5 < GSI < 40$
Geomechanical characterisation	
Reduced uniaxial compressive strength (Habimana et al., 2002)	$UCS_H=(GSI/100)^{0.55} \cdot UCS$
Water inflow	
Variable permeability of the rock mass → combined conduit-barrier	
(Most frequent) tunnelling problems	
Squeezing; flowing ground; instabilities in front of the cutterhead	

6.2.4 Class IV: crushed fault rocks

This last class takes into account the tectonically crushed fault rocks and disintegrated rock masses. This condition corresponds to the highest degree of tectonisation which entails a soil-like behaviour of the material and can be characterised by a non-cohesive nature. This class groups the rocks which encountered the highest level of mechanical and chemical degradation processes (i.e. significant worsening of the geomechanical properties).

As for Class III, the volumetric joint count (J_v) cannot be evaluated, but, according to the description given in section 6.2.1, totally crushed rock masses can be supposed for J_v greater than 35 joints/m^3. It is important to underline that this value is only an assumption because there is no enough information for an accurate estimation. As a matter of facts, the extremely high fracturing degree and no more evident discontinuity sets result in a total absence of blockiness.

In this context, the term "tectonisation" refers both to a significant mechanical fragmentation and to an important weathering of the rocks. This class corresponds to the poorly interlocked and heavily broken rocks included in the "disintegrated" category of the GSI chart (Figure 6.1). In particular, by considering the new version of GSI for heterogeneous rock masses (Figure 6.2), Class IV corresponds to rock masses of Type IX. With regard to the weathering conditions, the quality is supposed to vary from "poor" to "very poor". By combining the previous observations, the variation range of GSI narrows to:

$$5 < GSI < 30$$

As observed in Class III, the UCS_H can be considered as an appropriate parameter for describing the geomechanical behaviour of the rocks included in this class. Based on Equation 4.11a, the

strength of rock can undergo a reduction from 50% to 80% of UCS (depending on the GSI value).

Class IV can be associated to particular categories of fault rocks reported in the literature, specifically "fault breccia" and "fault gouge" (kakirite). As reported in Chapter 3, they are both described as non-cohesive (or slightly cohesive) material, where the main difference depends on the percentage of visible fragments in the rock mass (Sibson, 1977; Bürgi, 1999; Sausgruber and Bradner, 2003).

With regard to the water inflows, it is important to observe that the permeability of the rock masses described by Class IV is strongly related to the lithology of the host rocks. According to Sausgruber and Bradner (2003), a "fault breccia", resulting from the crushing of competent rocks, is characterised by high permeability that entails a significant risk of huge water inflows. On the contrary, a "fault gouge" originated from brittle deformation of incompetent host rocks is characterised by a lower permeability.

For what concerns the most frequent tunnelling problems relate to Class IV, in addition to a high risk of flowing ground, the cohesionless material of a "fault breccia" is subject to sudden and unexpected collapses, while a "fault gouge" is generally characterised by a higher squeezing potential. In Table 6.4 the main characteristics of Class IV are summarised.

Table 6.4 Class IV: crushed fault rocks

Fracturing degree	
Fault breccia and fault gouge → crushed rocks → no blockiness	
Weathering degree	
Highest degree of weathering (tectonisation) → "new version" of GSI	$5 < GSI < 30$
Geomechanical characterisation	
Reduced uniaxial compressive strength (Habimana et al., 2002)	$UCS_H=(GSI/100)^{0.55} \cdot UCS$
Water inflow	
Permeability related to lithology of host rock: higher permeability for competent rock (fault breccia); lower permeability for incompetent rock (fault gouge)	
(Most frequent) tunnelling problems	
Flowing ground and sudden collapses (fault breccia); squeezing (fault gouge)	

6.3 «Fault zone» classes in the TBM-performance database

Figure 6.3 summarises the procedure adopted for identifying the "fault zone" classes according to the description given in the previous sections. In this framework, the mechanical degradation refers to the fracturing degree of the rock. With reference to the field data collected for this research, Figure 6.4 shows the distribution of the "fault zone" classes within the TBM-performance database described in Chapter 4. As it is possible to observe from Figure 6.4, Class

I and Class II (i.e. highly fractured rock masses characterised by different degrees of weathering) represent the most common conditions encountered in the analysed tunnel projects. Based on what has been observed in Chapter 4 and Chapter 5, only tunnel sections excavated by gripper TBM have been considered since the geotechnical/geological information related to the shield TBM data were not enough to identify the different "fault zone" classes.

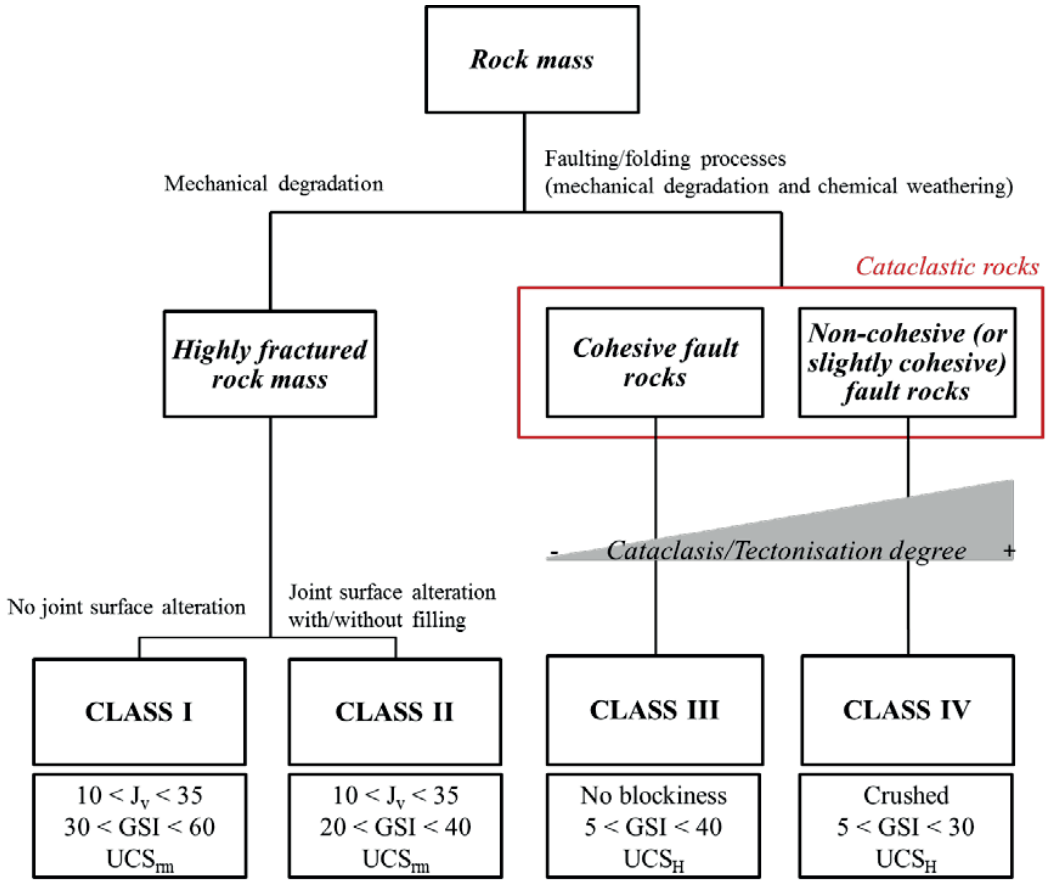

Figure 6.3 The procedure adopted for defining the four "fault zone" classes.

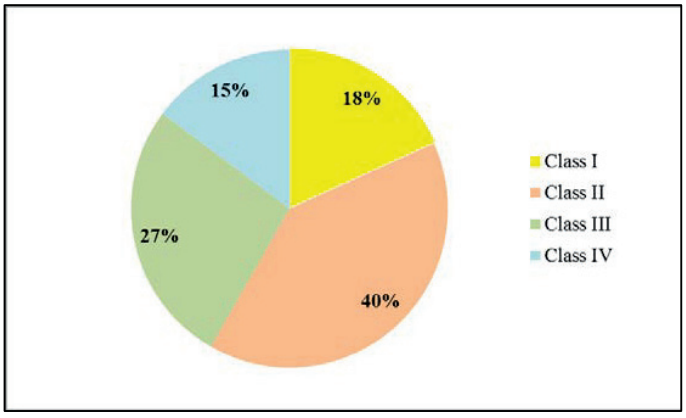

Figure 6.4 Percentages of tunnel sections representing the different "fault zone" classes in the TBM-performance database.

6.4 Numerical modelling of cracking process induced by a TBM cutter in highly fractured and faulted rocks

Since the classification has been developed for characterising the main problems encountered during tunnelling, thus describing the influence of rock degradation on TBM performance, a series of two dimensional numerical models have been performed in order to analyse the rock fragmentation process in a highly jointed and weathered rock mass, by simulating the rock response to TBM cutter penetration in the "fault zone" classes.

6.4.1 Brief state of the art

Generally, in geomechanics, two main approaches can be adopted for modelling a rock mass (Barla and Barla, 2000): the equivalent continuum approach and the discontinuum approach (see also Annex B).

In the equivalent continuum approach the rock mass is modelled as a continuum isotropic medium where the intact rock properties (such as the uniaxial compressive strength) are scaled down to the properties of the rock mass by using well known correlations with the most frequently used rock mass indexes (such as RMR and GSI). After the scaling process a proper constitutive relation, such as elastic or elasto-plastic, has to be adopted for describing the material behaviour. As reported by Barla and Barla (2000), the continuum method consists of two different approaches: the domain methods (including finite element methods and finite difference methods) and the boundary methods (including several types of boundary element methods). In a tunnelling problem, the boundary methods discretise the excavation boundaries while the rock mass is represented as an infinite continuum. On the contrary, in the domain methods, both the medium and the boundaries are discretised and modelled.

In the discontinuum approach the rock mass is modelled as a discontinuum medium, considering the blocky nature of the system characterised by rock matrix and discontinuities. Each block, which may be either rigid or deformable, interacts with the neighbouring blocks and large displacements may take place along the contacts. The discontinuum approach includes the family of Discrete Element Methods which (Cundall and Hart, 1993) define as those that allow finite displacements and rotations of discrete bodies (including complete detachment) and recognise new contacts automatically as the calculation progresses. The Distinct Element Method (DEM) belongs to the family of Discrete Element Methods. Besides simulating large movements in jointed rock masses (Cundall, 1971) and granular assemblies (Cundall and Strack, 1979), it has been also applied to a discontinuum medium modelled as discs in two dimensions or spheres in three dimensions (Bonded Particle Method) (Potyondy and Cundall, 2004). There are three main issues related to the application of DEM: the representation of contacts (discontinuities); the description of solid material (blocks) and the detection of new contacts during execution. Each block of the discretised domain is subjected to forces arising from the contacts, if any, from the surrounding blocks and from internal forces (e.g. gravity) and its displacement is governed by Newton's second law of motion (Bobet, 2010). A DEM code (such as UDEC, 3DEC PFC of Itasca®) is based on a dynamic (time domain) algorithm which solves the equation of motions by an explicit finite difference method. The choice between continuum and discontinuum modelling depends on the size (scale) of the discontinuities

(mainly the joint spacing) with respect to the size (scale) of the problem investigated (Bobet, 2010). At the design analysis stage, if the rock mass response to the excavation of a tunnel has to be predicted, the decision may be also based on the study of the likely mechanism, such as sliding along joints or block movement and rotation (Barla and Barla, 2000).

Both continuum and discontinuum numerical methods have been already used for simulate the rock fragmentation under the action of an indenter. Wang and Lehnhoff (1976) investigated the penetration of a blunt point, sharp wedge and cylindrical bits, using a finite element model, in which elements with variable stiffness were used to simulate the progressive strength failure of the rock. According to their results, a wedge bit, with the action of the inclined bit surfaces, shows a more efficient transmission of the lateral pressure to the side elements, resulting in an early chip formation and in a more effective bit penetration. Cook et al. (1984) experimentally analysed and employed a linear axisymmetric elastic finite element model to study the fracture process in a strong, brittle rock by a circular, flat-bottomed punch. They concluded that failure might occur either in tension or in compression. The numerical results (in agreement with the laboratory experience) showed that, at low confining stress, the region of tensile failure extends completely beneath the tool edge, while, for higher confining stress, it affects a zone adjacent to the tool edge corners developing downwards in a subvertical direction as the punch load increases. The authors highlighted that, immediately beneath the tool edge, the rock does not fail since it is in a state of quasi-hydrostatic compression. Kou et al. (1999) simulated the action of a non-symmetrical tool in heterogeneous rock. Furthermore, Chiaia (2001) simulated the penetration of a hard cutting indenter in heterogeneous materials, by means of a lattice model implemented in a FEM program. According to his results, plastic crushing and brittle chipping would be the dominant failure mode characterising the indentation process. Other simulation of brittle material penetration by high speed hard projectile using FEM and FDM methods were also described by Hanchak et al., (1992) and by Resnyansky (2002). In order to reproduce progressive rock fragmentation process characterising indentation, Liu et al. (2002) developed a numerical code R-T^{2D} (Tock–Tool interaction) where the failure process of the rock was simulated through a realistic cracks pattern. Innaurato and Oreste (2001) and Innaurato et al. (2007) modelled the rock-tool interaction and the rock breaking and chipping processes under high stress confinements. They pointed out the importance of the relative position between the disk cutter and a confinement-free area which simulates the formation of a groove near the tool. For what concerns discontinuum modelling of the fragmentation process, less examples can be found in the literature. (Gong et al., 2005 and 2006) employed DEM in order to study the rock-tool interaction and the chipping process. In the proposed model, the influence of joint spacing and orientation on the TBM penetration rate is investigated by simulating a portion of the tunnel face with one joint family. The obtained numerical results were in good agreement with the field observations. Other attempts were made for simulating the rock cutting process. For example, Su and Akcin (2011) tried to predict tool forces by modelling cutting tests in PFC^{3D}, with the aim to improve the performance prediction of the mechanical excavation. Onate and Rojek (2004) studied the rock fragmentation process by combining DEM and FEM models. Finally, Rojek et al. (2011) compared experimental data and numerical results obtained by simulating the rock cutting process under the action of roadheader picks.

6.4.2 Two dimensional discontinuum analyses

Model generation

In order to investigate the effects of high fracturing degree on the rock fragmentation process, in this framework, two dimensional numerical simulations have been performed by means of the DEM. The 2D Universal Distinct Element Code UDEC (Itasca®) has been used. As already reported, UDEC is a discontinuum code where the rock mass is treated as an assemblage of discrete blocks, which can be considered rigid or deformable, separated by joints.

As also previously done by Gong et al. (2005 and 2006), in this work the rock blocks are simulated as a deformable material and the Mohr-Coulomb yield criterion has been considered for describing their failure. With the aim to reproduce as closely as possible the rock mass conditions observed on a real tunnelling site, the material characterisation has been done by using results from laboratory tests performed on gneiss rock samples (i.e. the most frequent lithology present in the database described in Chapter 4) and reported by Ziegler et al. (2008) and Vuilleumier et al. (2006). The geomechanical properties are summarised in Table 6.5.

Table 6.5 Geomechanical properties of the rock material (rm)

Bulk density [kg/m^3]	2700
Young modulus, E [GPa]	30
Poisson ratio, ν	0.3
Bulk modulus, K [GPa]	25
Shear modulus, G [GPa]	11.5
Cohesion, $c_{(rm)}$ [MPa]	10
Friction angle, $\varphi_{(rm)}$ [°]	40
Tensile strength, $\sigma_{t(rm)}$ [MPa]	8
Dilation angle, $\psi_{(rm)}$ [°]	10

The bulk modulus (K) and the shear modulus (G) have been computed with Equations 6.1 and 6.2.

$$K = \frac{E}{3(1-2\nu)} \quad 6.1$$

$$G = \frac{E}{2(1+\nu)} \quad 6.2$$

For charactering the joints, in agreement to what has been done by Gong et al. (2005 and 2006), the Coulomb slip model has been considered, thus simulating elastic-perfectly plastic behaviour. The joint friction angle has been recovered from about 113 direct shear tests executed on several types of gneiss samples (i.e. paragneiss, migmatic gneiss, muscovite-gneiss, hornblende gneiss,

biotite gneiss, mica-gneiss) both on natural and artificial joints and compiled in a database at the Rock Mechanics Laboratory (LMR at EPFL). Figure 6.5 shows an histogram plot of the residual friction angle indicating the mean, mode, minimum, maximum values as well as the standard deviation In this framework the mean value (i.e. φ=30°) has been considered for characterising the joint shear strength.

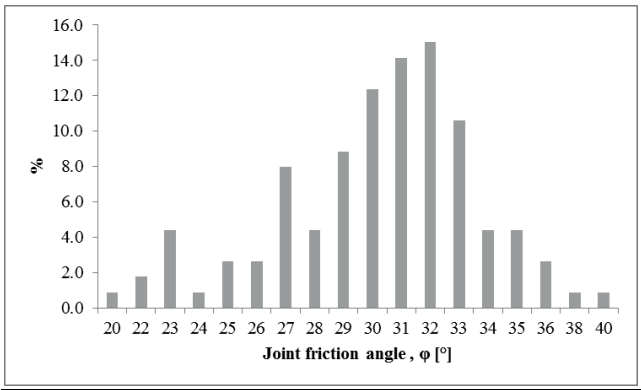

Minimum value [°]	20
Maximum value [°]	40
Mean value [°]	30
Mode value [°]	32
Standard deviation [°]	5.6

Figure 6.5 Histogram plot for friction angle derived by 113 direct shear tests performed on metamorphic rocks samples at the LMR-EPFL and compiled in a specific database.

In the model, the joint normal and shear stiffness (k_n and k_s) define the deformability characteristics of the discontinuities. In particular, k_n describes the rate of change of normal stress with respect to normal displacement (Equation 6.3) and k_s describes the rate of change of shear stress with respect to shear displacement (Equation 6.4) (Bandis et al., 1983):

$$k_n = \frac{\partial \sigma_n}{\partial v} \tag{6.3}$$

$$k_s = \frac{\partial \tau}{\partial u} \tag{6.4}$$

where σ_n is the normal stress, v is the normal displacement, τ is the shear stress and u is the shear displacement. The selected stiffness values must also respect the numerical constraint imposed by UDEC solver algorithm expressed by Equation 6.5 (Itasca, 2011):

$$k_n \; and \; k_s \leq 10.0 \left[max \left(\frac{K + 4/3G}{\Delta z_{min}} \right) \right] \tag{6.5}$$

where K and G are the bulk and shear moduli of the block material and Δz_{min} is the smallest width of the zone adjoining the joint in the normal direction. According to Equation 6.5, the joint normal and shear stiffness should be kept smaller than ten times the equivalent stiffness of the stiffest neighbouring zone in blocks adjoining the joint. In the presented models the

maximum equivalent stiffness of the zones is more than 5000 GPa (with Δz_{min} = 0.005 m), therefore the numerical constrain is respected. Although the joint stiffness does not seem to affect significantly the results of the models developed in this research (i.e. the chip formation under the cutter force), the normal stiffness might strongly influence the contact overlap between the blocks (i.e. the relative displacement). In particular, if the stiffness is too low the overlap becomes too large and the computation cannot be performed. Therefore, in order to avoid large block interpenetration, a fictive higher ("non-physical") value has been chosen to characterise the normal stiffness of the joints (i.e. k_n=100 GPa/m). For what concerns the shear stiffness, the value has been assumed referring to data coming from direct shear tests performed by Delisio (2014) at LMR-EPFL on joints in gneissic rock samples, which fit quite well data coming from the literature (e.g. Kulhawy, 1975).

The parameters chosen for characterising the joints (i.e. the interfaces between the rock blocks) are summarised in Table 6.6.

Table 6.6 Geomechanical properties adopted for modelling the joints (i.e. the interfaces between the blocs in the model) (j)

Normal stiffness. k_n [GPa/m]	100
Shear stiffness, k_s [GPa/m]	0.6
Cohesion, $c_{(j)}$[MPa]	0
Friction angle, $\varphi_{(j)}$[°]	30
Tensile strength,$\sigma_{t(j)}$[MPa]	0
Dilation angle, $\psi_{(j)}$[°]	0

With the aim to reproduce the highly fractured rock masses described by Class I and Class II of the "fault zone" classification, three joint sets are included in each model, by considering values of the volumetric joint count (J_v) between 10 and 35 (i.e. the fracturing degree range assumed for Class I and Class II). In particular, J_v is evaluated on the basis of the discontinuity spacing (Equation 4.8, Chapter 4) which has been supposed variable from 0.25 m to 0.09 m and equal, for a matter of simplicity, for the three joint sets in each model. It is important to observe that, in this framework, any distinction between the two classes is not made. This is due to the fact that the rock fragmentation is analysed at the cutter (tool) scale. As a matter of fact, the main difference of Class II with respect to Class I is represented by the weathering degree of the joints (i.e. absent for Class I and significant for Class II) and this aspect influences the excavation performance mainly at the tunnel diameter scale (i.e. at the TBM-scale) in terms of face and side-wall stability issues.

Similarly to Gong et al. (2006), all the models have a dimension of 0.6 × 0.6 m. The lower, upper and right boundaries are constrained in order to fix the displacements (velocities) along the horizontal (x) and vertical (y) direction and, as it was already done by Gong et al. (2005 and 2006), the cutter is simulated by applying a normal force at mid height of the left boundary (along x-direction) through contact thickness of 15 mm. By considering a maximum thrust per

cutter equal to 300 kN (i.e. according to data compiled in the TBM-performance database, Chapter 4), a reduced force (L_{xx}) of 100 kN (i.e. between 30 and 40% of the maximum value) is used to model the normal cutter load. The force is applied with an increment that can vary according to the fracturing degree from 0.5 kN to 1 kN at each computational cycle (i.e. the higher the fracturing degree the lower the increment). Since the models are only two dimensional, the rolling force of the cutter cannot be taken into account. Figure 6.6 shows the geometry adopted for the simulations (the model with the joint spacing assumed equal to 0.15 m is reported as example).

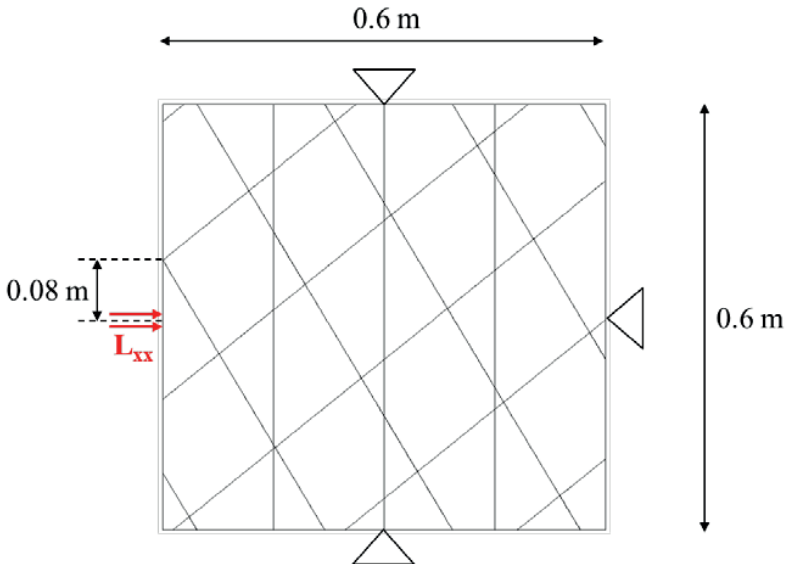

Figure 6.6 Model geometry adopted for the discontinuum analyses.

As already mentioned, and contrary to Gong et al. (2005 and 2006) who studied a single joint set, in this work three joint families with different spacing values have been considered for evaluating the influence of changing fracturing degrees (expressed by J_v) on the chip formation process. By varying the joint spacing in each simulation, six models have been created. The corresponding J_v values as well as the joint orientation are reported in Table 6.7.

The dip direction of the first joint set is chosen in the same direction as the cutter force, while the direction of the second joint set is assumed to be against the direction of the cutter load and the third one is assumed to be sub-vertical (thus perpendicular to the cutter force). The joint dip α represents the angle between the hypothetical tunnel axis (parallel to the cutter load direction) and the joint plane (an example with one joint set is reported in Figure 6.7). As reported by Sanio (1985) and Gong et al. (2005), the cutter penetration is affected by this angle and achieves the maximum value for $\alpha = 60^{\circ}$ when the excavation advances in the same direction of the discontinuity. In all the proposed models it has been decided to maintain the same joint orientation by only varying the joint spacing (i.e. thus by increasing the J_v). Moreover, as it can be seen in Figure 6.6, the joint outcrop is always fixed at 80 mm above the mid-point of the loaded area, assuming this value as the net spacing between two cutters.

Table 6.7 Description of fracturing degree and joint set orientation for each discontinuum model (represented also in Figure 6.6).

Model No.	**J_v [joints/m^3]**	**α [°]**		
		First joint set	Second joint set	Third joint set
1	> 10	60 *(with cutter load direction)*	(-) 40 *(against cutter load direction)*	90 *(⊥ cutter load direction)*
2	15			
3	20			
4	25			
5	30			
6	> 30			

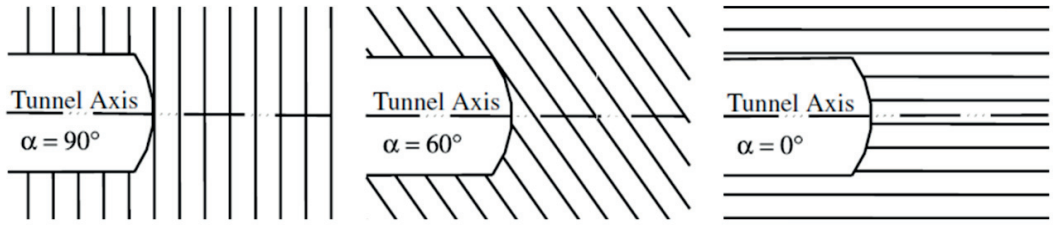

Figure 6.7 Orientation of one joint set with respect to the tunnel axis after (Gong et al., 2005).

Model results

Sanio (1985) affirmed that, as a direct result of high stress concentration, the rock is first crushed in a zone just below the tool, and then the approximate hydrostatic state of stress within the crushed zone causes tangential tensile stresses in the surrounding undamaged rock. Once the tensile strength is attained, tensile cracks start developing from the cutting edge in a radial direction. The chip is formed once these cracks reach the free surface of the rock.

According to Gong et al. (2005 and 2006), it is possible to identify two different modes of the rock chipping process depending on the orientation and spacing of a single joint set:

I. The crack initiates from the crushed zone (i.e. the zone of compressive failure induced by the cutter indentation) and propagates forward to the joint plane.
II. The crack, induced by the tensile failure, initiates from the joint plane and propagates forward to reach the free surface.

In order to observe and analyse the rock crack initiation and propagation, the plastic states are plotted at different iteration steps for all the six models. Figure 6.8, Figure 6.9 and Figure 6.10 show the results obtained for model 1 ($10 < J_v < 15$), model 2 ($J_v = 15$), and model 3 ($J_v = 20$).

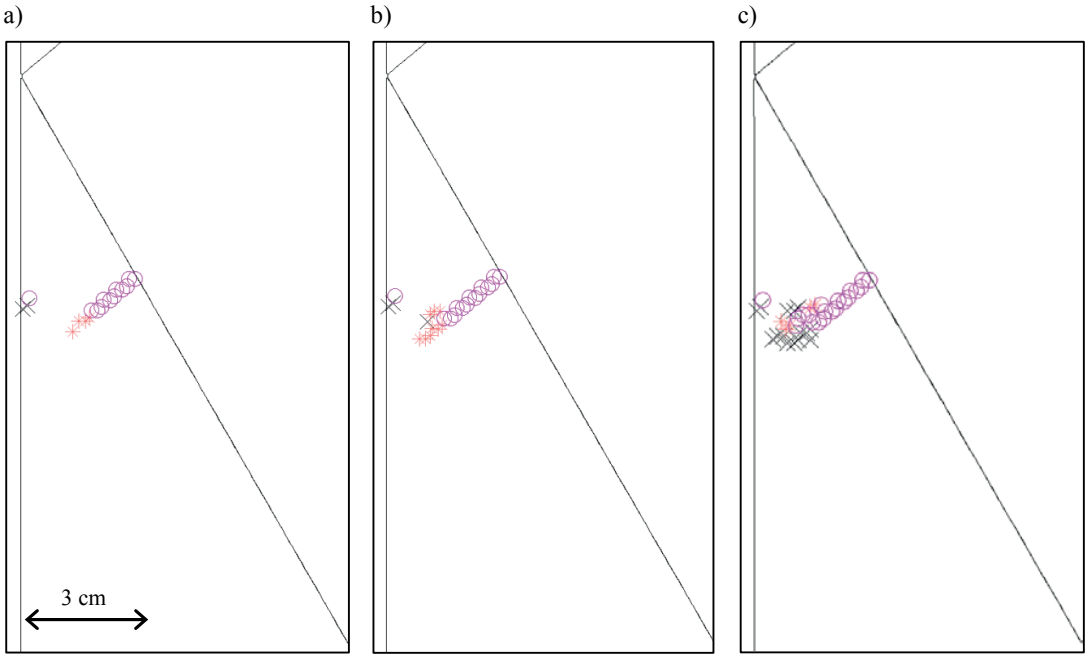

Figure 6.8 Failure status of rock in model 1 at selected step: a) step 300; b) step 400; c) step 600. Circle denotes tensile failure, cross denotes compressive failure.

In agreement with mode II of crack propagation described by Gong et al. (2005 and 2006), after the first load increment, due to the influence of the first joint set ($\alpha = 60°$), the element closest to the joint plane firstly fails (Figure 6.8a, Figure 6.9a and Figure 6.10a). Then, the crack propagates along the zone of tensile failure (Figure 6.8b, Figure 6.9b and Figure 6.10b) and the chip is formed once the free surface is reached (Figure 6.8c, Figure 6.9c and Figure 6.10c). In model 2 ($J_v = 15$), it can be observed from the plotted results (Figure 6.9c) that the tensile cracks are also initiated below the cutter edge. This is probably due to the higher influence of the second joint set ($\alpha = 40°$) characterised by a lower spacing with respect to model 1 ($10 < J_v < 15$). However, the crack below the cutter edge does not occur in model 3, when $J_v = 20$ (Figure 6.10c), although the spacing of the second joint set decreases. A possible reason for this can be the more significant spacing reduction, with respect to model 2, of the first and the third ($\alpha = 90°$) joint set resulting in a different stress redistribution within the block which is immediately under the cutter. This is probably due to the higher influence of the joint planes behind those that delimit the block. It is important to note that, after the first steps, compressive failure occurs immediately beneath the cutter and propagates together with the tensile crack. With the increase of J_v (i.e. joint spacing reduction) in models 4, 5 and 6, this zone of compressive failure does not develop anymore and the chip seems to form exclusively by the propagation of the tensile failure elements. This is in agreement with what has been observed by Gong et al. (2006) for lower spacing of the single joint set.

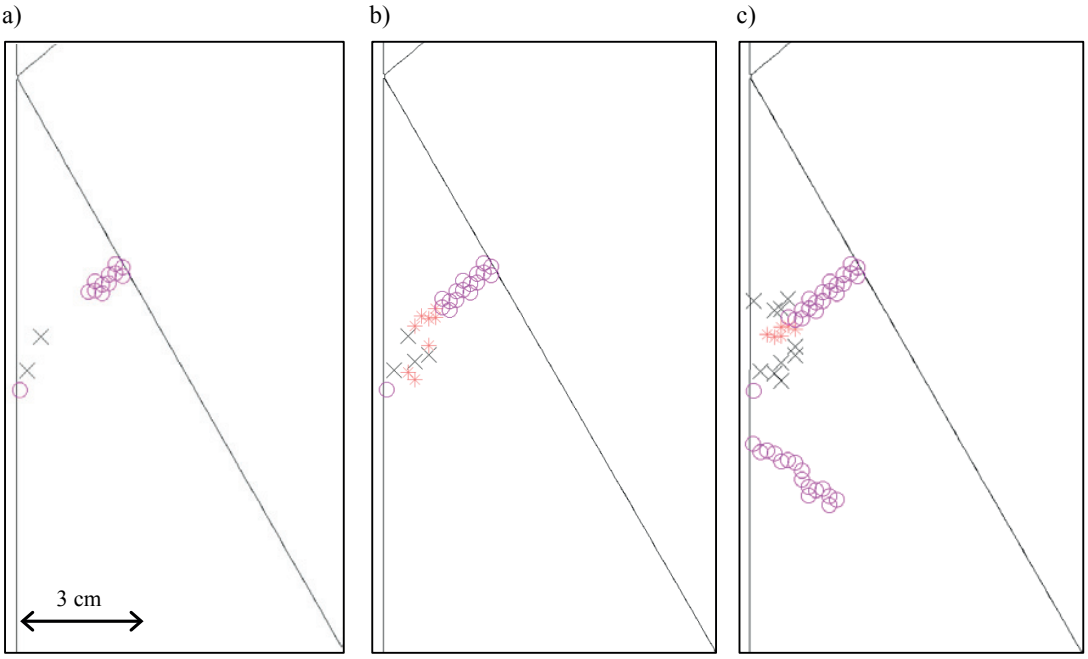

Figure 6.9 Failure status of rock in model 2 at selected step: a) step 200; b) step 300; c) step 500. Circle denotes tensile failure, cross denotes compressive failure.

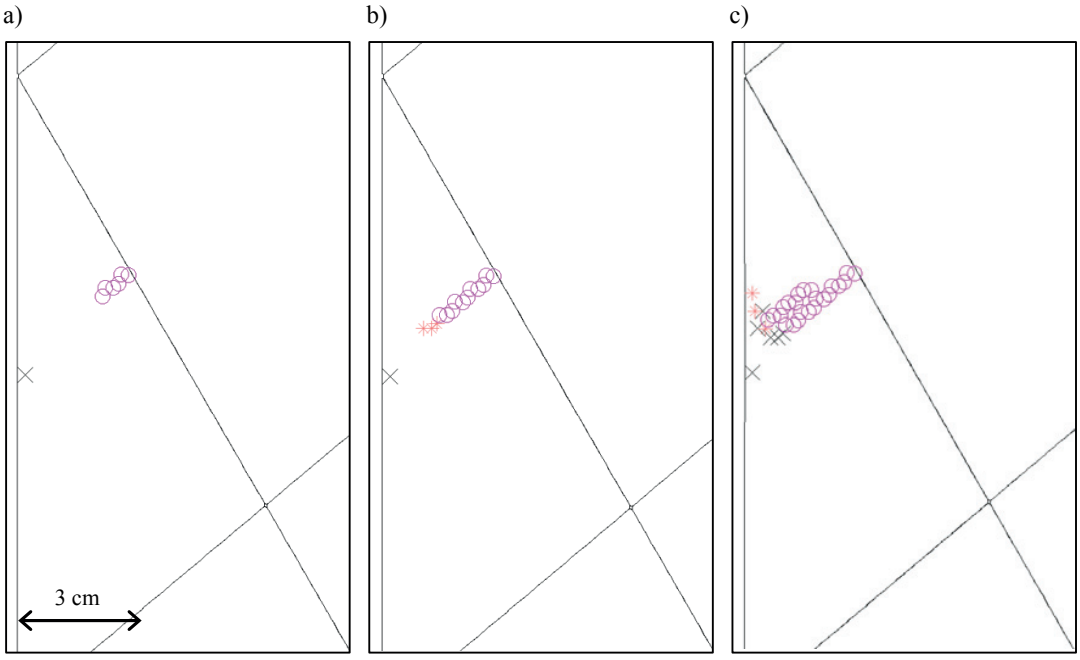

Figure 6.10 Failure status of rock in model 3 at selected step: a) step 200; b) step 300; c) step 700. Circle denotes tensile failure, cross denotes compressive failure.

While for models 1 to 3 a minimal load increment of 1 kN must be applied before the crack initiates , in models 4 (for J_v = 25) and 5 (for J_v = 30), shown in Figure 6.11 and Figure 6.12,

the tensile failures take place at the joint plane (Figure 6.11a and Figure 6.12a) also while the cutter force is kept constant (i.e. without applying any additional increments). As for the previous models, the crack starts to propagate downwards to the free surface (Figure 6.11b and Figure 6.12b) until the chip is formed (Figure 6.11c and Figure 6.12c).

Figure 6.13 shows the simulation results of model 6 (for $J_v > 30$). Also in this case the tensile failures take place on the joint plane, but in this case they initiate from the discontinuity characterised by $\alpha=40°$ (Figure 6.13a). This is due to the fact that, unlike the models 1 to 5, the distance of the mid-point of application of the cutter load from this joint plane is lower than the distance from the first joint set ($\alpha=60°$). As a result, the crack propagates upwards to the free surface forming more quickly a smaller chip (Figure 6.13b) with respect to the other models. Then, under a small increment of load (i.e. 0.5 kN), a second chip is formed, due to the new tensile crack which propagates from the second closest joint plane (Figure 6.13c). This results in a bigger chipping area, actually including two chips instead of only one as observed with the other models.

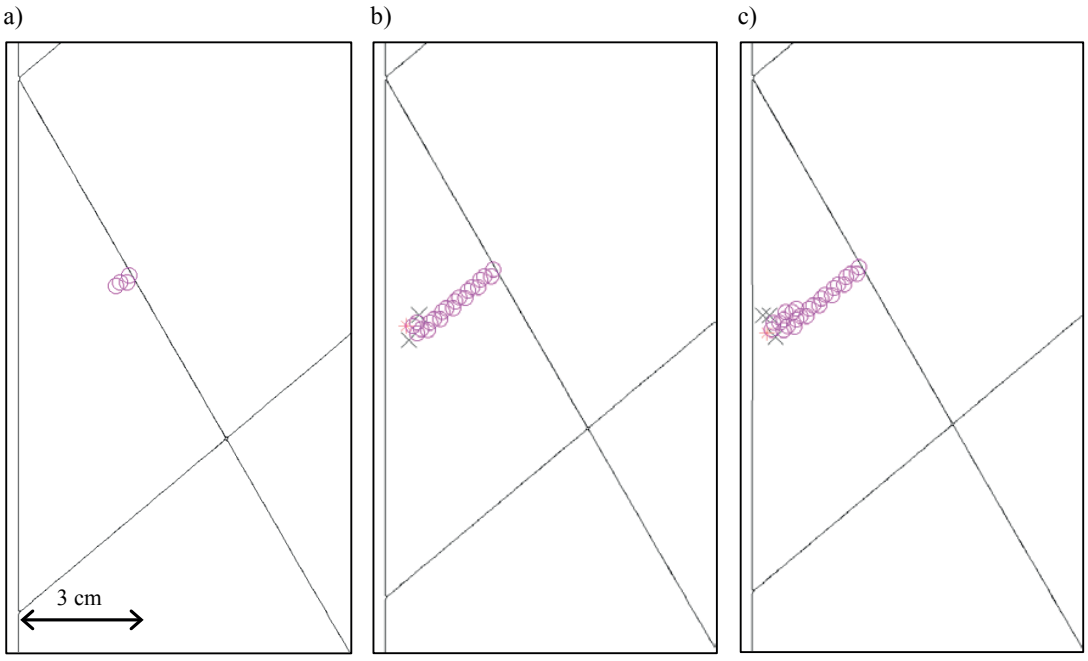

Figure 6.11 Failure status of rock in model 4 at selected step: a) step 400; b) step 700; c) step 1000. Circle denotes tensile failure, cross denotes compressive failure.

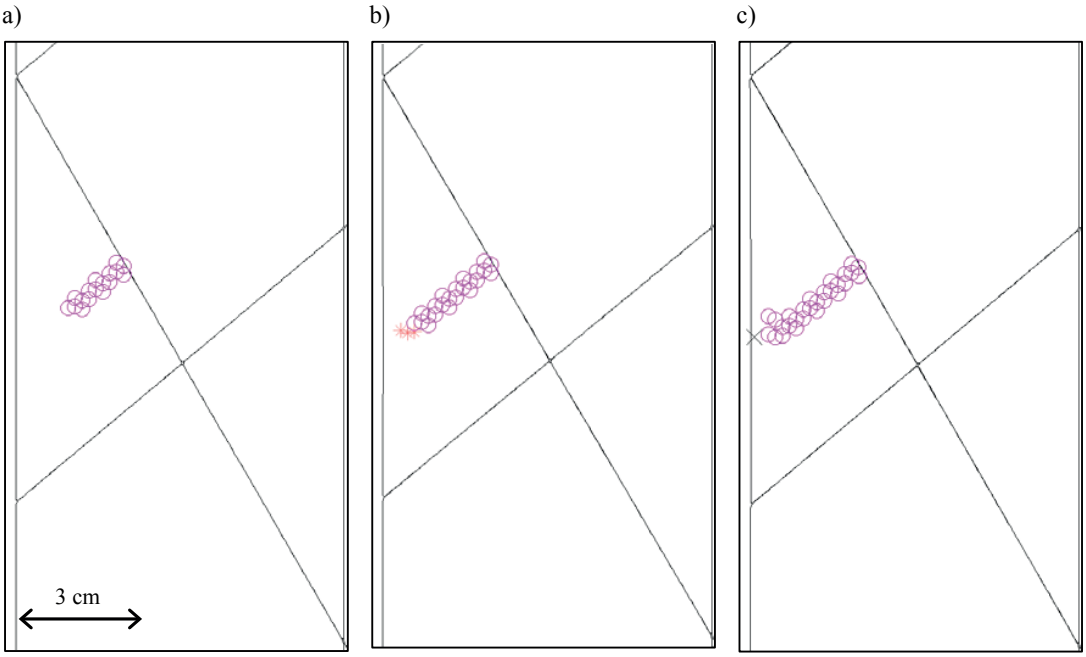

Figure 6.12 Failure status of rock in model 5 at selected step: a) step 400; b) step 700; c) step 1000. Circle denotes tensile failure, cross denotes compressive failure.

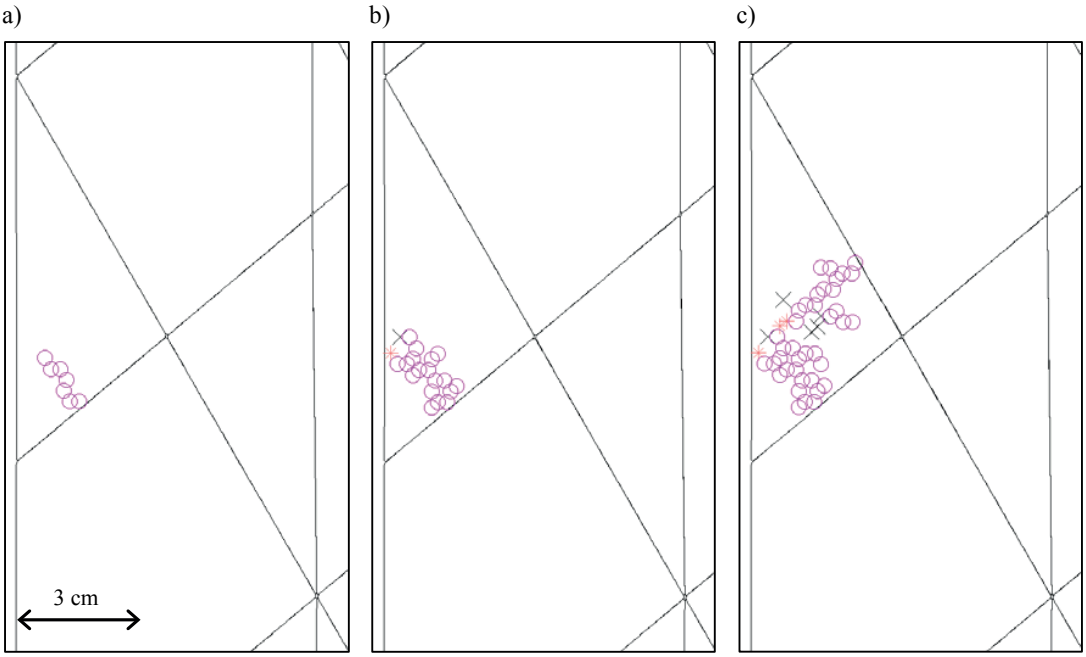

Figure 6.13 Failure status of rock in model 6 at selected step: a) step 1000; b) step 1200; c) step 1300. Circle denotes tensile failure, cross denotes compressive failure.

Figure 6.14 shows the main principal stress contour observed in each model. While in a homogeneous material the stress distribution is almost symmetrical, the stress field induced by

the cutter in highly jointed rock mass is deflected and the deviation seems to change with the variation of the fracturing degree.

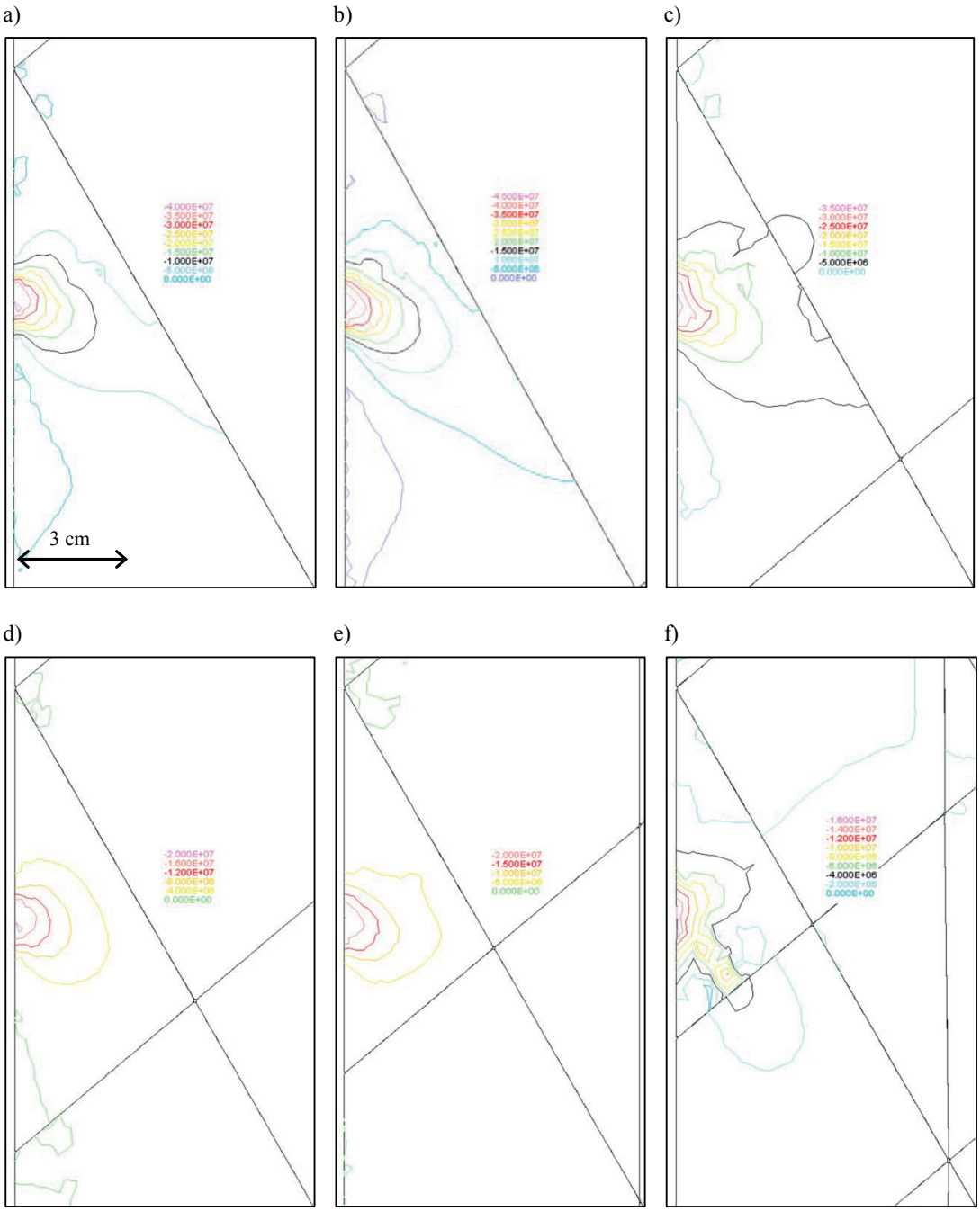

Figure 6.14 Main principal stress contour: a) model 1; b) model 2; c) model 3; d) model 4; e) model 5; f) model 6. Stess is expressed in Pa.

As it can be seen from Figure 6.14, high values of the main principal stresses are always concentrated in the vicinity of the loading area and they decrease with increasing distance from

the cutter. Due to the discontinuities, the stress contour tends to follow the joint plane closer to the loading area (Figure 6.14a and Figure 6.14b). As J_v increases (i.e. the spacing of all discontinuity families decreases), the stress deviation starts to be affected also by the presence of the other joint set, thus the stress contour, being deflected twice, tends to follow the block shape (Figure 6.14c and Figure 6.14d). For higher J_v the stress plot seems to be equally deflected towards the two joint planes (Figure 6.14e and Figure 6.14f) and the location of the tensile cracks becomes quite evident (e.g. the limits of the two chips obtained in model 6 can be easily detected in Figure 6.14f).

In case of lower values of J_v (Figure 6.14a and Figure 6.14b) it is interesting to observe that the stress contour induced by the cutter is interrupted at the joint interfaces. As reported by Gong et al. (2005), the joint plane "protects" from damage the neighbouring block because the failure is unlikely reached due to the non-uniformity in stress transmission at the interface. On the contrary, for higher J_v, the stress transmission seems to occur (Figure 6.14b, Figure 6.14c, Figure 6.14d, Figure 6.14e and Figure 6.14f) making possible the failure of the contiguous block once the cutter load is incremented. This might have an impact on the face stability which, however cannot be studied at this model scale.

6.4.3 Effect of the fracturing degree on the penetration rate

As already suggested by Gong et al. (2005 and 2006), in order to evaluate the penetration rate of the cutter, the chipping area (computed as the chip surface parallel to x-direction) has been estimated for each model as well as the chipping stress, which represents the threshold stress for the crack to initiate and propagate inside the rock. The results are reported in Table 6.8 and the effects of the fracturing degree (J_v) on chipping area and chipping stress are plotted in Figure 6.15 and Figure 6.16. The ratio of chipping area over chipping stress (P_{chip}), reported in Table 6.8, denotes the amplitude of the rock chip per unit cutter force for different J_v values and thus indirectly stands for the cutter penetration rate.

Table 6.8 The effect of J_v on the cutter penetration (P_{chip}), calculated according to previous work done by Gong et al. (2005 and 2006).

Model No.	J_v [joints/m^3]	Chipping stress [MPa]	Chipping area [cm^2]	P_{chip} [cm^2/MPa]
1	> 10	40	11.9	0.30
2	15	45	13.1	0.29
3	20	30	14.1	0.47
4	25	20	13.3	0.66
5	30	20	13.8	0.69
6	> 30	16	15.6	0.98

Both chipping area and chipping stress show good correlation with J_v. The best fitting for the chipping area is provided by a positive power fitting curve (Figure 6.15) that gives a quite good accuracy of the relationship (R^2=0.69). In particular, if the fracturing degree increases also the

chipping area seems to increase. On the contrary, the chipping stress decreases with J_v (i.e. the crack propagation proves to be easier for higher J_v) and the best fit is in this case provided by a negative power function (Figure 6.16), characterised by a very high accuracy (R^2=0.92). As a consequence of the increasing chipping area and decreasing chipping stress, the penetration rate (expressed as P_{chip}) also increases with J_v. The correlation between P_{chip} and J_v is shown in Figure 6.17a and it is characterised by a very good accuracy (R^2=0.95) if approximated by a positive power function. In order to compare the obtained results with the field data included in the TBM-performance database (Chapter 4), the preliminary analyses carried out with the aim to find possible relationships between the rock fracturing degree and the penetration rate in mm/rev (p) of the machine (see Chapter 5) have been used here as a target. In particular, only the tunnel sections classified as belonging to Class I and Class II (thus characterised by J_v values varying between 10 and 35) have been considered (Figure 6.17b).

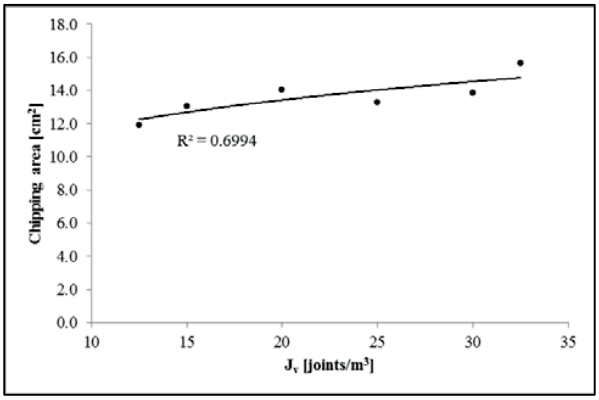

Figure 6.15 Correlation between J_v and the chipping area.

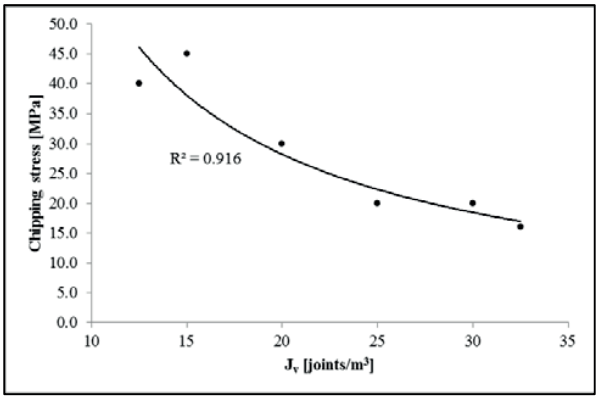

Figure 6.16 Correlation between J_v and the chipping stress.

Although they describe the same process, it is important to emphasize that the physical quantity expressed by the ratio between the chipping area and the chipping stress (P_{chip}) is different from the TBM penetration rate (p) expressed as mm/rev. The aim of this analysis and comparison is just to analyse the trend of the correlation that P_{chip} and p show with J_v. This is also done with the aim to understand if these models are reliable and correctly reproduce the fragmentation process of highly jointed rock masses. Though the different accuracy, the best fitting curve for

both p and P_{chip} is provided by a positive power fitting function (Figure 6.17a and Figure 6.17b). This seems to demonstrate that the significant fracturing degree of the rock generally does not represent a hindrance for the cutter penetration which, on the contrary, tends to increase for higher values of J_v.

As it has been already observed by Gong et al. (2005 and 2006), the simulated results (P_{chip}) represent only the instantaneous process happening when the cutter force is applied on the rock and cannot reproduce the continuous boring process of the TBM nor the interaction with neighbouring cutters. Moreover, it is important to consider that the penetration rate values (p) are based on a more significant amount of data (i.e. field data compiled in the database), characterised by a higher scattering than the results obtained by the numerical simulations.

a)

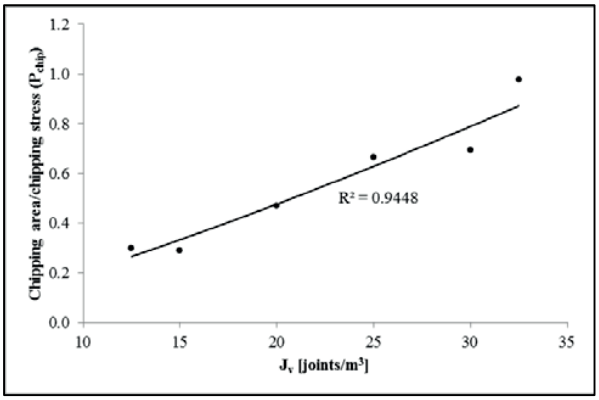

b)

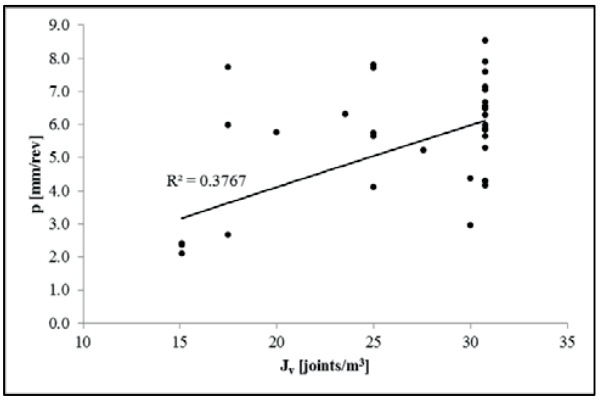

Figure 6.17 Correlation between J_v and the cutter penetration: a) penetration rate expressed as the ratio between chipping area and chipping stress (results of numerical modelling); b) penetration rate expressed as penetration per revolution, from data compiled in the database by considering only tunnel sections identified as belonging to Class I and Class II of the proposed fault zone classification system.

6.4.4 Two dimensional continuum analyses

Model generation

With the aim to investigate the rock fragmentation process in very poor and disturbed rocks representing Class III and Class IV, an equivalent continuum medium has been considered. This choice arises from the fact that the fracturing degree (i.e. J_v) is no longer a reference parameter for describing these two classes (see also sections 6.2.3 and 6.2.4). Therefore, it is not possible to explicitly reproduce the joints as interfaces of well-defined blocks. Although the same code (UDEC) has been used, in this model no joint set has been included. This corresponds to an equivalent continuum finite difference model, where the intact rock properties need to be properly scaled in order to take into account the effect of the extremely disturbed conditions.

According to the description of Class III and Class IV, which consist of tectonised and crushed rocks, the extension of the Hoek and Brown failure criterion to cataclastic rocks, proposed by Habimana (1999) and Habimana et al. (2002), has been adopted for estimating the rock strength in the modelling. As already reported in Chapter 3, the Authors modified the generalised form of Hoek and Brown including a parameter (t), which depends on the mechanical and chemical weathering undergone by rock mass and expressed by the Geological Strength Index (GSI). The suggested failure criterion is reported in Table 6.9 as well as the new variation ranges of the involved parameters which have been partly modified from the previous ones for better reproducing the behaviour of cataclastic rocks.

Table 6.9 The Hoek and Brown failure criterion modified by Habimana (1999) and Habimana et al. (2002). Where: k_p is the passive earth pressure coefficient; m_b and m_i are Hoek and Brown material constant, respectively for rock mass and intact rock; s and a are material constant function of GSI

$\sigma_1 = \sigma_3 + t\sigma_{ci}\left(m_b \frac{\sigma_3}{t\sigma_{ci}} + s\right)^a$	$t = \left(\frac{GSI}{100}\right)^{0.55}$
	$m_b = k_p - 1(m_i - k_p + 1)exp\left(\frac{GSI - 100}{28}\right)$
	$s = exp\left(\frac{GSI - 100}{9}\right)$
	$a = \frac{1}{2}\left[1 + exp\left(-\frac{GSI}{20}\right)\right]$

For the continuum modelling, the new geomechanical properties (Table 6.10) have been evaluated based on the information reported in the TBM-performance database (Chapter 4). Only the tunnel sections characterised by gneissic rocks and associated to Class III and Class IV have been considered. The reduced uniaxial compressive strength (UCS_H, corresponding to the product $t\sigma_{ci}$) is set equal to 49.8 MPa which corresponds to an average value computed by taking into account the considered tunnel sections (i.e. Class III and Class IV). For the Geological Strength Index the average interval (i.e. 10 < GSI < 20) has been assumed.

Table 6.10 Geomechanical properties of the rock material

Bulk density [kg/m^3]	2700
Bulk modulus, K [GPa]	1
Shear modulus, G [GPa]	0.5
UCS_H [MPa]	49.8
m_b	3.29
s	0.0001
a	0.69

Only one model (i.e. model 7) has been developed and it is characterised by the same geometry assumed for the discontinuum analyses, in particular:

- dimension of 0.6 × 0.6 m;
- constrained lower, upper and right boundaries with fixed displacements along x- and y-direction;
- normal cutter force (L_{xx}=50 kN with increment of 0.5 kN at each computational cycle) applied at mid height of the left boundary (along x-direction) through a contact thickness of 15 mm (evaluated according to the real values compiled in the TBM-performance database);
- no rolling force acting on the cutter.

Model results

In Figure 6.18 the plot of the plastic failures observed in model 7 after the simulation are reported at three different iteration steps.

As it can be observed, contrary to what has been obtained with the previous models (i.e. discontinuum analyses), shear failure seems to be the dominant fragmentation mechanism when a weak and degraded rock mass is modelled as an equivalent continuum medium. As a matter of facts, the strength is strongly reduced to account for the material alteration (Class III) and intense degree of fracturing (Class IV). As a consequence, failure is easily attained also for a lower cutter force. The plastic area initiates from the free surface, at the loaded area, and symmetrically expands.

The main stress contours (Figure 6.19) are almost symmetrical and the value strongly decreases with the increasing distance from the cutter. This is in well agreement with the results obtained by Liu et al. (2002) and Gong et al. (2006) for models studying the cracking process induced by a single cutter in a homogeneous material.

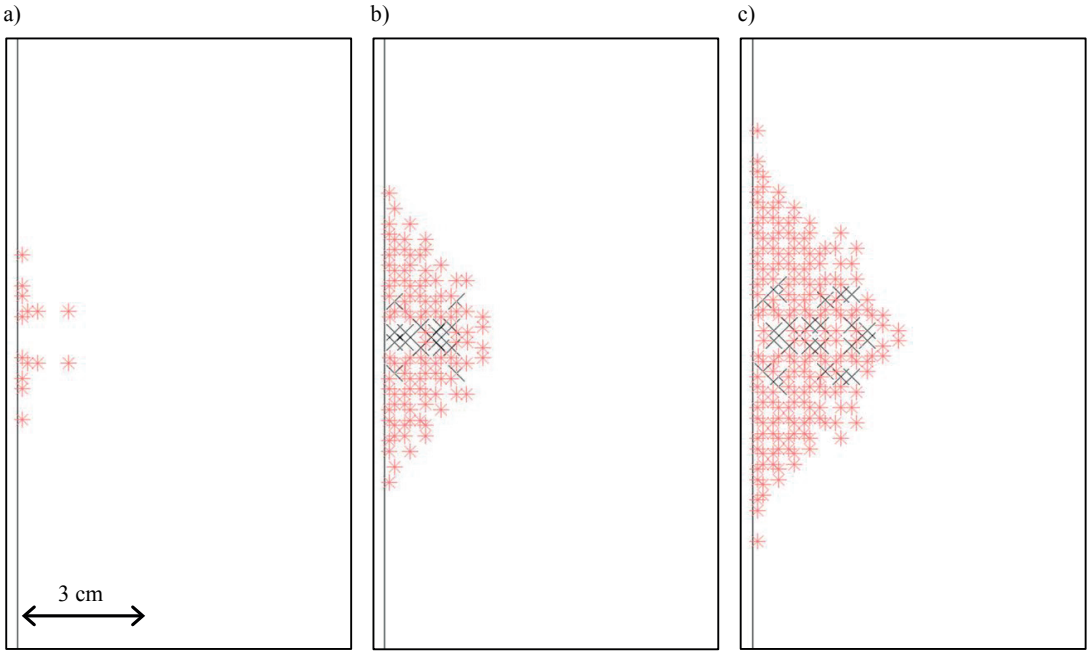

Figure 6.18 Failure status of rock in model 7 at selected step: a) step 10; b) step 30; c) step 50. Black cross denotes compressive failure (red star denote failure just occurred).

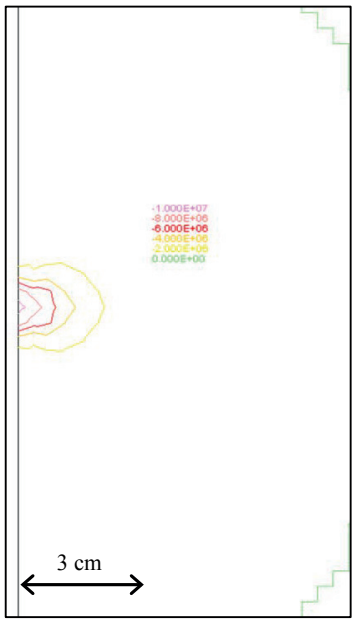

Figure 6.19 Main principal stress contour in model 7. Stress is expressed in Pa.

Also by considering what has been previously observed by several authors (Evans, 1958; Sanio, 1985; Barton, 2000; Liu et al., 2002; Gong et al. 2005; Gong et al. 2006), it can be concluded that the chipping process in rocks characterised by high brittleness and/or discontinuous nature is mainly due to tensile failure. On the other hand, shear failure is a realistic mechanism in continuum plastic material such as soft rock (Barton, 2000) and this behaviour seems to be

confirmed by the results of model 7. In this case, since no tensile cracks propagate from the crushed zone, it becomes impossible to identify and clearly isolate a chip. This seems to confirm the assumption according to which in faulted and crushed rocks at the tunnel face the excavation may not proceed anymore via the usual chipping process, but it becomes mainly a problem of removing material from the tunnel face.

6.5 Final remarks

In this chapter a specific classification system for the fault zones has been proposed, referring to highly fractured and faulted rocks (i.e. extremely difficult ground conditions for TBM tunnelling). The aim of this classification system is to develop a more global approach (i.e. combination of factors instead of specific parameters) for describing these particular environments characterised by a complex and heterogeneous structure. The main goal is to define different fault zone classes in order to study and predict the potential TBM-performance reduction for each of them.

In order to describe the classes, several geological/geotechnical factors have been considered. The selection of these parameters has been done based on the compilation of several sources (reported in Chapter 3) dealing with the geological and geomechanical characterisation of fault zones and fault rocks. In particular, the fracturing degree of the rock mass (expressed by the volumetric joint count, J_v) and the weathering degree of the rock and of the joint surfaces (expressed by the Geological Strength Index, GSI) represent in this framework the principal parameters for describing the characteristics and the behaviour of each "fault zone" class. As a result from these considerations, four classes could be defined:

I. Highly fractured rock mass;

II. Highly fractured weathered rock mass;

III. Cohesive fault rocks and heterogeneous rock masses;

IV. Crushed fault rocks.

The rock masses described by Class I and Class II are characterised by J_v from 10 to 35 joints/m^3 and by GSI respectively from 30 to 60 (Class I) and from 20 to 40 (Class II). The lower boundary values of the GSI range in Class II are due to the worse weathering conditions of the rock and/or of the joint surfaces. Both classes can be described by the Uniaxial Compressive Strength of the rock mass (UCS_{rm}), which actually depends on the UCS of the intact rock and on GSI.

In Class III and Class IV the weathering degree represents the results of faulting and folding activities (tectonisation). The most recent GSI system becomes the main reference factor in order to describe these classes due to the faulted structure (Class III) and to the total absence of blockiness (Class IV) of the rock mass. Moreover, the uniaxial compressive strength proposed by Habimana (1999) for the cataclastic rocks (UCS_H) is introduced for better characterising the rock mass. As a matter of facts, the UCS_H depends on GSI that varies from 5 to 40 in Class III and from 5 to 30 in Class IV, where the highest degree of tectonisation and degradation of the material is reached.

Then, in order to improve the geomechanical characterisation of the "fault zone" classes, both discontinuum and continuum numerical models have been performed. The aim of the numerical modelling is mainly to study the cracking and chipping process induced by a TBM cutter. The excavation performance of a cutter is strongly affected by the rock properties, such as the material strength and brittleness, and by the presence of geological structures, such as discontinuity sets. With reference to the "fault zone" classification, the rock fragmentation induced by a TBM cutter has been simulated both by discontinuum and continuum models. The discontinuum method seems to be the most appropriate approach in order to take into account the influence of the discontinuities on the chipping process (Class I and Class II). On the other hand, when the degradation of the material assumes a leading role in the characterisation of the rock mass and when the joint sets are not evident anymore (Class III and Class IV), an equivalent continuum medium (with reduced strength parameters) better simulates the poor quality of the rock mass.

The input parameters for the simulations have been defined based on data compiled in the TBM-performance database described in Chapter 4 and on laboratory tests previously performed at the Rock Mechanics Laboratory (LMR) at EPFL. For Class I and Class II, modelled as a discontinuum medium, the influence on the chipping area and on the chipping stress of the volumetric joint count (J_v) has been investigated. Therefore, the effects of the fracturing degree (independently from the chosen lithology) on the penetration rate of the cutter have been evaluated. The results seem to confirm what has been obtained in the preliminary analyses reported in Chapter 5. Higher degree of fracturing improves indeed the TBM performance in terms of cutter penetration, since the discontinuities assist the crushing and chipping of the rock during excavation. With increasing values of J_v, the simulated penetration rate (expressed in this framework as the ratio between chipping area and chipping stress) follows the same rising trend as the observed penetration rate (expressed in mm/rev). Due to the higher material brittleness (considered as the ratio between the tensile strength and the shear strength of the rock) of the discontinuum models, it is found that tensile failure seems to be the dominant chip forming mechanism due to the cutter, confirming the results obtained both experimentally and numerically by previous studies. On the contrary, in the continuum models, the rock fragmentation is due to shear failure, due to the important strength decrease of the material. In the continuum simulations the degraded and crushed rock, (Class III and Class IV), is described by new strength parameters reduced according to the failure criterion introduced by Habimana (1999) and Habimana et al. (2002). Moreover, the results show that it becomes impossible to identify a well-defined chip as no evident tensile crack forms and propagates. As a consequence, the estimation of the rate of penetration becomes in this case a very difficult task since the fragmentation process seems to be reduced to a problem of rock removal from the tunnel face.

Chapter 7 Fault zone classes and TBM performance reduction

In this chapter a detailed analysis of the TBM performance has been carried out for each "fault zone" class identified in Chapter 6. In particular, the penetration rate as well as machine advancement reductions have been evaluated with respect to the best and the most frequent performance recorded in favourable conditions. For this purpose a new section of data has been included in the TBM performance database (Chapter 4), compiling information about tunnel sections characterised by good tunnelling and rock mass conditions. Due to the difficulties encountered and described in the previous chapters (Chapter 2 and Chapter 5) by applying the existing TBM performance prediction models to difficult ground conditions (such as highly fractured and faulted rocks), it has been evaluated, for each "fault zone" class, a specific reduction rate to be applied to the TBM performance parameters. The results obtained in this section will be then used for the probabilistic analyses performed in the next chapter.

Based on the observations made in Chapter 4 and Chapter 5, only the data coming from tunnel projects excavated with gripper TBMs have been considered. As a matter of facts, the shield TBM performance parameters do not seem to be significantly affected by crossing disturbed zones (the shield provides protection during excavation). In addition, the available information is not enough in terms of rock mass characterisation (especially with regard to the fracturing degree). Therefore the different "fault zone" classes could not be identified for the projects excavated with this kind of machine.

7.1 TBM-performance database in good tunnelling conditions

Though it is quite difficult to evaluate with exactitude the TBM behaviour in a fault zone, the performance decrease of the machine in difficult ground conditions has been studied with respect to the best and the most frequent (i.e. mode) performance recorded in good tunnelling situations (i.e. normal conditions). Thus, for the same projects already included, the data about tunnel sections excavated in good conditions have been added to the existing TBM-performance database (see Chapter 4). In particular:

1) TBM specifications and TBM performance (RPM, thrust force, p, PR, daily AR);

2) geological-geotechnical characteristics of the rock mass (rock strength, water inflow, fracturing degree, weathering degree of rock and joint surfaces).

In order to choose the sections to be included, attention has been focused on stretches where a total advance rate greater than 15 m/day has been recorded. As a matter of facts, by considering what is reported in literature and the available data, this value seemed to be a reasonable and good compromise to define a lower limit for the advancement rate in normal tunnelling conditions. The chosen sections are generally characterised by unweathered rock masses with low or medium fracturing degree and insignificant water inflows, as detailed here below:

- volumetric joint count (J_v) $\leq$ 20 joints/m^3: massive to slightly fractured/fractured rock mass (see Table 4.7, Chapter 4), where the size of blocks varies from very large to medium, according to the description proposed by ISRM (1978);
- weathering degree almost negligible: the rock mass is described as unweathered or slightly weathered and the rock, defined as very strong or strong (UCS > 60 MPa), is characterised by a "good" or "fair" geomechanical behaviour (see Table 4.8, Chapter 4);
- low water inflows: if present, the amount of water does not exceed 60 l/min.

For each tunnel project, it has been decided to select more or less a number of sections equivalent to the number of sections previously compiled for the bad ground conditions.

The decrease of the machine performance, with respect to the good tunnelling conditions, has been assessed for each lithotype. This allowed evaluating the behaviour of the machine in the same lithotype with changing ground conditions. Table 7.1 shows the average values of daily advance rate (m/day) and penetration rate (m/hr, mm/rev) recorded for different lithotypes in favourable tunnelling situations. Since these values refer to several tunnel projects, each lithotype actually represents a "category" which can be slightly different from project to project. The lithotype "gneiss", for instance, might correspond to crystalline gneiss, gneiss with subordinate micaschist but also to gneiss with minor amounts of quartzite, calc-silicates and/or pegmatite. The best performance is given by the average between the two highest values recorded for each lithotype during construction, while the definition of the "mode" mainly based on the identification of ranges for each TBM parameter. As a matter of fact, due to the fact that each section is characterised by different performances, it is not possible to define a unique "mode" value for any lithotype. The mode value of the TBM-performance parameters, shown in Table 7.1, refers therefore to the weighted average of each range mode. As reported in the previous sections (Table 4.5, Chapter 4), TBM parameters such as PR and p have not been obtained for all tunnel projects, therefore some information is not available (e.g. greenstone). Existing prediction models have been used in order to identify whether it is possible to reliably predict the TBM performance in good rocks. In particular, it has been observed that the average penetration and daily advance rates recorded in good tunnelling conditions fit quite well (Figure 7.1) the performance predicted by the NTNU model (see Chapter 2 and Annex A), developed by Bruland (1998), which considers the fracturing degree of the rock as well as the thrust force of the cutterhead. However, it is important to underline that the predicted values are strongly affected by two main factors: the reduced thrust per cutter and the utilisation factor U. In this analysis, these parameters have been estimated according to most frequent values used in literature.

Table 7.1 Average, best and mode daily AR [m/day], PR [m/hr] and p [mm/rev] for different lithotype classes with good tunnelling conditions

Main lithotype	**Daily AR [m/day]**			**PR [m/hr]**			**p [mm/rev]**		
Gneiss	*Average*	*Best performance*	*Mode performance*	*Average*	*Best performance*	*Mode performance*	*Average*	*Best performance*	*Mode performance*
	22.1	27.7	20.1	1.70	2.02	1.63	5.26	6.25	5.38
Schist	*Average*	*Best performance*	*Mode performance*	*Average*	*Best performance*	*Mode performance*	*Average*	*Best performance*	*Mode performance*
	16.8	23.1	19.9	2.59	2.82	2.74	7.44	8.13	7.86
Limestone	*Average*	*Best performance*	*Mode performance*	*Average*	*Best performance*	*Mode performance*	*Average*	*Best performance*	*Mode performance*
	19.1	24.3	17.4	2.21	2.57	2.05	6.25	7.32	5.96
Granodiorite	*Average*	*Best performance*	*Mode performance*	*Average*	*Best performance*	*Mode performance*	*Average*	*Best performance*	*Mode performance*
	28.5	32.4	28.5	2.27	2.35	2.27	6.33	6.56	6.15
Greenstone	*Average*	*Best performance*	*Mode performance*	*Average*	*Best performance*	*Mode performance*	*Average*	*Best performance*	*Mode performance*
	23.8	31.8	21.9	-	-	-	-	-	-
Amphibolite	*Average*	*Best performance*	*Mode performance*	*Average*	*Best performance*	*Mode performance*	*Average*	*Best performance*	*Mode performance*
	29.7	31.7	31.1	1.76	2.02	1.73	5.74	6.60	5.14

(a)

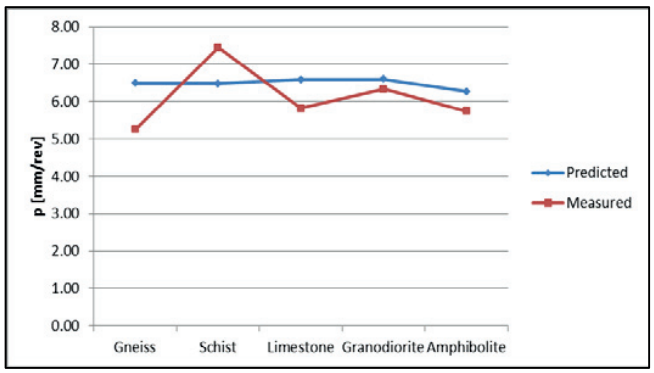

(b)

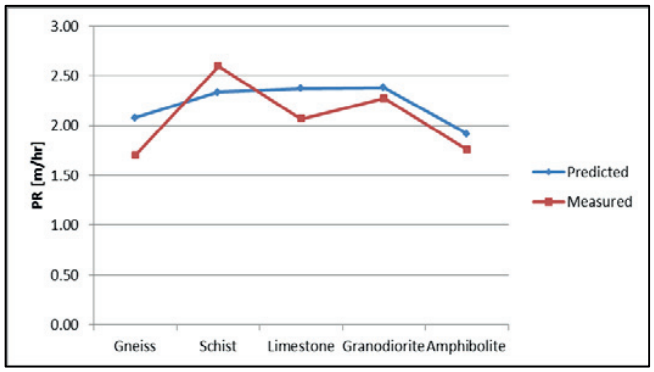

(c)

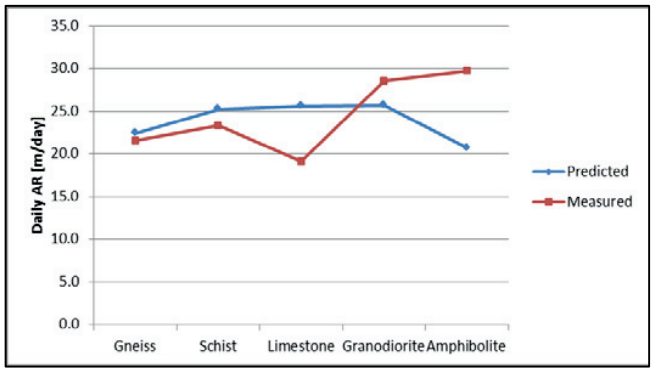

Figure 7.1 Comparison between predicted (by NTNU model, where U is supposed equal to 0.4 and the thrust per cutter is reduced to 80% of the maximum value) and measure TBM performance. (a) Penetration per revolution p; (b) penetration rate PR; (c) daily advance rate (daily AR).

7.2 TBM tunnelling in faulted rocks: the Q_{TBM}

The Q_{TBM} system (see Chapter 2 and Annex A) was proposed by Barton (2000) for extending the TBM performance prediction also to highly jointed and faulted rocks. Based on this observation, the Q_{TBM} seems to be the most appropriate existing method to adopt in the poor ground conditions considered in this research. However, as already underlined in Chapter 2, the great number of parameters (both rock mass- and machine-related) involved in the calculation

strongly limits its application, especially due to the low quality that often characterises the geological and geotechnical information coming from the field. Because of this "practical" limitation, the Q_{TBM} cannot be properly assessed in the tunnel projects studied in this work. However, very simplified assumptions have been considered (i.e. especially for what concerns the joint conditions), but the comparison with the real data did not prove to be meaningful. As it is possible to see from Figure 7.2, the predicted values (circles) seem to underestimate the actual PR recorded during the excavation (crosses).

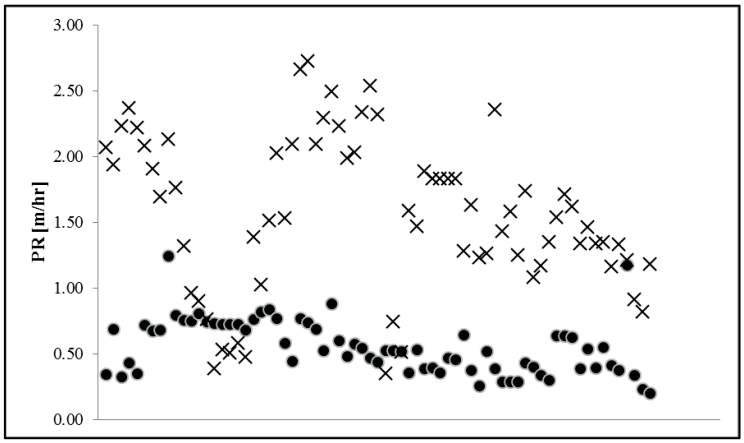

Figure 7.2 Comparison between the actual penetration rate PR (crosses) and the PR predicted by the Q_{TBM} (circles) according to the Equation 2.2 (see Chapter 2). Each cross (circle) represents a tunnel section. This chart refers only to a portion of the collected data, in particular to the tunnel sections where the information about the penetration rate was available (see paragraph 4.2, Chapter 4).

The difficulty to explain the poor correlations between Q_{TBM} and penetration has been already underlined by Sapigni et al. (2002) who did not find reasonable comparisons between actual and predicted performances. Based on statistical analyses on data from tunnel excavated in predominately hard metamorphic rocks, the Authors concluded that Q_{TBM} seemed to show low sensitivity to penetration rate and that the correlation was even worse than the one obtained with conventional Q or other basic parameters like UCS. It must be emphasised, as underlined also by Sapigni et al. (2002), that the reliability of the Q_{TBM} cannot be judged on the basis of a limited number of data (i.e. few tunnel projects with respect to the ones analysed by Barton) and on the basis of not full detailed information. However, the fact that the model takes into consideration too many parameters (some of them affected also by the human experience) represents an important issue to deal with.

7.3 TBM performance reduction analyses

Knowing the TBM behaviour in good excavation conditions, it is possible to estimate the decrease of performance due to difficult conditions. In each "fault zone" class, the penetration per revolution p (mm/rev), the cutterhead rotation speed RPM (rev/min), the penetration rate PR (m/hr) and the daily advance rate AR (m/day) have been "normalised" considering the average values of the best and of the most frequent performance as expressed in Table 7.1 for each lithotype.

Unfortunately, as previously said, while the computation of the daily advance rate has been possible for all tunnel sections included in the TBM-performance database, the values of p, RPM and PR are not available for some sections compiled in the database. However, it is possible to observe that the performed analyses can be always considered representative since data are available for more than 50% of the total tunnel sections included in each class. Table 7.2 shows the "representativeness" of each "fault zone" class per type of TBM parameter analysed.

Table 7.2 Percentages of tunnel sections considered in the estimation of the TBM-performance parameters (per "fault zone" class)

TBM parameter	Class I	Class II	Class III	Class IV
p, RPM, PR	76 %	52 %	61 %	71 %
Daily AR	100 %	100 %	100 %	100 %

7.3.1 Cutterhead rotation speed, RPM

The cutterhead rotation speed strongly depends on the dimension of the machine, therefore, to do a comparison among several different tunnel projects (i.e. characterised by different sizes of excavations diameters) might give not relevant results. For this reason, it has been decided to take into consideration the percentage of reduction with respect to the real (i.e. maximum) value of RPM of the TBM (RPM_{max}).

In Figure 7.3 the decrease of RPM, with respect to RPM_{max}, is represented for each "fault zone" class.

In Class I (Figure 7.3a) the RPM keeps constant for most of the sections where a minor reduction has been recorded. As a matter of fact, more than 80% of sections is characterised by RPM greater than, or equal to, 80% of RPM_{max}, while less than 10% is reduced up to 60% of the maximum value.

A similar behaviour has been observed in Class II (Figure 7.3b), where the high weathering degree of the joint surfaces seems not affecting the RPM of the TBM. However, a certain reduction with respect to Class I has been recorded: less than 70% of sections is characterised by a RPM greater than (or equal to) 80% of RPM_{max}, while more than 10% shows significant decrease with respect to the maximum value (down to 40% of RPM_{max}).

In Class III, i.e. faulted rocks, (Figure 7.3c) the reduction of RPM is more evident. Approximately 70% of sections is indeed characterised by a RPM lower than 80% of RPM_{max} and approximately 40% of them is reduced to values comprised between 40% and 60% of the maximum value.

An important reduction has been observed also in Class IV, described by crushed rock masses (Figure 7.3d). In this case about 40% of tunnel sections keeps the RPM close to the maximum

value, while a same number of sections is characterised by RPM between 40% and 60% of RPM_{max}.

The results obtained for the cutterhead rotation speed clearly show the influence of highly fractured and faulted rocks on the TBM performance, especially in the last two "fault zone" classes, which represent indeed the worst tunnelling conditions. The RPM shows an inevitable reduction in challenging environments (such as crushed rock masses) that hinder operational issues related, for instance, to the efficiency of the muck removal system.

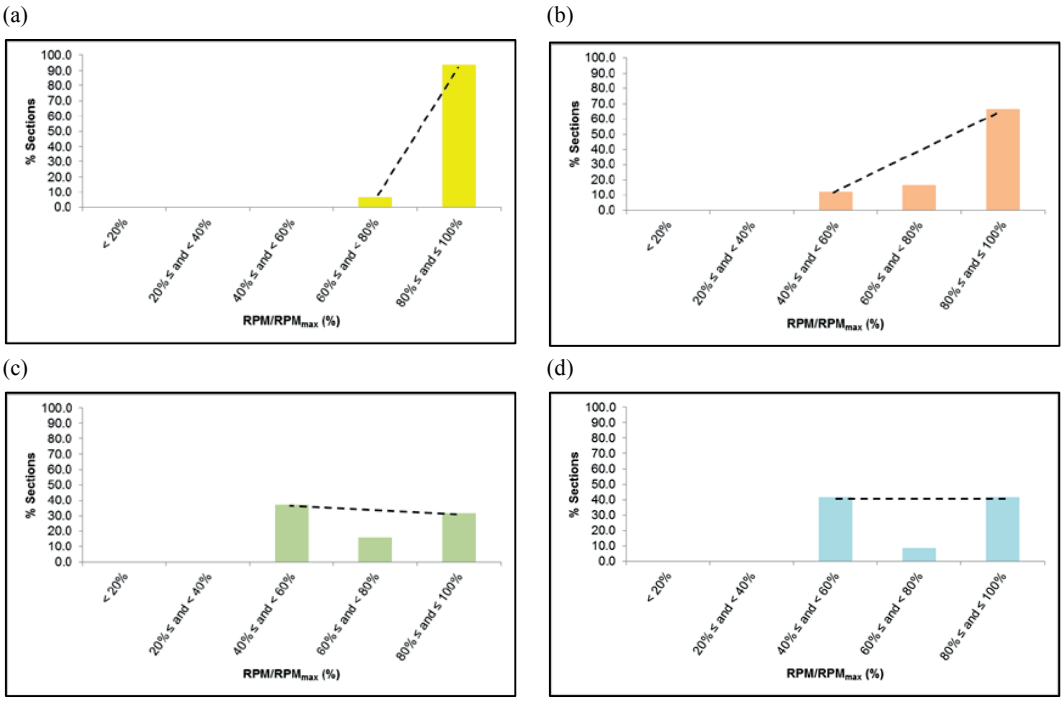

Figure 7.3 Reduction of the cutterhead rotation speed RPM (rev/min) with relation to the RPM_{max} of the machine. The broken line represents the average trend in each class. (a) Class I; (b) Class II; (c) Class III; (d) Class IV.

7.3.2 Penetration per revolution, p

In Figure 7.4 the decrease of the penetration per revolution (p), with respect to the best performance (p_{max}) and the most frequent performance (p_{mode}) recorded in good tunnelling conditions, is represented for each "fault zone" class.

In Class I, i.e. highly fractured rock masses (Figure 7.4a), the majority of the tunnel sections (i.e. more than 60%) is characterised by a p-value approximately equal to the best performance recorded in good tunnelling conditions (p greater than 80% of p_{max}). A reduction of about 40% to 60% is observed for only 10% of sections. This result seems to confirm the theory, already introduced in the previous chapters, that the high number of joint sets generally does not represent a hindrance to the boring process. For what concerns the most frequent (mode) performance recorded in good tunnelling conditions, about 50% of the tunnel sections is characterised by a p-value equal (or even greater) to p_{mode}. A decreasing trend can be observed

down to the range corresponding to 40 - 60% which interests less than 10% of sections. This result does not differ significantly from the p-reduction trend obtained by considering the best performance (p_{max}).

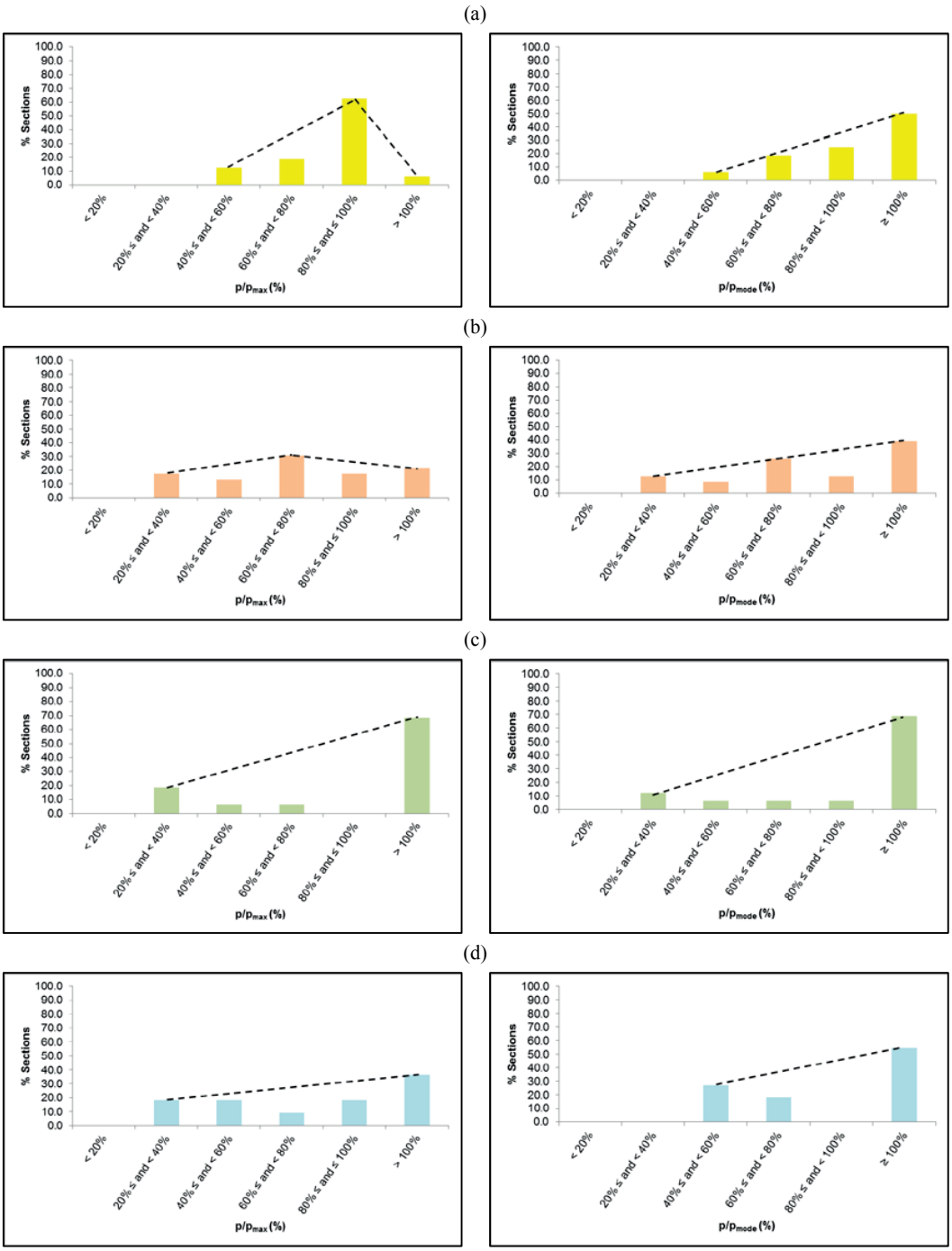

Figure 7.4 Reduction of the penetration per revolution p (mm/rev) with relation to the best performance p_{max} (on the left) and the most frequent performance p_{mode} (on the right) recorded in the same lithotype with good ground conditions. The broken line represents the average trend in each class. (a) Class I; (b) Class II; (c) Class III; (d) Class IV.

Similar results are observed for Class II. However, in this case, more variable values for p have been recorded. As it is possible to observe (Figure 7.4b), about 20% of the tunnel sections is affected by an important performance decrease, i.e. down to 20% of the best performance value. Unlike Class I, only approximately 30% of sections exceeds the 80% of the best performance recorded in good tunnelling conditions. Lower values of p can be explained by the decreased surface quality of the joints (poor and very poor), where a high weathering degree might signify soft clay joints-fillings. Actually, this can represent a problem for the interaction between rock mass and TBM cutters because the excavation may not proceed anymore via the usual chipping process. Also in the histogram describing the p-reduction with respect to the mode performance, about 20% of the tunnel sections is affected by an important decrease. Approximately 30% of sections exceeds the 100% of the reference performance recorded in good tunnelling conditions and more than 20% of sections is characterised by a reduction comprised between 60% and 80%. Compared to what has been obtained for the best performance, a peak shift to the right occurs for Class II. This is obviously due to the fact that the reference value is lower ($p_{mode} < p_{max}$). However, a similar range distribution can be observed in both situations.

Regarding Class III a totally different behaviour has been observed (Figure 7.4c). As a matter of fact, more than 70% of sections is characterised by a p-value greater than (or equal to) 100% of p_{max}. It is important to say that, in this class, the fracturing degree can be no longer considered as a reference parameter. Therefore, though it is not possible to justify the increasing of the penetration with a high number of joint sets, the apparently easier boreability of the rock can be explained by a significant strength reduction due to an intense faulting and folding process. Moreover, concerning the mode performance analysis, a significant peak (i.e. about 70% of tunnel sections) has been observed for the values equal to or greater than p_{mode} recorded in good rocks and approximately 10% of sections is characterised by a reduction down to 80%. This trend is almost equivalent to the one obtained for the analysis done by considering the best performance values, where more than 10% of tunnel sections is characterised by the greatest reduction (from 20% to 40% of p_{max}).

High values of p have been recorded also for the crushed rock masses described by Class IV (Figure 7.4d). As it is possible to observe, about 50% of the tunnel sections is characterised by p greater than or equal to 80% of p_{max}, while, only about 20%, by a reduction comprised between 20% and 40% of the best performance. In this class the rock is characterised by the highest degree of mechanical degradation and chemical weathering, reaching a soil-like state. This almost total loss of strength of the crushed material, seems, on one hand, leading to a better boreability of the rock mass but, on the other hand, could reduce the chipping efficiency. In the histogram showing the mode performance analysis, about 50% of the tunnel sections is characterised by p greater than or equal to 100% of p_{mode}, and about 30% is reduced to 40% of the mode performance. The p-reduction trend obtained for the best performance is almost confirmed. Only a slight increase of the tunnel sections characterised by a value greater than or equal to 100% of the reference performance can be observed as well as the shift to the right of the lowest reduction range. This is again explained by a lower reference value ($p_{mode} < p_{max}$).

Contrary to the effects that bad ground conditions have on the cutterhead rotation speed (RPM) which is affected by the excavation problems at the TBM scale, the results of this analysis clearly show that the penetration of the rock by the cutters (i.e. at the tool scale) does not

represent a particular issue in highly fractured and fault zones. Thus, the recorded p-values are not extremely low since a significant fracturing degree (together with the decrease of the rock strength) generally assists the crushing of the material by the cutting tools at the tunnel face. A similar effect has been observed by Delisio et al. (2013) and Delisio and Zhao (2014) in the case of TBM excavation in blocky rock conditions.

7.3.3 Penetration rate, PR

The penetration rate (PR), expressed as meters per hour, represents the distance excavated by the TBM in a continuous excavation phase. This parameter is a combination of the penetration per revolution (p) and the cutterhead rotation speed (RPM) as expressed by the Equation 4.2b (Table 4.3, Chapter 4).

In particular, if RPM increases (or decreases), PR can significantly increase (or decrease) independently from the value of p. This means that PR does not depend only on the real penetration at the cutter scale (mm/rev), but, being strongly related to the rotational speed of the cutterhead, it represents somehow the penetration at the TBM-scale (without considering downtimes and possible stops of the machine).

In Figure 7.5 the decrease of PR, with respect to the best performance (PR_{max}) and the most frequent performance (PR_{mode}) recorded in good tunnelling conditions, is represented for each "fault zone" class.

In Class I most of the tunnel sections (about 80%) is characterised by PR greater than or equal to 60% of PR_{max} (Figure 7.5a). For more than 50% of them, PR greater than or equal to 80% of PR_{max} has been recorded, while about 10% of sections shows a reduction down to 40% of the best performance. The same considerations already made for the penetration per revolution can be applied in this case: the penetration does not represent a big issue in highly fractured rocks and good performance can be achieved also in these conditions. Moreover, RPM shows a negligible reduction in this class, keeping a value close to RPM_{max} for the majority of the sections. The high values of p are therefore confirmed by the high values of PR. For what concerns, the analysis performed with respect to the mode performance recorded in good conditions, most of the tunnel sections (more than 90%) is characterised by PR greater than or equal to 60% of PR_{mode}. For more than 60% of them, PR greater than or equal to 80% of PR_{mode} has been observed, while less than 10% of sections is characterised by values comprised between 40% and 60% of the mode performance. The high values of p are again confirmed by the high values of PR and the p- and PR- reduction trends are almost the same.

In Class II characterised by a higher variability of p (see Figure 7.4b), the same behaviour is observed also for PR (Figure 7.5b). Also in this case a low percentage of tunnel sections (about 20%) exceeds the 80% of the best performance achieved in good tunnelling conditions. However, a greater reduction is observed for PR with respect to the reduction observed for p. As a matter of fact, more than 30% of sections shows a significant decrease and about 10% of them reaches values lower than 20% of PR_{max}. This reduction is due to the influence of the cutterhead rotation speed (RPM). In the mode performance analysis, 20% of tunnel sections exceeds the 100% of the reference value recorded in good tunnelling conditions but the general reduction trend is very similar to the one observed for the best performance.

(a)

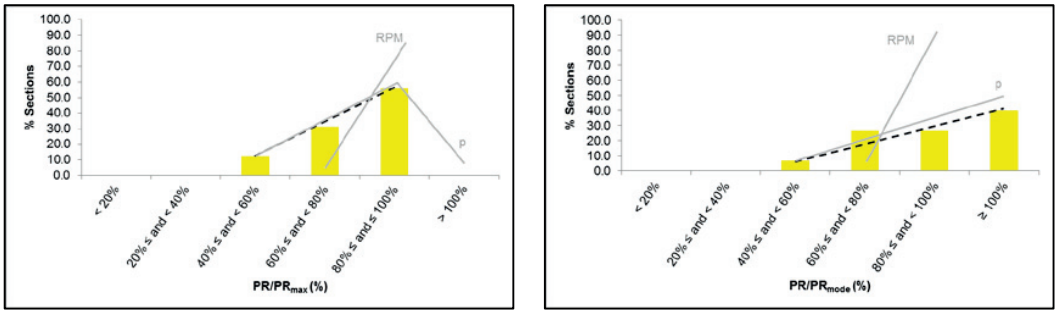

(b)

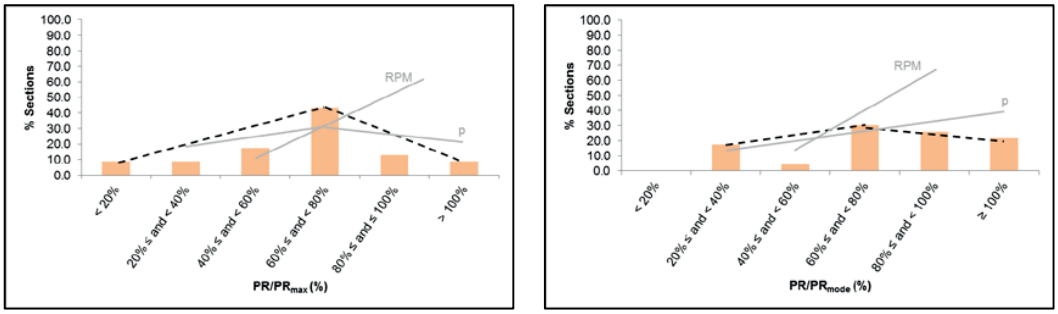

(c)

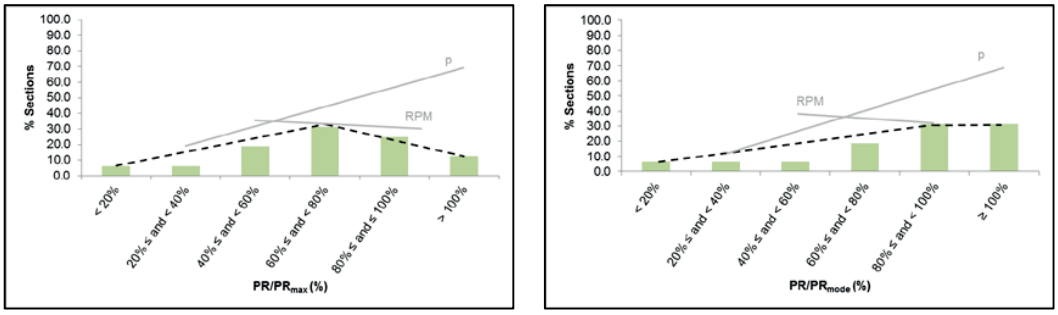

(d)

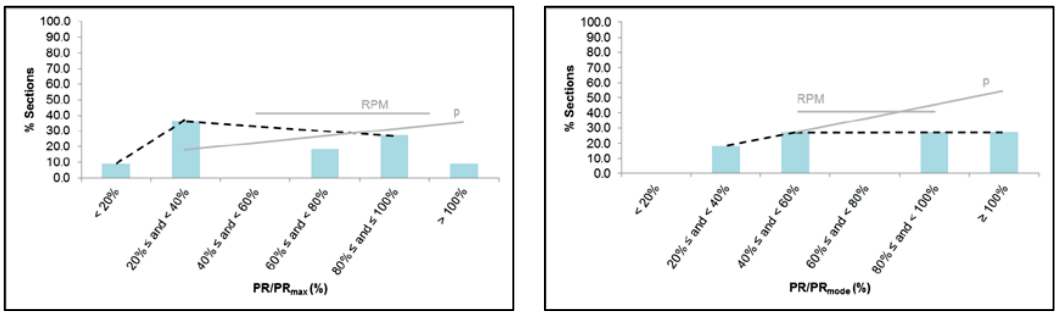

Figure 7.5 Reduction of the penetration rate PR (m/hr) with relation to the best performance PR_{max} (on the left) and the most frequent performance PR_{mode} (on the right) recorded in the same lithotype in good ground conditions. The broken line represents the average trend of PR in each class. The grey lines represent the average trend of p and RPM. (a) Class I; (b) Class II; (c) Class III; (d) Class IV.

In Class III the tunnel sections are characterised by rather high PR (Figure 7.5c). The reduction of RPM observed in this class (see Figure 7.3c) affects the percentage of sections interested by the highest values of PR. For about 30% of sections, values between 80% and 100% of PR_{max} have been recorded, while for p the values even exceed 100% for more than 60% of sections. By considering the most frequent PR (i.e. mode PR) recorded in good conditions, 30% of sections is characterised by values equal to (or even greater than) the mode performance. Some sections show an important reduction, down to reach PR lower than 20% of the PR_{mode}.

In Class IV the values of PR do not reflect what has been observed for p (Figure 7.5d). Despite approximately 30% of tunnel sections is characterised by PR greater than or equal to 80% of PR_{max}, for more than 40% of sections PR shows a strong decrease with respect to the best performance recorded in good conditions, down to values lower than 20% of PR_{max}. Moreover, the clear reduction of RPM in this class seems to affect more PR than in Class III. As a matter of fact, it has been observed that in crushed rocks a greater percentage of tunnel sections is affected by a significant decrease (40% to 60% of RPM_{max}) of the cutterhead rotation speed compared to the one in faulted rocks (i.e. Class III). Regarding the mode performance analysis, more than 50% of tunnel sections is characterised by PR greater than or equal to 80% of PR_{mode} and approximately 50% of sections by PR lower than 60% of the mode performance recorded in good conditions.

The results obtained for the reduction with respect to the mode performance do not differ from what has been observed for the best performance analysis. As a matter of fact, as it is possible to see, though a shift to the right of the histogram peak can be observed, due to the difference between PR_{max} and PR_{mode} ($PR_{mode} < PR_{max}$), the PR-reduction maintains the same trend for each "fault zone" class.

7.3.4 Daily advance rate, daily AR

The daily advance rate (daily AR) is expressed as meters per day and represents the real advancement of the TBM. Since it takes into account also downtimes and stops of the machine, it is probably the performance parameter more affected by uncertainties. Though, by referring to time-construction plans of the projects, it has been possible to exclude from the analyses holiday terms and TBM-maintenance intervals, the daily AR remains a function of the utilisation factor (U) of the TBM (as expressed in Equation 4.3, Table 4.3, Chapter 4) which is affected by several factors (e.g. geological conditions, performance and human component) extremely difficult to be predicted and evaluated. However, a certain trend can be defined for the daily AR reduction in each "fault zone" class.

Figure 7.6 shows the decrease of daily AR, with respect to the daily AR_{max} (i.e. the average value between the two best performances recorded in good tunnelling conditions) and the most frequent performance (i.e. daily AR_{mode}), for each "fault zone" class.

As reported in Table 7.1, unlike the other parameters (i.e. p, RPM and PR), the daily AR has been estimated considering all the tunnel sections included in the database. Therefore, it is the most representative of the collected data. In order to better describe the performance reduction in each class, and thus reach a higher degree of detail, smaller intervals have been considered for this analysis.

In Class I (Figure 7.6a) about 30% of tunnel sections is characterised by a daily AR comprised between 20% and 30% of the best performance (daily AR_{max}) while more than 10% of sections shows a significant reduction, down to values lower than 20%. Daily AR greater than 50% of daily AR_{max} is recorded for approximately 30% of sections, but it does not exceed 70% of the best performance. In the histogram concerning the mode performance analysis, about 30% of tunnel sections is characterised by a daily AR comprised between 30% and 40% of daily AR_{mode} while more than 10% of sections undergoes a significant reduction, reaching values lower than 20% of the mode performance. Daily AR greater than 50% of daily AR_{mode} is recorded for approximately 50% of sections, also exceeding 70% of the mode performance.

Class II shows a different trend (Figure 7.6b), where more than 60% of tunnel sections is characterised by a highly reduced daily AR (lower than 30% of daily AR_{max}). About 40% of sections reaches percentages lower than 20% of the best performance, while about 20% has daily AR comprised between 40% and 60% of daily AR_{max}. There is a very low percentage (about 5%) of tunnel sections where the daily AR exceeds the 90% of the best performance recorded in good conditions. However, this percentage is so low and so distant from the mean value of the class, that it is not taken into consideration for defining the average trend of the daily AR. Regarding the mode performance, approximately 50% of tunnel sections is characterised by values lower than 30% of daily AR_{mode}. About 25% of sections reaches percentages lower than 20% of the mode performance, while about 20% shows daily AR comprised between 30% and 40% of daily AR_{mode}. More than 10% of tunnel sections is characterised by daily AR comprised between 60% and 70% of the mode performance and, also in this case, about 5% of sections shows values greater than 90% of the reference performance in good rock conditions.

In Class III, the reduction of the performance is still evident but differently spread with respect to the first two classes (Figure 7.6c). A specific trend is not visible because the percentages are quite evenly distributed among the tunnel sections. The daily AR does not exceed 50% of the best performance and more than 60% of sections is characterised by values lower than 30% of daily AR_{max}. The lowest values (lower than 10% of the best performance) have been recorded for about 30% of sections. Unlike what has been observed for the best performance, a decreasing trend is visible in the reduction with respect to the daily AR_{mode}, up to reach values comprised between 60% and 70% of the mode value recorded in good tunnelling conditions. Also in this case, the lowest values (lower than 10% of the daily AR_{mode}) have been recorded for about 30% of tunnel sections.

The most significant reduction has been recorded in Class IV where the daily AR proves to be lower than 40% of daily AR_{max} in each tunnel section (Figure 7.6d). However, unlike the faulted rocks, the vast majority of the sections is characterised by values lower than 10% of the best performance (more than 45% of sections). About 90% of the tunnel sections shows values that do not exceed 30% of daily AR_{max}. With reference to the mode value, the daily AR proves to be lower than 50% of daily AR_{mode} in each analysed tunnel unit. Finally, a quite important number of sections (i.e. more than 40% of the total) is characterised by values lower than 10% of the mode performance. About 90% of tunnel sections shows values that do not exceed 30% of daily AR_{mode}.

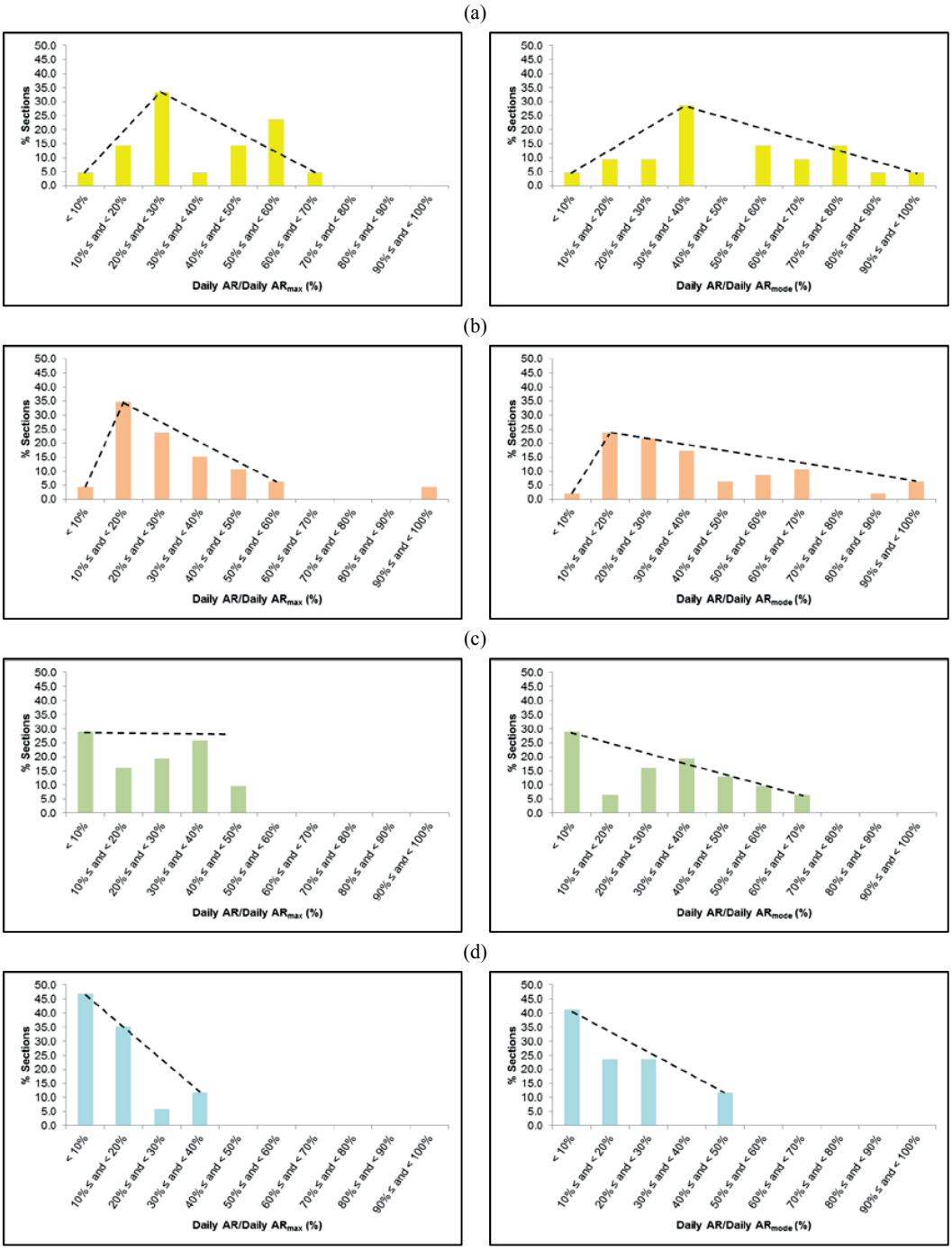

Figure 7.6 Reduction of the daily advance rate AR (m/hr) with relation to the best performance daily AR_{max} (on the left) and the most frequent performance daily AR_{mode} (on the right) recorded in the same lithotype in good ground conditions. The broken line represents the average trend of daily AR in each class. (a) Class I; (b) Class II; (c) Class III; (d) Class IV.

The reduction trends of the daily AR obtained referring to the mode performance recorded in good tunnelling conditions, are very similar to the ones observed in the analysis performed respect to the best performance. Only in Class I a shift to the right of the peak occurs (as already

said, mainly due to the fact that daily AR_{mode} < daily AR_{max}), while in Class III a more definite trend could be identified (in the best performance analysis the reduction percentages are more equally distributed among the sections).

7.4 Result discussion

The results allow affirming that the TBM rate of penetration (expressed as p or PR) does not seem to be the major issue in highly fractured and faulted rock masses. The penetration per revolution (p) does not show any significant reduction with respect to the good tunnelling conditions, quite the contrary, an increase has been even observed in Classes III and IV (Figure 7.7a). As already mentioned, the high fracturing degree, together with the strength reduction undergone by the rock material (especially for Class III and Class IV), seem facilitating the boring process rather than hindering it.

The RPM seems to be more affected by the worsening of the ground conditions. This is certainly connected to the different scale considered for the analyses. In particular, at the tool-scale (i.e. p) the face stability issues do not represent a hindrance to cope with, on the contrary, if the the tunnel diameter scale (i.e. RPM) is considered, the stability problems have to be taken into account. As a matter of facts, a certain decrease can be observed in the last two classes (which correspond to the worst tunnelling conditions), while in Classes I and II the values are very close to the maximum RPM of the machine (Figure 7.7b). However, it is important to remind that RPM is also affected by the skill of the TBM operator, as well as by the possibility to adapt the rotation speed according to the changing ground conditions right on time.

Thus, mainly due to the influence of the cutterhead rotation speed (RPM) of the machine, also in the case of PR the performance decreasing trend with decreasing ground conditions is more evident (Figure 7.7c).

Finally, the daily advance rate (daily AR) is the parameter which shows the most evident reduction. The decreasing trend could be observed from the first to the fourth “fault zone” class (Figure 7.7d). A quite important reduction of the daily AR (down to 40% of the best performance) can be observed with just an increasing degree of fracturing (Class I). Then, the difference between the reduction percentages becomes smaller from one class to the next one. The minimum is clearly reached with Class IV (representing the worst excavation conditions) where the majority of tunnel sections is characterised by daily AR lower than 10% of the best reference performance (see also Figure 7.6d).

Despite of this result, however, it is important to underline that the advance rate of the TBM strongly depends on the utilisation factor of the machine (U) for which it is extremely difficult to establish a direct correlation with the geological/geotechnical conditions of the rock mass, since it is affected by several other factors, including experience of the crew, contractual decisions, working conditions, etc. and thus it can be only estimated with a certain uncertainty degree (Einstein, 1996).

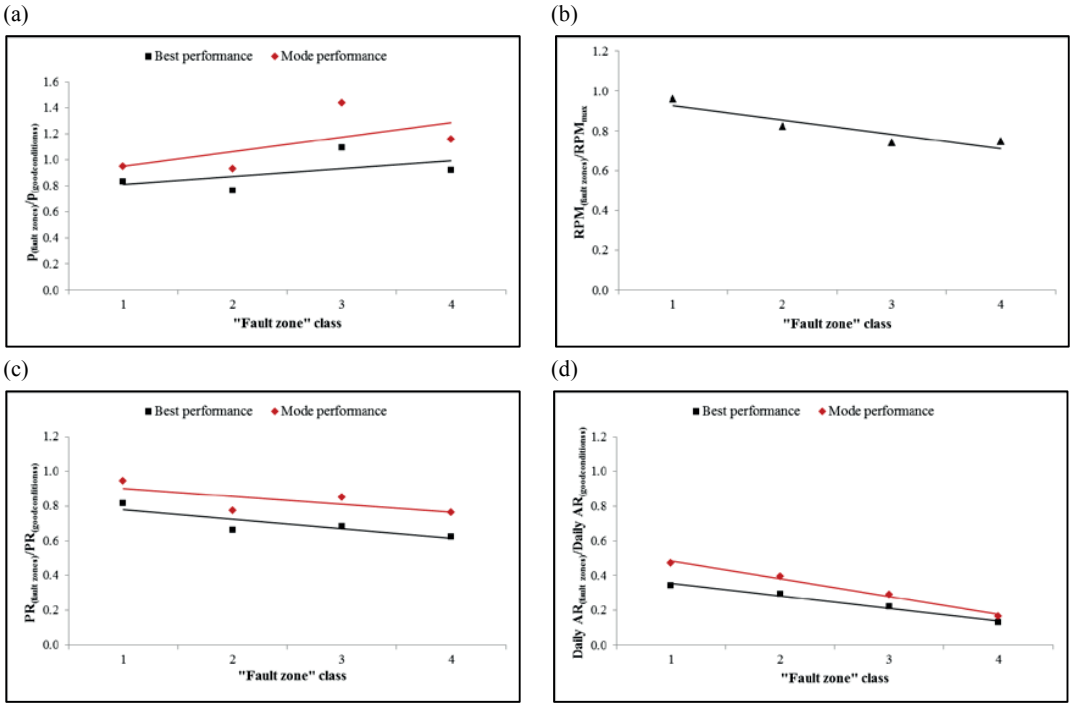

Figure 7.7 Average reduction of the TBM parameters, in each "fault zone" class with respect to the performances recorded in good tunnelling conditions. (a) average reduction of the penetration per revolution (p) with respect to the best (p_{max}) and the most frequent performance (p_{mode}); (b) average reduction of the cutterhead rotation speed (RPM) with respect to the maximum RPM of the TBM (RPM_{max}); (c) average reduction of the penetration rate (PR) with respect to the best (PR_{max}) and the most frequent performance (PR_{mode}); (d) average reduction of the daily advance rate (daily AR) with respect to the best (daily AR_{max}) and the most frequent performance (daily AR_{mode}).

7.5 Final remarks

After having classified the data compiled in the TBM performance database according to the classification method proposed in Chapter 6, for each of the four identified "fault zone" classes, a specific reduction of TBM performance has been estimated by taking into account the best and the mode performances characterising the TBM advancing in good tunnelling conditions. The reduction rates applicable to the TBM-performance parameters in each class are summarised in Table 7.3. The percentages refer to the reduction ranges covered by the histograms reported in Figure 7.3, Figure 7.5 and Figure 7.6 for what concerns the RPM, the PR and the daily AR. Since the reduction observed for each class is similar if considering the best performance or the mode (the difference is mainly related to the gap between the best performance and the relative mode performance), the table includes only the decrease with respect to the best performance. Moreover, in order to better distinguish the influence of each class on the TBM performance, the most frequent reduction (MFR) is also reported.

The reduction rates reported in Table 7.3 can be easily applied to the TBM-performance parameters estimated in normal/good tunnelling conditions by means of the existing prediction models (such as the NTNU model).

Table 7.3 The rates of reduction for each "fault zone:" class (estimated with respect to the best TBM performance and obtained by the histograms reported in Figure 7.3, Figure 7.5 and Figure 7.6) to be applied to the TBM-performance parameters evaluated by existing performance prediction models (e.g. the NTNU model) in ordinary tunnelling conditions (see also Annex C)

TBM parameter	**Rate of reduction (to be applied to the best predicted performance: RPM_{max}, PR_{max}, Daily AR_{max})**			
	Class I	**Class II**	**Class III**	**Class IV**
RPM [rev/min]	80% - 100%	60% - 100%	40% - 100%	40% - 100%
	MFR	***MFR***	***MFR***	***MFR***
	80% - 100%	*80% - 100%*	*40% - 60%*	*40% - 60%*
PR [m/hr]	40% - 100%	20% - 100%	20% - 100%	20% - 100%
	MFR	***MFR***	***MFR***	***MFR***
	80% - 100%	*60% - 80%*	*60% - 80%*	*20% - 40%*
Daily AR [m/day]	10% - 70%	10% - 60%	10% - 50%	10% - 40%
	MFR	***MFR***	***MFR***	***MFR***
	20% - 30%	*10% - 20%*	*< 10%*	*< 10%*

As it can been observed, though the obtained results are linked to the quality of the data collected in the database, and thus prone to be improved by introducing more data, it is important to underline that the outcomes of this analysis provide useful insights and give a first qualitative overview on the reduction of the TBM performance in difficult ground conditions such as highly jointed and fault zones.

Chapter 8 Probabilistic analysis of TBM tunnelling in highly fractured and faulted rocks with the Decision Aids for Tunnelling (DAT)

The results presented in the previous chapter, regarding the reduction of the TBM performance characterising each "fault zone" class, have been used to perform probabilistic analyses of the tunnel construction. The aim of these analyses is to obtain time and cost estimation of TBM tunnelling in highly fractured and faulted rocks. These analyses have been performed with the software package called "Decision Aids for Tunnelling" (DAT).

The DAT are a model and a computer software that can be used to evaluate the effect on tunnel construction cost and time of the uncertainties related to both the geological/geotechnical conditions and the construction process (Dudt et al., 1996; Einstein et al., 1999; Haas and Einstein, 2002).

In this section, the DAT have been used to determine the risks related to tunnelling in highly fractured and faulted rock masses. In particular, by taking into consideration the fault zone classification method presented in Chapter 6, the construction of a 10 km long tunnel (and then of a real tunnel) has been simulated to quantitatively assessing the effects that degrading ground conditions may have on TBM excavation in terms of construction time and costs.

8.1 The Decision Aids for Tunnelling

Tunnel construction is always characterised by a high degree of uncertainty, which is linked to two principal aspects (Einstein, 1996):

1) the geological conditions along the tunnel alignment, which are never exactly known;

2) the construction process, which includes the variable performance of crew and equipment, repairs and maintenance occurring at various intervals, as well as accidents/breakages.

These two aspects practically make impossible the prediction of advance rates and costs.

The DAT can formally quantify uncertainties in tunnelling thus providing a basis for determining the related risks. This is done by simulating the construction of a tunnel (or a network of many tunnels) in a number of different possible geological profiles. Most of the parameters governing the simulation can be defined in a probabilistic way, resulting in the overall uncertainty about a project with respect to construction cost and time (Haas and Einstein, 2002). The DAT have been applied in a number of cases (Einstein et al., 1999; Min et al., 2008) and have been further developed to consider details of resource modelling (Min, 2008) and applications to linear/networked infrastructure projects involving structures other than tunnels (Moret and Einstein, 2011). A recent application (Ritter et al., 2013) uses the DAT to model muck removal and reuse. Finally, the DAT have been also used to compare TBM excavation versus drill & blast excavation in difficult ground conditions (Paltrinieri et al., 2014).

The DAT are a toolbox consisting of two main modules, called "geology module" (description of geology) and "construction module" (simulation of construction). The geology module produces probabilistic geologic/geotechnical profiles indicating the probability related to particular geological conditions occurring at a specific tunnel location. The profiles are usually obtained by combining objective information and subjective estimations done by tunnel experts. A third module, called "resource module", allows taking into consideration production and consumption of resources (construction material, muck material, labour or equipment) and modelling the effect of interfering activities.

Following a hierarchical structure, the geology along a tunnel is initially subdivided into "zones". The term "zone" is used to identify a stretch of ground which may be described as a "geologically homogeneous zone" characterised by a set of ground parameters. Each of these zones consists of a sequence of "segments" in which a specific set of parameter states occurs (Einstein et al., 2012). An example of the hierarchy of the geological subdivision is represented in Figure 8.1.

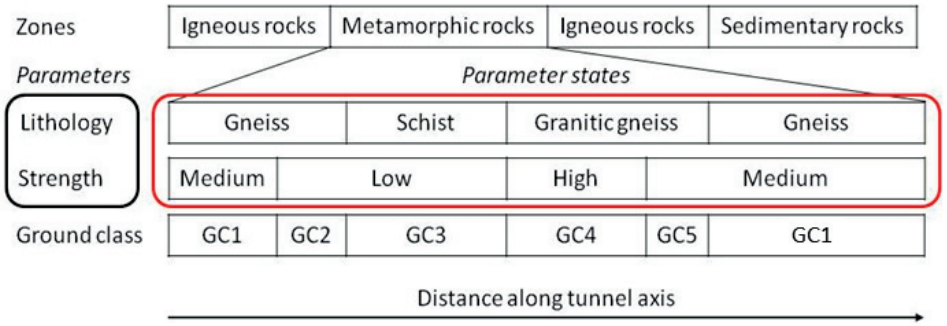

Figure 8.1 Hierarchical representation of the geological input in the DAT.

Usually, Markov chains are used to simulate the segment sequence of the parameter states along the zones. The Markov process is characterised by mean lengths of the states and transition probabilities from each state to the others (Einstein, 1996). The mean lengths and the transition probabilities of the parameter states are generally subjectively estimated. With reference to Figure 8.1, this is equivalent to define the mean lengths of the states "gneiss", "schist" and "granitic gneiss" and the probability with which these states will change from one to another (like gneiss to either schist or granitic gneiss). After computing possible Markov chains for each parameter, these are combined together into a possible ground class profile along each zone. Several simulations are then performed to obtain an equivalent number of possible ground class profiles along the tunnel alignment, in order to represent the whole range of geological conditions (in particular, Figure 8.1 shows for example the result of a single geology simulation). Alternatively, according to the available information, other approaches may also be used to generate the segments.

Once the geology simulations are completed, the construction module simulates tunnel excavation through each ground class profile generated by the geology module. In particular, each ground class is related to a particular "construction method" which defines the excavation procedure as well as the support requirements (Einstein et al., 2012). Each "method" is then associated to construction costs and time, which are generally defined in the form of cost per linear unit of tunnel and advance rate. The "construction methods" may be represented as a single activity or as a sequence of different activities (boring, supporting, mucking, etc.), each of them defined by representative time and cost equations. Triangular distributions are generally used for this purpose. However, uniform and lognormal distributions can also be used.

The construction of the tunnel network is then simulated by advancing round by round through one possible geological profile. For each simulation a specific value of final cost and final time is produced. Thus, running several simulations, a time-cost "scattergram" is produced (Figure 8.2), where each point represents the result of a single simulation.

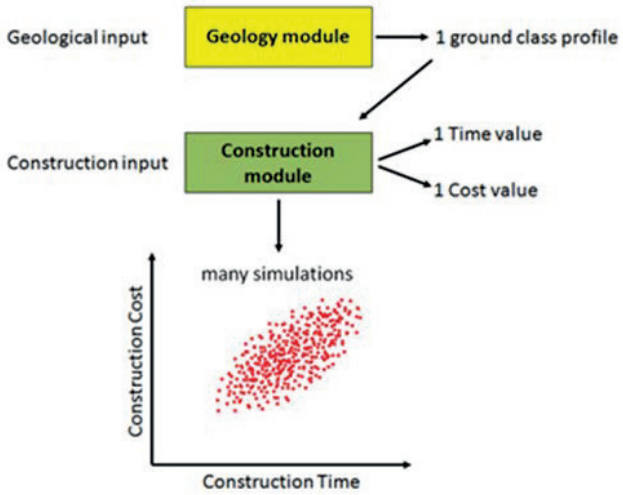

Figure 8.2 Schematic diagram of the DAT methodology, after Delisio (2014).

8.2 Effects of highly fractured and faulted rocks on TBM tunnelling simulations with DAT

As discussed in the previous chapters, TBM operational issues related to bad ground conditions represent a primary source of construction delays and cost increase.

In Chapter 7, the reduction of the TBM performance related to degrading tunnelling conditions has been investigated. In order to better analyse the influence that faulted and highly fractured rocks have on the tunnel construction time and costs, several DAT models have been built. The excavation of a circular, 10 km long tunnel has been considered and simulated. According to the DAT methodology, the input definition is based on two typologies of data set: the geology related and the construction related input, described in the following sections.

8.2.1 Geology related input

The first step in the development of a DAT model is the definition of the geology input. The considered tunnel lies in a single zone and the different ground conditions along the alignment are defined according to different factors (ground parameters). The uniaxial compressive strength (UCS) of the intact rock, the fracturing degree of the rock mass as well as the potential water inflows are taken into account as ground parameters for "ordinary" tunnelling conditions. These parameters can assume the values (or states) reported in Table 8.1. The fault zone classes described in Chapter 6 have been considered for representing the bad tunnelling conditions.

In particular, the "STRENGTH" parameter varies according to three possible intervals of values, corresponding to weak/medium strong (UCS $\leq$ 60 MPa), strong (UCS comprised between 60 MPa and 100 MPa) and very strong (UCS $\geq$ 100 MPa) rocks. As it can be seen in Table 8.1, the fracturing degree, the water inflows and the possible fault zones have been considered as one factor ("ROCK-MASS-CONDITIONS"). Three possible situations have been supposed for both the fracturing (massive, slightly fractured and fractured) and the water inflows (low/no, medium and high), while the four "fault zone" classes define the potential faulted and highly fractured rock masses:

1) Highly fractured rocks, C1 (corresponding to Class I of the classification).
2) Highly fractured, weathered rocks, C2 (corresponding to Class II of the classification).
3) Faulted rocks, C3 (corresponding to Class III of the classification).
4) Crushed rocks, C4 (corresponding to Class IV of the classification).

By combining the potential characteristics in terms of fracturing, water and faulted rocks, eleven possible values/states have been finally obtained for the "ROCK-MASS-CONDITIONS" ground parameter. With a simplifying assumption, it has been supposed that water inflows cannot occur in massive rock masses while they are not even specified for the highly fractured, faulted and crushed rocks. This is due to the fact that, according to what has been discussed in previous chapters, any further reduction of the TBM performance does not depend on the inflow degree in the fault zone classes.

Table 8.1 Ground parameters and possible values/states.

Ground parameter	
STRENGTH	ROCK-MASS-CONDITIONS
Values/states	
UCS ≤ 60 [MPa] (**S1**)	Massive (large blocks)-low (no) water inflow (**FW1**)
60 < UCS < 100 [MPa] (**S2**)	Slightly fractured-low water inflow (**FW2**)
UCS ≥ 100 [MPa] (**S3**)	Slightly fractured-medium water inflow (**FW3**)
	Slightly fractured-high water inflow (**FW4**)
	Fractured-low water inflow (**FW5**)
	Fractured-medium water inflow (**FW6**)
	Fractured-high water inflow (**FW7**)
	Highly fractured rocks (**C1**)
	Highly fractured/weathered rocks (**C2**)
	Faulted rocks (**C3**)
	Crushed rocks (**C4**)

The segments sequence along the alignment is simulated with a Markov process. After one simulation a ground class profile is obtained, where each combination between the ground parameters corresponds to a specific ground class (different combinations can give the same ground class).

An example of a possible ground class profile produced by the geology module is reported in Figure 8.3.

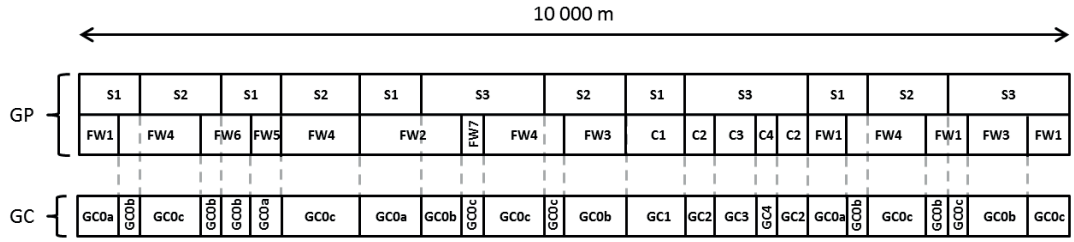

Figure 8.3 Example of a possible ground class (GC) profile obtained by the combinations of the different ground parameters (GP).

For the good tunnelling conditions, described by the combinations between the Si-states and the FWj-states (where i = 1 to 3 and j = 1 to 7, see Table 8.1), three ground classes have been defined:

1) GC0a: the most favourable tunnelling conditions, characterised by the best TBM performances.

2) GC0b: very good tunnelling conditions, characterised by high values of TBM performances which, however, never reach the best ones.
3) GC0c: quite good tunnelling conditions, characterised by acceptable TBM performances.

Concerning the bad tunnelling conditions, the Ck-states (where k = 1 to 4) define the ground classes GC1, GC2, GC3 and GC4 (corresponding to the four "fault zone" classes defined in Chapter 6) independently of the "STRENGTH" parameter value (Si), which, as previously said, is no more a representative characteristic for this kind of rocks.

Several DAT models have been developed in order to simulate different ground conditions. All models are characterised by about 55% of good tunnelling conditions (i.e. GC0a, GC0b and GC0c) and about 45% of bad tunnelling conditions (i.e. GC1, GC2, GC3 and GC4). For the bad tunnelling conditions, the percentage of each fault zone class has been fixed in each model. More in detailed, the following three scenarios have been considered (see Table 8.2):

1) **Model 1**: not extremely challenging geological conditions. In particular, 20% of class GC1 (and GC2) corresponds to 2000 m excavated in highly fractured rock masses (and in highly/weathered rock masses). In this model only 4% is considered as being excavated in very bad ground conditions (i.e. 3% in class GC3 and 1% in class GC4).
2) **Model 2**: degrading tunnelling conditions. The GC3 and GC4 classes cover about 26% of the tunnel alignment (i.e. 22% in class GC3 and 4% in class GC4), while both classe GC1 and class GC2 is reduced to 10%.
3) **Model 3**: the worst-case scenario. The GC1 and GC2 classes fall to 5%, while class GC3 covers 12%. Class GC4 reaches a maximum length of more than 2000 m (i.e. 24% of the tunnel alignment).

Table 8.2 Fault zone distribution (bad tunnelling conditions) along the tunnel alignment in each DAT model.

Model n.	GC1	GC2	GC3	GC4
1	20%	20%	3%	1%
2	10%	10%	22%	4%
3	5%	5%	12%	24%

An example of segment generation along the tunnel and the transition matrix adopted for the "STRENGTH" ground parameter is shown in Figure 8.4. Furthermore, the transition matrix of the "ROCK MASS CONDITIONS" parameter used in model 3 is reported in Figure 8.5 as example.

It is important to underline that, though in a real Markov chain an exponential distribution is considered for defining the parameter (i.e. segment length), in this framework triangular distributions have been adopted in order to avoid extremely short or extremely long segments.

In particular, the triangular distributions are characterised by the same values of minimum possible length (L_{min} = 50 m), most frequent length (L_{mode} = 100 m) and maximum possible length (L_{max} = 150 m). The probability to move from a given range of strength to another one is defined by the transition matrix (e.g. there is 50% of probability to go from S1 to S2 and from S1 to S3).

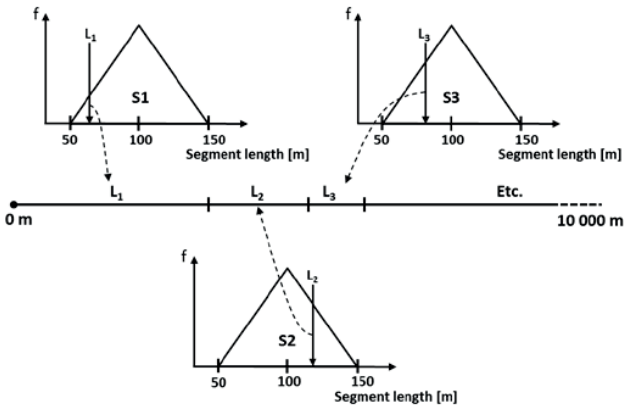

GP (from / to)	S1	S2	S3
S1	0.0	0.5	0.5
S2	0.5	0.0	0.5
S3	0.5	0.5	0.0

Figure 8.4 Example of segment sequence along the alignment and transition matrix of the ground parameter "STRENGTH" (Si, i=1, 2, 3). The length of each segment is picked with a Monte Carlo extraction from the triangular distribution defined for each ground parameter state.

GP (from / to)	FW1	FW2	FW3	FW4	FW5	FW6	FW7	C1	C2	C3	C4
FW1	0.0	0.1	0.1	0.15	0.15	0.15	0.15	0.05	0.05	0.05	0.05
FW2	0.1	0.0	0.1	0.1	0.15	0.15	0.15	0.05	0.05	0.05	0.1
FW3	0.1	0.1	0.0	0.1	0.1	0.1	0.1	0.05	0.05	0.1	0.2
FW4	0.1	0.1	0.1	0.0	0.1	0.1	0.1	0.05	0.05	0.1	0.2
FW5	0.1	0.1	0.1	0.1	0.0	0.1	0.1	0.05	0.05	0.1	0.2
FW6	0.1	0.1	0.1	0.1	0.1	0.0	0.1	0.05	0.05	0.1	0.2
FW7	0.1	0.1	0.1	0.1	0.1	0.1	0.0	0.05	0.05	0.1	0.2
C1	0.02	0.02	0.03	0.03	0.05	0.05	0.05	0.0	0.05	0.1	0.6
C2	0.02	0.02	0.03	0.03	0.05	0.05	0.05	0.05	0.0	0.1	0.6
C3	0.03	0.03	0.04	0.05	0.05	0.1	0.1	0.05	0.05	0.0	0.5
C4	0.03	0.03	0.04	0.05	0.05	0.08	0.08	0.12	0.12	0.4	0.0

Figure 8.5 The transition matrix adopted for the ground parameter "ROCK MASS CONDITIONS" (FWj, j=1, 2, 3, 4, 5, 6, 7 and Ck, k=1, 2, 3, 4) in model 3.

8.2.2 Construction related input

Tunnel construction is simulated with the DAT construction module. This allows combining the geological information and the construction process. In particular, for each combination of tunnel excavation system (i.e. drill and blast, gripper TBM, shield TBM etc.) and ground class, a so-called "construction method" is defined. As already mentioned each "construction method"

may be considered as a sequence of tunnelling activities, defined in terms of time and cost equations. The variables used in the equations are called "method variables" (as their Probability Density Function, PDF, varies from one "method" to another) and the combination of all the defined activities is called "activity network" (Einstein et al., 2012).

In the present analysis only one excavation system, corresponding to a gripper TBM, is considered and seven "construction methods" (referring to the different tunnelling conditions) have been defined:

1) **Method 0a**: TBM excavation in the best tunnelling conditions, corresponding to ground class GC0a.
2) **Method 0b**: TBM excavation in very good tunnelling conditions, corresponding to ground class GC0b.
3) **Method 0c**: TBM excavation in quite good tunnelling conditions, corresponding to ground class GC0c.
4) **Method 1**: TBM excavation in highly fractured rocks, corresponding to ground class GC1.
5) **Method 2**: TBM excavation in highly fractured and weathered rocks, corresponding to ground class GC2.
6) **Method 3**: TBM excavation in faulted rocks, corresponding to ground class GC3.
7) **Method 4**: TBM excavation in crushed rocks, corresponding to ground class C4.

Each of these "methods" is based on a single construction activity ("TBM advance") representing the total TBM advancement. It includes the TBM boring time and the production delays (due to support installation, maintenance, ground improvements, etc.). This is actually a common procedure for defining the construction module. In the DAT, activities are defined in terms of time and cost equations (generally expressed as a function of the advance rate and cost per meter respectively). Therefore, the results derived from the analysis of the TBM performance data (presented Chapter 7) have been considered for selecting the DAT input distributions.

In good tunnelling conditions (i.e. Method 0a, 0b and 0c) the data retrieved from the database described in Chapter 4 have been used. The three distributions of daily advance rate (called AR_0 in this section for simplicity) have been defined on the basis of the TBM performances recorded in favourable ground situations (Figure 8.6).

(a)

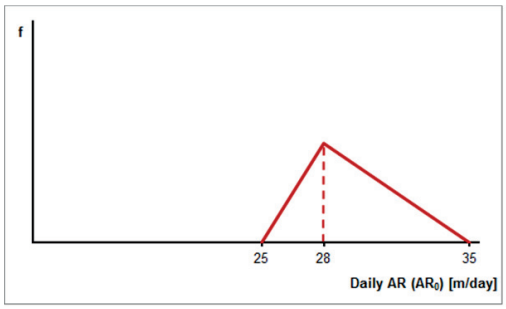

(b)

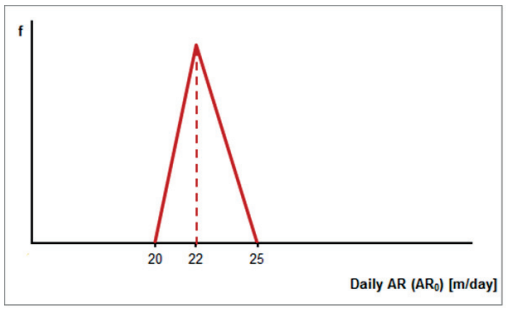

(c)

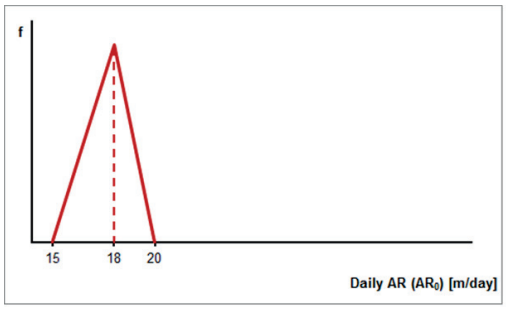

Figure 8.6 Triangular distribution function for AR_0 in good tunnelling conditions. a) Best performance (Method 0a); b) good performance (Method 0b); c) acceptable performance (Method 0c).

Unfortunately it is quite difficult to obtain information about the excavation costs. Therefore, the final costs have been defined by taking into account data used in past simulations performed, for similar modelling conditions, at the Laboratory of Rock Mechanics (LMR) at EPFL. Figure 8.7 shows the triangular distribution considered for representing the excavation cost per meter in good tunnelling conditions (EC_0). This distribution is representative of the excavation cost of a hard rock machine with a diameter of about 8 to 12 m (i.e. the same type of gripper TBM included in the TBM performance database).

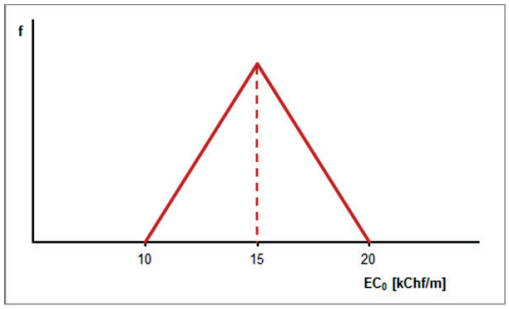

Figure 8.7 Triangular distribution function for the excavation cost EC_0 in good tunnelling conditions.

For what concerns the bad tunnelling conditions (Method 1, 2, 3 and 4) the performance reduction identified in Chapter 7 for each fault zone class has been used in order to take into account the TBM advance rate decrease due to degrading ground conditions. The excavation time t_i (where i= 1 to 4 refers to each "method" in bad conditions) is thus given by the following equation:

$$t_i = \frac{RL}{\left(AR_{0[best\ performance]} \times r_i\right)} \tag{8.1}$$

where:

- RL is the round length (set equal to 2.0 m, i.e. one TBM stroke);
- r_i is the reduction factor (probabilistic) computed for each "method" on the basis of the associated histogram plot (see Chapter 7) obtained for each "fault zone" class;
- AR_0 represents the best advance rate obtained in good tunnelling conditions (see Figure 8.6a).

The factor r_i is introduced in the DAT as triangular distribution for Method 1, Method 2, Method 4 (Figure 8.8a, Figure 8.8b and Figure 8.8d) and as uniform distribution for Method 3 (Figure 8.8c). As a matter of fact, while in the first, second and fourth classes it has been possible to define a mode value, in the third class only a maximum and a minimum advance rate have been identified (see Figure 7.6c). The uniform distribution function seemed therefore the best choice (i.e. same probability to pick any value comprised between the minimum and the maximum). Regarding the distribution adopted for Method 4, the mode value has been assumed equal to the minimum value (r_i = 0.1). This is due to the fact that the vast majority of the tunnel sections described by this class are characterised by advance rate lower than 10% of the best performance (see Figure 7.6d).

If the TBM advance rate reduces according to Equation 8.1 as the ground conditions get worse, the excavation costs increase accordingly. In particular, it has been assumed that the construction costs increase proportionally to $1/r_i$ (Equation 8.2):

$$c_i = RL \times EC_0 \times \frac{1}{r_i} \tag{8.2}$$

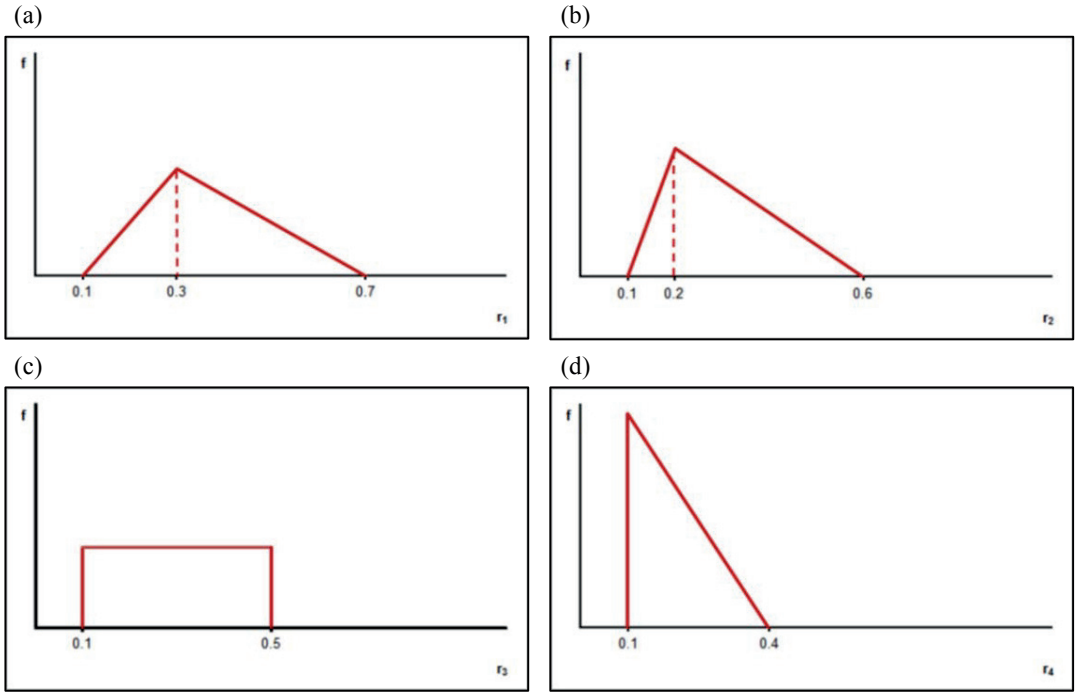

Figure 8.8 Distributions of the term r_i (i=1, 2, 3, 4) adopted for each method related to "fault zone" classes. The minimum value, the maximum value and the mode value are put in evidence. a) Method 1; b) Method 2; c) Method 3; d) Method 4.

8.3 Simulation results

The model results are represented in the form of a time-cost "scattergram". As already mentioned, each point of the diagram represents the result of a single construction simulation through a possible ground class profile.

In general, two different situations (schematically illustrated in Figure 8.9a and Figure 8.9b) can be identified if the results of the construction simulations are represented separately for each geology simulation. In both situations four geology simulations (G=1, 2, 3, 4) have been run, generating four different ground class profiles. On each profile 10 construction simulations (C1 to C10) have been performed, thus generating four clouds of 10 points.

In Figure 8.9a (representing the simulation results for Case 1) it is possible to distinguish four distinct clouds. This means that the geological conditions determine the tunnel construction time and cost as the scatter inter-clouds is much greater than the scatter intra-clouds. On the contrary, if the clouds overlap, as in Case 2 (Figure 8.9b), the final excavation time and cost do not significantly vary if the geological profile changes. In such a situation, the construction conditions have the largest influence on the estimation of the final construction time and cost.

(a) (b)

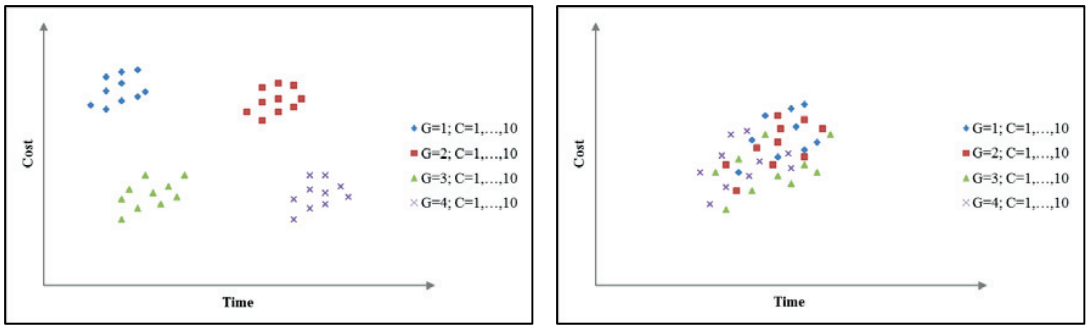

Figure 8.9 Time-cost scattergrams for the 4x10 DAT simulations. a) Case 1: the geology has the largest influence on the final excavation time and cost; b) Case 2: the construction has the largest influence on the final excavation time and cost.

In order to define the proper number of simulation for the proposed DAT models (model 1, 2 and 3), 10 x 10 simulations have been performed considering the input of model 3. For each geology simulation the associated 10 construction simulations have been plotted separately in a time-cost scattergram (Figure 8.10). The analogy of the chart shown in Figure 8.10 with Case 2 (Figure 8.9b) is evident and this means that the uncertainties related to the construction conditions have a greater influence than the geological profile on the final results.

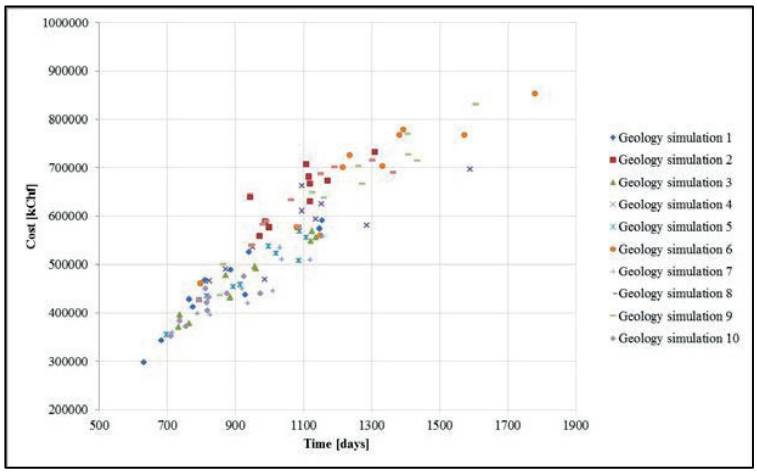

Figure 8.10 The time-cost scattergram for the 10x10 DAT simulations.

According to this analysis, 10 geology simulations have been run for the three models; each simulation produces a different ground class profile. Then, for each ground class profile, 100 construction simulations have been executed, thus giving 10x100 simulations of tunnel construction.

The results for the 10x100 DAT simulations of model 1, model 2 and model 3 are represented respectively in Figure 8.11, Figure 8.12 and Figure 8.13. The details of each simulation are

summarised in Table 8.3, and the resulting scattergrams of the three models are compared also in Figure 8.14.

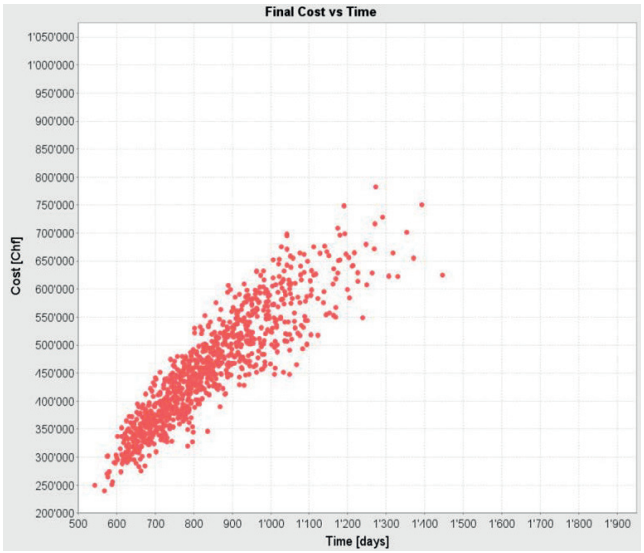

Figure 8.11 Time-cost scattergram for model 1 (20% of Class I; 20% of Class II; 3% of Class III; 1% of Class IV).

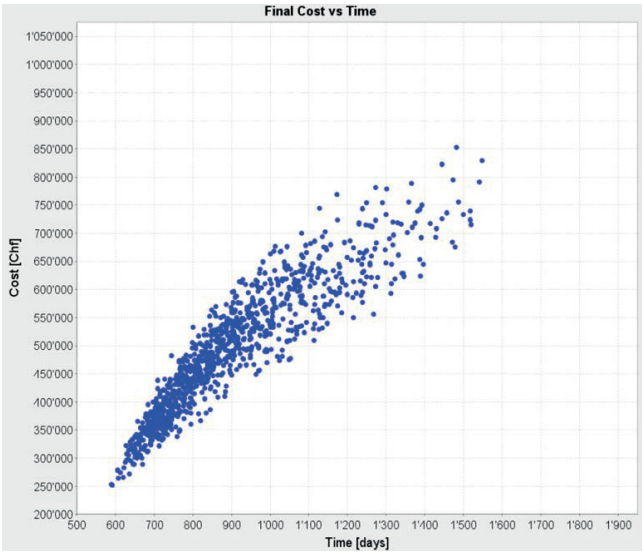

Figure 8.12 Time-cost scattergram for model 2 (10% of Class I; 10% of Class II; 22% of Class III; 4% of Class IV).

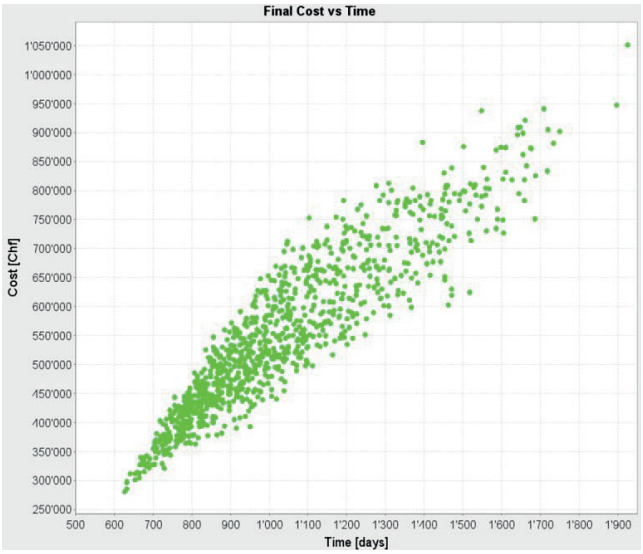

Figure 8.13 Time-cost scattergram for model 3 (5% of Class I; 5% of Class II; 12% of Class III 3; 24% of Class IV).

Table 8.3 Details of the DAT output for the three models. St. dev.= standard deviation and C. V.= coefficient of variation (i.e. st. dev./mean).

Model n.	Construction time [days]					Construction cost [millions CHF]				
	Min	Mean	Max	St. dev.	C. V.	Min	Mean	Max	St. dev.	C. V.
1	543	837	1446	151.2	0.18	240	455	782	96	0.21
2	589	903	1549	190.6	0.21	252	493	853	111	0.23
3	626	1032	1925	241.8	0.23	280	550	1051	135	0.25

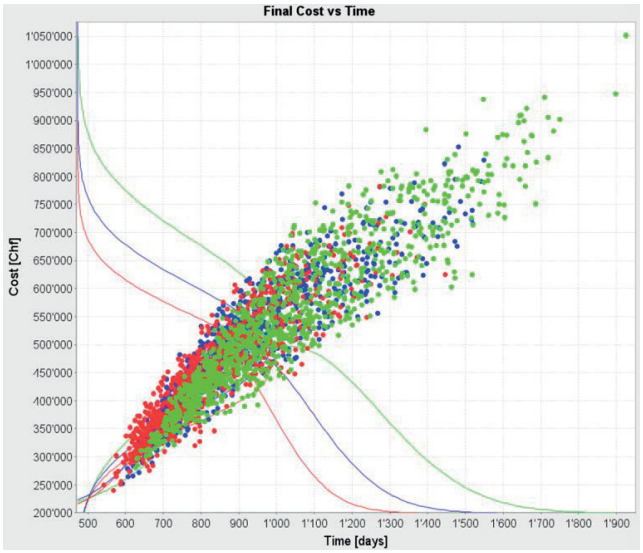

Figure 8.14 Time-cost scattergrams and normal distributions for the simulations performed for the three models. Red cloud: model 1; blue cloud: model 2; green cloud: model 3.

Table 8.3 and Figure 8.14 show clearly an increase of construction time and costs while moving from model 1 to model 3 (i.e. worsening tunnelling conditions). These results are represented by the shifting of the point clouds of models 2 and 3 towards higher values of time and costs. This increase is also evident in Figure 8.15a and in Figure 8.15b, where the minimum, mean and maximum values of the final construction time and cost are reported for the three models.

The results of these analyses show clearly:

- A certain increase of the mean construction time and costs (about 8% each) from model 1 to model 2. In addition, also the scatter of the points within the cloud (represented by the coefficient of variation C.V.) becomes more important. This stays for an increase of the uncertainty related to degrading tunnelling conditions moving from the first to the second set of simulations.
- A significant increase of the mean construction time (i.e. about 23%) and of the mean construction cost (i.e. about 21%) from model 1 to model 3. Moreover, in model 3 (i.e. worst-case scenario) the C.V. reaches its maximum, which means that in this case the estimation of the construction time and costs is characterised by the highest uncertainty degree.
- An increase of the maximum value of construction time and costs which is much more pronounced with respect to the variation of the mean and minimum values from model 1 and 2 to model 3. As a matter of fact, the risk of high/very high construction times (due in particular to longer machine delays) and cost overruns becomes more significant with worsening geological conditions.

Although the obtained results are quite interesting to get an idea of the possible delays and cost overruns in highly fractured and faulted rocks, it should be noted that the assumptions made may lead to a final construction cost higher than what can be observed in reality, especially for the worst case (model 3) which represents extremely bad conditions. This is due to the assumption done for the cost evaluation relationship, expressed by Equation 8.2, which generates very high cost values as the rock mass conditions get worse.

(a) (b)

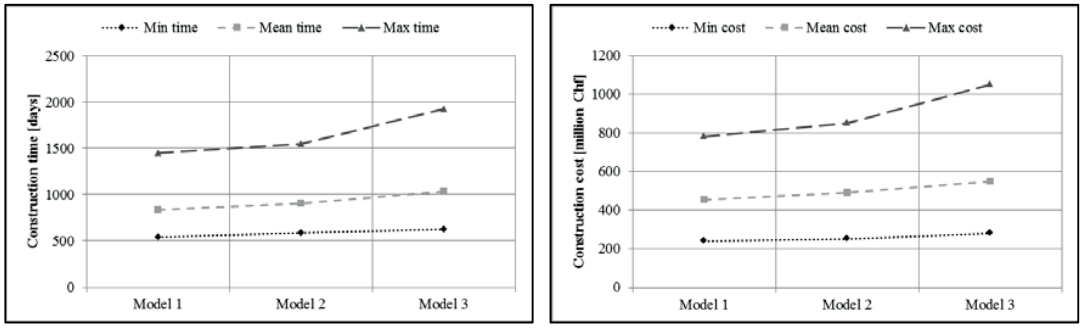

Figure 8.15 Construction time (a) and construction cost (b) for the three considered models.

The influence of the different percentages of the "fault zone" classes on the final construction time is more evident in the time-way diagram reported in Figure 8.16. Actually, in this graph each line represents the average envelope of the simulations performed for each model. The significant time increase can be observed as the ground conditions get worse (i.e. model 3 vs. model 1).

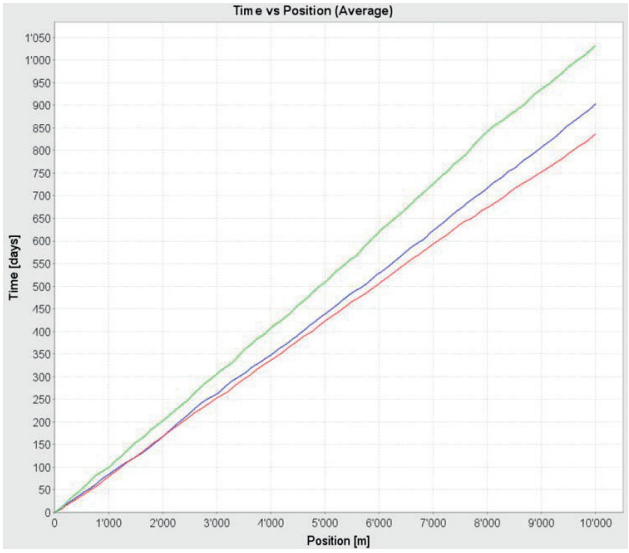

Figure 8.16 Average time-position curve. Red line: model 1; blue line: model 2; green line: model 3.

Finally, it is also interesting to compare the scattergrams previously described with the results of simulations performed without considering the "fault zone" classes and, therefore, without including any of the reduction ranges (obtained for each class in Chapter 7) for computing the advance rate. A new model (model 4) has been thus introduced. In model 4 the "ROCK MASS CONDITIONS" ground parameters refer only to FWj factors reported in Table 8.1 (without considering the Cj ones). In this case, the most challenging environments are represented by the ground classes characterised by highly fractured rocks and high water inflows. While in the previous models (model 1, 2 and 3) only the excavation times corresponding to favourable tunnelling conditions have been defined by using data retrieved from the database described in Chapter 4, in model 4 also the unfavourable conditions are based on the real values of performances collected in the database. Figure 8.17 shows the triangular distributions of daily advance rate (daily AR) and of the excavation cost (EC) adopted in model 4 (one single chart has been adopted for the daily AR distributions and for the EC distributions in order to better observe the extent of the value ranges). The final scattergram is shown in Figure 8.18.

Although the different "fault zone" classes are not identified within the "general" bad zones, model 4 is characterised by the same total percentage of difficult tunnelling conditions (i.e. about 45%) of models 1, 2 and 3. By comparing the results of model 4 with the scattergrams of model 1, 2 and 3 (Figure 8.19), it is evident how the extremely low advance rates (down to 1 m/day) affect the simulations. As a matter of facts, the possible construction time shows a minimum, a mean and a maximum value very close to the results of model 3 (the worst-case scenario described by the "fault zone" classes). Therefore, the results of this model show that,

without making any distinction among "fault zone" classes, the potential advance rates seem to be underestimated. This is true especially if compared to model 1 and model 2, characterised by a significant presence of highly fractured rock masses (i.e. Class I and II) which practically does not affect the final construction time as much as it happens in the case of faulted and crushed rocks (i.e. Class III and IV). This means that a more detailed characterisation of the difficult ground conditions, by distinguishing properly the impact of each identified "fault zone" class on the excavation process, seems to be quite helpful for a better prediction of construction time and costs.

(a)

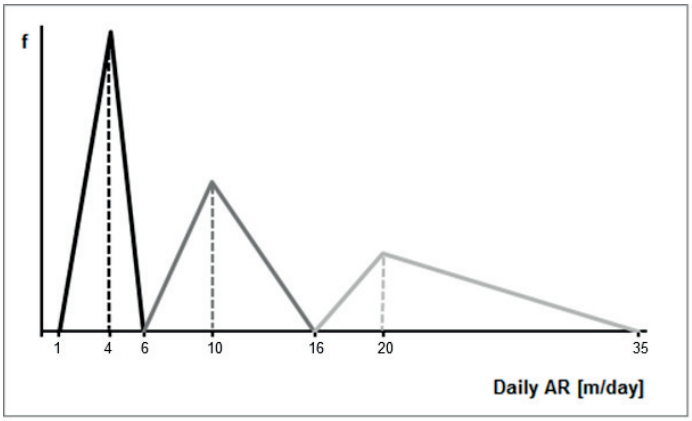

(b)

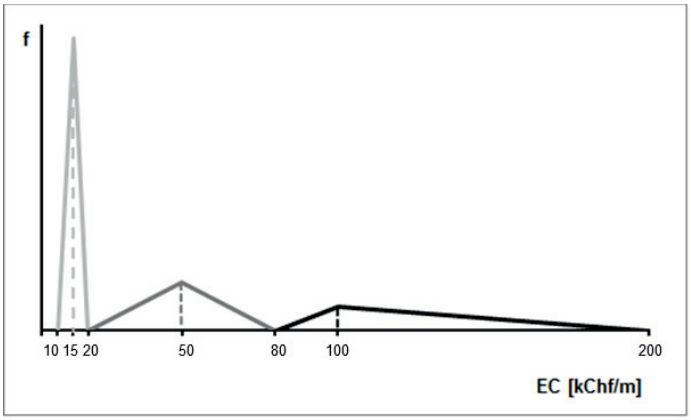

Figure 8.17 Triangular distribution function for daily AR and excavation cost (EC) adopted in model 4. Light grey line: good and very good tunnelling conditions. Dark grey line: bad tunnelling conditions. Black line: the worst tunnelling conditions.

It is important to underline that, due to the lack of real data, the cost triangular distributions used in model 4 are based on the author experience trying to be reasonable and as closer as possible to realistic values. Though a different method has been used for introducing this input (i.e. Equation 8.2 for models 1, 2 and 3 and the triangular distribution reported in Figure 8.17 in

model 4), the mean cost value obtained in model 4 is comparable to the mean costs of models 1, 2 and 3. In particular, as it has been already observed by the analysis of the final construction time, it is closer to the value obtained in the worst-case scenario (i.e. model 3).

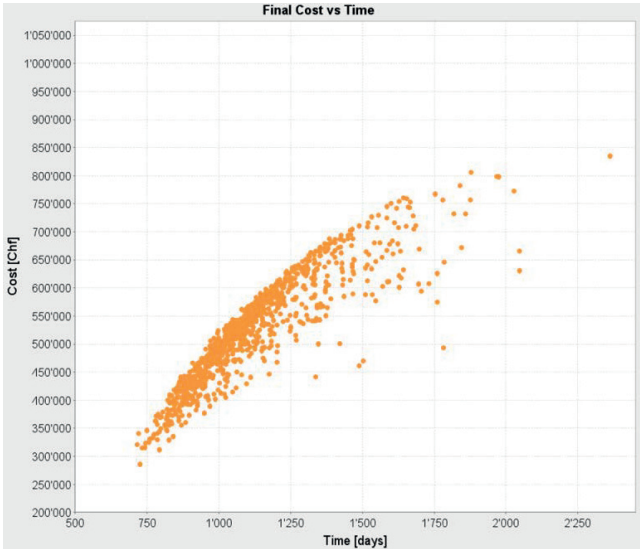

	Min	Mean	Max	St. dev.	C.V.
Construction time [days]	715	1125	2047	223.3	0.20
Construction costs [millions Chf]	286	525	806	93	0.18

Figure 8.18 Time-cost scattergram for model 4 and details of DAT output.

Figure 8.19 Time-cost scattergram for simulations performed without "fault zone" classes (i.e. model 4, orange cloud) and time-cost scattergrams of the "fault zone" models (i.e. models 1, red cloud; model 2, blue cloud; model 3, green cloud).

8.4 Application of DAT model to a real case

In order to have a better idea of the ability to represent reality, a DAT model has been applied to a real case-study. For performing this simulation it has been chosen a stretch of about 3000 m of the Lötschberg Base Tunnel (LBT, Switzerland). This high speed railway tunnel was constructed between 1999 and 2006 in the Swiss Alps, between Raron (Rhône Valley) and Frutigen (Lenker Valley). It has a length of 36.4 km and consists, for almost its whole length, of two tubes at a distance varying between 40 and 60 m to each other and linked together by transversal galleries approximately every 333 m. About 18.5 km of the tunnel has been excavated by two gripper TBMs (9.43 m in diameter). From a geological point of view, the tunnel is located between two different tectonic units, the Autochthon Gampel-Baltschieder and the Aar Massif. The Autochthon Gampel-Baltschieder is composed of several lithological units: the Lias zone (i.e. limestone and shale), the Dogger zone (i.e. slate, limestone and marl) and the Malm zone (i.e. limestone). The contact between sedimentary and crystalline rocks is at about 2800 m from the South portal. It represents the major tectonic disturbance of the region named Rote Kuh-Gampel fault. From this point on, the excavation proceeded into the Aar Massif, composed by granite and granodiorite, granitic gneiss and massive/schistose gneiss. The depth of cover along the alignment increases from 0 to 1950 m, reaching its maximum in the granitic gneiss at Tm 5600 from the south portal (Raron) (Ziegler et al., 2008; Delisio and Zhao, 2013).

The tunnel stretch chosen for the DAT model (red circle in Figure 8.20) consists only of one geological unit, the Autochthon Gampel-Baltschieder unit, where very high degree of fracturing and large water inflows were observed during construction.

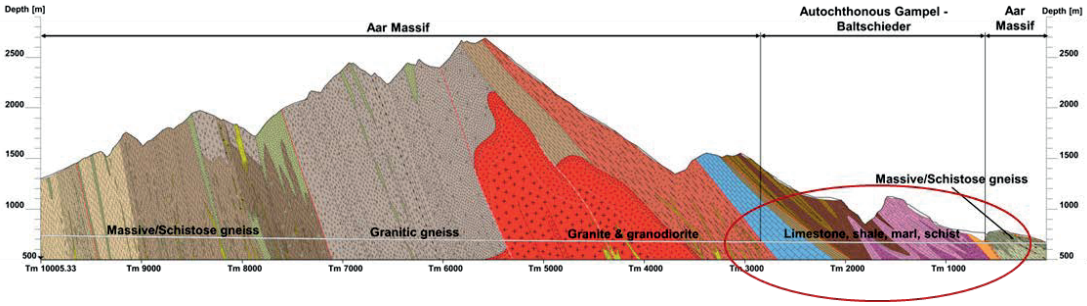

Figure 8.20. Geological longitudinal profile along the LBT (modified after Ziegler et al., 2008).

For this stretch, the classification methodology proposed in Chapter 6 has been applied and the different "fault zone" classes identified. The percentages reported in Table 8.4 have been observed.

Table 8.4 "Fault zone" classes distribution along the selected tunnel stretch (total length 3 km).

GC1	GC2	GC3	GC4
5%	4%	2%	1%

The DAT model has been then developed using the distribution of classes reported in Table 8.4 for defining the geology module while, for the construction module, the advance rate and cost triangular distributions described in section 8.2.2 for model 1, 2 and 3 have been adopted. As mentioned before, since the real cost information is not available, the analysis of the results will be mainly focused on the final construction time values. The real excavation progress recorded in the analysed LBT sections is reported in Figure 8.21, while the scattergram of the performed simulations is shown in Figure 8.22.

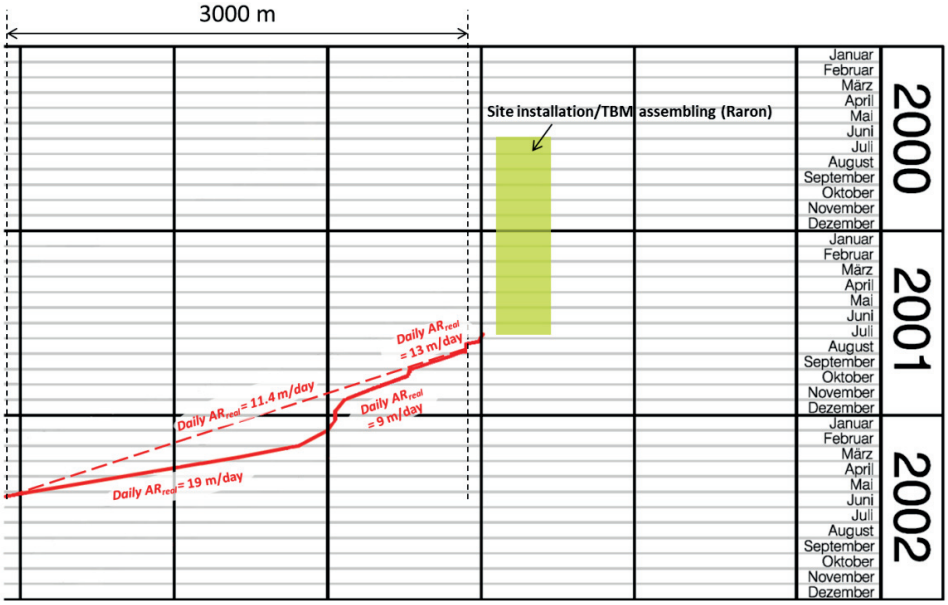

Figure 8.21 The excavation progress in the LBT for the stretch simulated with the DAT model (Vuilleumier et al., 2006).

As it is possible to observe, the time results are very close to the performances recorded in the reality. It is interesting to highlight that the real mean daily advance rate (average daily AR_{real} = 11.4 m/day) is extremely close to the minimum performance (the worst scenario) computed by the DAT model (minimum daily AR_{DAT} = 11.3 m/day). In addition, the real best daily AR (maximum daily AR_{real} = 19 m/day), recorded along the two-thirds of the analysed tunnel stretch, is almost equal to the highest advancement estimated by the DAT (maximum daily AR_{DAT} = 19.1 m/day). The daily AR_{real} (i.e. 9 m/day and 13 m/day in Figure 8.21) recorded along shorter but significantly long tunnel sections (i.e. 400 m and 380 m) are comprised between the minimum and the mean daily AR_{DAT} (i.e. respectively 11.3 m/day and 15.4 m/day). However, it is important to underline that each DAT simulation provides the average daily AR along the whole tunnel length (3000 m in the case-study). Therefore, it may not be proper to compare these values with the advancement corresponding to each single segment in the excavation progress chart (Figure 8.21). Nevertheless, on the basis of the obtained results, it can be concluded that the DAT model was able to reproduce this real case, allowing correct quantification of the influence of the most difficult ground conditions on the total excavation time.

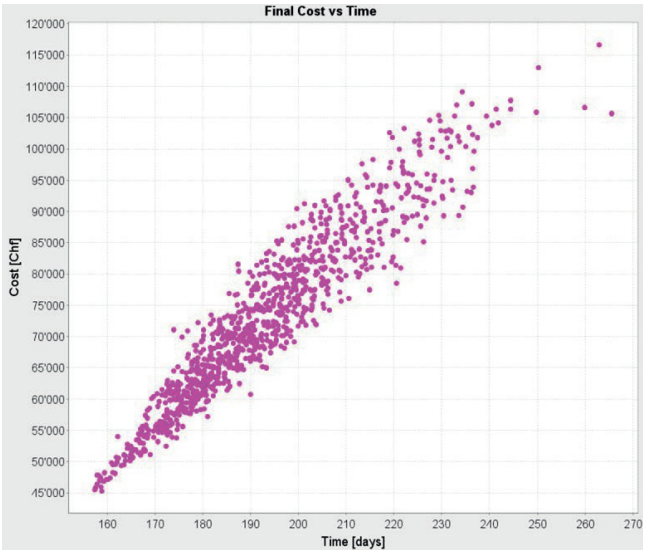

	Min	Mean	Max	St. dev.	C.V.
Construction time [days]	157	193	266	18.4	0.09
Daily AR_{DAT} (3000 m/construction time) [m/day]	11.3	15.4	19.1	-	-
Construction costs [millions Chf]	45	73	117	13.4	0.18

Figure 8.22 Time-cost scattergram for simulations performed on the selected stretch and details of the DAT output (in terms of time, cost and daily advance rate).

Moreover, the outcomes of this analysis confirm the importance of considering a more detailed and comprehensive characterisation of the zones characterised by difficult ground conditions which may hinder good advancement during the tunnel construction (such as extremely highly fractured and faulted rocks), in order to model more realistic situations. Furthermore, the classes described by the "fault zone" classification (see Chapter 6) as well as the introduction of specific reduction ranges applied to the TBM performance (in particular for what concerns the daily advance rate), seem to be a valid approach for obtaining more reliable predictions in terms of excavation time.

8.5 Final remarks

The Decisions Aids for Tunnelling are a very useful tool for quantifying uncertainties affecting tunnel excavation as well as estimating construction time and costs under variable/uncertain conditions. In this framework, the DAT have been used for estimating the distributions of tunnel construction time and costs that can be experienced during tunnelling in highly fractured and faulted rocks. In particular, this analysis allows to more deeply investigating the effect of the identified "fault zone" classes on the tunnel construction. Based on the classification system proposed in Chapter 6, the following ground conditions have been used as input for the DAT geology module:

- Good, massive to slightly jointed rock (ground classes GC0a, GC0b and GC0c), i.e. good tunnelling conditions
- Highly fractured rock (ground class GC1), i.e. Class I
- Highly fractured and weathered rock (ground class GC2), i.e. Class II
- Faulted rock (ground class GC3), i.e. Class III
- Crushed rock (ground class GC4), i.e. Class IV

By considering different lengths for each ground type (i.e. variable within a fix total percentage of bad geological conditions) the DAT models allow considering different rock mass configurations ranging from a predominance of highly fractured rocks to extremely bad conditions, in which highly weathered faulted and crushed rock are encountered on a considerable percentage of the whole tunnel alignment.

The tunnel excavation has been simulated by taking into account the results obtained from the analyses performed in Chapter 7. In particular, for classes GC0, GC0b and GC0c the good performance recorded in favourable ground conditions has been considered, while for classes GC1, GC2, GC3 and GC4 the rates of reduction obtained for each "fault zone" class have been introduced for estimating the final advancement. An assumption of increasing costs proportional to increasing excavation times has also been made. The results of the simulations demonstrate how highly fractured and faulted rocks can influence tunnel construction conditions. A significant increase of the construction time and cost occurs while changing from "better" to "worse" ground conditions. Furthermore, a greater uncertainty of simulation results is also observed with degrading rock mass conditions, thus underlining the increasing difficulty in estimating a representative value of tunnelling performance.

A comparison of these results with simulations performed without considering the "fault zone" classes and their specific performance reduction has been also carried out. In particular, the TBM performances compiled in the database introduced in Chapter 4 have been retrieved for describing both good and bad tunnelling conditions. The obtained results seem to show that a proper distinction among the effects of different "fault zone" classes on the excavation process provides a better prediction of time and cost (i.e. in case of classification-based analysis the results are less affected by higher values of variability).

Finally, DAT simulations have been run to model a real case-study with the aim of validating the use of the "fault zone" classification (as well as the relative advance rate reductions) for the estimation of the tunnel construction time. The analysis gave satisfying results since the predicted times are very close to the values recorded in the field.

These results confirm once more the importance of the methodology presented in the previous chapters (i.e. TBM-performance reduction associated to a specific "fault zone" class), showing how this approach allows obtaining a more reliable estimation and evaluation of the final time of tunnel construction in changing tunnelling conditions.

Chapter 9 Conclusions and outlook

The mechanical excavation by Tunnel Boring Machines (TBMs) is nowadays more and more considered a valuable alternative to conventional methods and its application in mining and tunnelling engineering has significantly increased in recent years. In good rocks, generally, the main advantages of TBMs can be summarised as follows: continuous operation, safe working conditions, reduced damage of the surrounding ground, and high advance rate. At the same time, TBM operations may be seriously affected by difficult ground conditions, such as highly fractured and fault zones, with a consequent significant reduction of the TBM performance with respected to the expected one.

"Fault zone" is commonly used to identify brittle shear zones generated in the upper part of the Earth's crust ranging from decimetres to kilometres in magnitude. Their extreme complex structure and heterogeneous nature, due to combined contribution of weak and strong rock components, make their geotechnical characterisation very difficult. For example, rocks resulting from brittle faulting processes (e.g. cataclastic rocks) can show properties typical of hard rocks to soil-like materials. This is mainly depending on the character of the material, cohesive or non-cohesive, in relation to the variable ratio of gouge matrix to rock blocks. Therefore, weak rocks resulting from these processes are characterised by quite low mechanical strength and can be described by behaviour somewhere between rocks and soils. They also show high deformability involving non-linear constitutive laws, strong dependence of the strength on water saturation and temperature, and great susceptibility to weathering.

The most common geotechnical problems resulting from tunnelling in these kinds of rocks include excessive deformations and strongly anisotropic wall displacements, instability of both the excavation face and the side-walls (also resulting in large overbreaks of the tunnel profile), frequent changes of stresses in terms of magnitude and direction, high water inflows, etc. Thus, a significant reduction of the TBM advance rate is generally recorded (e.g. in worst cases a stop, jamming, of the machine can be observed) also due to the construction delays associated to the need of ground treatment, heavier supports and additional waterproofing measures. Furthermore, the presence of a faulted/heavily jointed tunnel face might strongly affect the interaction between rock mass and TBM cutters since the excavation may not proceed anymore via the usual chipping process, causing unexpected wearing of the disc tools and thus requiring more frequent maintenance of the cutterhead.

In these last decades many TBM performance prediction models have been developed in order to estimate the optimum TBM advance rates for standard ground conditions (expected as good). Due to the fact that in highly fractured rocks and fault zones many events can take place at the same time (e.g. major high pressure inflows, outwash of fines, large tunnel deformations and formation of cavities at the tunnel crown or ahead of TBM), those models, however, are generally not representative of the bad tunnelling conditions. The research performed in this framework proposes a new approach for better estimating the TBM performance in challenging ground.

TBM-performance database and preliminary analyses

In order to better analyse the TBM performance in difficult grounds and to investigate the relationships existing between machine performance parameters and geological/geotechnical parameters of the rock mass, a TBM-performance database has been created. The tunnel sections included in the database have been selected from different tunnel projects (excavated by both gripper and shield TBMs) where highly jointed rock masses and/or fault zones have been encountered. The database is mainly subdivided into two parts: the first one contains the tunnel characteristics, TBM specifications and TBM performance parameters (e.g. penetration rate, advance rate, etc.); the second one considers the geological-geotechnical parameters of the rock mass (e.g. rock strength, fracturing and weathering degree of joints, etc.).

Concerning the data collection, the calculation of the basic machine parameters has been generally performed on the basis of the measures carried out by the TBM on-board acquisition system during construction. However, it was not possible to gain complete TBM data for all tunnel projects included in the database. As a matter of facts, the contractors are often unable to share easily the data from the site especially when on-going claims have not been resolved yet. Regarding the compilation of the geological and geotechnical parameters, it is important to underline that they have been directly gathered from the tunnel projects or estimated from laboratory tests through formula commonly used in rock mechanics. Although the degree of detail of data varies from one project to another, enough information has been collected in order to have an idea of the distribution of important parameters related to the boring process and the TBM advancement.

In order to identify the correlations between the performance parameters of the machine and the geological/geotechnical characteristics, preliminary analyses have been carried out based on the information collected in the TBM-performance database. Due to the variable quality of data and because of the different structural characteristics of the machines, gripper and shield data have been studied separately. Though an important variation between gripper and shield machines has been observed in terms of advancement (i.e. a better performance for shield TBM probably related to the higher penetration rate and to the fact that the rock supporting time does not change significantly from one section to another), no consistent correlations could be found between the shield TBM parameters and the geomechanical characteristics. On the contrary, more significant observations could be made in the case of gripper TBMs, where further investigations have been done.

The first results obtained for the open-type machine, confirm the difficulties in selecting, within the most common parameters used in the existing prediction models, the ones affecting the most the TBM performance while degrading the ground conditions. As a matter of facts, in highly fractured rocks and fault zones, the delays associated to the increasing need of heavy temporary supports, rock jams, gripper bearing failure, additional drainage system, etc., are partially balanced by the rather high TBM penetration rates generally observed in fractured/very fractured rock masses. Moreover, find a correlation between the TBM advancement and the rock mass quality is a quite difficult task because of the huge number of parameters, both rock mass- and construction- related, involved in its definition, as well as the unpredictable events, often due to the human factor which is almost impossible to quantify (TBM utilisation factor). In order to partially solve this problem, the reduced uniaxial compressive strength (Habimana, 1999; Habimana et al., 2002), which takes into account the weathering degree of rock mass, has been introduced for characterising the strength of disturbed rocks. Despite a significant lowering of strength values (thus more representative of the real conditions), the correlation with the TBM performance parameters remains almost meaningless, due to the large scattering of data. The uncertainties related to the behaviour of disturbed zones are one of the major causes of this large data scattering. Thus it has been decided to investigate the correlations between the TBM performance parameters (i.e. penetration rate and advance rate) and the Rock Mass Rating (RMR), in order to consider the rock mass as a combination of several factors (i.e. RMR). The obtained results are consistent with the previous work made by Sapigni et al. (2002). However, in order to predict the TBM performance, the RMR system proved to be not sufficient for characterising the rock mass behaviour in difficult ground conditions (although some trends have been identified). As a matter of facts, it has been observed that some parameters, which are basic factors for the evaluation of the RMR (e.g. the rock strength), and thus extremely significant for estimating performance while boring in hard rocks, may actually play a very marginal role in the definition/estimation of the machine performance in highly fractured and faulted zones.

Fault zone classification and numerical modelling

In order to consider the complex structure of fault zones and bearing in mind that a more global approach is required for characterising their behaviour (i.e. combination of factors instead of specific parameters approach), the next step has been the development of a classification system of these particular environments. In order to identify the specific classes describing highly fractured and faulted rocks, several geological/geotechnical factors have been taken into account. The choice of specific parameters has been done by compiling several literature sources dealing with fault rock characterisation, both from geological and geotechnical point of view. In particular, the fracturing degree of the rock mass (expressed by the volumetric joint count, J_v) and the weathering degree of rock and joints (expressed by the Geological Strength Index, GSI) represent, in this framework, the main factors involved for characterising the behaviour of each "fault zone" category. Four classes have been defined:

I. Highly fractured rock mass: the rock mass is characterised by a high fracturing degree ($10 < J_v$ [joints/m^3] < 35); there are no visible signs of discolouration and decomposition of the rock material and/or of the joint surfaces. This class can be

described by the Uniaxial Compressive Strength of the rock mass (UCS_{rm}), depending on UCS of the intact rock and on GSI ($30 < GSI < 60$).

II. Highly fractured rock mass, with weathered joints: in addition to the high fracturing degree ($10 < J_v$ [joints/m^3] < 35), surface weathering starts to appear but there are still no signs of alteration in composition and structure of the rock material (no results of faulting activities). This class is still described by UCS_{rm}, although the range of GSI decreases with respect to the first class ($20 < GSI < 40$).

III. Cohesive fault rocks (and heterogeneous rock masses): the fracturing degree (i.e. J_v) is no longer a reference parameter and the weathering degree becomes the main factor for describing this class, presented as the result of faulting and folding activities (tectonisation). In this framework, the uniaxial compressive strength proposed by Habimana (1999) and by Habimana et al. (2002) for the cataclastic rocks (UCS_H) becomes a valid parameter for better characterising the rock mass from the geomechanical point of view. Actually this parameter, mainly depends on GSI ($5 < GSI < 40$) that decreases according to the degree of tectonisation undergone by the rock material.

IV. Crushed fault rocks: disintegrated rock mass representing the highest degree of tectonisation and degradation of the material. The extremely high fracturing degree and no more evident discontinuity sets result in a total absence of blockiness (J_v is assumed to be greater than 35 joints/m^3). The UCS_H remains the most appropriate geomechanical parameter in order to describe this class, where GSI reaches the lowest values ($5 < GSI < 30$).

With the aim to better characterise the "fault zone" classes from a geomechanical point of view, the rock response to TBM cutter penetration has been simulated by discontinuum models (for the highly fractured rock masses described by Class I and Class II) and by continuum models (for the degraded and/or crushed rock masses described by Class III and Class IV). The Universal Distinct Element Code UDEC (Itasca®) has been used. Concerning the discontinuum approach, several models characterised by different values of J_v have been developed, while in the equivalent continuum medium no joint sets have been included in the simulations and the strength parameters have been reduced according to the failure criterion introduced by Habimana (1999) and Habimana et al. (2002). The performed simulations allow observing that:

- Discontinuum models (developed for simulating the rock mass described by Class I and Class II): according to the results obtained by previous authors, the tensile failure seems to be the dominant chip forming mechanism under the cutter load (probably due to the high material brittleness). Moreover, in agreement with the trend observed for the field penetration rate (p) compiled in the TBM-performance database, the simulated rate of penetration (P_{chip}) increases for increasing J_v (this means that the discontinuities assist the crushing and chipping of the rock).
- Continuum models (developed for simulating the rock mass described by Class III and Class IV): the shear failure seems to be the dominant mechanism inducing the rock fragmentation; this can be explained by the significant strength decrease of the material. Since it is not possible anymore to identify a defined chip (i.e. there are no tensile

cracks), the estimation of the penetration rate becomes more difficult. The fragmentation process seems actually to be reduced to a problem of rock removal from the tunnel face, as it is commonly observed in reality.

TBM-performance reduction in "fault zone" classes

Once the "fault zone" classes have been defined, for each of them the TBM performance has been evaluated in terms of penetration rate and daily advance rate. The existing database has been improved by including tunnel sections characterised by good tunnelling conditions. The aim was to analyse the best (and the most frequent) TBM performance recorded during the excavation and to compare them with the behaviour of the machine in difficult ground conditions (i.e. faulted and highly fractured rock masses). Moreover, in this step, only tunnel sections excavated by gripper TBMs have been classified according to the proposed "fault zone" classification system (because of the lack of data in shield TBM projects with regard to the rock mass description).

For each "fault zone" class it has been possible to obtain a reduction factor to be applied to the best (and the most frequent) performance recorded in good tunnelling conditions. The following parameters have been studied separately: cutterhead rotation speed RPM (rev/min), penetration rate PR (m/hr) and daily advance rate AR (m/day). Interesting observation could be done for the penetration rate (penetration per revolution, p) expressed in mm per revolution. Despite to expectations, a certain increase has been even observed especially in the last two "fault zone" classes (i.e. Class III and IV) where the strength reduction undergone by rock material, seems to facilitate the boring process rather than to hinder it. Contrary to PR, p somehow refers to the penetration at the tool-scale, where the face stability problems do not represent a hindrance to cope with. On the other hand, for analysing PR, where the tunnel diameter scale needs to be introduced due to its dependence on RPM, the issues related to face instability seems to affect the performance values. Finally, regarding the advance rate AR, a decreasing trend from the first to the fourth "fault zone" (representing decreasing tunnelling conditions) could be observed.

The "Decision Aids for Tunnelling" (DAT)

The TBM performance reduction (in terms of advancement) observed for each "fault zone" class obviously traduces in potentially longer tunnel construction times and higher costs. In order to more deeply investigate the influence that faulted and highly fractured rocks may have on the final time and cost, probabilistic analyses of the tunnel construction have been performed with the Decision Aids for tunnelling (DAT). The DAT are computer based tools that allow engineers to simulate the construction by keeping into consideration the uncertainties related to geology and to excavation processes. The DAT consist of two main modules describing respectively the geological conditions ("geology module") and the construction process in terms of methods and sequence ("construction module"). The "geology module" produces probabilistic ground class profiles indicating the probabilities of particular geological conditions occurring at a particular tunnel location. The excavation of the tunnel network through these profiles is then simulated by the construction module. The input is usually obtained through a

combination of objective information and subjective estimation done by experts. Based on the proposed classification system, the following ground conditions have been used as input for the DAT geology module:

1. Good, massive to slightly jointed rock (corresponding to good tunnelling conditions)
2. Highly fractured rocks, C1 (corresponding to Class I of the classification).
3. Highly fractured, weathered rocks, C2 (corresponding to Class II of the classification).
4. Faulted rocks, C3 (corresponding to Class III of the classification).
5. Crushed rocks, C4 (corresponding to Class IV of the classification).

The construction of the tunnel has been simulated by taking into account the outcomes of the analyses performed on the data compiled in the TBM-performance database (developed both in good and bad conditions). The results of the DAT analyses confirmed the significant construction time (and costs) increase that may take place while changing from "good" grounds to "disturbed" ground conditions. Thus, according to the different TBM-performance reductions evaluated for each "fault zone" class, it has been possible to obtain a reliable estimation of the final tunnel construction time and cost for different excavation scenarios. Beside the results achieved in terms of time and costs quantification, it is important to underline how the information obtained from the analyses carried out on the TBM-performance database contributes to the reduction of the uncertainties related to the subjective estimation, which is generally made by the DAT users. These uncertainties are higher in difficult ground conditions, such as fault zones, where the machine performance (in terms of advancement) is hard to assess. The proposed fault zone classification system and the reduction rates of the daily advancement characterising each class have been then implemented and used in a DAT simulation of a real case. Satisfactory results have been obtained since the predicted construction times proved to be very close to the values recorded on the field.

Perspectives and outlook of this research

Although the results of this study allow obtaining a better evaluation of the TBM behaviour in highly jointed rocks and fault zones, it is important to underline that this work is characterised by several limitations which might be tackled and eventually solved in future research.

Regarding the development of the TBM-performance database, the characterisation of the "fault zone" classes, the performance analyses in each identified category as well as the assessment of possible final construction time and cost, further improvements can be listed as follows:

- Although the quality of the geological/geotechnical information and the problems related to the accessibility of TBM data represent important issues hardly negligible, a logical continuation of this work is the improvement of the database by compiling information from other tunnel projects. Furthermore, the analyses of the TBM performance should be deepened not only for open-type TBM but also for shield (and double-shield) machines, which have not been well investigated in this framework due to the lack of data.

- For what concerns DAT simulations, although it has been observed that obtaining detailed information about tunnelling projects in difficult conditions can be extremely hard, the possibility to include a larger number of tunnel projects where fault zones (defined according to the proposed classification) are encountered can provide more reliable input data. Moreover, a careful analysis of time and cost related to the different construction activities (e.g. TBM boring, rock supporting, cutter replacement, conveyor system maintenance, etc.) would contribute to reduce the uncertainty characterising the construction method. This would allow better investigating the impact of worsening TBM performance (due to difficult ground conditions) on tunnel construction.

- A better geomechanical/geological characterisation of the "fault zone" classes, mainly based on accurate field investigations and laboratory testing programs on fault zone and fault rocks, would certainly allow for further improvements in the analysis of the influence of other important aspects, such as rock anisotropy and stress level.

- Finally, a more comprehensive description of the rock-machine interaction can be obtained by quantifying the variation of other operational parameters (apart from RPM) in the "fault zone" classes, with respect to the good tunnelling performances.

Other potential developments of the research can be identified by considering the numerical simulations of rock response to TBM cutter penetration; in particular the following improvements can be suggested:

- The simulation of different types of rocks would allow taking into account the influence on the chipping process of geomechanical parameters such as rock strength and deformability.

- More indenters should be modelled in order to better represent the chipping process as result of the interaction between adjacent cutters.

- High confinement stresses should be considered in order to model more realistic situations in terms of boundary conditions. Furthermore, this would also allow better analysing the influence of in-situ stresses on the rock breakage process induced by TBM cutting tools.

- Finally, an important step forward of this study would be the implementation and development of 3D models where the cutter rolling force can be also simulated and its effect on the chipping process taken into account.

ANNEX A

TBM-PERFORMANCE PREDICTION: THE PARAMETERS USED BY NTNU AND Q_{TBM} MODELS

The NTNU (NTH) model

The NTNU model makes use of two main groups of factors. The first one includes the main rock mass properties, relevant to TBM performance, that are based on a series of measurements and indexes which were originally developed for drillability testing of hard rock (first column of Table A-1). The second group of parameters includes the main TBM specifications (second column of Table A-1).

Table A-1 Parameters used by the NTNU model (after Bruland, 1998)

Rock mass properties	TBM parameters
Rock mass degree of fracturing	Average cutter thrust
Angle between tunnel axis and planes of weakness	Average cutter spacing
Drilling Rate Index (DRI)	Cutter diameter
Porosity (for some rock types)	Cutterhead rotation speed (RPM)
	Installed cutterhead power

Rock mass parameters

Intact rock properties

The NTNU model makes use of the Drilling Rate Index (DRI) to represent the properties of the intact rock material. The DRI is calculated on the basis of two tests, the Brittleness Test and the Sievers' Miniature Drill Test, which are briefly described below.

The brittleness test gives a measure of the ability of the rock to resist crushing from repeated impacts (Figure A-1). The volume of test material corresponds to 500 grams of specific gravity 2.65 of the fraction 16 ± 11.2 mm. The Brittleness Value (S_{20}) is defined as the percentage of material passing the 11.2 mm sieve after 20 impacts of a 14 kg weight, taken as the mean value of 3-4 parallel tests (Bruland and Nilsen, 1995).

The Sievers' Miniature Drill Test gives a measure of the surface hardness of the rock. The test is performed on a precut rock sample. The Sievers' J-value (SJ) is the drill hole depth, in 1/10 mm, after 200 rotations of the drill bit, taken as the mean value of 4-8 drill holes (Figure A-2). The precut surface of the sample must be parallel or perpendicular to the foliation of the rock. The SJ value measured parallel to the foliation is used to calculate the DRI (Bruland and Nilsen,

1995). The DRI is finally calculated starting from the brittleness value S_{20} and the SJ-value with the chart represented in Figure A-3.

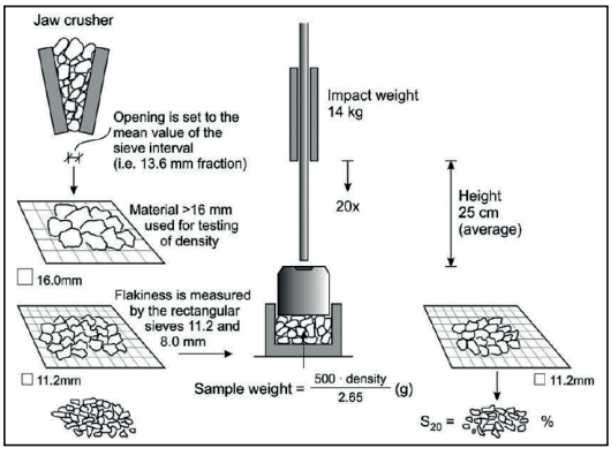

Figure A-1 The brittleness test (after Bruland and Nilsen, 1995).

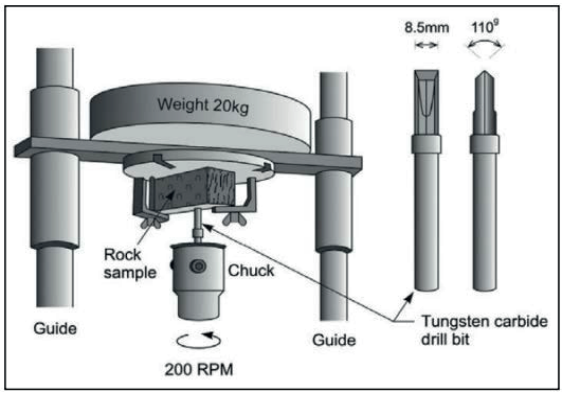

Figure A-2 The Seviers' miniature drill test (after Bruland and Nilsen, 1995).

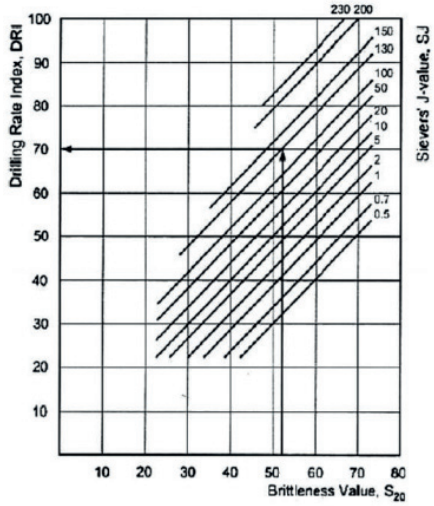

Figure A-3 Calculation of DRI (after Bruland, 1998).

The tests presented above are generally difficult to be performed in standard rock mechanics laboratories. For this reason a correlation between the drilling rate index and the compressive strength of intact rock has been proposed (Figure A-4). This correlation may be also expressed with Equation A-1.

$$DRI = E\sigma_{ci}^{-0.6} \quad \text{A-1}$$

where σ_{ci} is the uniaxial compressive strength of the rock and E is a factor representing various groups of rocks which assumes the following values:

- E = 1000 for most non-schistose, hard rocks (σ_{ci} > 40 MPa);
- E = 750 for metamorphic schist (σ_{ci} = 30-150 MPa);
- E = 500 for argillaceous rocks (σ_{ci} = 10-100 MPa).

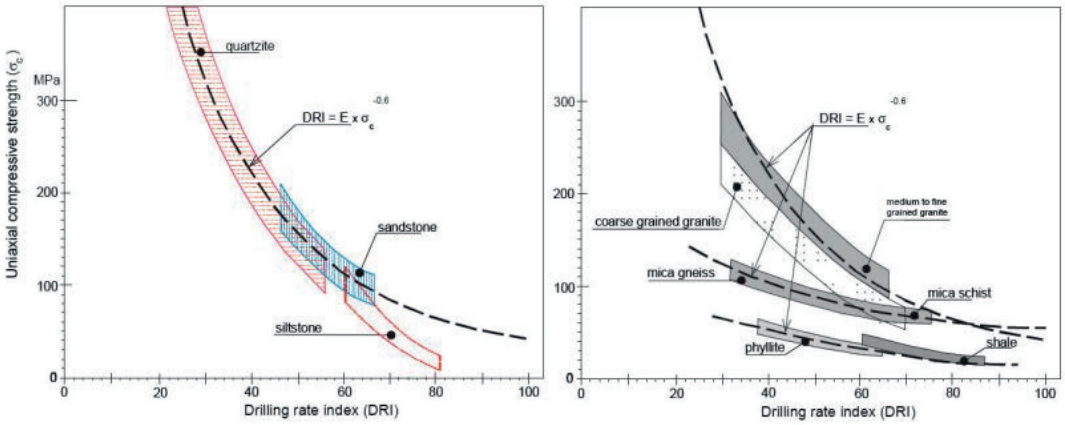

Figure A-4 DRI versus compressive strength ($\sigma_c = \sigma_{ci}$) grouping according to rock type (after Palmström, 1995).

Joint parameters

The NTNU model places great emphasis on rock jointing, which is regarded as the most important parameter influencing the advance rate of a TBM. In particular, rock mass jointing is described in the model as (Bruland, 1998):

- Systematically jointed rock masses, formed by:
  - parallel oriented joints (one set);
  - parallel oriented fissures and foliation planes or bedding planes (one set);
  - two or more joint sets and/or fissure sets.
- Massive rock masses.

Joints (Sp) are defined as pervasive joints which can be traced along the whole tunnel profile. They can be open (as in stress relief joints) or clay - coated with weak/smooth minerals (such as calcite, chlorite, etc.)

Fissures (St) include discontinuous joints which only partly can be observed around the tunnel profile. Healed joints with low shear strength and foliation or bedding planes (as in mica schist or mica gneiss) are also considered as fissures.

Massive Rock includes rock masses without joints or fissures, or with healed joints with filling of high shear strength (for example quartz, epidote, etc.). The degree of fracturing of a rock mass is then subdivided into seven classes (Table A-2).

Table A-2 NTNU fracture classes (after Bruland, 1998)

Fracture Class (Joints Sp/Fissures St)	**Distance between plane of weakness [cm]**
0	-
0-I	160
I-	80
I	40
II	20
III	10
IV	5

Finally, the rock mass fracturing degree is described by the fracturing factor k_s, which depends on fracture type and frequency and the angle between the tunnel axis and the plane of weakness, α. The latter can be computed according to Equation A-2 (Bruland, 1998):

$$\alpha = arcsin\left(sin\alpha_f \cdot sin(\alpha_t - \alpha_s)\right) \quad \text{A-2}$$

where α_f is the dip angle of weakness planes, α_t is the direction of the tunnel axis and α_s is the strike angle of weakness planes. Based on the angle α and the fracturing classes shown in Table A-2, the fracturing factor k_s is then obtained with the chart presented in Figure A-5 (Bruland, 1998). The k_s factor represents rocks with DRI = 49. For other values of DRI, k_s has to be adjusted. This is done according to the upper chart in Figure A-5. The correction factor is called k_{DRI}.

When more than one set of weakness planes are included in the model (maximum 3 recommended), the total fracturing factor must be calculated with Equation A-3:

$$k_{stot} = \sum_{i=1}^{s} k_{si} - 0.36 \cdot (s-1) \quad \text{A-3}$$

where k_{si} is the fracturing factor of set i and s is the number of joint families.

Finally, the rock mass properties for TBM boring are expressed by the equivalent fracturing factor:

$$k_{eq} = k_{stot} \cdot k_{DRI} \quad \text{A-4}$$

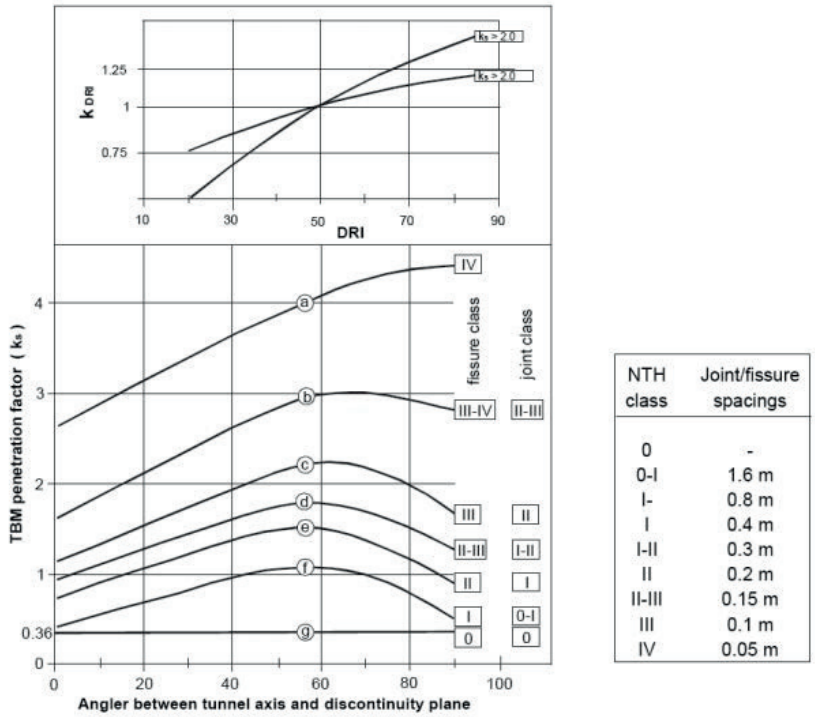

Figure A-5 Computation of the NTNU fracturing factor (after Bruland, 1998).

Machine parameters

The basic penetration or net rate of TBM penetration i_0, expressed in mm/rev, is a function of the equivalent thrust M_{eq} and the equivalent fracturing factor previously introduced. It can be derived from Figure A-6.

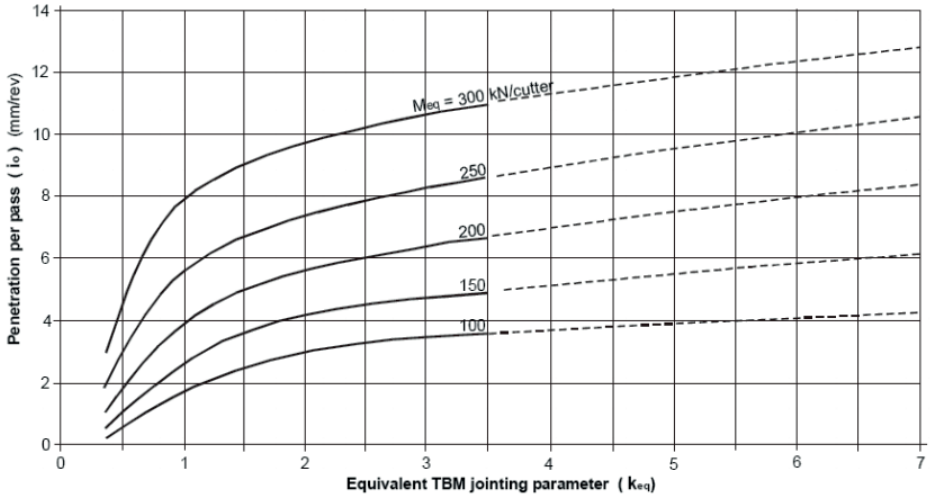

Figure A-6 Basic penetration i_0. Cutter diameter 483 mm and cutter spacing 70 mm (after Palmström, 1995).

The chart is valid for cutter diameter 483 mm (19 inches) and an average cutter spacing of 70 mm. In all the other cases the equivalent thrust M_{eq}, may be computed with Equation A-5:

$$M_{eq} = M_b \cdot k_d \cdot k_a \quad \text{A-5}$$

where M_b is the applied thrust per cutter (kN), k_d is the correction factor for cutter diameter and k_a is the correction factor for cutter spacing. k_d and k_a in Equation A-5 can be determined with the charts shown in Figures A-7 and A-8, respectively.

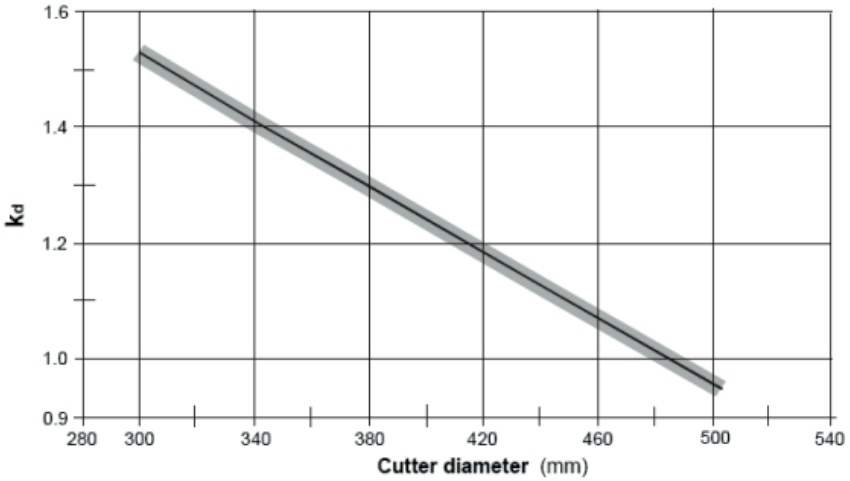

Figure A-7 Correction factor k_d for different cutter size (after Bruland, 1998).

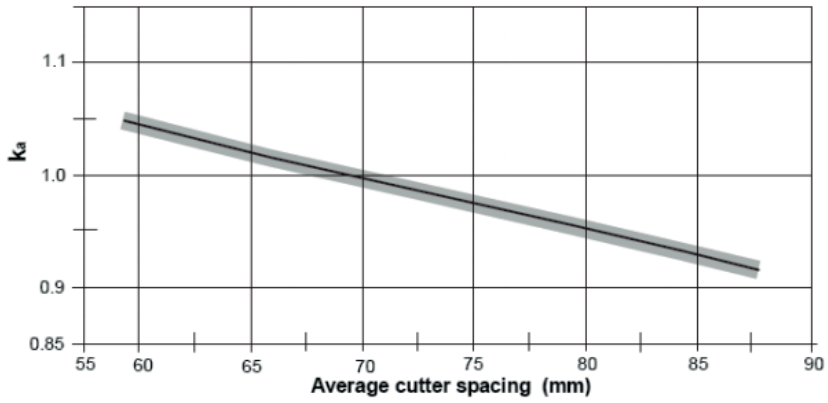

Figure A-8 Correction factor k_a for different cutter spacing (after Bruland, 1998).

Penetration rate estimation

The TBM penetration rate PR (m/hr) is finally calculated with Equation A-6:

$$PR = \frac{i_0 \cdot RPM \cdot 60}{1000} \quad \text{A-6}$$

Where RPM is the cutterhead revolutions per minute and i_0 (mm/rev) is the penetration per revolution (called p in the thesis), which can be evaluated with Figure A-6 or alternatively with Equation A-7:

$$i_0 = F \cdot k_{eq}^{G} \quad \text{A-7}$$

where:

$$F = 0.0015 \cdot M_{eq}^{1.5} \quad \text{A-8}$$

$$G = 30 \cdot k_{eq}^{-0.5} \cdot M_{eq}^{-0.8} \quad \text{A-9}$$

The TBM advance rate can be then calculated after selection of an appropriate utilisation factor U of the machine.

The Q_{TBM} model

The Q_{TBM} model (Barton, 2000) is an extension of the Q-system where some rock mass and machine parameters, relevant to TBM performance, have been introduced (e.g. the strength and abrasiveness of the rock, the cutter load etc.). The Q_{TBM} is calculated by Equation A-10:

$$Q_{TBM} = \frac{RQD_0}{J_n} \cdot \frac{J_r}{J_a} \cdot \frac{J_w}{SRF} \cdot \frac{SIGMA}{F^{10}/20^9} \cdot \frac{20}{CLI} \cdot \frac{q}{20} \cdot \frac{\sigma_\vartheta}{5} \quad \text{A-10}$$

with:

- RQD_0 = RQD (%) interpreted in the tunnelling direction
- J_n, J_r, J_a, J_w = joint parameters (unchanged from the original Q system)
- SRF = Strength Reduction Factor (unchanged from the original Q system)
- SIGMA = rock mass strength expressed as $SIGMA_{cm}$ (Equation A-11) or $SIGMA_{tm}$ (Equation A-12), based on the predominantly failure process (compressive or tensile). If α is the joint angle:

$$SIGMA_{cm} = 5 \cdot \gamma \cdot Q_c^{1/3} \ \ with\ unfavourable\ \alpha\ (generally\ greater\ than\ 60^\circ) \quad \text{A-11}$$

$$SIGMA_{tm} = 5 \cdot \gamma \cdot Q_t^{1/3} \ \ with\ favourable\ \alpha\ (generally\ lower\ than\ 30^\circ) \quad \text{A-12}$$

with Q_c and Q_t expressed as functions of the Q-value computed in the tunnelling direction (Q_0), according the following formulations:

$$Q_c = \frac{\sigma_{ci}}{100} Q_0 \quad \text{A-13}$$

$$Q_t = \frac{I_{50}}{4} Q_0 \quad \text{A-14}$$

where σ_{ci} is the uniaxial compressive strength and I_{50} is the point load index on 50 mm diameter core.

- F = average cutter load (tnf) through the same zone, normalised by 20 tnf
- CLI = Cutter Life Index
- q = quarts content (%)
- σ_9 = induced biaxial stress on tunnel face (MPa) in the same zone, normalised to an approximate depth of 100 m

The relationships between Q_{TBM}, penetration rate (PR) and advance rate (AR) was based on a process of trial and error using case records from literature. They are expressed by the Equations A-15 and A-16.

$$PR \approx 5 \cdot Q_{TBM}^{-1/5} \quad \text{A-15}$$

$$AR = PR \cdot U \approx 5 \cdot Q_{TBM}^{-1/5} \cdot T^{m} \quad \text{A-16}$$

where T is the time (hours) and m is a negative gradient (LT^{-2}- deceleration) that expresses the decelerating average advance rate which is observed as the unit of time (hours, days, weeks, months) increases (Figure A-9).

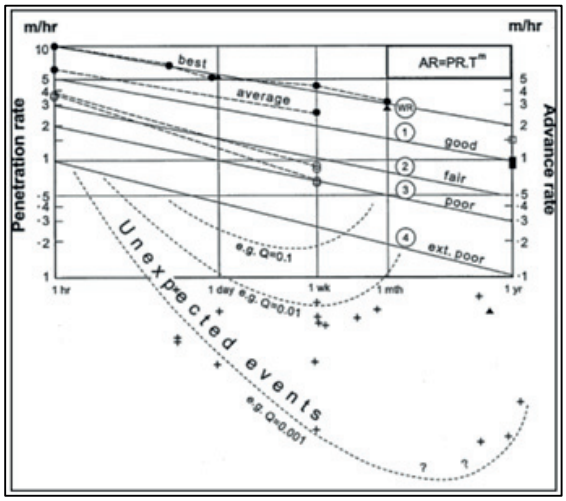

WR (world record)	m=-0.13 to -0.17
1 (good)	m=-0.17
2 (fair)	m=-0.19
3 (poor)	m=-0.21
4 (ext. poor)	m=-0.25

Figure A-9 Decelerating average advance rate observed as the unit of time (day, week, month) and tunnel length increase, based on 145 TBM tunnels totalling > 1000 km (e.g. crosses refer to diverse fault zones from widely different geologies) (after Barton, 2000).

The gradient m includes the abrasiveness of rock via the cutter life index CLI, and so includes the cutter wear. It also includes the percentage of quartz (%), rock porosity and tunnel dimension via the tunnel diameter (Equation A-17).

$$m \approx m_i \left(\frac{D}{5}\right)^{0.20} \left(\frac{20}{CLI}\right)^{0.15} \left(\frac{q}{20}\right)^{0.10} \left(\frac{n}{2}\right)^{0.05} \quad \text{A-17}$$

where m_1 is a factor depending on the Q-value, D is the tunnel diameter, CLI is the cutter life index, q is the quartz content (%) and n is the porosity. Suggested values for m_1 are reported in Figure A-10 (the subscript "1" is added to m for evaluation of Equation A-17).

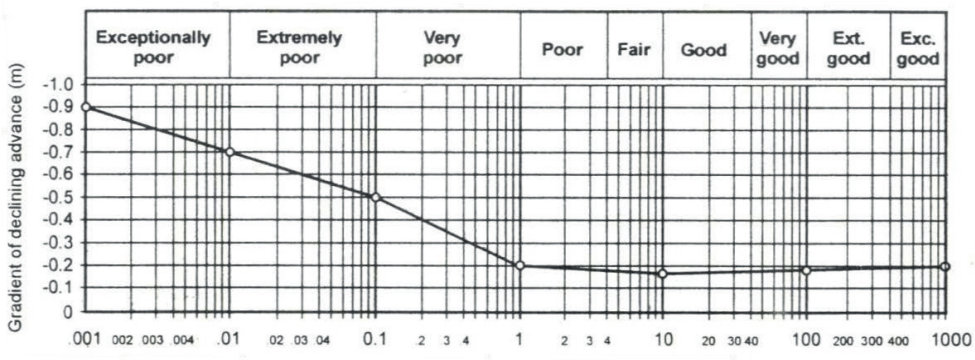

Figure A-10 Preliminary estimate of declining advance rate gradient (-)m, as a function of Q-value.

The time T to bore a length of tunnel L with an average advance rate of AR is obviously L/AR. Therefore, Equation A-18 can be derived:

$$T = \left(\frac{L}{PR}\right)^{\frac{1}{1+m}} \qquad \text{A-18}$$

In Figure A-11 the final log-linear versions of Equations A-15 and A16 are reported.

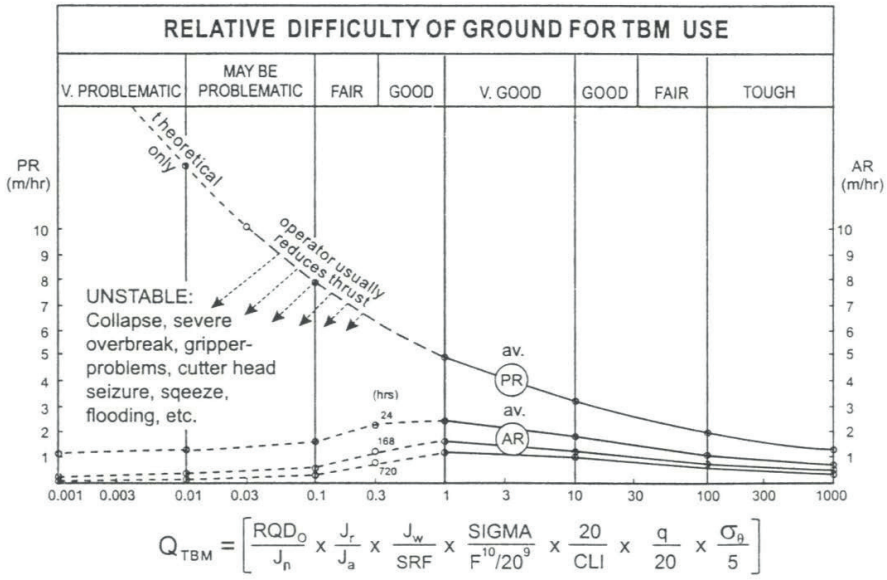

Figure A-11 Suggested relationship between PR, AR and Q_{TBM} (Barton, 2000).

ANNEX B

NUMERICAL MODELLING – MAIN APPROACHES IN GEOMECHANICS

Continuum modelling

The rock mass response to excavation is simulated by introducing a continuum/equivalent continuum where the intact rock properties (such as the uniaxial compressive strength) are scaled down to the properties of the rock mass by using well known correlations with the most frequently used rock mass indices (such as RMR and GSI). By means these correlations (which depend on the rock type and on the excavation method) rock mass parameters such as m_b and s of the Hoek-Brown criterion can be estimated.

After the scaling process (Figure B-1) a proper constitutive relation has to be adopted for the material. When the progressive failure of the rock mass is analysed, the post-peak response can be described by different elasto-plastic models. In Figure B-2 the stress-strain laws most frequently used for the solution of tunnelling problems are reported. Based on the rock mass quality the constitutive relations generally adopted in practice are (Hoek and Brown, 1997; Barla and Barla, 2000):

a) Elastic-perfectly brittle behaviour (very good quality hard rock mass): when the rock mass is exceeded a sudden strength drop occurs (Figure B-2a);
b) Elastic-strain softening behaviour (average quality rock mass): after yielding the rock strength is reduced from the in situ to the broken state; once the final "residual" state is reached deformation continues at a constant stress level (Figure B-2b).
c) Elastic-perfectly plastic behaviour (very poor quality rock mass): after yielding deformation continues at a constant stress level and no volume change is associated with the ongoing failure (Figure B-2c).

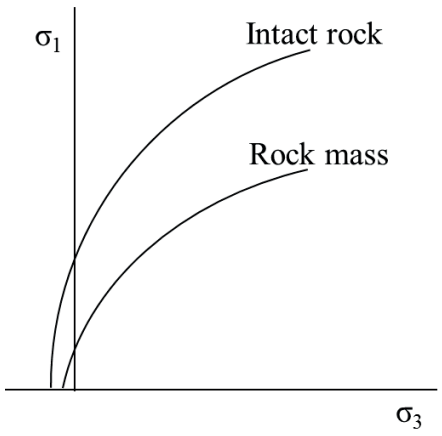

Figure B-1 Hoek-Brown failure criteria for the intact rock material and the rock mass.

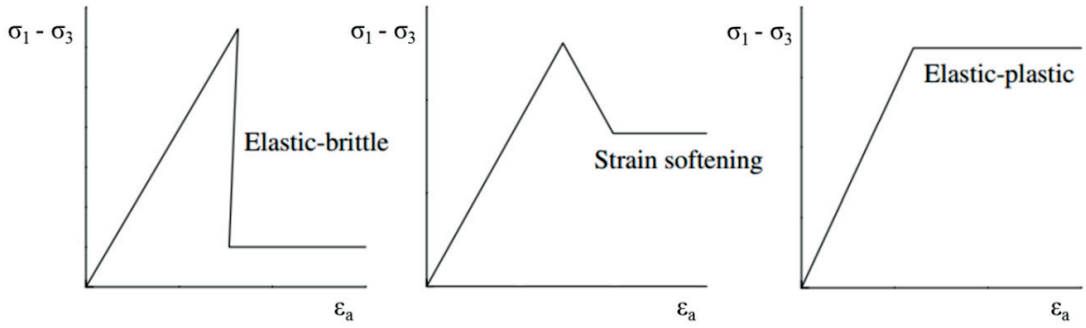

Figure B-2 Stress-strain laws for different rock mass qualities: a) elastic-perfectly brittle law; b) elastic-strain softening stress-strain law; c) elastic-perfectly plastic stress-strain law; (after Barla and Barla, 2000).

As reported by Barla and Barla (2000), the continuum method can be summarized in two groups: the domain methods (including finite element methods and finite difference methods) and the boundary methods (including several types of boundary element methods). In a tunnelling engineering problem, the boundary methods subdivide into elements the boundary of the excavation while the interior of the rock mass is represented mathematically as an infinite continuum. On the contrary, in the domain methods, both the medium and the boundaries are discretized into zones or elements.

Finite Element Method, FEM

In the Finite Element Method (FEM), the most used method in geomechanics, the continuum is discretized into small elements that intersect at their nodes (Figure B-3). The method is based on the principle of virtual displacements according to which for any small virtual displacement applied to a body in equilibrium, the total internal work associated with the virtual displacement field must be equal to the total virtual external work. It is assumed that the displacements at any point within the element can be obtained from the displacements of the nodes by appropriately chosen interpolation functions (Bobet, 2010). FEM computer programs can tackle a variety of rock mechanics problems. They are capable to model elastic, plastic and viscous materials and can incorporate anisotropic behaviour, 'no-tension zones', joints and faults (Blake, 1989).

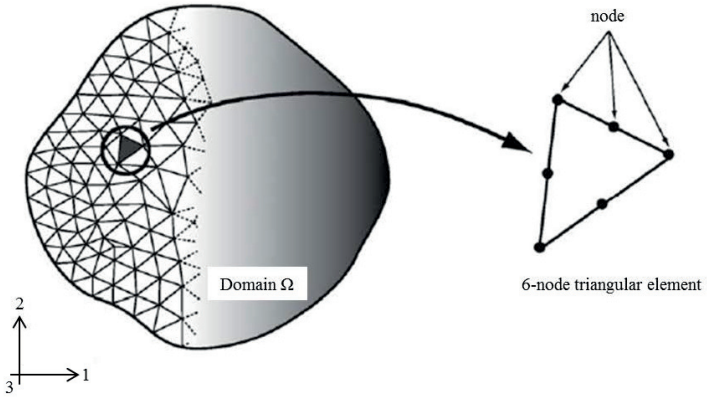

Figure B-3 Continuum model: 2D finite element discretization (after Bobet, 2010).

Finite Difference Method, FDM

In the Finite Difference Method (FDM), the oldest among the numerical methods in geomechanics, partial different equations which define material behaviour and boundary conditions (i.e. equilibrium, strain compatibility) are approximated by finite difference formulas. In this approach grid is superimposed to the domain (Figure B-4) and the discontinuities can be included by using grid points on each side of the discontinuity. The slip along the joint plane is determined by the relative displacement between corresponding grid points. Normal and shear displacements can also be related to the shear and normal stiffness of the discontinuity and friction laws (e.g. Coulomb) can be included to the system of equations that relate shear stress with normal stress. FDM is very well-suited to incorporate non-linear behaviour. The desired final state is reached on a stepwise process, involving sufficiently small loading increments. The displacements at the grid points are obtained at the end of each loading step then, based on the non-linear behaviour of the material, stress are updated and another small loading increment is added (Bobet, 2010).

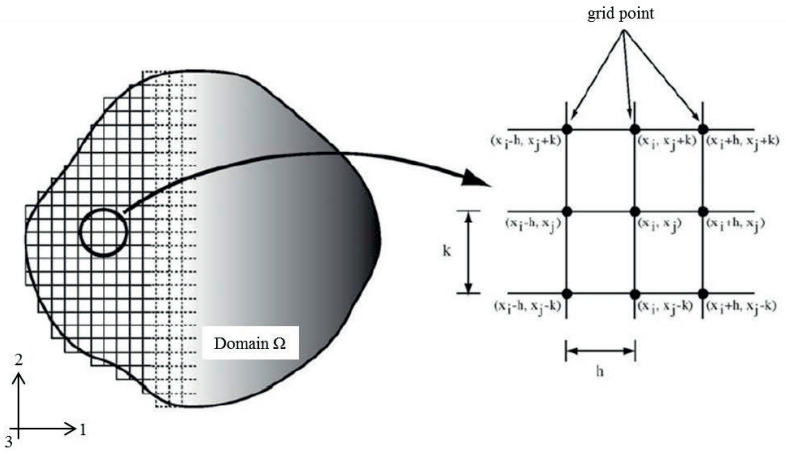

Figure B-4 Continuum model: 2D finite difference grid (after Bobet, 2010).

Boundary Element Method (BEM)

In the Boundary Element Method (BEM) only the boundaries of the continuum is discretized (Figure B-5). Being the problem reduced from 3D to 2D surface problem or from 2D to 1D line problem, this method is highly effective for problems where the volume to boundary surface ratio is large. The governing differential equations are formulated as integral equations which only consider boundary values. While the solution is approximated at the boundaries (unlike FEM and FDM where the approximations are made inside the medium), the equilibrium and compatibility are satisfied within the domain (Bobet, 2010).

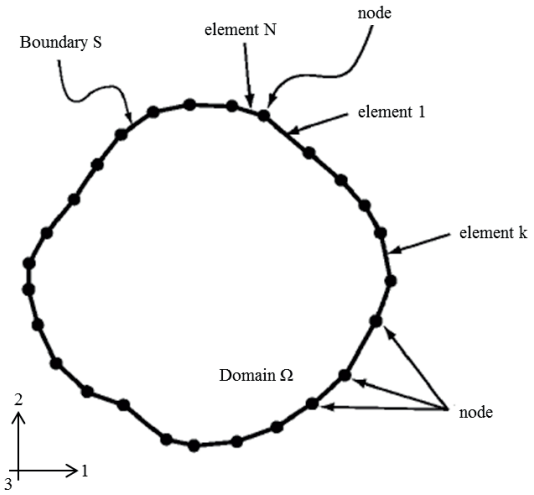

Figure B-5. Example of 2D discretization with boundary elements (after Bobet, 2010).

Discontinuum modelling

The continuum methods is not always suitable to model highly jointed rock masses where the use of the discontinuum modelling has been gaining progressive attention in tunnelling engineering (Barla and Barla, 2000). A discontinuous medium, unlike the continuous medium, is characterised by contacts (interfaces) between the discrete blocks that make up the system. The blocks are defined by the discontinuities and may be either rigid or deformable. The discontinuum approach includes the family of Discrete Element Methods which Cundall and Hart (1992) define as those that:

- Allow finite displacements and rotations of discrete bodies, including complete detachment;
- Recognizes new contacts automatically as the calculation progresses.

Without the first attribute, the model cannot reproduce some important mechanisms in a discontinuous medium; without the second, the model is limited to small numbers of bodies for which the interactions are known in advance (Itasca, n.d.).

Distinct Element Method (DEM)

The Distinct Element Method (DEM) belongs to the family of Discrete Element Methods. Besides simulating large movements in jointed rock masses (Cundall, 1971) and granular assemblies (Cundall and Strack, 1979), it has been also applied to a discontinuum medium modelled as discs in two dimensions or spheres in three dimensions (Bonded Particle Method, Potyondy and Cundall, 2004). There are three main issues related to the application of DEM: the representation of contacts (discontinuities); the description of solid material (blocks) and the detection of new contacts during execution. Each block of the discretized domain (Figure B-6) is subjected to forces arising from the contacts, if any, from the surrounding blocks and from internal forces (e.g. gravity) and its displacement is governed by Newton's second low of motion (Bobet, 2010).

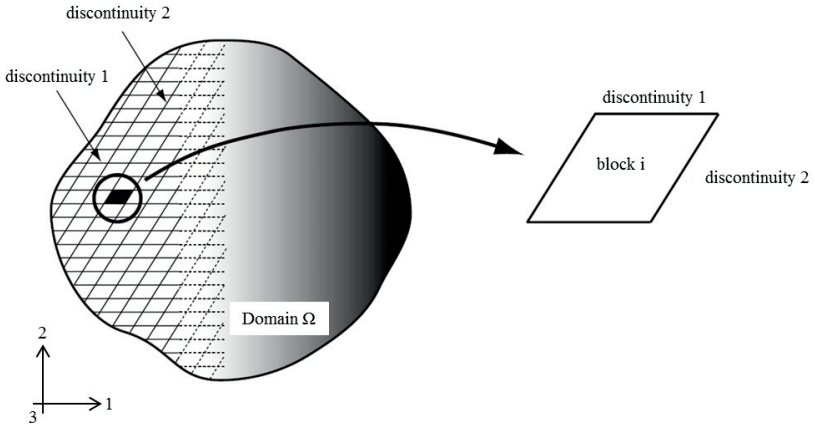

Figure B-6 Discontinuum model: DEM discretization (Bobet et al., 2009).

The calculations performed in the distinct element method alternate between application of Newton's second law at all blocks and a force-displacement law at all contacts. The force-displacement law is used to find contact forces from known (and fixed) displacements. If the blocks are deformable, motion is calculated at the grid points of the triangular finite-strain elements within the blocks. Then, the application of the block-material constitutive relations gives new stresses within the elements (Itasca, n.d.). In Figure B-7 the cycle of mechanical calculation is reported.

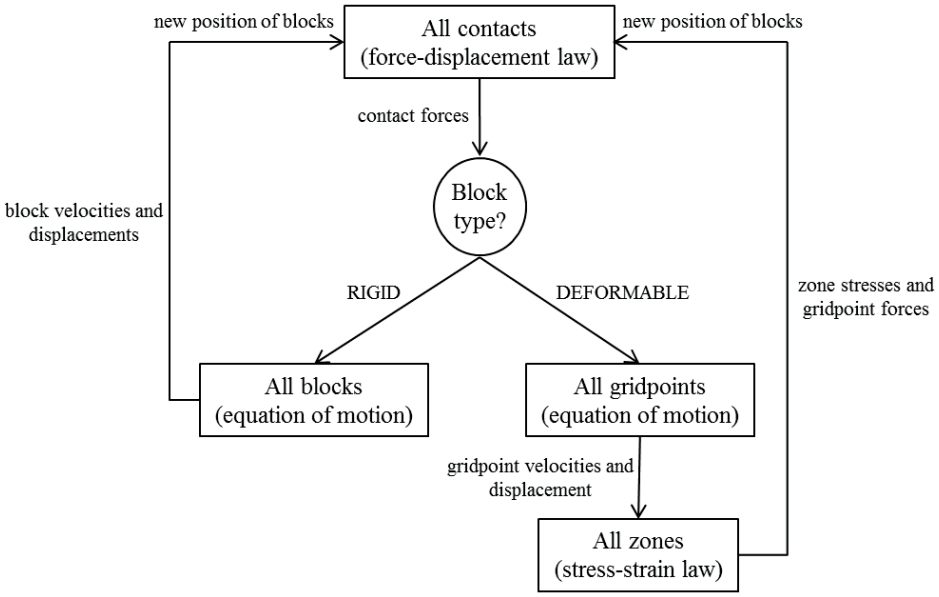

Figure B-7 Calculation cycle for a DEM code (after Itasca, n.d.).

A DEM code (such as UDEC, 3DEC PFC of Itasca®) is based on a dynamic (time domain) algorithm which solves the equation of motions by an explicit finite difference method.

The size of the timestep in the "timestepping" algorithm is limited by the assumption that velocities and accelerations are constant within the timestep. The distinct element method is based on the concept that the timestep is sufficiently small enough that disturbances cannot propagate between one discrete element and its immediate neighbours during a single step (i.e. there is a limited speed at which information can be transmitted in any physical medium). For rigid blocks, the timestep limitation is defined by the block mass and interface stiffness between blocks; for deformable blocks, the zone size is used, and the stiffness of the system includes contributions from both the intact rock modulus and the stiffness at the contacts (Itasca, n.d.).

ANNEX C

HOW TO APPLY THE "FAULT ZONE" CLASSIFICATION

General procedure

By following a simple procedure (summarised in Figure C-1), the "fault zone" classification can be used only for tunnel projects excavated by gripper (open) machine. As it can be seen in Figure C-1, both the ordinary (good) and the difficult tunnelling conditions have to be analysed in order to correctly apply the reduction rate of the TBM performance identified for each "fault zone" class.

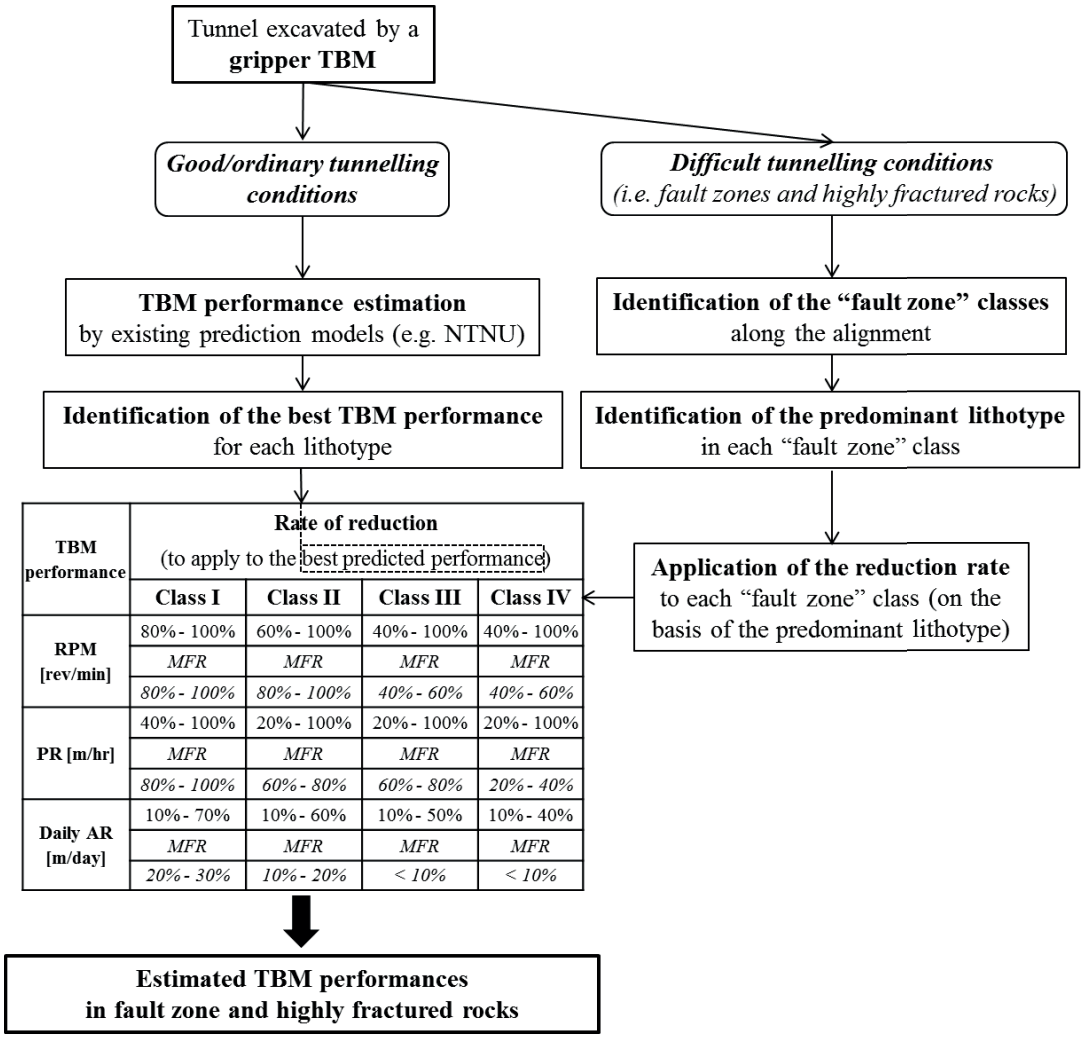

TBM performance	Rate of reduction (to apply to the best predicted performance)			
	Class I	**Class II**	**Class III**	**Class IV**
RPM [rev/min]	80% - 100%	60% - 100%	40% - 100%	40% - 100%
	MFR	*MFR*	*MFR*	*MFR*
	80% - 100%	*80% - 100%*	*40% - 60%*	*40% - 60%*
PR [m/hr]	40% - 100%	20% - 100%	20% - 100%	20% - 100%
	MFR	*MFR*	*MFR*	*MFR*
	80% - 100%	*60% - 80%*	*60% - 80%*	*20% - 40%*
Daily AR [m/day]	10% - 70%	10% - 60%	10% - 50%	10% - 40%
	MFR	*MFR*	*MFR*	*MFR*
	20% - 30%	*10% - 20%*	*< 10%*	*< 10%*

Figure C-1 Procedure to be followed to apply the "fault zone" classification.

In the preliminary phase of the tunnel construction, the penetration rate (PR) and the advance rate (AR and daily AR) can be estimated in the tunnel sections characterised by favourable environments through the existing performance prediction models (e.g. NTNU).

Once the TBM behaviour has been investigated in good/ordinary tunnelling conditions, the best performance (PR_{max} and daily AR_{max}) can be identified for each lithotype. Together with the maximum RPM installed on the machine (RPM_{max}), the best penetration and advance rates represent the parameters to which the reduction rates obtained for the "fault zone" classes have to be applied.

The "fault zone" classes have to be identified along the alignment (by means an adequate investigation activity before and during excavation) and for each of them the main lithotype (generally the host rock) has to be defined.

The reductions rates can be applied, on the basis of the lithotype, to the best performances previously estimated (or recorded during excavation) in good/ordinary tunnelling conditions. The TBM performances, in terms of cutterhead rotation speed, penetration rate and daily advance rate, are therefore estimated also in the fault zones and highly fractured rock masses.

Practical example

1. TBM-performance estimation in the tunnel sections characterised by good and ordinary tunnelling conditions. The existing prediction models can be used:
   - *NTNU model* (see Annex A) → Once the penetration rate (PR) is estimated for each tunnel section, the (daily) AR is obtained by assuming a reasonable utilization factor (U) for the machine (e.g. 0.4 for all lithologies).

Penetration per revolution [mm/rev], p	i_0 in the *NTNU model* (see Annex A)
Penetration rate [m/hr], PR	$PR = \frac{p \cdot RPM \cdot 60}{1000}$
Daily advance rate, daily AR [m/day]	$Daily\ AR = (PR \times U) \times 24$

2. Identification of the best (highest value) TBM-performance predicted for each lithotype (and the maximum RPM installed on the machine):

Lithotype	**Best performance**		***RPM installed on the machine, RPM_{max} [rev/min]***
	PR_{max} [m/hr]	**Daily AR_{max} [m/day]**	
Gneiss	2.2	21.1	6
Schist	2.6	25	6
Limestone	2.4	23	6
Granodiorite	1.9	18.2	6

3. Identification of the "fault zone" class along the alignment:

- three fault zones of the I CLASS;
- one fault zone of the II CLASS;
- two fault zones of the III CLASS
- one fault zone of the IV CLASS.

4. Identification of the predominant lithotype in each identified fault zone:

"Fault zone" class	**Main lithotype (host rock)**
I CLASS	Gneiss
	Schist
	Granodiorite
II CLASS	Schist
III CLASS	Gneiss
	Limestone
IV CLASS	Limestone

5. Estimation of the TBM-performance in each identified fault zone:

Example I CLASS

TBM performance	**Rate of reduction** (to apply to the best predicted performance)			
	Class I	**Class II**	**Class III**	**Class IV**
RPM [rev/min]	80% - 100%	60% - 100%	40% - 100%	40% - 100%
	MFR	*MFR*	*MFR*	*MFR*
	80% - 100%	*80% - 100%*	*40% - 60%*	*40% - 60%*
PR [m/hr]	40% - 100%	20% - 100%	20% - 100%	20% - 100%
	MFR	*MFR*	*MFR*	*MFR*
	80% - 100%	*60% - 80%*	*60% - 80%*	*20% - 40%*
Daily AR [m/day]	10% - 70%	10% - 60%	10% - 50%	10% - 40%
	MFR	*MFR*	*MFR*	*MFR*
	20% - 30%	*10% - 20%*	*< 10%*	*< 10%*

- $RPM = (0.8 \div 1) \times RPM_{max}$

  $RPM\ (Most\ Frequent\ Reduction) = (0.8 \div 1) \times RPM_{max}$

- $PR = (0.4 \div 1) \times PR_{max}$

  $PR\ (Most\ Frequent\ Reduction) = (0.8 \div 1) \times PR_{max}$

- $Daily\ AR = (0.1 \div 0.7) \times Daily\ AR_{max}$

  $Daily\ AR\ (Most\ Frequent\ Reduction) = (0.2 \div 0.3) \times Daily\ AR_{max}$

where:

	RPM $_{max}$ [rev/min]	PR_{max} [m/hr]	Daily AR_{max} [m/day]
1st fault zone (Gneiss)	6	2.2	21.1
2nd fault zone (Schist)	6	2.6	25
3rd fault zone (Granodiorite)	6	1.9	18.2

6. Final (complete) results:

Fault zone class		**Variation range of the TBM-performances**					
		RPM [rev/min]	*RPM [rev/min] (MFR)*	**PR [m/hr]**	*PR [m/hr] (MFR)*	**Daily AR [m/day]**	*Daily AR [m/day] (MFR)*
I CLASS	1st fault zone	**4.8 ÷ 6**	*4.8 ÷ 6*	**0.9 ÷ 2.2**	*1.8 ÷ 2.2*	**2.1 ÷ 14.8**	*4.2 ÷ 6.3*
	2nd fault zone	**4.8 ÷ 6**	*4.8 ÷ 6*	**1 ÷ 2.6**	*2.1 ÷ 2.6*	**2.5 ÷ 17.5**	*5 ÷ 7.5*
	3rd fault zone	**4.8 ÷ 6**	*4.8 ÷ 6*	**0.8 ÷ 1.9**	*1.5 ÷ 1.9*	**1.8 ÷ 12.7**	*3.6 ÷ 5.5*
II CLASS		**3.6 ÷ 6**	*4.8 ÷ 6*	**0.5 ÷ 2.6**	*1.6 ÷ 2.1*	**2.5 ÷ 15**	*2.5 ÷ 5*
III CLASS	1st fault zone	**2.4 ÷ 6**	*2.4 ÷ 3.6*	**0.4 ÷ 2.2**	*1.3 ÷ 1.8*	**2.1 ÷ 10.5**	*< 2.1*
	2nd fault zone	**2.4 ÷ 6**	*2.4 ÷ 3.6*	**0.5 ÷ 2.4**	*1.4 ÷ 1.9*	**2.3 ÷ 11.5**	*< 2.3*
IV CLASS		**2.4 ÷ 6**	*2.4 ÷ 3.6*	**0.5 ÷ 2.4**	*0.5 ÷ 1*	**2.3 ÷ 9.2**	*< 2.3*

References

Afrouz, A.A. (1992). Practical Handbook of Rock Mass Classification Systems and Modes of Ground Failure: Boca Raton, FL : CRC Press.

Aydan, Ö. , Akagi, T., & Kawamoto, T. (1993). The squeezing potential of rock around tunnels: theory and prediction. Rock Mechanics and Rock Engineering, 2, 137-163.

Bandis, S.C., Lumsden, A.C., & Barton, N.R. (1983). Fundamentals of rock joint deformation. International Journal of Rock Mechanics and Mining Sciences & Geomechanics Abstracts, 20(6), 249-268.

Barla, G. (2002). Tunnelling under squeezing rock conditions. Advances in Geotechnical Engineering and Tunnelling, 169-268.

Barla, G., & Barla, M. (2000). Continuum and discontinuum modelling in tunnel engineering. Rudarsko Geolosko Naftni Zbornik (12), 45-57.

Barla, G., & Pelizza, S. (2000). TBM tunnelling in difficult ground conditions. Paper presented at the GeoEng2000 - An International Conference on Geotechnical and Geological Engineering, Melbourne, Australia.

Barton, N., Lien, R., & Lunde, J. (1974): Engineering classification of rock masses for the design of tunnel support. Rock Mechanics, Vol. 6, No. 4, pp. 189-236.

Barton, N. (2000). TBM Tunneling in Jointed and Fault Rock. Rotterdam: Balkema.

Barton, N. (2006). Fault zones and TBM. Paper presented at the Geotechnical Risks in Rock Tunnels.

Bieniawski, Z.T. (1976). Rock mass classification in rock engineering. Paper presented at the Exploration for rock engineering, proc. of the symp., (ed. Z.T. Bieniawski), Cape Town.

Bieniawski, Z.T., Celada, B. , Galera, J.M. , & Tardaguila, I. (2008). New applications of the excavability index for selection of TBM and predicting their performance. Paper presented at the ITA-AITES World Tunnel Congress 2008, Agra, India.

Bieniawski, Z.T., Celada, B., & Galera, J.M. (2007). TBM Excavability: Prediction and machine-rock interaction. Paper presented at the RETC, Toronto.

Bieniawski, Z.T., Celada, B., & Galera, J.M. (2007). Predicting TBM Excavability. Tunnels & Tunnelling International.

Bieniawski, Z.T., Celada, B., Galera, J.M., & Álvares, M. (2006). Rock Mass Excavability (RME) index. Paper presented at the ITA World Tunnelling Congress, Seoul.

Bilgin, N., Balci, C., Acaroglu, O., Tuncdemir, H., Eskikaya, S., Akgul, M., & Algan, M. (1999). The performance prediction of a TBM in Tuzla-Dragos Sewerage Tunnel. Challenges

for the 21st Century. Proceedings of the World Tunnel Congress '99, Oslo, June 1999. (2 vols). 817-822.

Bilgin, N., Balci, C., Tuncdemir, H., Eskikaya, S., Akgul, M., & Algan, M. (1999). The performance prediction of a TBM in difficult ground conditions. Paper presented at the AFTES Conference, Paris.

Bilgin, N., Nasuf, E., & Cigla, M. (1993). Stability problems effecting the performance of a full face tunnel boring machine in Istanbul Baltalimani Tunnel. Assessment and prevention of failure phenomena in rock engineering, 501-506.

(Edited by) Blake, L.S., Civil Engineer's Reference Book (Fourth Edition). Rock Mechanics and Rock Engineering. Butterworths. 1989.

Bobet, A. (2010). Numerical methods in geomechanics, The Arabian Journal for Science and Engineering, 35, Number 1B, 27-48.

Brosch, F.J., Kurz, W., & Klima, K. (2006). Definition and Characterisation of Faults and Fault Rocks. Felsbau 24 (5), pp. 13-20, Essen: VGE.

Bruhn, R.L., Parry, W.T., Yonkee, W.A., & Thompson, T. (1994). Fracturing and hydrothermal alteration in normal fault zones. Pure Appl. Geophys., 142, 609-644.

Bruland, A. (1998). Hard rock tunnel boring. (PhD), Norwegian University of Science and Technology, Trondheim.

Bruland, A., Dahlø, T.S., & Nilsen, B. (1995). Tunnelling performance Estimation Based on Drillability Testing. Paper presented at the ISRM Congress, Tokyo.

Bruland, A., & Nilsen, B. (1995). Tunneling Performance Estimation based on Drillabİlİty Testing. Paper presented at the ISRM Congress on Rock Mechanics.

Büchi, E. (1984). Einfluss geologischer Parameter auf die Vortriebsleistung einer Tunnelbohrmaschine (mit besonderer Berücksichtigung der Gesteinsanisotropie). (PhD), University of Bern.

Bürgi, C. (1999). Cataclastic fault rocks in underground excavations: a geological characterisation. (PhD), EPFL.

Burgi, C. , Parriaux, A., & Franciosi, G. (2001). Geological characterization of weak cataclastic fault rocks with regards to the assessment of their geomechanical properties. Q J Eng Geol Hdyrogeol, 34, 225–232.

Caine, J.S., Evans, J.P., & Forster, C.B. (1996). Fault zone architecture and permeability structure. Geology, 24(11), 1025-1028.

Chester, F.M., & Logan, J.M. (1986). Implications for mechanical properties of brittle faults from observations of the Punchbowl Fault Zone, California Pure Appl Geophys, 124, 79–106.

Chiaia, B. (2001). Fracture mechanisms induced in a brittle material by a hard cutting indenter. Int. J. Solids Struct. 38, 7747–7768.

Christe, P. (2009). Geological characterization of cataclastic rock samples using medical X-ray computerized tomography : towards a better geotechnical description. (PhD), EPFL.

Coli, N., Berry, P., & Boldini, D. (2011). In situ non conventional shear tests for the mechanical characterisation of a bimrock. Int J Rock Mech Min Sci, 48, 95-102.

Cook, N.G.W., Hood, M., & Tsai, F. (1984). Observations of crack growth in hard rock loaded by an indenter. Int. J. Rock Mech. Min. Sci. Geomech. Abstr. 21(2), 97–107.

Cundall, P.A. (1971). A computer model for simulating progressive large-scale movements in block rock mechanics. Proc. Symp. Int. Soc. Rock Mech. Nancy, p. 2.

Cundall, P.A., & Hart, R.D. (1993). Numerical modeling of discontinua. Comprehensive rock engineering. Vol. 2, 231-243.

Cundall, P.A., & Strack, O.D.L. (1979). DISCRETE NUMERICAL MODEL FOR GRANULAR ASSEMBLIES. Geotechnique, 29(1), 47-65.

Davis, G.H., & Reynolds, S.J. (1996). Structural Geology of rocks and regions, 2nd edition. John Wiley & Sons, Inc. New York.

Dearman, W.R. (1976). Weathering classification in the characterization of rock: A revision. Bulletin International Association Engineering Geologist, 13, 373-381.

Deere, D.U., Peck, R.B., Monsees, J.E., & Schmidt, B. (1969). Design of tunnel liners and support systems: Report prepared for U.S. Department of Transportation. OHSGT 3-0152. NTIS.

Delisio, A. (2014). Field and numerical studies on the causes and effects of blocky rock conditions on TBM tunnelling. (PhD), EPFL.

Delisio, A., & Zhao, J. (2013). Review of the TBM performance in blocky rocks with potential face stability issues.

Delisio, A., & Zhao, J. (2014). A new model for TBM performance prediction in blocky rock conditions. Tunnelling and Underground Space Technology, 1(43), 440-452.

Delisio, A., Zhao, J., & Einstein, H.H. (2013). Analysis and prediction of TBM performance in blocky rock conditions at the Lötschberg Base Tunnel. Tunnelling and Underground Space Technology, 33(0), 131-142.

Dollinger, G., & Raymer, J. (2002). Rock mass conditions as baseline values for TBM performance evaluation. Paper presented at the North American Tunnelling.

Dudt, J.P., Descoeudres, F., & Einstein, H.H. (1996). Risk assessment in design and construction of deep tunnels – Example of the Gotthard Base Tunnel. Paper presented at the European Conference on Deep tunnels: design, construction and service life, Verona, Italy.

Ehrbar, H. , & Pfenniger, I. . (1999). Umsetzung der Geologie in technische Massnahmen im Tavetscher Zwischenmassive Nord. Paper presented at the Vorerkundung und Prognose der Basistunnels am Gotthard und am Lotschberg.

Einstein, H.H. (1996). Risk and risk analysis in rock engineering. Tunnelling and Underground Space Technology, 11(2), 141-155.

Einstein, H.H., Indermitte, C., Dudt, J.P., Sangyoon, M., Yvonne, M., & Cédric, M. (2012). Decision Aids for Tunnelling - Simjava. Massachussets Institute of Technology, Cambridge, Massachussets.

Einstein, H.H., Indermitte, C., Sinfield, J., Descoeudres, F.P., & Dudt, J.P. (1999) Decision Aids for Tunneling. (pp. 6-13).

Evans, I. (1958). Theoretical aspects of coal ploughing. In: W.H. Watton, Editor, Mechanical Properties of Non-Metallic Brittle Materials, Butterworths, London, pp. 451–468.

Fasching, F., & Vanek, R. (2011). Engineering geological characterisation of fault rocks and fault zones. Geomechanics and Tunnelling, Vol. 4(3), pp. 181-194, Berlin: Ernst & Sohn.

Ferrari, A. (2006). Tunneliers en zones instables. Tracés 22, Les failles d'Alptransit. Bulletin téchnique de la Suisse Romande, 19-26.

Gehring, K. (1995). Leistungs-und Verschleissprognosen in maschinellen Tunnelbau. Felsbau 13 (6).

Geological Society Engineering Group Working Party. (1995). The description and classification of weathered rock for engineering purposes. Quarterly Journal Engineering Geology, 28(3), 207-242.

Goel, R.K., Jethwa, J.L., & Paithakar, A.G. (1995). Indian experiences with Q and MR systems. Tunnelling and Underground Space Technology, 10, 97-109.

Gong, Q.M., Jiao, Y.Y., & Zhao, J. (2006). Numerical modelling of the effects of joint spacing on rock fragmentation by TBM cutters. Tunnelling and Underground Space Technology, 21(1), 46-55.

Gong, Q.M., & Zhao, J. (2009). Development of a rock mass characteristics model for TBM penetration rate prediction. International Journal of Rock Mechanics and Mining Sciences, 46(1), 8-18.

Gong, Q.M., Zhao J., & Jiao Y.Y. (2005). Numerical modeling of the effects of joint orientation on rock fragmentation by TBM cutters. Tunnelling and Underground Space Technology, 20(2), 183-191.

Goodman, R.E., & Ahlgren, C.S. (2000). Evaluating safety of concrete gravity dam on weak rock: Scott Dam. J Geotech Geoenvir Eng, 126(5), 429–442.

Graham, P.C. (1976). Rock exploration for machine manufacturers. Paper presented at the Symposium on exploration for rock engineering, Johannesburg.

Grandori, R., Jaeger, M., Antonini, F., & Vigl, L. (1995). Evinos-Mornos Tunnel, Greece-construction of a 30 km long hydraulic tunnel in less than three years under the most adverse geological conditions. Paper presented at the RECT, San Francisco.

Haas, C., & Einstein, H.H. (2002). Updating the Decision Aids for Tunneling. Journal of Construction Engineering and Management, 128(1), 40-48.

Habimana, J. (1999). Caractérisation géomécanique de roches cataclastiques rencontrées dans des ouvrages souterrains alpins. (PhD), EPFL.

Habimana, J., Labiouse, V., & Descoeudres, F. (2002). Geomechanical characterisation of cataclastic rocks: experience from the Cleuson-Dixence project. International Journal of Rock Mechanics & Mining Sciences, 39, 677-693.

Hanchak, S.J., Forrestal, M.J., Young, E.R., Ehrgott, J.Q. (1992). Perforation of concrete slabs with 48 MPa and 140 MPa unconfined compressive strengths. Int. J. Impact Eng. 12 (1), 1–7.

Hartman, H.L. (1992). SME Mining Engineering Handbook (Second ed.). Society of Mining, Metallurgy and Exploration, Inc., Littleton, Colorado.

Hassanpour, J., Rostami, J., & Zhao, J. (2011). A new hard rock TBM performance prediction model for project planning. Tunnelling and Underground Space Technology, 26(5), 595-603.

Higgins, M.W. (1971). Cataclastic rocks. US Geological Survey Professional Paper, 687.

Hoek, E. (1983). Strength of jointed rock masses. Géotechnique, 23(3), 187-223.

Hoek, E (1994). Strength of rock and rock masses. ISRM News J 2: 4–16.

Hoek, E. (2001). Big tunnels in bad rock. Terzaghi Lecture. ASCE Journal of Geotechnical and Geoenvironmental Engineering, 127(9), 762–740.

Hoek, E., & Brown, E.T. (1988). The Hoek-Brown failure criterion - a 1988 update. Paper presented at the 15th Canadian Rock Mech. Symp., Toronto.

Hoek, E., & Brown, E.T. (1997). Practical estimates of rock mass strength. International Journal of Rock Mechanics & Mining Sciences, 34(8), 1165-1186.

Hoek, E., Carranza-Torres, C. , & Corkum, B. (2002). Hoek-Brown criterion – 2002 edition. Paper presented at the 5th North American Rock Mechanics Symp., Toronto.

Hoek, E., & Marinos, P. (2000). Predicting tunnel squeezing problems in weak heterogeneous rock masses. Tunnels and Tunnelling International, 45-51: part 41; 33-36: part two.

Hoek, E., Marinos, P., & Bennissi, M. (1998). Applicability of the Geological Strength Index (GSI) classification for the very weak and sheared rock masses. The case of the Athens schist formation. Bull Eng Geol Environ, 57, 151-160.

Hudson, J. A., & Priest, S. D. (1979). Discontinuities and rock mass geometry. International Journal of Rock Mechanics & Mining Sciences & Geomechanics Abstracts, 16, 339-362.

Hughes, H.M. (1986). The relative cuttability of coal measures rock. Min. Sci. Technol., 3(2), 95-109.

Innaurato, N., & Oreste, P.P. (2001). Theoretical approach for assessment of the mechanics of rock failure in the TBMs tools-rock interaction. In: Proc., AITES – ITA World Tunnel Congress 2001, Progress in Tunnelling after 2000, Milan (Italy). Patron, Bologna, 227–236.

Innaurato, N., Oggeri, C., Oreste, P.P., & Vinai, R. (2007). Experimental and Numerical Studies on Rock Breaking with TBM Tools under High Stress Confinement. Rock Mech. Rock Engng. 40 (5), 429–451.

ISRM. (1978). Metodologie per la descrizione quantitativa delle discontinuita` nelle masse rocciose: Rivista Italiana di Geotecnica 2/93.

Itasca Consulting Group (2011). UDEC (Universal Distinct Element Code), Version 5.0. User's Guide. Minneapolis, Minnesota.

Itasca Consulting Group (n.d.). UDEC^{TM}, Version 6.0, Distinct-Element Modeling of Jointed and Blocky Material in 2D. Avaliable from: http://www.itascacg.com/software/udec/distinct-element-method

Jethwa, J.L., Singh, B., & Singh, B. (1984). Estimation of ultimate rock pressure for tunnel linings under squeezing rock conditions - a new approach. Paper presented at the Design and Performance og Underground Excavations, ISRM Symposium, Cambridge.

Kahraman, S., & Alber, M. (2008). Triaxial strength of a fault breccia of weak rocks in a strong matrix. Bull Eng Geol Environ, 67, 435–441.

Kahraman, S., & Alber, M. . (2006). Estimating the unconfined compressive strength and elastic modulus of a fault breccia mixture of weak rocks and strong matrix Int J Rock Mech Min Sci 43, 1277–1287.

Kahraman, S., Alber, M., Fener, M., & Gunaydin, O. (2008). Evaluating the geomechanical properties of Misis fault breccia (Turkey). International Journal of Rock Mechanics & Mining Sciences, 45, 1469–1479.

Kaiser, P.K., Diederichs, M.S., Martin, C.D., Sharp, J., & Steiner, W. (2000). Underground works in hard rock tunnelling and mining. Paper presented at the GeoEng2000, Melbourne, Australia.

Klein, S. (2001). An approach to the classification of weak rocks for tunnel projects. Paper presented at the Proc. Rapid Excavation and Tunn. Conf., San Diego, CA, USA.

Klein, S., Schmoll, M., & Avery, T. (1995). TBM performance at four hard rock tunnels in California.

Koenig, A., Straumann, U., & Inniger, M. Geologische Herausforderungen beim Tunnel Moutier. Tunnelbau - Schweizer BauJournal - SBL 3/06.

Kou, S.Q., Lindqvist, P.A., Tang, C.A., & Xu, X.H. (1999). Numerical simulation of the cutting of inhomogeneous rocks. Int. J. Rock Mech. Min. Sci. Geomech. Abstr. 36(5), 711–717.

Kulhawy, F.H. (1975). Stress Deformation Properties of Rock and Rock Discontinuities. Engineering Geology, Vol. 9, No. 4, Dec. pp.327-350.

Laws, S. , Eberhardt, E., Loew, S. , & Descoeudres, F. (2003). Geomechanical properties of shear zones in the Eastern Aar Massif, Switzerland and their implication on tunnelling. Rock Mech Rock Eng, 36(4), 271–303.

Lee, S.G. , & De Freitas, M.H. (1989). A revision of the description and classification of weathered granite and its application to granites in Korea. Quarterly Journal Engineering Geology, 22(1), 31-48.

Lindquist, E.S. , & Goodman, R.E. (1994). Strength and deformation properties of a physical model melange. I. Paper presented at the The 1st North American rock mechanics symposium.

Little, A.L. (1969). The engineering classification of residual tropical soils. Paper presented at the ntern. Conf. Soil Mech.& Found. Engng. 7th, Mexico.

Liu, H.Y., Kou, S.Q., Lindqvist, P.A., & Tang, C.A. (2002). Numerical simulation of the rock fragmentation process induced by indenters. Int. J. Rock Mech. Min. Sci. 39, 491–505.

Loew, S., Barla, G., & Diederichs, M. (2010). Engineering geology of Alpine tunnels: Past, present and future. Paper presented at the 11th IAEG Congress, Auckland.

Maher, H.D. (2014). Description and classification of faults and fault rock types. On-line course of Structural Geology-Geology.

Marinos, P., & Hoek, E. (2000). GSI – A geologically friendly tool for rock mass strength estimation. Paper presented at the GeoEng2000 Conference, Melbourne.

Marinos, P., & Hoek, E. (2001). Estimating the geotechnical properties of heterogeneous rock masses such as flysch. Bulletin of the Engineering Geology & the Environment (IAEG), 60, 85-92.

Marinos, P.G., Marinos, V., & Hoek, E. (2007). The Geological Strength Index (GSI): A Characterization Tool For Assessing Engineering Properties For Rock Masses. Paper presented at the International Workshop on Rock Mass Classification in Underground Mining.

Medley, E.W. (1994). The engineering characterization of melanges and similar “block-in-matrix”-rocks (bimrocks). (PhD), University of California, Berkeley.

Medley, E.W. (2002). Estimating block size distribution of melanges and similar block-in-matrix rocks (bimrocks). Paper presented at the The 5th North American rock mechanics symposium, University of Toronto, Canada.

Medley, E.W. (2001). Orderly characterization of chaotic Franciscan Melanges. Felsbau Rock Soil Eng 19, 20–33.

Medley, E.W., & Goodman, R.E. (1994). Estimating the block volumetric proportions of melanges and similar block-in-matrix rocks (bimrocks). . Paper presented at the The 1st North American rock mechanics symposium

Min, S.Y. (2008). Development of the Resource Model for the Decision Aids for Tunnelling (DAT). Massachusetts Institute of Technology, Boston, US.

Min, S.Y., Kim, T.K., Lee, J.S., & Einstein, H.H. (2008). Design and construction of a road tunnel in Korea including application of the Decision Aids for Tunneling – A case study. Tunnelling and Underground Space Technology, 23(2), 91-102.

Moret, Y., & Einstein, H.H. (2011). Cost and time correlations in linear infrastructure construction. London: Taylor & Francis Group.

Nickmann, M., Spaun, G., & Thuro, K. (2006). Engineering geological classification of weak rocks. Paper presented at the 10th International IAEG Congress 2006, Nottingham.

Nilsen, B., & Ozdemir, L. (1993). Hard rock tunnel boring prediction and field performance. Paper presented at the RETC, Boston.

Onate, E., Rojek, J. (2004).Combination of discrete element and finite element methods for dynamic analysis of geomechanics problems. Comput. Methods Appl. Mech. Engrg. 193 3087–3128.

Palmström, A. (1995). RMi- a rock mass characterization system for rock engineering purposes. (PhD), University of Oslo.

Palmström, A., & Berthelsen, O. (1988). The significance of weakness zones in rock tunnelling. Paper presented at the International conference on Rock Mechanics and Power Plants, Madrid, Spain.

Paltrinieri, E., Dudt, J.P., Sandrone, F., & Zhao, J. (2014). Comparison of excavation methods in different grouns conditions with the Decision Aids for Tunnelling. Paper presented at the 15th Australasian Tunnelling Conference, Sydney, NSW.

Paltrinieri, E., & Sandrone, F. (2014). A study of the TBM performance in fault zones and highly fractured rocks. Paper presented at the World Tunnel Congress,, Iguassu Falls, Brazil.

Passchier, C.W., & Trouw, R.A.J. (1996). Microtectonics: Springer-Verlag, Heidelberg.

Potyondy, D.O, & Cundall, P.A. (2004). A bonded-particle model for rock. International Journal of Rock Mechanics & Mining Sciences; 41(8):1329–64.

Proctor, R.J. (1971). Mapping geological conditions in tunnels. Bull. Ass. Engn. Geol, VIII, 1-31.

Ramezanzadeh, A., Rostami, J., & Kastner, R. (2005). Influence of Rock Mass Properties on Performance of Hard Rock TBMs. Paper presented at the RETC 2005, June 27-29, Seattle, Washington, USA.

Ramezanzadeh, A., Rostami, J., & Tadic, D. (2008). Impact of rock mass characteristics on hard rock tunnel boring machine performance.

Ramoni, M., & Anagnostou, G. (2010). Tunnel boring machines under squeezing conditions. Tunnelling and Underground Space Technology, 25(2), 139-157.

Ramsay, J.G. , & Huber, M. (1987). The Techniques of Modern Structural Geology, Volume 2: Folds and Fractures. Academic Press, London.

Resnyansky, A.D. (2002). DYNA-modeling of the high-velocity impact problems with a split-element algorithm. Int. J. Impact Eng. 27 (7), 709–727.

Riedmüller, G., Brosch, F.J., Klima, K., & Medley, E.W. (2001). Engineering Geological Characterization of Brittle Faults and Classification of Fault Rocks. Felsbau, 19(4), 13-19.

Ritter, S., Einstein, H.H., & Galler, R. (2013). Planning the handling of tunnel excavation material – A process of decision making under uncertainty. Tunnelling and Underground Space Technology, 33(0), 193-201.

Robbins, R.J. (1980). Present trends and future directions in tunnelling. Paper presented at the The Yugoslav Symp. on Rock Mechanics and Underground Actions.

Rojek, J., Onate, E., Labra, C., & Kargl, H. (2011). Discrete element simulation of rock cutting. International Journal of Rock Mechanics & Mining Sciences, 48, 996-1010.

Rostami, J. (1997). Development of a force estimation model for rock fragmentation with disc cutters through theoretical modelling and physical measurement of crushed zone pressure. (PhD), Colorado School of Mines.

Rostami, J., & Ozdemir, L. (1993). A new model for performance prediction of hard rock TBMs. Paper presented at the Rapid excavation and tunneling conference, Boston, MA.

Rostami, J., Ozdemir, L., & Nilsen, B. (1996). Comparison between CSM and NTH Hard Rock TBM Performance Prediction Models. Paper presented at the Annual Technical Meeting: Institute of Shaft Drilling Technologys, Las Vegas.

Sanio, H.P. (1985). Prediction of the performance of disc cutters in anisotropic rock. Int J Rock Mech Min Sci. 22(3),153-61.

Santi, P.M. (1995). Classification and Testing of Weak and Weathered Rock Materials: A Model Based on Colorado Shales. (PhD), Colorado School of Mines, Golden, CO.

Santi, P.M., & Doyle, B.C. (1997). The locations and engineering characteristics of weak rock in the U.S. Denver, CO: Association of Engineering Geologists, Special Publication #9.

Santi, P.M. (2006). Field Methods for Characterizing Weak Rock for Engineering. Environmental & Engineering Geoscience, 12(1), 1-11.

Sapigni, M., Berti, M., Bethaz, E., Busillo, A., & Cardone, G. (2002). TBM performance estimation using rock mass classifications. International Journal of Rock Mechanics and Mining Sciences, 39(6), 771-788.

Sausgruber, T., & Bradner, R. (2003). The relevance of brittle fault zones in tunnel construction - Lower inn valley feeder line north of Brenner Base tunnel, Tyrol, Austria. Mitt. Osterr. Geol. Ges., 94, 157-172.

Schubert, W., & Riedmüller, G. (2000). Tunnelling in Fault Zones-State of the Art in Investigation and Construction. Felsbau, 18(2), 7-15.

Schubert, W., & Riedmüller, G. (1997). Influence of Faults on Tunnelling. Felsbau 15(6), 483-488.

Sibson, R.H. (1977). Fault rocks and fault mechanisms. J. Geol. Soc. London, 133, 191-213.

Singh, B., Jethwa, J.L., Dube, A.K., & Singh, B. (1992). Correlation between observed support pressure and rock mass quality. Tunnelling and Underground Space Technology, 7, 59-74.

Sonmez, H., Gokceoglu, C., Medley, E.W., Tuncay, E., & Nefeslioglu, H.A. (2006). Estimating the uniaxial compressive strength of a volcanic bimrock. Int J Rock Mech Min Sci 43, 554–561.

Sonmez, H., Gokceoglu, C., Tuncay, E., Medley, E.W., & Nefeslioglu, H.A. (2004). Relationship between volumetric block proportion and overall UCS of a volcanic bimrock. Felsbau Rock Soil Eng, 22, 27–34.

Sturk, R., Dudouit, F., Aurell, O., & Eriksson, S. (2011). Summary of the first TBM drive at the Hallandsas project. Paper presented at the Rapid Excavation and Tunneling Conference San Francisco, CA.

Su, O., & Akcin, N.A. (2011). Numerical simulation of rock cutting using the discrete element method. International Journal of Rock Mechanics & Mining Sciences, 48, 434-442.

Tarkoy, P.J. (1974). Predicting Tunnel Boring Machine (TBM) Penetration Rates and Cutter Costs in Selected Rock Types. Paper presented at the The 9th Canadian Rock Mechanics Symposium, Montreal.

Terzaghi, K. (1946). Rock defects and loads on tunnel supports. In R. V. P. a. T. L. White (Ed.), Rock tunneling with steel supports (pp. 15-99). Youngstown, OH.

Thuro, K., & Plinninger, R.J. (1999). Roadheader excavation performance - geological and geotechnical influences.

Thuro, K., & Plinninger, R.J. (2003). Hard rock tunnel boring, cutting, drilling and blasting: rock parameters for excavatability. Paper presented at the ISRM 2003.

Thuro, K., & Scholz, M. (2003). Deep weathering and alteration in granites - a product of coupled processes. Paper presented at the International Conference on Coupled T-H-M-C in Geosystem: Fundamentals, Modelling, Experiments and Application, GeoProc 2003, Stockholm, Royal Institute of Technology (KTH).

Thuro, K., & Spaun, G. (1996). Drillability in hard rock drill and blast tunnelling. Felsbau 14, 103-109.

Vibert, C. , Gupta, S.C. , Felix, Y., Binquet, J. , & Robert, F. (2005). Dul Hasti Hydroelectric Project (India): Experience gained from backanalysis of the excavation of the headrace tunnel. Paper presented at the GEOLINE 2005 International Symposium, Lyon.

Vuilleumier, F., Keller, M., Straumann, U., Aeschbach, M., & Marclay, R. (2006). Schlussbericht Rohbau Nr. 13 – Felsmechanik, Ausbruch, Sicherung. Unpublished Report.

Wang, J.K., & Lehnhoff, T.F. (1976). Bit penetration into rock: a finite element study. Int J Rock Mech Min Sci 13:11–16.

Wanner, H., & Aeberli, U. (1979). Tunnelling machine performance in jointed rock. Paper presented at the The 4th Int. Congr. ISRM, Montreux

White, S. (1982). Fault rocks of Moine Thrust Zone: A guide to their nomenclature. Textures and Microstructures, 4, 211-221.

Wise, D.U., Dunn, D.E., Engelder, J.T., Geiser, P.A., Hatcher, R.D., Kish, S.A., & Schamel, S. (1984). Fault-related rocks: Suggestions for terminology. Geology, 12, 391-394.

Zhang, X.G., Han, W.F., & Nie, D.X. (1986). Engineering geological classification of fault rocks. Paper presented at the 5th Int. Congr. Int. Assoc. Engin. Geol., Buenos Aires.

Ziegler, H.J., Giovanoli, F., & Isler, A. (2008). Basistunnel Steg/Raron Geologischer Bericht. Raron-Ferden, Lötschberg Basistunnel Schlussdokumentation. Unpublished report.

Curriculum Vitae

Personal Information	
First Name/Surname	**Erika Paltrinieri**
E-mail	erika.paltrinieri@epfl.ch paltrinieri.e@gmail.com
Nationality	Italian
Date of birth	05.06.1984
Education and Training	
Dates	2012-to date
	Ph.D. in Geomechanics
Principal topics	TBM tunnelling in difficult ground conditions Numerical modelling of TBM excavation in highly fractured and faulted rocks Probabilistic analysis of tunnel construction with the Decision Aids For Tunnelling (DAT) Thesis title: Analysis of TBM tunnelling performance in faulted and highly fractured rocks Supervisor: Prof. Jian Zhao Co-supervisor: Dr. Federica Sandrone
Name and type of organization providing education and training	Ecole Polytechnique Fédérale de Lausanne (EPFL), Laboratoire de Mécanique des Roches
Dates	2013
	Attendance of the theoretical classes of the Master of Advanced Studies (MAS) in Tunnelling at the Ecole Polytechnique Fédérale de Lausanne (EPFL), Laboratoire de Mécanique des Roches

Dates	2010
Title of qualification awarded	**Qualification for Engineering practice**
Name and type of organization providing education and training	Politecnico di Torino – C.so Duca degli Abruzzi, 24 – 10129, Torino (TO)
Dates	2007-2009
Title of qualification awarded	**Master of Science in Environmental Engineering, Geoengineering specialization** Final grade: 110/110 Thesis: Study of debris flow events in Upper Susa Valley Supervisor: Chiara Deangeli
Principal subjects covered	Rock Mechanics and Rock Engineering, Slope Stability, Tunnelling and Underground Structures, Applied Geophysics, Geological Survey.
Name and type of organization providing education and training	Politecnico di Torino – C.so Duca degli Abruzzi, 24 – 10129, Torino (TO)
Level in national or international classification	M. Sc. Degree / Dottore Magistrale in Ingegneria per l'Ambiente e il Territorio
Dates	2003-2006
Title of qualification awarded	**Bachelor of Science in Environmental Engineering** Final grade: 110/110 Thesis: Environmental applications of gamma spectrometry
Principal subjects covered	Structural Engineering, Soil Mechanics, Hydraulic Engineering, Geology
Name and type of organization providing education and training	Università degli Studi "La Sapienza" di Roma – Piazzale Aldo Moro, 5 – 00185, Roma (RM)
Level in national or international classification	Bachelor Degree / Dottore in Ingegneria per l'Ambiente e il Territorio
Dates	1998-2003
Title of qualification awarded	**Scientific High School Degree** Final grade: 100/100
Level in national or international classification	Liceo scientifico G.B Grassi di Latina – Via P. Sant'Agostino, 8 – 04100, Latina (LT)

Work and Teaching Experience	
Dates	2012-to date
Main activities	**Teaching assistant** in the courses: Analysis I and II Rock mechanics and tunnel engineering Underground construction technology
Dates	2009-2011
Occupation or position held	**Fellowship in Geotechnical Engineering**
Main activities and responsabilities	Assessment of debris flow hazard in different geological and climatic conditions.
Name and address of employer	Politecnico di Torino – C.so Duca degli Abruzzi, 24 – 10129, Torino (TO)
Type of business sector	University Research
Date	2009-2010
Occupation or position held	**Collaboration to a project of national relevance (PRIN 2007)**
Main activities and responsabilities	Characterization of materials involved in debris flow phenomena located in the Upper Susa Valley; Numerical modelling and definition of deposition areas of debris flow.
Name and address of employer	Politecnico di Torino – C.so Duca degli Abruzzi, 24 – 10129, Torino (TO)
Type of business sector	University Research
Date	2010-2011
Occupation or position held	**Scientific collaboration to the European Project PARAmount "iMproved Accessibility: Reliability and security of Alpine transport infrastructure related to mountainous hazards in a changing climate"**.
Main activities and responsabilities	Development of a 3D numerical model for the assessment of deposition areas of debris flow in alpine environment
Name and address of employer	Contract between: Politecnico di Torino – C.so Duca degli Abruzzi, 24 – 10129, Torino (TO) Arpa Piemonte – Via Pio VII, 9 – 10135, Torino (TO)
Type of business sector	University Research and scientific consultancy

Personal skills and competences

Mother tongue **Italian**

Other languages

Self - Assessment	Understanding				Speaking				Writing	
European level (*)	Listening		Reading		Spoken interaction		Spoken production			
English	B1	Independent user	B2	Independent user	B1	Independent user	B1	Independent user	B2	Independent user
French	A2	Basic user	B1	Independent user	A2	Basic user	A2	Basic user	A2	Basic user

(*) Common European Framework of Reference for Languages

Certificates Cambridge P.E.T. "Pass with merit"

Social skills and competencies Motivated, organized, competent and dynamic. High problem solving approach

Technical and computer skills and competencies Basic command of the Fortran programming language. Good command of MS. Office, MS. Windows and AutoCAD 2D. Good command of analytical codes (RocScience Dips, Swedge, RocSupport, Unwedge). Good command of UDEC and DAT software.

Driving licence Private Swiss Driving Licence (Cat. B)

List of publications

Scientific publications

Paltrinieri E., Sandrone F. and Zhao J. (2014). Analysis and estimation of the TBM performance in highly fractured and faulted rocks. (Under revision - Tunnelling and Underground Space Technology).

Presentations, conferences or seminars held by the candidate

Paltrinieri E. and Sandrone F. (2014). A study of the TBM performance in fault zones and highly fractured rocks. World Tunnel Congress 2014, Iguassu Falls, Brazil.

E. Paltrinieri, J.P. Dudt, F. Sandrone, and J. Zhao (2014). Comparison of excavation methods in different grounds conditions with the Decision Aids for Tunnelling, in 15th Australasian Tunnelling Conference 2014: Sydney, NSW.

E. Paltrinieri, F. Sandrone, J.P. Dudt, and J. Zhao (2015). Probabilistic simulations of TBM tunnelling in highly fractured and faulted rocks, in International Conference on Tunnel Boring Machines in Difficult Grounds (TBM DiGs) Singapore, 18–20 November 2015.

Other publications

Paltrinieri E. and J. Zhao (2015). TBM Tunnelling in Faulted and Folded Rocks. Final report for the research project FGU 2007/004.